Hygrothermal Assessment of Wall Constructions in the Arctic

Friis, Naja Kastrup

Link to article, DOI:
10.11581/DTU.00000275

Publication date:
2023

Document Version
Publisher's PDF, also known as Version of record

Department of Civil and Mechanical Engineering
PhD thesis

Hygrothermal Assessment of Wall Constructions in the Arctic

Naja Kastrup Friis

Hygrothermal Assessment of Wall Constructions in the Arctic

PhD thesis
September 2023

Author
Naja Kastrup Friis
nfri@dtu.dk

Cover photo: Naja Kastrup Friis
Published by: Department of Civil and Mechanical Engineering
Technical University of Denmark (DTU)
Building 118
2800 Kgs. Lyngby, Denmark
www.construct.dtu.dk

DOI: https://doi.org/10.11581/dtu.00000275
ISBN: 978-87-7475-755-9
DCAMM: S333

Preface

The present thesis, “Hygrothermal Assessment of Wall Constructions in the Arctic”, was conducted as partial fulfilment of the Doctor of Philosophy (PhD) degree from the Technical University of Denmark (DTU). The research presented within this thesis was carried out from February 2020 to April 2023 in the section of Design and Processes at DTU Construct (previously DTU Byg). This PhD was supervised by Professor Eva B. Møller and Associate professor Tove Lading.

Through a combination of theoretical calculations, field measurements, and numerical simulations, the research contributes to identifying the necessary initiatives for achieving robust, durable, and sustainable constructions in Greenland, especially concerning the suitability of the construction and the impact of weather conditions present in the Arctic.

This is a paper-based thesis comprising five papers, constituting the second part of the thesis. The papers include three first-authored journal articles, one conference paper, and one second-author journal article. Additionally, the research contributed to the development of a calculation tool for determining the optimal insulation thickness in exterior walls.

Originally, my interest in this field of research was lit by a deep fascination and curiosity about Greenland. Specifically, I have, from an early age, been intrigued by many aspects of Greenland, from the culture and language to environmental and climatic challenges. Thus, when the opportunity arose to combine this interest with my knowledge of buildings and sustainability, I had to go for it. During the research work, I found great motivation in the opportunity of contributing to better Greenlandic living conditions. The project offered two wonderful trips to Greenland, where I had some of my life’s most magnificent and overwhelming nature experiences.

The research project was financially funded by the interdisciplinary research project Arctic Building and Construction, which aimed to improve the quality and processes in the construction sector in Greenland.

Kgs. Lyngby, Denmark

September 2023

Naja Kastrup Friis

Abstract

There are many challenges when building in the Arctic. These challenges include harsh weather conditions, limited infrastructure, financial circumstances, and lack of local resources, e.g., building materials, skilled labour, factories, and machinery. In this study, Greenland was selected as a case study for the Arctic region.

Due to the current building traditions being implemented by the Greenlandic Technical Organisation in 1950 and forward, the modern Greenlandic construction industry is relatively new. As of 2023, it consists mainly of refined single-family half-timber houses and multistorey concrete and half-timber constructions. The newest tendency is cross-laminated timber (CLT) constructions. The Greenlandic building stock is of varying quality, and around 11 % of the government-owned residents are uninhabitable due to either mould or wear and tear. The consequences of poor buildings are many, including unhealthy indoor climate, short service life, large heat loss, and environmental issues.

Consequently, this thesis aims to identify how to achieve a better and more robust building stock in Greenland. To this end, two hypotheses were formulated, each with three research questions. The hypotheses are:

- Mould problems in Greenlandic wall constructions are caused by faulty design
- Optimal wall construction designs depend on the location in Greenland

Two field studies were conducted, collecting experimental data from constructions in Nuuk and Sisimiut. Three construction types were tested and monitored for temperature and relative humidity. The investigated construction types were half-timber, CLT, and concrete. In the first study, data from a meticulously constructed test facility with a controlled indoor climate was analysed. In the second field study, data from multiple residential houses was evaluated. Thus, the two data sets account differently for buildability and user behaviour. The performances of the constructions were evaluated by comparing the measured data to hygrothermal simulations of fitted models conducted in the simulation programme Delphin. Furthermore, the risk of mould growth was quantified with the Viitanen model and used to evaluate the buildings' suitability. The constructions in the test facility were tested for multiple Greenlandic locations with reanalysis weather data.

A theoretical study was conducted based on a developed tool, calculating the optimal insulation thickness for minimising greenhouse gas emissions. The tool was compared to two other methods, evaluating future Arctic and subarctic climate scenarios.

Despite critical mould conditions in air cavities, none of the constructions were concluded to have faulty designs and, therefore, were not considered unsuitable for the Arctic climate based on mould growth risk. Most essentially, the buildability and the labour quality ensuring wind, air, and vapour-tight constructions were found to be key for the suitability, though the presence of wind and vapour barriers is not crucial. Such barriers might, however, reduce the consequences of building errors if implemented correctly. The suitability of a construction at a specific location was found to be closer related to town size and available facilities and resources than to the weather conditions. This is despite the fact that the weather conditions across Greenland were significantly different.

Dansk resumé

Der er mange udfordringer forbundet med at bygge i Arktiske egne. Disse udfordringer inkluderer barske vejrforhold, begrænset infrastruktur, finansielle forhold og mangel på lokale ressourcer, såsom råmaterialer, kompetent arbejdskraft og faciliteter som fabrikker og maskinel. I dette studie fungerer Grønland som case for hele Arktis.

Eftersom de nuværende byggetraditioner udspringer af Grønlands Tekniske Organisations (GTO) arbejde i 1950 og frem, er den moderne Grønlandske byggeskik relativt ny. I dag består bygningsmassen primært af videreudviklede enfamilies-bindingsværkshuse, fleretages beton- og bindingsværks-konstruktioner samt krydslaminerede trækonstruktioner, som den nyeste byggetendens. Den Grønlandske bygningsmasse er af varierende kvalitet, og omtrent 11 % af Selvstyrets boliger står tomme på grund af enten skimmel eller ekstrem slitage. Konsekvenserne ved dårlige bygninger er mange og inkluderer usundt og ukomfortabelt indeklima, reduceret levetid grundet hurtig nedbrydning, øget varmetab og miljømæssige udfordringer.

Målet med denne afhandling at identificere, hvordan Grønlands bygningsmasse kan blive bedre og mere robust. Nedenstående hypoteser er formuleret, hver med tre tilhørende forskningsspørgsmål:

- Skimmelproblemer i Grønlandske vægkonstruktioner skyldes dårligt design
- Optimale facadedesigns afhænger af den geografiske lokation i Grønland

Der blev udført to feltstudier, hvor der blev indsamlet data for temperatur og relativ luftfugtighed fra tre konstruktionstyper i Nuuk og Sisimiut. Konstruktionstyperne var bindingsværk, CLT og beton. Det ene studie er en omhyggeligt konstrueret testbygning med kontrolleret indeklima, og det andet evaluerer data fra beboede boliger. Derfor forholder de to studier sig forskelligt til bygbarhed og brugeradfærd. Kvaliteten af facaderne er evalueret ved at sammenligne de målte data med hygrotermiske simuleringer af tilpassede modeller i simuleringsprogrammet Delphin. Derudover er skimmelrisici kvantificeret ved brug af Viitanen modellen og brugt som mål for egnethed. Med reanalyse data blev facaderne i testbygningen testet for flere lokationer.

Derudover indeholder afhandlingen et teoretisk studie baseret på et værktøj, der er udviklet til at beregne den optimale isoleringstykkelse og derved sikre minimal drivhusgasudledning. Resultaterne fra værktøjet blev analyseret og sammenlignet med to andre metoder, ved at evaluere fremtidsscenarier for Arktisk og subarktisk klima.

På trods af kritisk skimmelindeks i ventilerede hulrum blev ingen af konstruktionerne konkluderet fejlagtigt designet og derved uegnet til det Arktiske klima baseret skimmelrisiko. Desuden blev bygbarhed fundet signifikant, imens måden at sikre dette var uvæsentlig. Håndværkskvaliteten, der sikrer vind-, luft- og fugttætte konstruktioner, blev fundet afgørende for egnetheden, men tilstedeværelsen af vind- og dampspærrer var underordnet. De kan dog reducere konsekvenser ved byggefejl, hvis de implementeres korrekt. Egnetheden af en konstruktion på en specifik lokation blev i højere grad defineret af byens størrelse, faciliteter og ressourcer end af vejrforholdene, selvom vejrforholdene over Grønland er signifikant forskellige.

Acknowledgements

I would like to use this opportunity to thank my supervisors, Professor Eva B. Møller and Associate Professor Tove Lading, for this fantastic opportunity, both in terms of scientific development and the wonderful experiences that came with it. Eva B. Møller has been my eternal anchor during this process. I am forever grateful for the encouragement, discussions, small talk, laughs, and, most importantly, trust in my abilities. I am not sure I could have done this without you. Tove Lading has been vital to the success of this project. I truly appreciate your enthusiasm when sharing your love for Greenland and introducing me to the construction industry, challenges, and small gems to enjoy while travelling the country. You always have a sharp eye on the essential challenges and a priceless overview of how to overcome all kinds of unforeseen obstacles. Thank you both for having me on board during this project.

I also want to express my deepest gratitude to all the incredible researchers in the ZEB-lab at the Norwegian University of Science and Technology, NTNU. Thank you very much, Tore Kvande and Berit Time, for the opportunity and for inviting me for a second trip with further collaboration. In the Klima2050 office, I was lucky to be seated next to Jørn Emil, with whom I have co-authored two papers and had many great talks and cups of coffee. I am also grateful for knowing the sugar pushers Vegard and Erland and the great company of Silje and Martin. I also want to thank my welcoming office neighbours Tonje and Ørjan for spending time with me and introducing me to an authentic May 17th celebration. It was an absolute pleasure to be included in your scientific community and join you for discussions as well as cake breaks, waffle afternoons, and climbing trips.

Furthermore, I would like to thank my colleagues at DTU Construct and Arctic DTU in Sisimiut. My fellow PhDs, both former and present, for cheering me on and ensuring me that one day, I would be able to proudly hand in my PhD thesis – I guess that day is today. A special thanks to my office mates, Andreas and Panagiota, for all the small talk, procrastination, and discussions, and to Ioannis, Adam, and Pablo for making sure that I would sometimes take time for a bite to eat, a beer, a laugh, or some fresh air.

I could not have succeeded with this massive project without my exceptional rock-steady support crowd. My deepest gratitude goes to you, Richard, for always encouraging me to follow my dreams, trust my intuition, and support me unconditionally. You make the world a better place, and I cherish being a part of yours. I sincerely appreciate my parents and family for encouraging me, rooting for me, and letting me join them for holiday lunches while abroad. And my dear friends. Thank you for understanding my absence during travels and busy periods, always cheering me on, and listening to my frustrations, insecurities, and scientific challenges. I truly appreciate you thinking the best of me – even when I could not be the best version of myself.

Finally, I would like to thank my selected critics for helping me perfect this thesis and asking me many great questions to ensure the best reader experience for everyone who decides to read past the table of contents. Sabine, Adam, Kathrine, Mia, and Charlotte. You are my heroes.

Acronyms

AAU	Aalborg University
ACH	Air Change Rate per hour
AHO	Oslo School of Architecture
BR06	Building Regulation of 2006 (Greenlandic)
CLT	Cross-Laminated Timber
CON	Concrete construction
CPH	Copenhagen, the capital of Denmark
CV(RMSE)	Coefficient Variation of Root Mean Square Error
DGNB	Deutsche Gesellschaft für Nachhaltiges Bauen (sustainability certification)
DH	District Heating
DMI	Danish Meteorological Institute
DTU	Technical University of Denmark
ECMWF	European Centre for Medium-Range Weather Forecasts (weather data)
EoL	End-of-Life
ERA5	ECMWF Reanalysis 5th Generation
ESL	Estimated Service Life
GHG	Greenhouse Gasses
GTO	Greenlandic Technical Organisation
HAM	Heat, Air, and Moisture simulation
HDD	Heating Degree Days
HT	Half-timber construction
IAQ	Indoor Air Quality
IDA ICE	IDA Indoor Climate and Energy (software)
IPCC	Intergovernmental Panel on Climate Change
ITO	Insulation Thickness Optimiser (Excel tool)
LCA	Life Cycle Assessment
LCI	Life Cycle Inventory
MBE	Mean Bias Error
MD	Difference in means
NOAA	National Oceanic and Atmospheric Administration
NTNU	Norwegian University of Science and Technology
RH	Relative Humidity
RMSE	Root Mean Square Error
RQ	Research Question
$Scen_{ins}$	ITO scenario considering only the insulation
$Scen_{wall}$	ITO scenario considering the insulation and additional wall layers
TRY	Test Reference Year (weather data)
VB	Vapour barrier
VOC	Volatile Organic Compounds
WB	Wind barrier
WUFI	Wärme Und Feuchte Instationär (software)

List of symbols

Greek letters

α	Slope curve	[°]
Δ	Difference	
θ	Temperature	[°C]
λ	Thermal conductivity for heat transport	[W/(m·K)]
μ	Vapour diffusion resistance factor	[-]
ρ	Density	[kg/m^3]
ϕ	Relative humidity	[%]

Roman letters

d	Thickness	[m]
d_{opt}	Optimal insulation thickness	[m]
D	Distance	[km]
E	Emissions	[kg$CO_{2\text{-eq}}$]
E_{factor}	Emissions related to energy production	[kg$CO_{2\text{-eq}}$/kWh]
E_{heat}	Emissions related to heat loss, Q	[kg$CO_{2\text{-eq}}$/m^2]
$E_{material}$	Emissions related to insulation material production	[kg$CO_{2\text{-eq}}$/m^3]
E_{opt}	Total emissions at d_{opt}	[kg$CO_{2\text{-eq}}$/m^2]
HDD	Heating Degree Days	[K/a]
ν	Vapour content	[g/m^3]
$\Delta\nu$	Interior moisture load	[g/m^3]
W	Waste factor	[%]
W_{dist}	Waste factor of energy due to distribution	[%]
$W_{material}$	Residual waste factor of insulation material	[%]
P	Air pressure	[Pa]
Q	Heat loss from transmission	[W/m^2]
U	Thermal transmittance	[W/(m^2·K)]

Subscripts

opt	Optimal
int	Interior
ext	Exterior
inc	Incineration
land	Landfill

List of papers

This PhD thesis is based on the papers listed below. The papers are all appended in the second part of the thesis.

Paper I. **Friis, N.K**., Møller, E.B., and Lading, T. (2021) '*Can Collected Hygrothermal Data Illustrate Observed Thermal Problems of the Façade? - A Case Study from Greenland*',
Journal of Physics: Conference Series, 2069(1).
doi: 10.1088/1742-6596/2069/1/012071.

Paper II. **Friis, N.K**., Gaarder, J.E., and Møller, E.B. (2022) '*A Tool for Calculating the Building Insulation Thickness for Lowest CO2 Emissions—A Greenlandic Example*',
Buildings, 12(8).
doi: 10.3390/buildings12081178.

Paper III. Gaarder, J. E., **Friis, N.K**., *et al.* (2023) '*Optimisation of Thermal Insulation Thickness Pertaining to Embodied and Operational GHG Emissions in Cold Climates – Future and Present Cases*',
Building and Environment, 234.
doi: 10.1016/j.buildenv.2023.110187.

Paper IV. **Friis, N.K.**, Møller, E.B., and Lading, T. (2023) '*Hygrothermal Conditions in Greenlandic Test Pavilion – Measurements and Simulations*',
Building and Environment, 238.
doi: 10.1016/j.buildenv.2023.110347.

Paper V. **Friis, N.K.**, Møller, Eva B., and Lading, T. (2023) '*Hygrothermal Conditions in the Façade of Residential Buildings in Nuuk and Sisimiut*',
Building and Environment, 243.
doi: 10.1016/j.buildenv.2023.110686.

Other scientific work

Tool Friis, N.K. (2022) 'Insulation Thickness Optimizer, ITO'.
doi: 10.11583/DTU.19672470.

Contents

Part I

Summary

1 Introduction

The modern Greenlandic building tradition is relatively new, mainly originating from the middle of the 20th century. The turning point was the establishment of the Greenlandic Technical Organisation with the purpose of improving the construction industry. Since then, the development has happened rapidly, with the phase-out of peat houses, improvement of the existing half-timber houses, and later the introduction of concrete blocks. However, the effort to maintain existing buildings has been inadequate, resulting in short service life for many industrial, institutional, and residential buildings (Naalakkersuisut, 2012). The lack of maintenance and improvement of the building stock has contributed to an extreme housing shortage, as older buildings are demolished or uninhabitable before their estimated service life (Marott Brandt, 2021).

While developing new construction methods, little effort has been made to learn more about the performance of the introduced constructions; at least, there has been limited systematically compiled documentation on building performance in Greenland. Consequently, the underlying knowledge is inadequate, and almost no evidence has been gathered to define the optimal constructions of the future. This knowledge gap is an issue, as many residents in Greenland experience thermal discomfort, draught, and mould.

Furthermore, due to the anticipated extensive population growth in Nuuk (Kommuneqarfik Sermersooq, 2021), there is considerable potential for implementing better constructions. Specifically, the municipality, Kommuneqarfik Sermersooq, intends to expand Nuuk with housing for approximately 11,000 persons by 2030 (Kommuneqarfik Sermersooq, 2021). Meanwhile, there is a waiting time of 10-12 years for ordinary housing in Nuuk (Nordisk Samarbejde, 2020). This is further challenged by the insufficient maintenance and lack of knowledge on how to build well-functioning buildings, which make it difficult to expand the building stock effectively.

The primary motivation for this PhD is founded on these three challenges: 1) lack of maintenance and improvement of existing building stock, 2) lack of documentation of appropriate building practises, and 3) anticipated need for immense expansion of the building stock. This PhD aims to assess hygrothermal issues in current buildings based on experimental data to provide evidence for proper practices in Greenland.

The remainder of this thesis is structured as follows. First, the background information is provided in Chapter 2, including historical insights, essential information about Greenland, and related research projects. Furthermore, the chapter describes the relevant technical theory and the current state-of-the-art of Greenlandic building practices. The investigated hypotheses and research questions are introduced in Chapter 3. Chapter 4 explains the central methodologies from the papers with a level of detail necessary for the following discussion. Chapter 5 contains the main findings, which are discussed in Chapter 6 based on the defined hypotheses and research questions. Finally, Chapter 7 summarises the findings of the conducted work, presents the conclusions, and describes recommendations for future work.

2 Background

The following provides the necessary information to understand the challenges and conditions when constructing in the Arctic. The focus is primarily on Greenland, as this country served as a case for the research and experiments.

2.1 Definition of the Arctic

The Arctic region is the geographic area surrounding the North Pole. The region's boundaries vary depending on the chosen definition, i.e., vegetation and forest line, the Arctic Circle, culture, and political boundaries such as Arctic Council Working Groups (Arctic Centre University of Lapland, 2023b, 2023a). One of the most common definitions is the 10 °C July isotherm, which corresponds to the area where the monthly average temperature is consistently below 10 °C (Arctic Centre University of Lapland, 2023b). The boundary corresponding to the 10 °C July isotherm is illustrated in Figure 2.1 and is the definition applied in this thesis. Most definitions of the Arctic include all of or parts of Canada, the United States, Russia, Finland, Sweden, Norway, Iceland, and Greenland (an autonomous part of Denmark). The region inhabits approximately 4 million people, of which 10 % are indigenous (Arctic Centre University of Lapland, 2023b). The Arctic Circle corresponds to a latitude of 66°33’ N. It also marks the border north of which all areas experience polar night, meaning that the sun never sets during at least one day of the year.

Figure 2.1. Map of the Arctic region defined by the 10 °C July isotherm, marked with the orange line. The dashed line marks the Arctic Circle (Arctic Portal, 2016).

Compared to other countries within the Arctic, Greenland has some of the most challenging circumstances for achieving a healthy construction industry with a thriving economy, sufficient skilled labour, and quality buildings with long service lives. The current challenges include the lack of natural building materials, a lack of infrastructure

causing island operations, and an unhealthy economy (Lading, 2015). The lack of sufficiently skilled workers is also an issue due to the small population, though bigger cities are more likely to have a more capable workforce (Grydehøj, 2014; Abrahamsen, 2019). During this study, “Island operation” refers to a society of multiple remote communities (towns and settlements) that are desolated from each other. The island operation causes unequal conditions for the towns and settlements across Greenland.

Since the Greenlandic construction industry is the most challenged within the Arctic, it is assumed that a solution is functional in the entire Arctic region if it is suitable for Greenland. Therefore, the title of this thesis includes the whole Arctic region despite the explicit focus on Greenlandic conditions. However, melting permafrost is more challenging to houses in other Arctic areas, e.g., Svalbard, as most Greenlandic buildings stand on bedrock. This perspective is not included in this study, which concentrates on exterior walls.

2.2 Greenland today

Globally, Greenland is known for its serene nature, harsh climate, northern lights, societal challenges, and strategic military position. This section aims to paint a more detailed picture of the current conditions and demography.

Figure 2.2. Map of Greenland, with the approximate location of relevant towns and settlements. The horizontal line represents the Arctic Circle (latitude: 66°33’ N).

The population of Greenland is currently 57 000, of which approximately 60 % of the population live in one of the five largest towns: Nuuk (34 %), Sisimiut (10 %), Ilulissat, Aasiaat, and Qaqortoq. The largest towns are all located on the west coast, as shown in the map in Figure 2.2. Only 3,000 residents currently live on the east coast of Greenland, of which approximately 2,000 live in the largest town, Tasiilaq (Statistics Greenland, 2022). According to the Arctic Human Development Report from 2015, 60 % of the Greenlandic population is indigenous (AHDR, 2015).

Greenland is the largest island on Earth, with the approximate size of Central Europe (Hendriksen, 2016), but an ice cap and smaller glaciers cover 80 % of it. According to Hendriksen (2016), only 3 % of Greenland is suitable for living, resulting in large distances between inhabited areas. Due to the extreme weather conditions and large distances between towns and settlements, Greenland is island operated. This means that each settlement needs to be self-sufficient regarding energy and, to some extent, institutions, health care, food, and other skilled labour, depending on the population size.

2.3 Historical development of Greenlandic buildings

Understanding the historical development of Greenland's construction sector is essential to understanding the current building practice. Prior to the colonisation, the Greenlandic building practice consisted of only locally available natural materials. The main resources were peat and stone for winter housing, while leather tents were used in the summer during fishing and hunting. North of the Arctic Circle, the construction style was influenced by access to vast amounts of large whale bones, while the south had access to Siberian driftwood (Vadstrup and Schultz-Lorentzen, 1994).

The contact between Greenland and the rest of Europe was sporadic until whaling activities increased in the 1600s. In 1721, the Danish king Frederik the 4th became interested in whale oil products, e.g., for use as fuel in street lamps, manufacturing lubricants, grease for machines, and soap (Engelbrechtsen and Jørgensen, 2023). Then, the Danish king sent Hans Egede to convert Greenland to Christianity, which marked the beginning of colonisation (Greenland National Museum, 2016).

Due to the island operation, the construction tendencies varied across Greenland. Nevertheless, until 1950, the Greenlandic building culture can be divided into four construction techniques according to the Greenlandic National Museum and Archive, Nunatta Katersugaasivia Allagaateqarfialu (see Figure 2.3). Although, the construction types were sometimes combined into new house types (Vadstrup and Schultz-Lorentzen, 1994; Greenland National Museum, 2016). The four main construction techniques are shown in Figure 2.3 and include:

a. Peat houses
b. Stone houses
c. Log houses (Norwegian: “laftehus”, Danish: “stokværkshus”)
d. Timber frame houses

(a) Peat house. Credit: Eva B. Møller.

(b) Stone house. Credit: Morten Frederiksen.

(c) Log house. Credit: Ernst J. de Place.

(d) Timber frame house.

Figure 2.3. Examples of the four traditional construction methods from Greenland.

Prior to the colonisation, peat houses were used for permanent residence during winter. The peat houses had leather roofs, used for tents during summer when the Innuits moved to better hunting and fishing areas. The peat houses were repaired and reused during the following winter – possibly with new leather roofs (Greenland National Museum, 2016). The decline in the nomadic lifestyle resulted in changed user behaviour; specifically, the skins were no longer removed during summer, which had served an important function of airing the peat houses and thus reducing bugs and bacteria in the construction. The lifestyle change resulted in a poor indoor climate, which in turn led to the fatal development of tuberculosis. One-third of the population died of tuberculosis in the town of Ilulissat in 1867 (GEUS, 2023).

When colonisation began in the 1720s, single-family houses and multifamily dwellings were built as a combination of peat and stones, with windows of intestine skins to let in light. This construction type was further developed during the 19th century based on inspiration from European buildings and increased material availability. Over time, the houses were equipped with refined details like glass windows, weather porches, and stone or wooden walls insulated externally with peat. These houses were named “Danish-Greenlandic houses” (Vadstrup and Schultz-Lorentzen, 1994). This type of house was further refined; in particular, Ph. Rosendahl attempted to redesign the construction to improve self-construction, aiming to improve the poor indoor climate and reduce the adverse effects on human health (Andersen, 1976). However, the design

never gained widespread adoption due to the beginning of World War 2. At the end of the war, peat houses were replaced by timber frame constructions. At this time, the residential buildings consisted partly of self-built homes due to easier accessibility of conventional building materials, e.g., plywood, insulation, and paint (Andersen, 1976), and partly of more organised buildings controlled by the Department of Greenland (Andersen, 1976; Vadstrup and Schultz-Lorentzen, 1994).

The Norwegians introduced log houses in the 1730s, when “Bergenkompagniet” (the Bergens Company) established trade posts. The advantage of log houses was that they could be disassembled entirely and quickly rebuilt at the next trade location.

In 1950, the Greenlandic Technical Organisation (GTO) was established, and in the following years, they developed the bright-coloured wooden standard houses, which are still characteristic of Greenland today (Greenland National Museum, 2016). This period was characterized by an increasing population, causing a need for additional and better residential buildings and larger schools and institutions. The structure of society changed as production became more efficient, demanding larger factories and leading more people to the bigger towns (Vadstrup and Schultz-Lorentzen, 1994).

The urbanisation of Greenland resulted in a building shortage in multiple towns, and consequently, larger and taller buildings were constructed. For example, in 1965, “Blok P”, with 64 apartments, was built as the first building block in Nuuk, followed by blocks 1 to 10 in 1968 and “Radiofjeldet” with 600 apartments in 1972-1977 (Grydehøj, 2014; Steenholdt, 2019). Figure 2.4 shows an example of this building type, which was introduced in multiple towns. There are many political perspectives and opinions on the cultural consequences related to the building blocks (Nordatlantens Brygge, 2020), but from a construction perspective, the blocks introduced modern facilities to the area. Unfortunately, maintenance was neglected in many cases, and most of the constructions have either been declared due for demolition or been levelled to the ground. Block P was demolished in 2012, less than 50 years old (Nordatlantens Brygge, 2020).

Figure 2.4. Example of concrete block construction. Credit: Eva B. Møller.

Today, the most common building tendency is multilevel tower buildings of either timber-frame or concrete. The advantage of these buildings is a reduced need for site maturing, which is expensive due to the rocky ground. On a smaller scale, cross-laminated timber (CLT) is also implemented in the Greenlandic building stock (Møller and Lading, 2020). Many of the traditions and challenges from the past still prevail, including the culture of self-built “catalogue” houses, especially in the settlements (Statistics Greenland, 2010), and building shortage. For example, the waiting time for an apartment in Nuuk is 10-12 years (Nordisk Samarbejde, 2020). Furthermore, tuberculosis is a sustained problem, occurring 20 times more often in Greenland than in the rest of the Nordic countries (Statistics Greenland, 2022).

2.4 The ABC project and related field studies

This PhD thesis was part of the six-year research project “Arctic Building and Construction,” in daily speaking, the ABC project (Technical University of Denmark, 2022). The project was a collaboration between the Technical University of Denmark (DTU), Aalborg University (AAU), Oslo School of Architecture (AHO), and Ilisimatusarfik (the University of Greenland) (Arctic Building and Construction, 2022). The project aims to investigate and document constructions in the Arctic, with Greenland as a reference point. Five subtopics are included: (1) processes, (2) sustainability, (3) architecture and urban spaces, (4) user satisfaction, and (5) building physics and interior climate. This thesis is especially concerned with subtopic 5 but also engages with subtopics 1 and 2.

The ABC project has carried out three major field studies, namely, a test pavilion, several monitored residential buildings, and a test house. Common for all three field studies is monitoring using hygrothermal sensors, which measure the conditions indoors, in the air cavities, and on each side of the implemented wind and vapour membranes. The data collected from the pavilion and the residential houses are fundamental to the research conducted and presented in this thesis. Therefore, a short introduction to the field studies is presented below. Note that the test house field study is included for completeness. Additional information about the ABC project can be found in Arctic Building and Construction (2018) and Technical University of Denmark (2022).

2.4.1 The test pavilion

The test pavilion is a simple construction with a controlled indoor climate. It was located in Nuuk next to the test house, as shown in Figure 2.5. The purpose of the pavilion was to test five different typical Greenlandic façade and roof solutions. The data from the pavilion consisted of hourly hygrothermal measurements from the building envelope. The data from the wall constructions was investigated in this study, while data related to the roof constructions was not investigated in this study.

Figure 2.5. The test house in Nuuk (left) and the test pavilion (right).

2.4.2 Monitored residential buildings

A monitoring program collecting hygrothermal data from the façades of 14 residential buildings was made. The buildings were located in Nuuk, Sisimiut, and Sarfannguit (a settlement east of Sisimiut). The installation time was individual for each building; hence, the available amount of data varied. Some houses were excluded after sensor installation due to technical or practical circumstances. As a result, data from nine houses in Nuuk and Sisimiut were analysed in this thesis.

2.4.3 The test house

The test house, the construction to the left in Figure 2.5, had a more extensive setup, i.e., measuring temperature and relative humidity (RH) in the rooms, walls, and roofs, measuring the energy supply, and monitoring the need for ventilation and solar shading (Møller and Lading, 2021). It was built in 2020 to test multiple unconventional design solutions, including a double façade solution, where the insulation and the weather protection were separated, creating an unheated semi-indoor zone.

The test house was preliminarily evaluated by Møller and Lading (2021) and later analysed by Slyngborg (2021). The evaluation and analysis illustrated some common problems and challenges when building and developing construction practices in Greenland. The preliminary assessment by Møller and Lading (2021) thoroughly described the design and development process, including some of the design elements delaying the construction process. As this thesis focuses on current building practices and the test house is designed rather unconventionally, the data collected from this building was not assessed in this study.

2.5 Hygrothermal theory

The façade construction of a building is part of the building envelope protecting the interior from the weather. When designing façades, many parameters must be considered to obtain an optimal building design regarding material and energy consumption, sufficient daylight, adequate indoor air quality (IAQ), and a comfortable

indoor climate. At the same time, it is of high interest to construct a well-functioning wall that can endure the outdoor environment for a long time without compromising the indoor climate.

2.5.1 Indoor air quality

In existing literature, the evaluation of IAQ considers multiple parameters. Some of the most common are temperature, RH, CO_2 level, and volatile organic compounds (VOC) (Kotol *et al.*, 2014). VOC covers many organic chemicals, which can have short or long-term health consequences and are emitted from furniture, building materials, surface treatments, people, and microorganisms such as mould (Larsson *et al.*, 2021).

The four IAQ parameters depend on the installations, including heating and ventilation, but also the building envelope and the user behaviour, which can impact the installations and contribute to both heat, moisture, and particles. Users or residents of a building contribute to moisture directly through sweating and breathing and indirectly, e.g., by cooking, showering, cleaning, and drying clothes.

2.5.2 Hygrothermal conditions in wall constructions

The temperature profile through the wall depends mainly on the wall thickness, thermal conductivity of the materials, and boundary conditions (i.e., the indoor and outdoor temperature). The moisture profile through a wall depends on multiple parameters, including material properties, temperatures, internal vapour conditions, internal and external pressures, and ambient weather, including wind pressure, wind-driven rain, and solar radiation. Relative humidity is temperature-dependent, i.e., warm air can contain more vapour than cold air, and condensation occurs when the relative humidity reaches 100 %. Thus, the vapour content of the air can be constant while the RH varies with temperature. Eq. 1 presents the formula for calculating vapour content, ν (g/m^3), from air temperature, θ (°C), and relative humidity, ϕ (-) (ISO, 2012).

$$For\ \theta \geq 0\ °C,\ \ \nu = \phi \cdot \frac{610.5 \cdot e^{\frac{17.269 \cdot \theta}{237.3+\theta}}}{0.4615 \cdot (\theta + 273.15)}$$

$$For\ \theta < 0\ °C,\ \ \nu = \phi \cdot \frac{610.5 \cdot e^{\frac{21.875 \cdot \theta}{265.5+\theta}}}{0.4615 \cdot (\theta + 273.15)} \quad [\mathrm{g/m^3}] \quad \text{Eq. 1}$$

The interior moisture load, $\Delta\nu$ (g/m^3), is defined as the increase in moisture inside the building, ν_{int} (g/m^3), compared to the external climate, ν_{ext} (g/m^3). Thus, the internal moisture load can be calculated as:

$$\Delta\nu = \nu_{int} - \nu_{ext} \quad [\mathrm{g/m^3}] \quad \text{Eq. 2}$$

Five humidity classes are defined in ISO 13788:2012 (ISO, 2012) to classify the moisture loads. The humidity classes are calculated from the monthly mean outdoor temperature and either the interior moisture load, $\Delta\nu$, or the air pressure difference Δp [Pa]. The correlation is illustrated in Figure 2.6. The indoor climates of residential buildings are usually in humidity class 2 or 3, i.e., $\Delta\nu$ between 2 and 6 g/m^3.

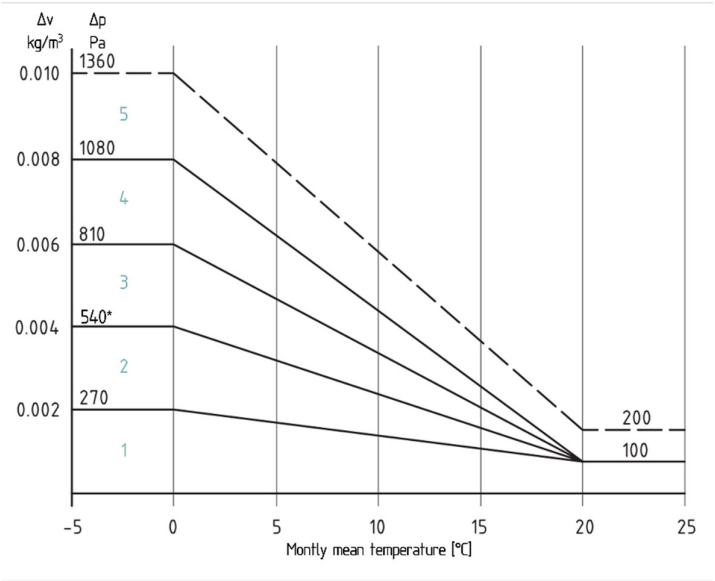

Figure 2.6. Correlation between vapour content, air pressure, and the monthly mean outdoor temperature (ISO, 2012). The number denoted by an asterisk (*) is corrected from 640 due to an error in the standard. Blue numbers are the moisture load classes.

2.5.3 Robustness and membranes

According to ISO 22111 (ISO, 2019) and SBI 258 (Statens Byggeforskningsinstitut, 2017), a building is considered robust when the sensitivity to errors in the construction parts, which are essential to the quality of the building, is minor. The robustness can be challenged by different situations and conditions, e.g., fire, water, or inexpedient human behaviour.

Robustness issues in façades can occur when the vapour content in the construction gets too high and the water condensates. Condensation can have multiple consequences, e.g., reduced effect of the thermal insulation, degradation of materials due to fungi and rot, and finally, negative impact on the IAQ due to mould growth (see Section 2.5.4). To avoid condensation in building envelopes, a vapour barrier can be implemented. The vapour barrier hinders vapour transport from the interior side of the wall (which is exposed to the moisture load) to colder parts of the wall (where condensation might occur). In Greenland, the vapour barrier is usually placed a maximum of 1/4 into the insulation from the inner side, as it must be placed somewhere warm enough to avoid condensation.

Another membrane that can reduce the risk of condensation is a wind barrier. The primary function of a wind barrier is to reduce the risk of air penetrating the construction layers in the façade. Cold air can cause condensation – even on the interior side of the vapour barrier if the exterior layers do not hinder the airflow.

Wind and vapour barriers can also reduce heat loss through surfaces and joints. In the current Greenlandic building regulation (Direktoratet for Boliger og Infrastruktur, 2006),

there are no requirements for the airtightness of the general building. However, such requirements are expected to be implemented in the new regulations introduced in Section 2.6.8. Regardless of the chosen building design, securing a certain tightness of the construction is essential to prevent heat loss and undesirable vapour transport.

2.5.4 Mould growth

Mould growth depends on nutrition in the surrounding materials, temperature, relative humidity, and time. Mould growth is not dependent on condensation. In pure wood at 10 °C, mould thrives when the relative humidity exceeds 85.4 % (Brandt *et al.*, 2023). Multiple methods exist to estimate the risk of mould growth for given conditions. The most widely used is the Viitanen model (Hukka and Viitanen, 1999), which quantifies mould growth risk on a scale from 0 to 6. The Viitanen model has been implemented in this study with the software WUFI Mould Index VTT (Fraunhofer Institute for Building Physics, 2022). A mould growth index of 2 is considered acceptable, while an index above 3 is considered critical. For a mould index between 2 and 3, additional assessments must be made to assess the risk. When using the WUFI software, it is essential to be aware that it only uses the time frame of the data implemented. For field studies, data are usually collected for a relatively short period. Therefore, it is advisable to run the model using repeated datasets to investigate potential long-term effects.

2.6 State-of-the-art

The purpose of this section is to introduce the reader to the current state-of-the-art background, methods, and results related to hygrothermal assessments and buildings in a Greenlandic context. Only themes, results, and conclusions that are relevant to the method or discussion are included.

2.6.1 Indoor air quality in Greenlandic buildings

The indoor air quality of Greenlandic residential buildings is a topic that has been thoroughly investigated and documented. The indoor climate, including CO_2 levels, humidity, and temperature, can significantly impact well-being and health (Kotol *et al.*, 2014). Generally, it is estimated that humans spend 90 % of their time indoors (Klepeis *et al.*, 2001), of which it is estimated that Danes spend approximately 13-16 hours at home (Patursson and Sode, 2020). This emphasizes the importance of creating well-balanced interior environments – especially during winter when the days are short.

2.6.1.1 Field studies

Multiple field studies have been conducted in Greenland to determine the indoor air quality in residential buildings. For example, Kotol *et al.* (2014) monitored the IAQ in the bedrooms of 79 dwellings for seven days in June 2011 and January to February 2012 in Sisimiut. The collected data included temperature, RH, and CO_2 concentration. The study used absolute humidity and CO_2 concentration as indicators of insufficient ventilation. For CO_2 concentration, the accepted content was 1000 ppm, and the difference in absolute humidity in the living room compared to the outside was acceptable (below 2.5 g/kg). Based on these parameters, 73 % of the bedrooms were determined to be insufficiently ventilated, with dwellings built after 1990 more likely to underperform due to increased airtightness of the building envelopes. The study described how a high moisture load (the difference of absolute humidity above 2.5 g_{water}/kg_{air}) is not reflected

by RH, which had a mean of 26 %. Overheating was also an issue, as 19 % of all measured bedroom temperatures were above 26 °C during summer (Kotol *et al.*, 2014).

A smaller study of 20 dwellings was conducted almost ten years later, in March 2021 (Andersen, 2021). The study investigated both bedrooms and bathrooms using the same parameters as Kotol *et al.* (2014). The bedroom results showed that it is easier to maintain a decent temperature range than CO_2 concentration during night-time. The measured RH was generally low, i.e., within 20 to 30 %. In comparison, the recommended RH level is 25-60 % for optimal comfort, whereas 1/3 of the monitored bedrooms had a lower RH (Andersen, 2021).

Both field studies (Kotol *et al.*, 2014; Andersen, 2021) were accompanied by questionaries (Kotol, 2012). Of the 20 households questioned in 2021, 2/3 reported experiencing discomfort, including draft, cold floors, or generally low room temperatures during winter (Andersen, 2021). There were no neutral reports about the overall perceived indoor environment. Additionally, the residents were asked to consider their satisfaction with temperature, air quality, acoustics, daylight, and overall perception. The distribution of answers was similar for both surveys (Kotol *et al.*, 2014; Andersen, 2021). Only a few residents reported mould or condensation, though only “sometimes” or “almost never” (Andersen, 2021).

Despite the low humidity levels, mould is a common issue experienced in residential buildings in Greenland. A report from 2020 performed by the Danish Institute of Human Rights (Institut for Menneskerettigheder, 2020) stated that in Greenland, 151 residential dwellings were renovated due to mould from 2015 to 2019 as part of a project called “Smiling Houses.” The report also stated that 300 dwellings owned by the Greenlandic home-government were empty due to mould in 2015. Additionally, 399 dwellings were abandoned due to extreme wear and tear. Similar problems have also been reported for multiple public buildings, including primary public schools (Naalakkersuisut, 2012) and other institutions, e.g., the shelter in Sisimiut and the family centre in Maniitsoq.

2.6.1.2 User behaviour in Greenland

When the functionality of a building does not fulfil the users' needs and the IAQ is insufficient, it is almost certain that the users will intervene. User intervention includes opening or closing windows and adjusting the settings, e.g., temperature or ventilation. In typical ventilation systems without heat recovery, the outdoor air is flowing in through inlets. If the system is incorrectly designed, it can cause draught or low room temperatures. Many residents would attempt to fix this problem either by blocking the airflow from the inlet with textiles and tape, as shown in Figure 2.7, or by turning up the heat and thus increasing heat losses and energy consumption. Lack of ventilation increases the relative humidity and the risk of mould growth, as described in Section 2.5.4. Insufficient ventilation can also result in high levels of increased VOC and CO_2 concentration, which can have health consequences.

Figure 2.7. Blocked ventilation inlet in Greenland. Credit: Eva B. Møller.

User behaviour was also investigated in the previously mentioned surveys from 2012 and 2021 (Kotol, 2012; Andersen, 2021). The results revealed that appliances for improving the IAQ were unavailable in many dwellings. Of the respondents, 18 % reported not having a kitchen hood, and 37 % did not have an exhaust in the bathroom (Kotol, 2012). Additionally, some of those with such installations did not always use them.

2.6.2 Hygrothermal simulations

When evaluating measured data, it is common practice to produce a theoretical framework of reference to identify the consistency between practice and theory. The framework can either be calculations or simulations. The latter is most common as it is associated with higher accuracy. Examples include Wang et al. (2020) evaluating moisture-safe attic designs in Quebec with WUFI (Fraunhofer Institute for Building Physics, 2022) and Kukk et al. (2022) using Delphin (Baumklimatik-Dresden, 2022) to evaluate how the initial moisture content in CLT impacts the risk of mould growth.

In other cases, simulations are used as a theoretical tool only, as the results are not compared to measurement data. For example, Ghazaryan and Tariku (2021) investigated the hygrothermal performance of natural cork insulation in combination with other materials in seven walls using WUFI. Such assessments can be used prior to field studies to evaluate relevant combinations to construct and monitor. There are also many examples of studies using hygrothermal simulations to test the accuracy of developed models. For example, Månhardt et al. (2021) used WUFI to test a model for simulating the airflow and moisture safety in ventilated cathedral roofs.

Common for these cases is that either Delphin (Baumklimatik-Dresden, 2022) or WUFI (Fraunhofer IBP, 2018) are used to produce the simulations. Both software programs can simulate the coupled transport process of Heat, Air, and Moisture (HAM) and can consider one or multiple dimensions. Studies reveal that results from the two software programs are very similar and consistent, although minor discrepancies can occur (Hejazi *et al.*, 2019; Defo, Lacasse and Laouadi, 2022). Regardless of the purpose of the simulations or the software applied, the simulations require weather data for a minimum of one year. Optimally, the data are measured for the investigated period, but Test Reference Years (TRY) can also be applied.

2.6.3 Evaluation methods

When comparing measured experimental data with modelled data (theoretical framework), it is important to consider how the information is evaluated. Often, the most intuitive way is to compare the data visually, but the results can be complicated to interpret. Fortunately, many statistical indicators have been developed for quantifying the performance of a model, all with certain advantages and limitations. The choice of statistical indicators depends on the purpose of the comparison and the investigated parameters. The statistical indicators can also be used for model calibration. Lower errors indicate a model that better fits the measurements.

For studies like this thesis, there are multiple statistical indicators which are commonly used. Among others, these include Root Mean Square Error (RMSE) (Månhardt *et al.*, 2021; Kukk *et al.*, 2022), Coefficient Variation of Root Mean Square Error, CV(RMSE), and Mean Bias Error (MBE) (Huerto-Cardenas *et al.*, 2020; Abdul Hamid, Arfvidsson and Harderup, 2022).

2.6.4 Energy production and climate conditions

Most of Greenland's water and energy supply is facilitated by an independent government-owned utility company, Nukissiorfiit. According to Nukissiorfiit's annual report from 2021 (Nukissiorfiit, 2022), the utility provides services to 20,000 consumers. Of the energy generated by Nukissiorfiit, 66 % is from renewable sources, i.e., hydro, solar, and wind power. Of these sources, hydropower is the most dominant, with an installed capacity of 91 MW (Nukissiorfiit, 2022). The five Greenlandic hydropower plants are located in Ilulissat, Sisimiut, Nuuk, Qaqortoq, and Tasiilaq. In 2021, it was decided to build new hydropower plants in Qasigiannguit and Aasiaat. There are also several waste incineration plants that generate heat and electricity, which, from 2023 and 2024, respectively, will be centralised in Nuuk and Sisimiut. Currently, waste incineration supplies 6 % of the energy demand (Nukissiorfiit, 2022). Finally, 28 % of the energy supply by Nukissiorfiit was generated from fossil fuels.

Figure 2.8. Example of local production of solar energy in Tasiilaq. Photo credit: Eva B. Møller 2022.

Due to the large distances, Nukissiorfiit cannot reach all residents in Greenland, and therefore, many households need to be self-supplying with energy. Energy consumption, not facilitated by Nukissiorfiit, usually includes oil as a heating source. However, Figure 2.8 shows an example of private production of renewable energy. According to current statistics, 82.5 % of the total energy consumption, including the energy provided by Nukissiorfiit, is supplied by fossil fuels (Statistics Greenland, 2021).

Within Greenland, the energy mix varies greatly, resulting in different emission factors, E_{factor}. The E_{factor} quantifies the emitted $CO_{2\text{-eq}}$ in kg when producing 1 kWh. The energy mix is presented for selected Greenlandic towns and settlements in Table 2.1. The table also contains information on the local heating demand quantified by heating degree days (HDD) obtained from Statistics Greenland (Grønlands Statistik, 2021). HDD represents the sum of the daily difference between an indoor temperature of 19 °C and the average outdoor temperature. Copenhagen is included for reference; however, the HDD is only considered for the heating period from October to May (Guldborgsund Forsyning, 2021).

Table 2.1. Heating degree days (HDD) (Grønlands Statistik, 2021) and emission factor (E_{factor}) for 2020 and 2021 (Nukissiorfiit, 2020, 2022) for selected locations. Locations are ordered according to ascending latitude. Unavailable data is represented by a dash (-).

Location	**HDD [K/a]**	$\mathbf{E_{factor}\ 2020}$ **[kg$CO_{2\text{-eq}}$/kWh]**	$\mathbf{E_{factor}\ 2021}$ **[kg$CO_{2\text{-eq}}$/kWh]**
Reference			
Copenhagen	2500	0.050	0.035
West coast			
Qaqortoq	6210	0.218	0.176
Paamiut	6740	0.190	0.184
Nuuk	7080	0.009	0.015
Maniitsoq	6820	0.176	0.164
Kangerlussuaq	8420	-	-
Sisimiut	7570	0.161	0.110
Aasiaat	7970	0.207	0.231
Qasigiannguit	7740	0.136	0.146
Ilulissat	7890	-	0.004
Uummannaq	7908	0.002	-
Upernavik	8990	-	-
Qaanaaq	9580	0.107	0.222
East coast			
Tasiilaq	6820	-	-
Ittoqqortoormiit	8830	-	-

Even though the $E_{factors}$ given in Table 2.1 are provided by the supplier in 2020, they must be considered with a degree of uncertainty, e.g., the E_{factor} for Nuuk (9 g$CO_{2\text{-eq}}$/kWh) and Uummannaq (2 g$CO_{2\text{-eq}}$/kWh) are very low. Both locations have access to renewable energy, i.e., hydropower and solar power, but they also depend on oil for heat production. 1 litre of oil produces approximately 10 kWh of energy and emits 335 g$CO_{2\text{-eq}}$/kWh (SimaPro, 2022). Furthermore, the IPCC states that the greenhouse gas (GHG)

emissions related to hydropower are usually estimated to be 4-14 $gCO_{2\text{-}eq}$/kWh (Kumar *et al.*, 2018). Nuuk includes 0.003 litre of oil per kWh, which produces 0.03 kWh of heat. Considering only the emissions related to the oil, the E_{factor} in Nuuk is 10 $gCO_{2\text{-}eq}$/kWh. In Uummannaq, heat production consumes 0.001 litre of oil, equal to 3.35 $gCO_{2\text{-}eq}$/kWh. This is more than the total emissions stated (Nukissiorfiit, 2020). The emission factors were updated in the recent year report from Nukissiorfiit. The $E_{factors}$ for Copenhagen are obtained from HOFOR (2022).

According to the National Oceanic and Atmospheric Administration (NOAA), climate change will decrease HDD globally, especially in the Arctic region (Lindsey and Dahlman, 2021). IPCC has defined multiple Representative Concentration Pathways (RCP) to evaluate possible future climate conditions. RCP8.5 is considered the worst-case scenario, while RCP2.6 is the least critical prediction (Schwalm, Glendon and Duffy, 2020).

2.6.5 Construction types

Currently, there are three common wall construction types used in new buildings in Greenland: structural elements of concrete, cross-laminated timber (CLT), and half-timber of wood or steel. Regardless of the construction type, the façades are equipped with a ventilated air cavity and finished with a cladding material, typically wood, thermowood, or fibre cement boards.

As described in Section 2.3, constructions were historically built as single-family houses, whereas buildings today are generally taller, facilitating more residential units on less space. Taller buildings have two main advantages. First, they require less space, which can be a limited resource due to restrictions caused by mountains, bodies of water, and other topological obstacles. Second, multi-story buildings reduce the per-unit expense for site development, which is expensive when building in the Arctic (Sermitsiaq AG, 2010; Statistics Greenland, 2017). One reason for this is that Greenland's subsurface geology consists mainly of rocks, which must be blasted away to make space for sewage and water distribution pipes.

2.6.6 Air change rate in ventilated air cavities

As described in Section 2.6.5, typical Greenlandic façade structures usually have a ventilated air cavity on the inner side of the external cladding. Therefore, the air change rate or air changes per hour (ACH) in the air cavity is relevant when investigating these structures. However, quantifying airflow is challenging and, thus, a hot topic in many studies – especially where the intention is to make hygrothermal simulations of structures.

According to a comprehensive study by Rahiminejad and Khovalyg (2021), airflow depends on many factors, including wind speed, solar radiation, air temperature, and material properties of the air cavity surfaces. Other driving mechanisms include the stack effect and wind effect (Rahiminejad and Khovalyg, 2021). Furthermore, a recent literature study found that the ACH in ventilated air gaps can vary from 0 to 650 h^{-1} for a 19 mm air gap and up to 1000 h^{-1} in a 40 mm air gap (Brozovsky, Nocente and Rüther, 2023).

Lastly, there are multiple experimental and theoretical ways of estimating the air change rate, though all methods are inherently associated with significant uncertainties. Therefore, the ACH is often considered constant in numerical studies, such as (Kukk *et al.*, 2022; Brozovsky, Nocente and Rüther, 2023), both of which used 150 h^{-1} in their hygrothermal simulation models.

2.6.7 Concrete in the construction sector

Concrete is widely used, as most of the required raw materials are available locally, which saves money and reduces delivery time. Originally, concrete was in-situ casted, i.e., locally at the building site. However, the establishment of three new concrete element factories in Nuuk, Sisimiut, and Ilulissat has made prefabricated elements desirable (Sermitsiaq, 2020).

According to Jeppe Mortensen from BJ Enterprise, there are several advantages to building with prefabricated elements. Some advantages include the possibility of using local unskilled labour, utilising the winter period for casting the concrete elements, and finally, closing the building envelope quickly, protecting the building interior from harsh and unpredictable weather conditions (Sermitsiaq, 2020).

Furthermore, building with prefabricated elements makes it easier to fulfil the requirements of tolerances, as they are produced under controlled conditions. Unfortunately, using such concrete elements requires high demands for infrastructure and cranes and is thus not profitable in smaller towns and settlements (Departementet for Boliger og Infrastruktur, 2019b).

2.6.8 Regulations

The present official building regulation in Greenland is the building regulation from 2006, BR06 (Direktoratet for Boliger og Infrastruktur, 2006). In BR06, the allowed energy consumption for different construction types is divided into two zones defined by the Artic Circle: a northern and a southern. There are additional requirements specified in circulars, specifications, and instructions (BygInfo, 2019), but only a few of these consider the climatic differences across the country. However, some requirements do consider climatic differences, e.g. when calculating heat losses; the outdoor design temperature is based on latitude, spanning from -20° in south Greenland to -40 °C in the northern part of Greenland (Bygge og Anlægsstyrelsen, 1995; Kragh and Svendsen, 2004). The building regulation is currently under revision, and a preliminary proposal has already been published (Naalakkersuisut - Government of Greenland, 2021).

2.6.9 Sustainability and DGNB certification

The German sustainability certification system, DGNB - “Deutsche Gesellschaft für Nachhaltiges Bauen,” has attracted considerable interest from the construction industry. Therefore, adjusting the requirements for a Greenlandic setting has been initiated to motivate building owners, engineers, and contractors to aim higher regarding building performance. This development may increase the sustainability profile of the Greenlandic construction industry environmentally, socially, and economically.

When discussing sustainability in the Greenlandic building sector, there are two fundamental perspectives to consider. The most obvious is environmental awareness in terms of emissions and climate impacts, which is currently a hot topic in practically all contexts. However, sustainable and robust development of the building stock must also be considered to ensure long service lives of new buildings. The latter is addressed in multiple plans, interviews, and agendas. The economy and administration are often mentioned in this context. Naalakkersuisut, the Greenlandic self-government, describes their awareness and ambitions of building with a focus on buildability, robustness, and environmental sustainability (Departementet for Boliger og Infrastruktur, 2019a). Already in 2002, the effectivization of the Greenlandic construction industry was evaluated (IAPP's committee, 2002). Here, the perspective of good building practice was considered a part of sustainability. It is described as a wish for pilot projects to test new ideas and demonstrate robustness and quality. This is followed by a need for a web-based knowledge centre where generated knowledge can be shared and used in practice (IAPP's committee, 2002).

Only a few Greenlandic studies have considered environmental sustainability in terms of life cycle assessments (LCA). Although from a broader context, many studies are relevant, e.g., studies concerning reduction of heat losses, energy consumption, and waste or optimisation of installations.

A comparative study by Ryberg *et al.* (2021) investigated the environmental impacts of the three typical construction types presented in Section 2.6.5, i.e., CLT, concrete, and half-timber. A fourth scenario was also included, representing the renovation of concrete buildings, e.g., by implementing more insulation than originally to reduce heat losses. The study concluded that renovation had the lowest environmental impact and, thus, was the best solution in terms of sustainability. There was no unanimous answer when considering new constructions, although the wooden structures (i.e., CLT and half-timber) outperformed new concrete structures (Ryberg *et al.*, 2021). Another lesson learned from this study was the low impact contribution from infrastructure, construction, end-of-life, and transportation, which accounted for less than 15 % on average across all impact categories. The exception was the CLT case, for which transportation accounted for 13 %. All in all, transportation was found to have less significance to the results than could be expected from the remote geographic locations (Ryberg *et al.*, 2021).

Another study by Ryberg *et al.* (2022) investigated a construction with significant errors and aimed to identify whether it was better, in a sustainability context, to correct the error or not. It was stated that this study could not be generalized but only used to gain insight into construction errors' environmental consequences. The study included a baseline scenario, being the original building without errors. Three additional scenarios were defined: 1) No correction of errors, 2) implementing a new element to reduce the consequences of the error, and 3) redoing the elements of the errors. Although the study concluded that the errors significantly impacted the performance of the façade, correcting the errors was also found to have a considerable impact. Thus, it should be evaluated for the individual case whether the overall emissions would be greater by correcting the error than leaving it as is. Of the two correction scenarios, the second scenario was the

best, as it resulted in less material waste and performed better than Scenario 3 on all impact categories. The main takeaway from the study is the importance of avoiding errors by designing specifically for Arctic conditions, especially concerning moisture and wind, and controlling the building process to ensure high quality (Ryberg *et al.*, 2022).

2.6.10 Previous field studies

In 2005, a Low Energy House in Sisimiut was constructed to test the possibilities of building more sustainable and passive houses in the Arctic. The definition of a low-energy house is discussed widely (Karlsson and Moshfegh, 2013). In this context, it was defined as a house that consumes half of the energy allowed in the building regulation (Svendsen and Kragh, 2004). Despite the allowed 230 kWh/m^2/year given in the building regulation for the northern part of Greenland (Direktoratet for Boliger og Infrastruktur, 2006), the aim was to produce a house consuming only 80 kWh/m^2/year. The reason was an expected energy reduction of 70 kWh/m^2/year due to the implementation of a ventilation system with heat recovery. The house was constructed in collaboration between the Technical University of Denmark (DTU) and Arctic DTU with local contractors and consulting engineers (Ottosen, 2006).

Figure 2.9. Photos of the Low Energy House in Sisimiut (March 2021).

In 2004, a simulation study showed that the energy goal of the Low Energy House was achievable (Svendsen and Kragh, 2004). However, when assessed in 2010, the building had a much higher energy consumption than anticipated (up to 150 kWh/m^2/year). The main reasons were inadequately constructed joints causing air leaks and an inefficient heat exchanger with a high energy consumption due to frost accumulation in the system (Vladykova *et al.*, 2012). After improving the building by repairing the heat exchanger and improving the air tightness, the targeted energy consumption was almost achieved with a consumption of only 90 kWh/m^2/year (Vladykova *et al.*, 2012). Studies of the Low Energy House in Sisimiut concluded that commissioning must be a central part of constructing passive houses in the Arctic. As a minimum, commissioning should include both blower door tests and measurements during the first year of use.

Another case study investigated a typical wooden construction with non-traditional elements, i.e., extra insulation in building envelopes resulting in low U-values, triple-glazed windows, and a mechanical ventilation system with a rotary heat exchanger (Luc, Kotol and Lading, 2016). The energy consumption and IAQ in the investigated house

were monitored for one year and compared to building simulations conducted in IDA ICE (EQUA, 2018). Measurements were compared to an alternative traditional Greenlandic building without heat recovery. The study concluded that the increased insulation layers and the heat exchanger could decrease space heating requirements by 45 %. When interviewing the residents, there were no reports of issues with dry air, moisture/condensation, draught, or cold surfaces. The only reported problem was overheating during sunny days – even for cold periods with outdoor temperatures of -15 °C.

3 Hypothesis and research questions

As described in Chapter 2, there are many challenges related to the construction industry in Greenland. For example, the importance of air tightness was identified through previous field studies such as the Low Energy House presented in Section 2.6.10. Along with the moisture theory and the tendencies of mould growth, the membranes are in focus during this thesis. The impact of the membranes was investigated in relation to the design and building process because of the findings in the preliminary assessment of the Test House in Nuuk presented in Section 2.4.3 and the inadequate performance of the Low Energy House.

As island operation is an inevitable premise for constructing in Greenland, it was essential to identify the importance of the location within the island. The research questions are formulated to aid the investigation of the hypotheses.

Hypothesis 1: Mould problems in Greenlandic wall constructions are caused by faulty design.
Research questions:

1.1 Are wind barriers essential?
1.2 Are vapour barriers essential?
1.3 How important is buildability?

Hypothesis 2: Optimal wall construction designs depend on the location in Greenland.
Research questions:

2.1 Does the climate decisively affect façade performance?
2.2 Is the difference between towns and settlements impactful?
2.3 How does location influence sustainability?

The hypotheses and research questions focus on three key concepts, i.e., suitability, buildability, and sustainability, defined below with examples.

In this study, "*suitability*" defines if a building is robust to the conditions it is exposed to. A building is considered suitable if it can perform satisfactorily under the given conditions. There are multiple parameters which indicate how satisfactory a building is performing. These parameters include the risk of mould, thermal comfort, including draught and surface temperatures, energy consumption, heat loss, and durability. This study does not consider the whole building but only the outer walls. Consequently, some of the indicators for suitability cannot be properly assessed. Instead, based on the mould growth model of Viitanen (Hukka and Viitanen, 1999), the risk of mould growth will be used to evaluate the design. The agreement between measurements and simulations and the risk of mould growth have been used as criteria to assess the actual performance of the walls. Major deviances from simulations are thus assessed further. In cases where the measured performance of the façade is significantly worse than the modelled performance, the deviances are interpreted as being due to faulty execution of the construction that negatively affects the suitability of the solution.

The "*buildability*" of a construction describes the level of complexity or difficulty of a specific design. A higher level of buildability corresponds to greater chances of a building being well-executed. Buildability is mainly ensured during the design phase and requires thorough consideration of detailed aspects, focusing on realistic solutions. Evaluation of given tolerances and the likelihood that these can be fulfilled is also essential to buildability. Furthermore, the need for special competencies or design solutions can challenge buildability. In this study, buildability has mainly been evaluated by comparing the hygrothermal performance of walls of existing buildings with similar walls in a meticulously constructed test facility. Major deviances are considered a symptom of low buildability.

"*Sustainability*" is a commonly used term that traditionally expresses considerations regarding reduced impact on the environment, economy, and people. In this thesis, the measure of sustainability is primarily based on theoretical calculations of total emissions of CO_2, as this indicator is known to increase global warming, which has a significant impact on the ecosystem. The social end economic sustainability is not considered.

3.1 Thesis outline

This thesis is based on four appended journal articles, a conference paper, and a calculation tool called Insulation Thickness Optimiser (ITO). The papers are denoted using Roman numerals, ranging from I-V. This thesis summarises the findings and provides the answers to the hypotheses and research questions based on an overall evaluation. Table 3.1 identifies how each paper (I-V) relates to the hypotheses and research questions.

Table 3.1. Contributions of research papers to research questions (RQ).

Papers	Hypothesis 1			Hypothesis 2		
	RQ 1.1	RQ 1.2	RQ 1.3	RQ 2.1	RQ 2.2	RQ 2.3
I	x		x	x		
II				x	x	x
III				x		x
IV	x	x		x		
V	x	x		x		

3.2 Scope

The methods of **Papers II-III** are theoretical and do not include any experiments. The research presented in **Paper I** and **Papers IV-V** is based on information from the presented wall constructions and hygrothermal measurements of these walls. In a few cases, it was possible to include photographic documentation to supplement the investigation of potential reasons for the significant deviances between thermal simulations and measurements.

4 Methodology

This chapter presents the main methods applied in this thesis. The chapter only includes information from the appended **Papers I-V,** which is relevant to the discussion (Chapter 6) and conclusions regarding the hypotheses and research questions (Chapter 7). The intention is to provide a resumé of the work presented in the appended papers. Thus, additional details and information can be found there. Figure 4.1 elaborates on the relationship between the content of the individual appended papers. As illustrated in Figure 4.1, there are two overall fundamental approaches: experimental field studies (red boxes) and theoretical investigations (green boxes). The theoretical study focuses on optimal insulation thicknesses, and the methods related to this will be explained in Section 4.1. The methods used in the two field studies described in Section 2.4.1 are explained together in Section 4.2, as they are almost identical.

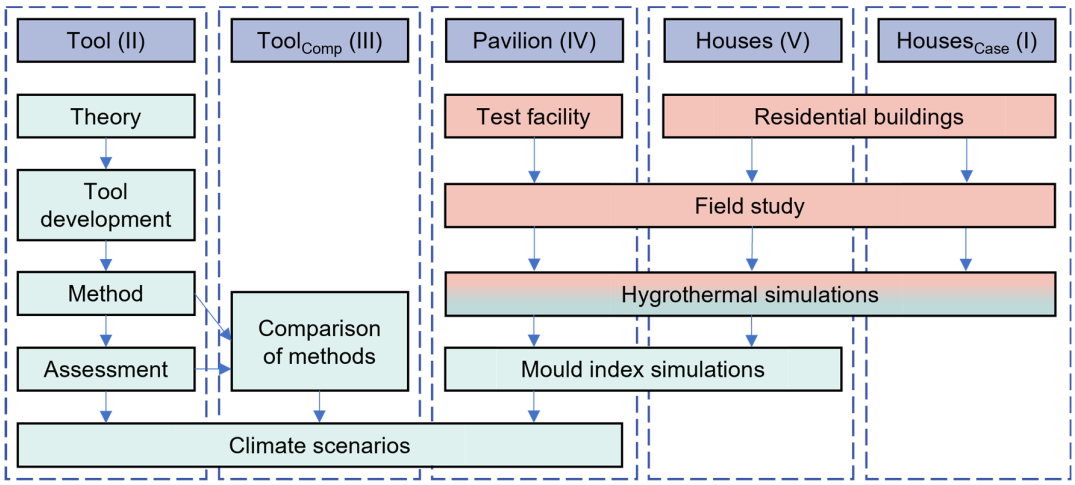

Figure 4.1. Relationship between research papers, denoted by Roman numerals, and research methods. The green colour indicates theoretical work, while the red colour indicates experimental endeavours. The box with both colours indicates that the research method relies on both theoretical and experimental work.

4.1 Optimal insulation thickness

The insulation thickness affects both the heat loss through a building envelope and the environmental impact of the insulation material. Simultaneously, the energy savings per added centimetre of insulation is reduced with increasing insulation thickness. Therefore, there is an optimal insulation thickness (d_{opt}) where additional insulation is no longer efficient in minimising greenhouse gas emissions. The flow chart in Figure 4.2 illustrates the evaluation process. This section is based on **Paper II** (Friis, Gaarder and Møller, 2022) and **Paper III** (Gaarder *et al.*, 2023).

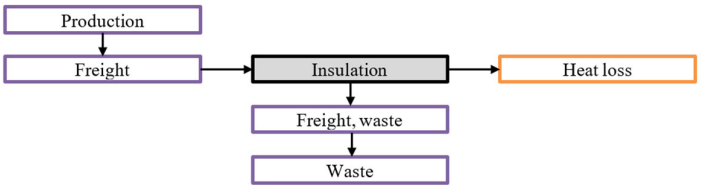

Figure 4.2. Simple flow chart for insulation material in a façade (Friis, Gaarder and Møller, 2022).

4.1.1 Purpose of the ITO tool

Due to the tradition of people building their own houses based on standard houses from catalogues, only few parameters are generally considered, e.g., building style, size, and materials. Therefore, the goal was to create a tool to identify the optimal insulation thickness to easily quantify sustainable considerations, regardless of the user's background and prior knowledge. However, sustainability perspectives are complex to disseminate to building owners with no construction background. Thus, easy access and user-friendliness were central. During the development process, it became clear that for people with some construction insight, the tool could be further refined, and additional parameters could be considered.

The tool was developed in Excel for easy access and was named Insulation Thickness Optimiser (ITO) (Friis, 2022). The initial success criterion was to obtain the minimum amount of emitted greenhouse gasses for a specific setup. The tool does not consider other parameters related to façade constructions, e.g., thermal comfort, daylight, safety, risk of mould growth, and regulations.

4.1.2 Development of the ITO tool

The development of the ITO tool was based on theoretical approaches and values from available databases. The underlying calculations depend on the location, material choices, and, if available, the building design. Table 4.1 presents the parameters contributing to these topics. Users with more background knowledge and detailed information about the materials and building design can redefine the default values to better fit the project.

Table 4.1. Parameters related to location, material choice, and building when calculating the optimal insulation thickness in ITO. An asterisk (*) indicates that the information is used to calculate additional results; however, the tool functions without this information.

Materials	Location	Building type
Transportation (due to ρ)	Transportation	Estimated service life
Environmental impacts	Energy mix	Additional material layers*
Thermal conductivity (λ)	Climate	Slab material*
Production location	Future Energy mix*	

The flow chart displayed in Figure 4.2 does not account for the parameters with asterisks (*) in Table 4.1., as these are extra considerations and demand additional knowledge about the building.

Initially, ITO includes information on eight different insulation products and ten different locations (Copenhagen and nine Greenlandic towns). The major limitation of which locations the software can include is related to available data and documentation regarding climate and energy production. However, once the necessary information has been obtained, adding new locations and materials to ITO is easy.

4.1.2.1 Materials

The environmental impact of the insulation material contributes to the calculation of d_{opt}. Figure 4.3 presents the phases of the building, which are included and excluded in terms of consideration of the insulation. In the figure, the hatched areas correspond to the excluded stages, assuming equal performance regardless of the insulation material and location.

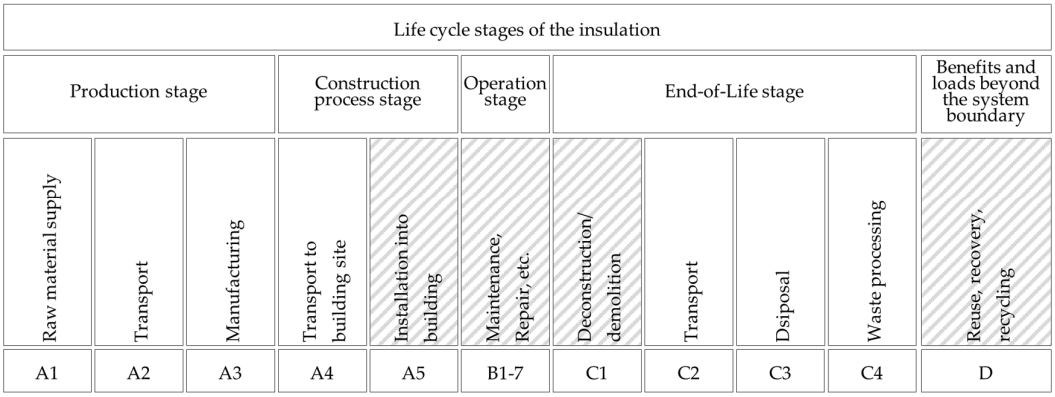

Figure 4.3. Life cycle stages of the insulation (One Click LCA, 2021). The stages shown by the hatched boxes are not considered in the ITO tool.

The emissions related to the insulation materials' life cycle are calculated in Eq. 3 and Eq. 4, where E_{A1-3}, E_{C3}, and E_{C4} refer to the life cycle stages of the insulation materials presented in Figure 4.3. $W_{material}$ (%) is an estimated amount of discarded material before end-of-life (5 % per default).

$$E_{production} = E_{A1-3} \cdot (1 + W_{material}) \quad [kgCO_{2\text{-}eq}/m^3] \quad \text{Eq. 3}$$

$$E_{waste} = (1 + W_{material}) \cdot (E_{C3} + E_{C4}) \quad [kgCO_{2\text{-}eq}/m^3] \quad \text{Eq. 4}$$

4.1.2.2 Transportation

The emissions from the transportation of 1 m^3 insulation, $E_{freight}$, depend on building location, location of material production, and the material density, ρ (kg/m^3). The emissions from transport depend on the method, including boat, truck and plane, based on the infrastructure patterns in 2022 (Friis, Gaarder and Møller, 2022). Initially, transport by plane is not used for any materials or locations, but it can be chosen if desired. The transportation emission data is extracted from the Ecoinvent 3 database (Ecoinvent, 2022). The ReCiPe 2016 Midpoint (H) impact assessment method is applied (Huijbregts *et al.*, 2017). Emissions due to transportation occur twice during the life cycle of the

materials: during transport from the factory to the building site (stage A4 in Figure 4.3) and from the building to the waste handling facility (stage C2). It is assumed that half of the produced waste, $W_{material}$, is transported to the building site, while the other half is assumed discarded at the factory. The distances, D, are estimated based on route plans (for trucks) and measuring tools (for boats) in Google Maps (Google, 2022). The calculation of the emissions related to freight, $E_{freight}$, is presented in Eq. 5, and must be calculated for A4 and C2, respectively.

$$E_{freight} = \frac{\rho}{1000} \cdot \left(1 + \frac{W_{material}}{2}\right) \cdot \left(E_{boat} \cdot D_{boat} + E_{truck} \cdot D_{truck} + E_{plane} \cdot D_{plane}\right) \quad [\mathrm{kgCO_{2\text{-}eq}/m^3}] \quad \text{Eq. 5}$$

4.1.2.3 Heat loss and climate change

The emissions related to heat losses, E_{heat}, is defined as the product of the heat loss through the walls caused by transmission, Q $[W]$, and the emission factor of the heating source, E_{factor} (see in Section 2.6.4). Q depends on the estimated service life (ESL) of the building and material, HDD, and thermal conductivity, λ (W/(m·K)). The equation also accounts for the heat loss from distribution, W_{dist}, defined as a percentage of the consumed heat. The standard waste factor, W_{dist}, in ITO is 5 %. The equation for calculating heat loss, E_{heat}, is presented in Eq. 6. Examples of $E_{factors}$ and HDD for multiple locations can be found in Table 2.1.

$$E_{heat} = Q \cdot E_{factor} = \frac{1}{d/\lambda} \cdot ESL \cdot HDD \cdot (1 + W_{dist}) \cdot \frac{24}{1000} \cdot E_{factor} \quad [\mathrm{kgCO_{2\text{-}eq}/m^2}] \quad \text{Eq. 6}$$

Furthermore, the tool is designed to make different climate scenarios easily available. ITO always presents the results of a constant climate and three evolving climate scenarios, which are named “Conservative”, “Moderate”, and “Extreme”. The evolving climate scenarios can be adjusted as a temperature change per 10 years, in °C/10 years. Initially, the temperature changes are defined as 0.2 °C/10 years, 0.4 °C/10 years, and 2.7 °C/10 years, respectively.

HDD is used to estimate the heat loss while keeping the calculations simple. The uncertainty related to this simplified method, compared to, e.g., thermal simulations, is considered insignificant due to the relatively high uncertainties in other parameters.

4.1.2.4 Success criterion

The total emissions related to the material, $E_{material}$, is the sum of the emissions from production (A1-3), product transport from the factory to the building site (A4), waste transport from the building site to where the waste is handled at the end-of-life (EoL) (C2), and finally, the waste handling at EoL (C3 and C4). Eq. 7 describes the equation for total emissions.

$$E_{material} = E_{production} + E_{freight} + E_{waste} + E_{freight,waste} \quad [\mathrm{kgCO_{2\text{-}eq}/m^3}] \quad \text{Eq. 7}$$

The optimal insulation thickness, d_{opt}, is the thickness with the minimum sum of emitted $CO_{2\text{-}eq}$. E_{opt} is the sum of emitted $CO_{2\text{-}eq}$ at the optimal insulation thickness. The

equations for E_{opt} and d_{opt} are given in Eq. 8 and Eq. 9, respectively. Both are performed for every centimetre, starting from 5 cm and ending with 195 cm.

$$E_{opt} = \min_{d \in [0.05, 1.95]} E_{material}(d) + E_{heat}(d) \quad [\mathrm{kgCO_{2\text{-}eq}/m^2}] \quad \text{Eq. 8}$$

$$d_{opt} = \operatorname{argmin}_{d \in [0.05, 1.95]} E_{material}(d) + E_{heat}(d) \quad [\mathrm{m}] \quad \text{Eq. 9}$$

4.1.2.5 Alternative success criteria and additional calculations

The significance of the success criterion was investigated by introducing two alternative and less strict criteria, which are defined as follows:

1) Accepting additional GHG emissions, e.g., 10 % more than for d_{opt}
2) Redefining the optimal angle of the slope curve, α, which is 0° for the initial definition of d_{opt}

Initially, the tool did not account for the consequences caused by significant amounts of insulation. For example, too much insulation can have consequences such as reduced sunlight (and thus reduced heat gain) and impose requirements for larger horizontal construction layers due to thicker walls (e.g., foundation, slabs, and roof). Therefore, the tool was expanded to account for some of these parameters to investigate their impact. The added parameters were:

a. The two alternative success criteria defined as 1) and 2) above
b. The insulating properties of additional wall layers ($\mathrm{Scen_{wall}}$)
c. Environmental contributions from an increased area of horizontal elements due to the wall thickness (simplified to slabs only)

4.1.2.6 Overview of inputs

Table 4.2 presents the information that is necessary to include when using ITO. The first rows are for the basic use, while the following table sections are for expanded use of the tool. The Table is first presented in **Paper II**.

Table 4.2. Introduction to the necessary inputs for Scenins as well as the mandatory information for Scenwall and Scenslab. The * marks an additional option called “User-defined”.

	Parameter	Type	Range	Unit	Note
Insulation only	Town	Dropdown menu	10 options*	-	
	Heat loss by distribution	Manual input	0–100	%	Usually 2–10%
	Insulation type	Dropdown menu	8 options*	-	Defines λ, ρ and prod. country
	Est. material waste	Manual input	0–100	%	Usually 2–10%
	Waste handling	Dropdown menu	2 options	-	Landfill or Incineration
	Estimated Service Life	Dropdown menu	11 options	year	10-110 years
	Temperature increase	Manual input	-	°C/10 yr	Optional
Wall	λ for additional layers	Manual input	-	W/(m·K)	
	Thicknesses of add. layers	Manual input	-	m	
Incl. slab	Floor height	Manual input	-	m	From slab to slab
	No. of slabs per floor	Manual input	-	-	Decreases with more floors
	Slab type	Dropdown menu	3 options *	-	Defines $E_{A1–3}$ for the slab

Table 4.3 presents the material properties and emissions for each considered insulation material. Columns A1-3 to $C4_{land}$ refer to life cycle phases in Figure 4.3. Sum_{inc} is the sum of emissions in a scenario where the waste material is incineration, whereas sum_{land} is for a landfill scenario. The table was first presented in **Paper II**.

Table 4.3. Presentation of materials included in the tool. Descriptions of Life Cycle Stages are presented in Figure 2.

Type	λ	ρ	A1-3	$C3_{inc}$	$C4_{inc}$	$C4_{land}$	Sum_{inc}	Sum_{land}	Prod.
	[W/(m·K)]	[kg/m^3]			[kg $CO_{2\text{-eq}}$]				[–]
Cellular glass	0.041	115.00	151.80	0.00	1.57	1.57	153.37	153.37	Belgium
Cellulose fibre, batts	0.041	80.00	−19.99	176.10	0.00	1.09	156.11	−18.90	Germany
Cellulose fibre, loose	0.039	45.00	−73.37	99.08	0.00	0.61	25.71	−72.76	Germany
EPS 18 kg/m^3	0.040	18.00	52.50	59.50	0.00	0.25	112.00	52.75	Germany
EPS 22.7 kg/m^3	0.035	22.70	59.50	0.00	75.20	0.31	134.70	59.81	Germany
Mineral wool, batts	0.034	30.00	40.31	0.72	0.40	0.41	41.43	40.71	Germany
Mineral wool, loose	0.034	50.00	64.02	1.25	0.69	0.68	65.96	64.71	Germany
Wooden fibre	0.036	51.70	−61.11	85.10	0.00	0.71	23.99	−60.40	France

4.1.3 Comparison of ITO and alternative methods

Paper III includes a comparative study of ITO and two alternative methods for identifying the optimal insulation thickness in terms of GHG (Gaarder *et al.*, 2023). The two investigated alternative models were designed for the Norwegian climate. Model 1 is a unit-level model based on a house located in a subarctic continental climate in Elverum, Norway. Model 2 is ITO, focusing only on the Arctic climates in Nuuk and Aasiaat. Model 3 is a full-scale building model in the subarctic continental climate in Oslo, Norway. All assessments of the models were based on glass wool insulation. The main topics of interest in the study were how the optimal insulation thickness changes with respect to future climate conditions and energy emission factors in cold climates.

4.2 Field studies

As presented in Section 2.4, two field studies with similar methodologies were conducted. There were two main differences between the studies. The pavilion (**Papers I and IV**) was located in Nuuk and had a controlled interior climate, whereas the nine monitored houses (**Paper V**) were located in Nuuk and Sisimiut and had varying interior climates based on user behaviour. The two field studies formed the basis of **Papers I**, **IV**, and **V**. The methods for both field studies are presented in this section, and the relation between these and the papers is visualised in Figure 4.1. **Paper I** focus on one specific case from the monitored residential buildings (CON_{Nuuk}), while **Paper V** includes all of them.

4.2.1 The test pavilion and wall constructions

The test pavilion in Nuuk had integrated five different façade constructions, each found in both the north and south-facing façade. The elements, which are referred to as “units” in this thesis, are named from A to E. The structure and orientation of the units are illustrated in Figure 4.4. The entrance to the pavilion is placed in Unit A_W. The east gable is made up of a Unit E element.

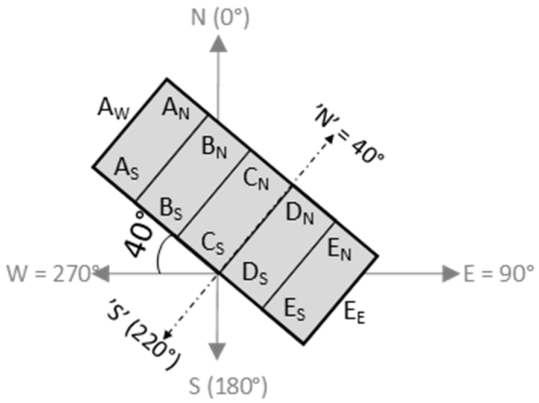

Figure 4.4. The structure and orientation of the test pavilion. Notice the angle of the pavilion, as the “north” façade almost faces northeast.

The construction of each unit is given in Figure 4.5. There is one sensor inside the room and at least one sensor for each direction in the ventilated air cavities. Additionally, there are sensors on both sides of implemented barriers in each unit. Sensor B also has a sensor inside the replication of the concrete layer, which is constructed with fibre cement boards. This is further described in **Paper IV**.

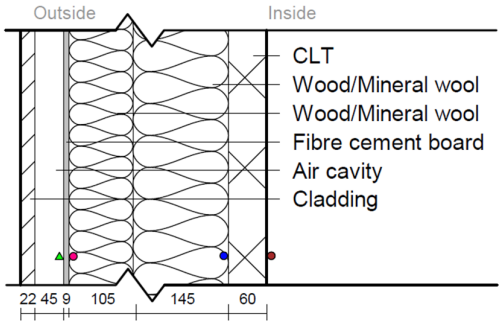

Unit A. U = 0.13 W/(m²·K).

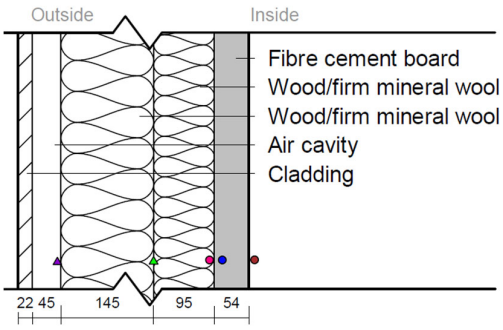

Unit B. U = 0.15 W/(m²·K)

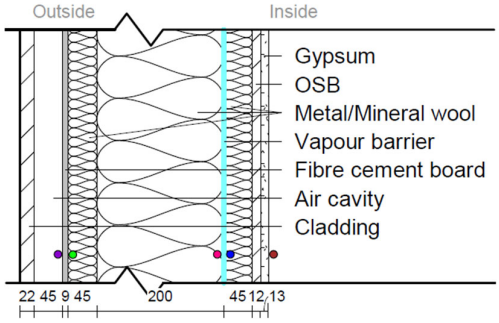

Unit C. U = 0.13 W/(m²·K)

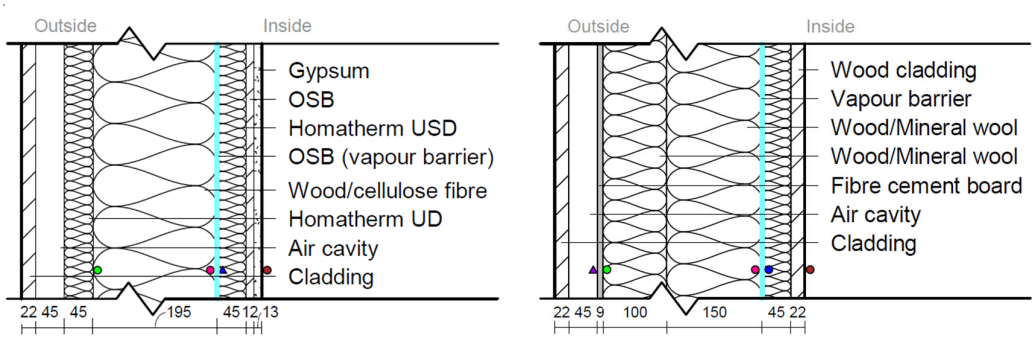

Unit D. U = 0.15 W/(m^2·K)

Unit E. U = 0.11 W/(m^2·K)

Figure 4.5. Cross-sectional drawings of each construction unit. Sensor locations are represented as dots (multiple orientations) or triangles (single orientation). The sensor colour corresponds to the lines in the graphs in Section 5. The sensors are named s0 to s4, starting from the interior side of the wall.

4.2.2 Houses and wall constructions

All rooms in the nine monitored residential houses had independent interior climates, depending on the implemented installations and usage of the buildings. The houses are named based on construction type and location. A number is added if multiple buildings fit the same naming. Figure 4.6 presents each evaluated wall construction, including dots to indicate the placement of the sensors. The colours of the dots correspond to the graphs in Chapter 6.

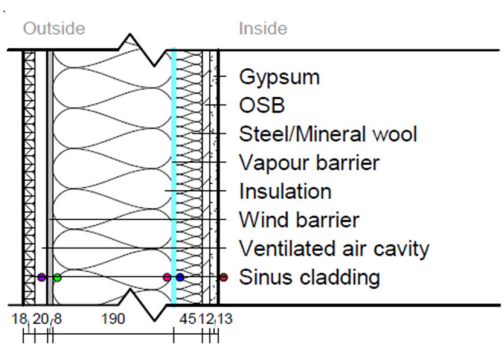

HT$_{sis1.}$ U = 0.15 W/(m^2·K) [W]

Legend

- Sensor 0 (s0) brown
- Sensor 1 (s1) blue
- Sensor 2 (s2) pink
- Sensor 3 (s3) green
- Sensor 4 (s4) violet

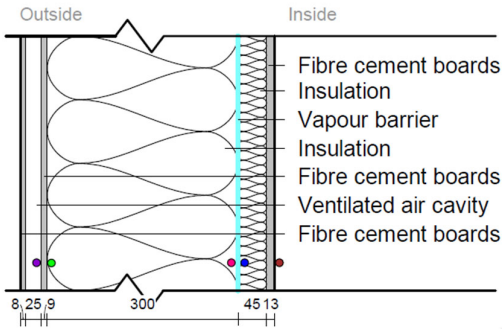

HT$_{sis2}$. U = 0.09 W/(m^2·K) [NE] [SE]

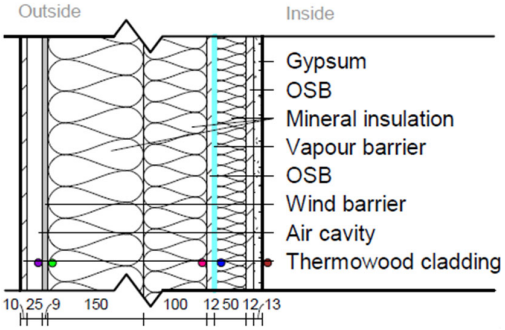

HT$_{sis3,}$ U = 0.12 W/(m^2·K) [NE]

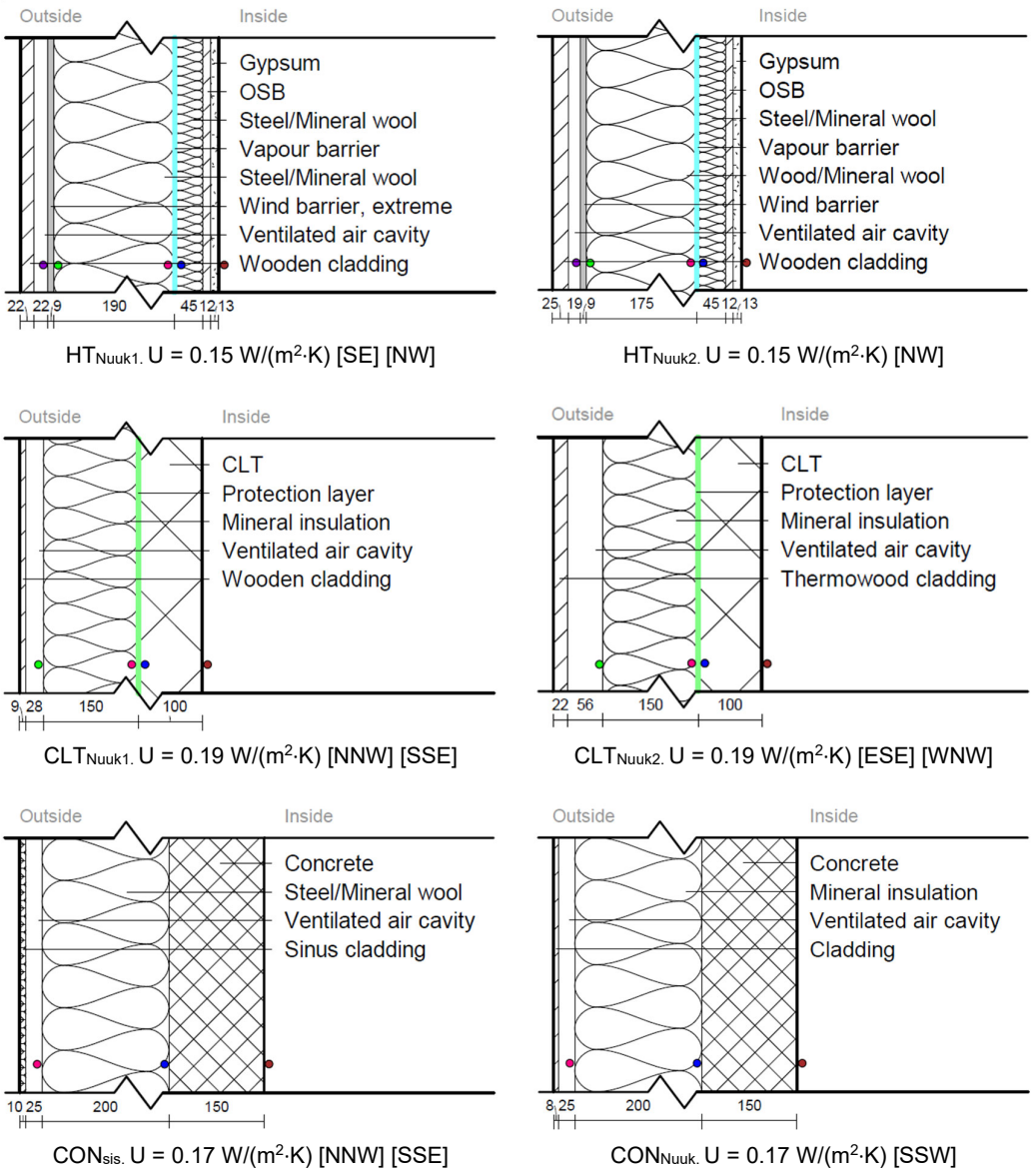

Figure 4.6. Cross-section drawings of the wall constructions in the monitored residential buildings. The dots indicate the placement of sensors, and the colours refer to the graphs in Chapter 5. The U-values and orientations are presented below each drawing.

The half-timber constructions were built of either wood or steel, but they all had vapour and wind barriers. The sensors were placed on each side of the membranes. Hence, each construction had four to five sensors depending on sensor installation in the air cavity. The studies investigated a total of eight half-timber examples (three in the pavilion and five houses). The insulation thickness varied from 220 mm to 345 mm. The residential half-timber constructions are named “HT” and identified with the respective location. A number is added if there are multiple constructions of the same construction type in that town. For example, the first of the two half-timber façades in Nuuk is named HT_{Nuuk1}.

Three CLT constructions were investigated (one in the pavilion and two houses), all located in Nuuk. None of the CLT constructions included a vapour barrier, but the two façades in the residential buildings had wind barriers. However, the wind barriers were placed untraditionally, as the purpose was to protect the CLT element from the weather conditions during construction. Therefore, the elements had three to five sensors depending on the presence of a wind barrier and air cavity sensor. The insulation thickness was 150 mm in the residential buildings and 250 mm in the pavilion.

There were three concrete structures (one in the pavilion and two houses), none of which included any membranes. In the pavilion, the concrete was replaced by multiple fibre cement boards because of the practical challenges of implementing concrete in the test facility. The number of sensors varied from three to five, as the element in the pavilion had an extra sensor installed between two layers of insulation and an additional sensor applied inside the “concrete” element. A description of this placement is provided in **Paper IV**. The insulation thickness varied from 200 mm in the residential buildings to 240 mm in the pavilion. The concrete layer was almost 100 mm thicker in the residential buildings than in the pavilion.

4.2.3 Sensors

All field studies were equipped with the same type of calibrated and temperature-compensated hygrothermal sensors. The implanted HYT 221 sensors from iST measured both temperature and relative humidity (Innovative Sensor Technology, no date). The measurement range of the sensors was -40 to +125 °C with a stated accuracy of ±1.8 % RH and ±0.2 K within specific ranges. The intention was to measure the hygrothermal conditions on each side of the potential implemented wind and vapour barriers. Nevertheless, photo documentation from the implementation of the sensors in the test pavilion and the monitored residential buildings revealed that the sensors were orientated opposite, as shown in Figure 4.7. Thus, instead of measuring on the membrane surfaces, the sensors measured the conditions a few centimetres away from the membranes. The sensors were new and calibrated at the factory and were not calibrated again before and after the field studies.

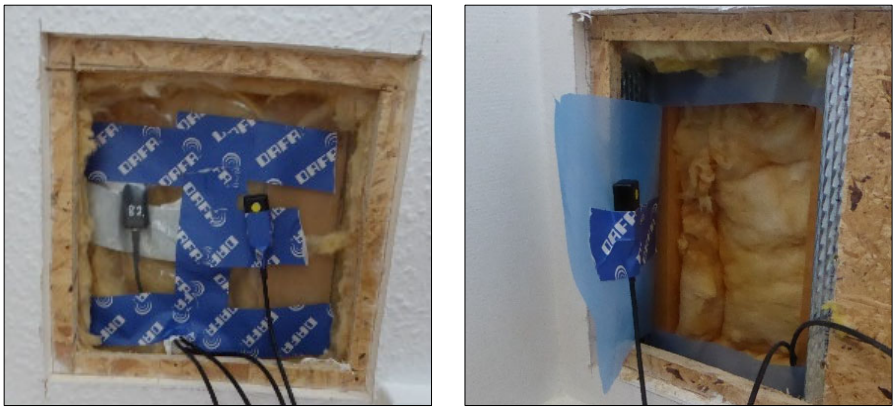

(a) Monitored residential building HT_{Nuuk2}. (b) Monitored residential building HT_{sis1}.

Figure 4.7. The orientation of hygrothermal sensors in test facilities. The yellow dot on the sensors is the sensing part. Both (a) and (b) are examples of half-timber constructions.

4.3 Hygrothermal simulations

As described in Section 2.6.2, it is common to produce a theoretical frame of reference to evaluate measurement data. In this study, Delphin 6.1 (Vogelsang, Fechner and Nicolai, 2013; Baumklimatik-Dresden, 2022) has been used to simulate the hourly conditions of the field studies in one dimension.

The simulations had multiple purposes. Mainly, they were used in combination with graphic visualisations to evaluate the performance of each façade construction. Furthermore, the models for the pavilion units were exposed to various Greenlandic climates and increased moisture loads. Finally, some of the constructions were analysed for different combinations of membranes, further explained in Section 4.4. Table 4.4 Table 4.5 presents an overview of the conducted simulations for the pavilion and monitored residential houses, respectively. Both tables refer to simulation scenarios, which are introduced later.

Table 4.4. Based on the data from the pavilion, the following simulations were conducted during this research. The italic definitions in the scenarios are the initial conditions for the fitted models. The conditions in the pavilion are represented by analysing the data from 2021.

Pavilion				
Unit	**No of sensors**	**Orientation**	**Scenarios**	
			Interior conditions	**Weather data**
A_W	3	W	*Measured* RH = 70 % RH = 85 %	*Nuuk (DMI)* Ilulissat (ERA5) Qaqortoq (ERA5) Sisimiut (ERA5) Tasiilaq (ERA5)
A_N	3	N		
A_S	4	S		
B_N	4	N		
B_S	4	S		
C_N	5	N		
C_S	5	S		
D_N	4	N		
D_S	4	S		
E_E	5	E		
E_N	4	N		
E_S	4	S		

Table 4.5. The simulations were conducted based on data from the residential houses during the research. The period of data collection presented in this thesis is from 2018 to 2022. The asterisks (*) indicate that the façade was analysed for multiple membrane combinations regarding mould growth, as presented in Section 4.4.2.

Houses					
City	**House**	**No. of sensors**	**Orientation**	**Simulated years**	**Weather data**
Sisimiut	HT_{sis1}	5	W	2018, 2021	*Sisimiut (ERA5)*
	HT_{sis2}	5	NE, SE	2021, 2022	
	HT_{sis3}	5	NE	2018	
	CON_{sis}	3	NNW, SSE	2020 - 2022	
Nuuk	HT_{Nuuk1}	5	SE*, NW	2021, 2022	*Nuuk (DMI)*
	HT_{Nuuk2}	5	NW	2021	
	CON_{Nuuk}	3	SSW*	2020 - 2022	
	CLT_{Nuuk1}	4	NNW, SSE	2022	
	CLT_{Nuuk2}	4	ESE*, WNW	2020 - 2022	

4.3.1 Evaluation of data

As described in Section 2.6.3, there are multiple commonly used evaluation methods to compare measured data with a theoretical frame of reference. The Coefficient Variation of Root Mean Square Error, CV(RMSE), is often applied, as it is easy to interpret with a unit in percentage. For the assessments during this study, a relative unit as percentages gives an uneven interpretation of errors due to the temperature and moisture profiles in the wall constructions. Instead, RMSE, which has the same unit as the evaluated parameter, is used. This method has two disadvantages as it is sensitive to outliers and is unable to identify if too high or too low values cause the error (Månhardt *et al.*, 2021; Kukk *et al.*, 2022). A third considered method is Mean Bias Error (MBE), which also has the same unit as the evaluated data. The disadvantage of this method is the risk of error cancellation (when the sum of positive and negative errors results in low overall error) (Huerto-Cardenas *et al.*, 2020; Abdul Hamid, Arfvidsson and Harderup, 2022).

When fitting the models, it is valuable to define an evaluation method to identify if an implemented change in the model resulted in a better or worse match to the measured data. The evaluation method could also help determine when the model was “good enough” by stating an accepted margin of error. Combined with visualisations of the data, the numerical evaluation was an essential tool for benchmarking the performance of the buildings. It was important to be aware that if the comparison was based on a poor model, the quality of the façade could easily be misinterpreted. As described in Section 2.6.3, there are many existing evaluation methods of the model quality, and they all have advantages and disadvantages. In **Paper I**, considering only temperatures in CON_{Nuuk}, the difference in means, MD, was used. The deviation was calculated as presented in Eq. 10.

$$MD = \frac{\sum \theta_{delphin} - \sum \theta_{sensor}}{N}$$ Eq. 10

In **Papers IV** and **V,** analysing multiple wall constructions, it was chosen to assess the model performance using the root mean square error (RMSE). The mathematical expression for RMSE is given in Eq. 11 and is based on the difference between the modelled data points, $x_{delphin,i}$, and the corresponding measured data points, $x_{sensor,i}$. There is a total of N data points, which are individually denoted by i.

$$RMSE = \sqrt{\frac{\sum_{i=1}^{N}(x_{delphin,i} - x_{sensor,i})^2}{N}}$$ Eq. 11

RMSE does not indicate if the error is positive or negative. Therefore, graphs comparing measured and simulated data are also included when evaluating the models. The unit of RMSE is equal to the unit of the evaluated data. The ambition was to define models where the temperature and humidity errors were below 5 °C and 10 % RH, respectively.

4.3.2 Material properties

The simulations require information about the materials in the investigated constructions. All material properties were based on similar existing materials from the Delphin database to ensure that the materials had reasonable properties, especially regarding vapour transport. Afterwards, the material properties were fitted to match the material properties given for the specific construction. Through an iteration process, the properties were adjusted to achieve results that fit the measurements of each construction based on the evaluation method described in Section 4.3.1.

All façade constructions were evaluated simultaneously for the test pavilion, as the five constructions were built simultaneously using the same materials in all units. The façade models were developed individually for the residential buildings because of the independent design and construction processes. If multiple walls in one house were monitored and simulated, the models were calibrated simultaneously. Figure 4.2 presents examples of the most important properties of selected materials, i.e., density (ρ), specific heat capacity (Cp), thermal conductivity (λ), and vapour diffusion resistance factor (μ). Additional material properties for the analysed constructions are presented in **Paper IV** (Friis, Møller and Lading, 2023a) and **Paper V** (Friis, Møller and Lading, 2023b)**.**

Table 4.6. Examples of material properties. Not all applied material of the same type has the same properties.

Material	ρ	Cp	λ	μ
	[Kg/m³]	[J/kgK]	[W/(m·K)]	[-]
Gypsum [81]	850	850	0.200	10
OSB [172]	630	1880	0.13	280
Insulation [730]	37	840	0.032	1.2*
Vapour barrier [174]	1500	2100	0.23	100,000
Insulation [648]	168	840	0.040	1.7*
Fibre cement [265]	1424 (Mukhopadhyaya *et al.*, 2007)	900 (Cembrit, 2017)	0.24 (Mukhopadhyaya *et al.*, 2007)	20 (Cembrit, 2018)
Air cavity 40 mm [17]	1.3	1050	0.138	0.4
Sinus cladding [778]	7700	460	25,000	-
Thermowood [654]	1158.7	1188	0.313	26.40
CLT [626]	425	1245	0.120	73
Wind barrier [28]	1200	2000	0.145	15,000
Concrete [569]	2104.2	1000	2.100	76.12
Sinus cladding [778]	7700	460	25,000	-

4.3.3 Boundary conditions

The hygrothermal boundary conditions were defined according to the circumstances of each field study. The boundary conditions correspond to the indoor climate and the exterior weather conditions.

The indoor conditions, including temperature and RH, were measured for all evaluated façades. In the test pavilion, the indoor climate was maintained constant at 20 °C and 50 % RH for all façade elements with the exception of short interruptions. In contrast, the indoor conditions in the measured residential houses depended on user behaviour. The interior sensor location is named s0.

The external weather conditions were obtained from two sources providing fundamentally different data types:

a. Measured and quality-assessed hourly weather data (e.g., from DMI or Asiaq)
b. Reanalysis weather data from ERA5

DMI (2020) is the official Danish Meteorological Institute directed by the Ministry of Energy, Utilities and Climate. Asiaq Greenland Survey is a survey institute owned by the Greenlandic government (Asiaq, 2023). ERA5 is a reanalysis dataset provided by the European Centre for Medium-Range Weather Forecasts (ECMWF) (European Centre for Medium-Range Weather Forecasts, 2022).

All weather data included temperature (θ), relative humidity (ϕ), air pressure, wind direction, wind velocity, rain, and solar radiation. Global horizontal solar irradiance was decomposed into diffuse and direct irradiance, using either the Orgill & Holland method

(Orgill and Hollands, 1977) or the Erbs method (Erbs, Klein and Duffie, 1982). All missing data, except solar radiation, were interpolated linearly. For solar radiation, it was essential to consider daytime and night-time when filling in the missing data. Nevertheless, short periods of missing solar irradiance were filled using interpolation. However, for longer periods of missing solar irradiance data, the missing data were replaced using interpolations of data obtained at the same time from the preceding and subsequent day. The weather data are further described in **Paper I**, **Paper IV**, and **Paper V.**

Five selected parameters, i.e., global irradiation, wind speed, temperature, and relative humidity, were statistically compared for each climate. As the weather data were not normally distributed, two-sided Wilcoxon tests were used to identify if the climate conditions were significantly different.

4.3.4 Air change in air cavities

All investigated façade structures had a ventilated air cavity. Therefore, the air change rate in the air cavities was accounted for in the simulation models. As described in Section 2.6.6, ACH is difficult to quantify. None of the field studies included attempts to quantify the airflow experimentally. Therefore, the values used for the simulation model were based on theory and literature. According to Brozovsky, Nocente and Rüther (2023), an air change rate from 0 h^{-1} to 650 h^{-1} is reasonable for a 19 mm gap. In the test pavilion, ACH was set to 60 h^{-1}, while it was defined iteratively for the monitored residential buildings within the limitations specified by Brozovsky et al. (2023). In **Paper IV**, the sensitivity of the model accuracy regarding the ventilation rate was investigated and concluded to be very low.

4.3.5 Simulation scenarios for the pavilion

The performance of the five construction types in the test pavilion was tested for multiple Greenlandic climates. This was done by running the Delphin models using ERA5 weather data for locations with different climates (see Section 4.3.3). The investigated locations were Sisimiut, Ilulissat, Qaqortoq, and Tasiilaq. Additionally, the simulations were run with higher internal RH (70 % and 85 %) compared to the original 50 % RH.

4.4 Mould growth index and suitability

The façade's robustness towards the climate conditions, and consequently the suitability for the Arctic conditions, was tested. As described in Chapter 3, suitability can be evaluated based on different aspects, but in this study, it is assessed by considering mould using the Viitanen method (Hukka and Viitanen, 1999). The Viitanen method is implemented in the free software WUFI Mould Index VTT (Fraunhofer Institute for Building Physics, 2022). The software can identify the risk of mould growth based on a minimum of one year of coherent hygrothermal data, including temperature and RH.

As described in Section 2.5.4, the risk of mould growth depends on temperature, RH, nutrition of the material, and time span. As the buildings are only monitored for a relatively short period, i.e., less than 5 years, this is a significant limitation to the risk assessment. Ojanen et al. (2010) did, however, show that low indexes are unlikely to increase significantly during an extended period. It takes only 20 weeks to attain a mould index of

5 for susceptible materials exposed to critical conditions. The index ranges from 0 to 6 and is considered critical above 3 inside a construction. Therefore, the constructions were considered suitable for the Arctic climate when the mould index was lower than 3 in all construction layers except the ventilated air cavity.

4.4.1 The test pavilion

In the test pavilion, the mould growth index was investigated for all the units based on the measured data and for simulated results of selected Units (C_N and C_S). Units C_N and C_S had some of the most critical hygrothermal conditions based on the graphs for RH, temperature, and mould indexes. Therefore, they were chosen for further investigation. The scenarios with alternative locations and increased RH, presented in Section 4.3.5, were also tested for mould growth.

4.4.2 The monitored residential buildings

The mould growth indexes were also calculated for all monitored walls in the residential buildings. Additionally, the simulation results of the corresponding Delphin models for the critical measured data were analysed for mould growth, and the indexes were compared. For the monitored residential buildings, four scenarios were tested (on one of each construction type) to identify the impact and consequences of implementing or omitting vapour and wind membranes. The four scenarios were:

1. Applied wind barrier but no vapour barrier
2. Applied vapour barrier but no wind barrier
3. No barriers
4. Applied wind and vapour barriers

Pine sapwood was chosen as the surrounding material for all mould risk assessments. This material is susceptible to mould growth and can thus quantify the worst-case risk levels. The mould growth indexes were also calculated for medium-resistant material properties (corresponding to glass wool) in selected layers for the four membrane scenarios. There were raw wooden battens in most air cavities in half-timber constructions. Therefore, these remained classified as very sensitive. The mould growth index is acceptable if it is below 2, while an index above 3 is considered critical.

4.5 Buildability

The buildability, defined in Chapter 3, is difficult to quantify, and therefore, the evaluation is an indirect assessment of the collected data. The evaluation is primarily based on the differences between the data collected in the pavilion and the data from the monitored residential houses. The reason is that the construction was performed rather meticulously in the pavilion, and consequently, the houses can reveal if the complexity of the design was too high for the local construction industry in Greenland. Thus, large errors (high RMSE) are considered an indication of too high complexity if they appear only for the monitored residential buildings. RMSE is used to compare the data from the two field studies and identify the buildability.

5 Main findings

This chapter presents the main findings from the research described in Chapter 4. Additional results can be found in the appended papers.

5.1 Optimal insulation thickness

The following results relate to the Insulation Thickness Optimiser tool, which was developed as described in Section 4.1. The purpose of the tool, ITO, is to quantify the insulation thickness, which emits the least GHG emissions. The results are also presented and further explained in **Paper II** and **Paper III**.

5.1.1 Outputs from ITO

When applying ITO to identify the optimal insulation thickness for a specific scenario, there are many parameters to define. Table 4.2 gives an overview of the parameters and their implementation in the tool. Table 5.1 presents the fundamental results from ITO, E_{opt} and d_{opt} for different scenarios combining different insulation materials and locations. The additional parameters are constant. A key finding is that the optimal insulation thickness is larger for Copenhagen (CPH) than for Nuuk. The reason is that the GHG emissions related to heating, E_{factor}, are much higher for Copenhagen than for Nuuk due to Nuuk's access to hydropower. Additionally, the table shows that the wooden fibres and loose cellulose fibres result in the minimum amount of GHG emissions at optimum. Cellular glass and batts of cellulose fibres emit the most $CO_{2\text{-eq}}$.

Table 5.1. Optimal insulation thicknesses (d_{opt}) and corresponding $CO_{2\text{-eq}}$-emissions (E_{opt}) were calculated with ITO for different scenarios. E_{d25} is the emissions for an insulation thickness of 0.25 m. The applied E_{factor} (shown in brackets under the location names) and HDD are for 2020, presented in Table 2.1.

Insulation material	**CPH (0.0499)**			**Nuuk (0.009)**			**Sisimiut (0.161)**			**Aasiaat (0.207)**			**Qaanaaq (0.107)**		
	d_{opt}	**E_{opt}**	**E_{d25}**	**d_{opt}**	**E_{opt}**	**E_{d25}**	**d_{opt}**	**E_{opt}**	**E_{d25}**	**d_{opt}**	**E_{opt}**	**E_{d25}**	**d_{opt}**	**E_{opt}**	**E_{d25}**
	[m]	**[$kgCO_{2\text{-eq}}$]**		**[m]**	**[$kgCO_{2\text{-eq}}$]**		**[m]**	**[$kgCO_{2\text{-eq}}$]**		**[m]**	**[$kgCO_{2\text{-eq}}$]**		**[m]**	**[$kgCO_{2\text{-eq}}$]**	
Cellular glass	0.2	77	78	0.2	54	60	0.7	234	361	0.8	273	473	0.6	217	311
Cellulose fibre, batts	0.2	76	77	0.2	54	61	0.7	238	362	0.8	277	474	0.6	219	312
Cellulose fibre, loose	0.5	33	40	0.3	24	25	1.5	103	311	1.7	120	417	1.3	96	263
EPS 18 kg/m^3	0.3	62	62	0.2	44	46	0.8	193	340	0.9	225	449	0.7	178	291
EPS 22.7 kg/m^3	0.2	64	64	0.2	45	51	0.7	199	307	0.8	231	403	0.6	183	264
Mineral wool, batts	0.4	37	39	0.3	26	26	1.2	113	275	1.4	132	368	1.1	105	234
Mineral wool, loose	0.3	46	47	0.2	33	33	0.9	143	283	1.1	167	376	0.8	133	241
Wooden fibre	0.4	34	39	0.3	22	23	1.5	95	287	1.7	110	385	1.3	89	243

Figure 5.1 visualises the optimal insulation thicknesses for specific cases. Specifically, Figure 5.1.a. shows the optimal insulation thicknesses in Nuuk and Sisimiut for the two heating sources, oil and district heating (DH), when considering the four different climate scenarios described in Section 4.1.2.3. The climate scenarios most significantly impact d_{opt} when d_{opt} is larger. Furthermore, the graph shows that it is essential to consider the

E_{factor} of the heating source. In Sisimiut, the optimal insulation thickness decreases by 50 cm for constant or conservative climate scenarios when changing the heating source from oil to DH. For Nuuk, where the E_{factor} for DH is the lowest, the reduction is more than 100 cm. In comparison, the most significant reduction of the d_{opt} caused by climate scenarios is 25 cm, achieved with the extreme climate scenario for DH in Nuuk.

Figure 5.1.b. shows the relation between insulation thickness and emissions for the same four cases as Figure 5.1.a for a constant climate. The dots indicate the optimal insulation thicknesses. The graph shows that the location (impacting the HDD and transportation emissions) has less impact when oil is used as the heating source.

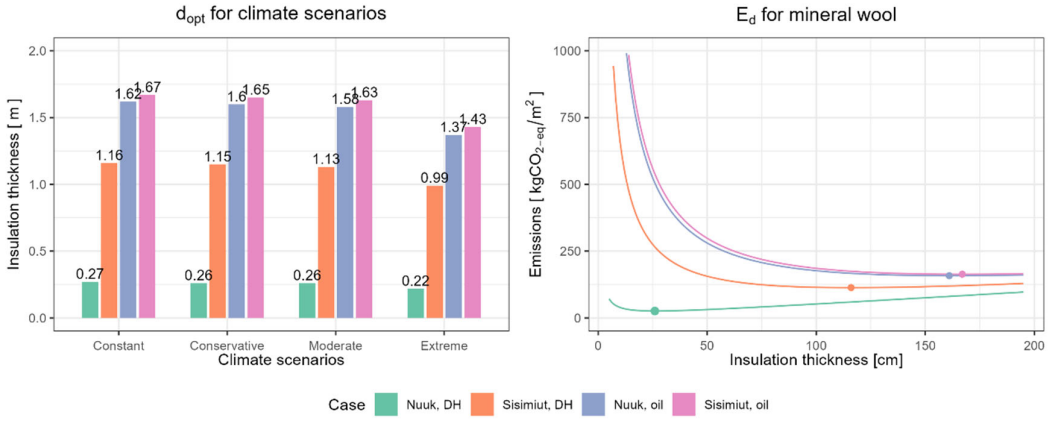

(a) (b)

Figure 5.1 Graphs presenting selected results from ITO. (a) shows the impact of the climate scenarios for four cases, while (b) shows the development of emissions at different thicknesses for mineral wool in the same cases considering a constant climate. The ESL is 60 years.

The optimal insulation thicknesses presented in Figure 5.1.a are very large for all scenarios except DH in Nuuk. As the cross-sectional drawings of the considered wall constructions in Figure 4.5 and Figure 4.6 indicate, the common building practices include significantly less insulation. A typical insulation thickness is 0.15 m to 0.35 m.

5.1.2 Comparison of incineration and landfill

The graphs in Figure 5.2 are not results from ITO but a visualisation of some of the inputs. More specifically, they show how each phase of the material lifecycle contributes to the $CO_{2\text{-eq}}$ emissions depending on the waste handling at EoL.

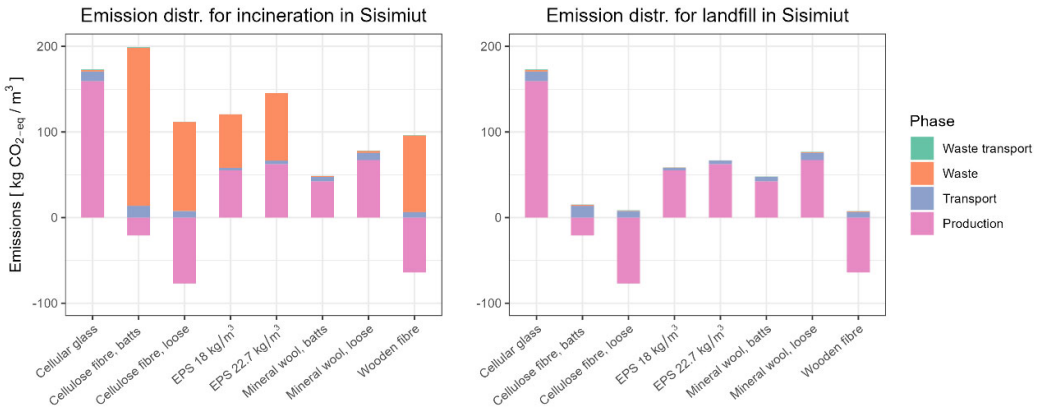

Figure 5.2. $CO_{2\text{-eq}}$ emissions from the different phases of 1 m^3 insulation material. The two graphs differentiate between the handling of waste at EoL. See **Paper II** for specific data on each material.

The tendency for most materials, excluding organic materials, i.e., cellulose fibre and wooden fibre, is that production is the primary contributing phase. For all materials, it was also found that transportation is an insignificant factor. Finally, waste handling is most significant for incineration, while it almost has no impact on the landfill scenario. However, this tendency does not necessarily mean that landfill is more sustainable than incineration, as there are other impact categories to consider in a broader context. Additionally, incineration of materials substitutes other fuels for heat production.

The functional unit for this small assessment is 1 m^3 of insulation. However, this does not account for the need for varying amounts of insulation due to the thermal conductivity of the material. The thermal conductivity of the materials varies from 0.034 W/(m·K) to 0.041 W/(m·K) (Friis, 2022). Considering the thermal conductivity does not change the interpretations above.

5.1.3 Effect of chosen criterion and additional considerations

There is an optimal insulation thickness because of the insulation's decreasing effect (the first centimetre reduces heat loss more than the last centimetre), resulting in a point where the additional emissions from the production and transportation of the insulation material exceed the saved emissions related to the reduced heat loss. The curve in Figure 5.3 for "insulation only" ($Scen_{ins}$) visually expresses the optimum.

As described in Section 4.1.2.5, two additional parameters were added to the calculation tool: 1) Insulating properties of the additional layers and 2) Environmental impacts from the increased areas of horizontal slabs caused by increased wall thicknesses.

Figure 5.3 shows the difference in d_{opt}, for $Scen_{ins}$, compared to $Scen_{wall}$, and a scenario considering concrete slabs. In this case, the additional wall layers include concrete, a ventilated air cavity, and cladding, further described in **Paper II**.

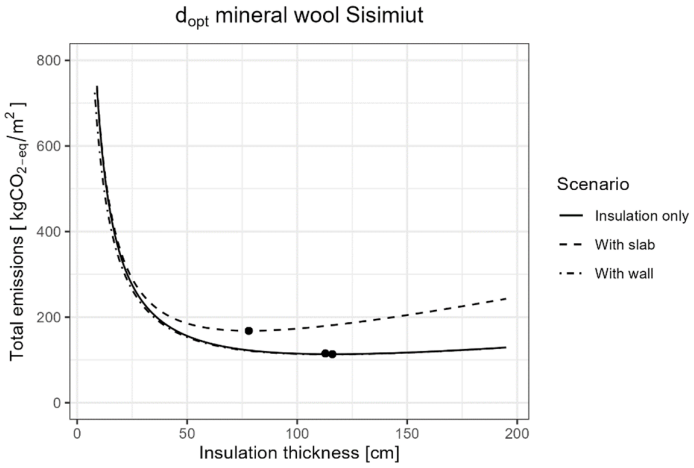

Figure 5.3. Example of optimal insulation thickness (represented by dots) for multiple scenarios. See more details in **Paper II**).

The graph shows that the additional wall layers are insignificant for the optimal insulation thickness. In contrast, considering the demand for additional horizontal layers is relevant to the decision process. The impact will, however, change depending on factors such as wall height, number of floors, and environmental footprint of the slab.

The consequences of the alternative success criteria for d_{opt} and E_{opt}, which are defined in Section 4.1.2.5, are shown for $Scen_{ins}$ in Figure 5.4. The general tendency is that the definition of the success criterion greatly impacts the results of the optimal insulation thickness and the relative emissions. However, the scenarios “5 %” and “10 %” had a more significant reduction of thickness than the increase in emissions, i.e., a 30 % and 37 % reduction, respectively, for Nuuk and a 27 % and 36 % reduction for Aasiaat.

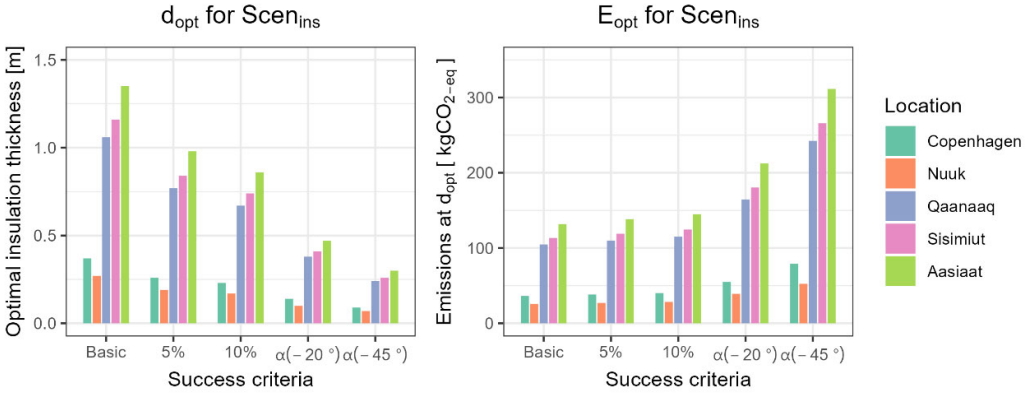

Figure 5.4. Changes in d_{opt} and E_{opt}, when adjusting the success criterion.

5.1.3.1 Sensitivity analysis

The optimal insulation thickness and the total emitted GHG are investigated with a sensitivity analysis, both for $Scen_{ins}$ and $Scen_{wall}$. Specifically, the GHG emission change is analysed when varying selected parameters with ±10 %. When considering the

insulation alone, E_{opt} is insensitive to the transportation distance, D. However, when the additional material layers are included, reducing the heat loss further, the change in GHG emissions is higher, indicating a sensitivity to this parameter. Generally, the sensitivity to parameters is a maximum of 5 % with few exceptions. The most sensitive parameter is the production phase, $E_{A1\text{-}3}$, for wooden fibres, regardless of the considered scenario ($Scen_{ins}$ or $Scen_{wall}$). For other materials, it is the least sensitive parameter, and thus, it is the one that varies the most depending on the material choice.

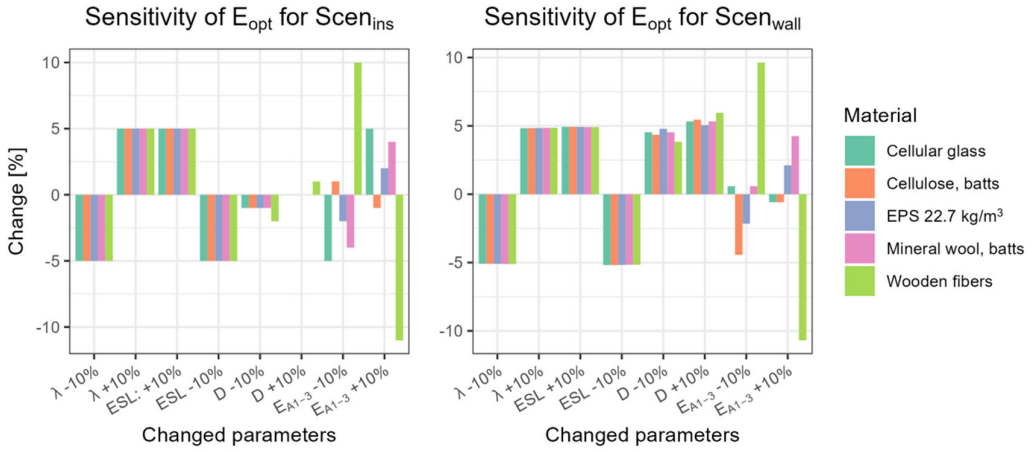

Figure 5.5. Sensitivity analysis of E_{opt} with and without additional concrete wall layers.

5.1.4 Comparison of alternative methods

As described in Section 4.1.3, the ITO tool was compared to two other methods in **Paper III**. Model 1 was based on a wall construction in Elverum, while Model 3 was unit-based, considering a complete building envelope in Oslo. Both locations are in Norway. ITO was considered Model 2.

For all three models, it was found that the assessment of the optimal insulation thickness is most relevant for cases with low E_{factor}. Model 1 demonstrated that if the E_{factor} was 17 $gCO_{2\text{-}eq}$/kWh, reducing d_{opt} by 100 mm, equivalent to a change of 21 %, would increase the GHG emissions by 3.5 %. The results of the models were consistent.

5.2 Field studies

This section presents the collected data from the two field studies presented in Section 4.2 in relation to the hygrothermal simulations. Most of the results presented here originate from appended **Papers I**, **IV** and **V**. These papers contain additional information and details; however, new assessments are included here to evaluate the correlation between the results of the papers.

5.2.1 Evaluation of Delphin models

Table 5.2 contains the errors of the simulations where RMSE exceeded the accepted limit of 5 °C for temperatures. As shown in Table 4.4, other simulations were performed as well. The results from these can be found in **Paper IV** and **Paper V**. In the test pavilion presented in **Paper IV**, the measured temperatures never significantly deviated from the

simulation results, and the RMSE never exceeded the defined limit of 5 °C, which is why they are not shown in the table.

Table 5.2. RMSE of the simulations, where RMSE of temperature exceeds 5 °C. Values exceeding the threshold limits are marked with yellow. This is a reduced version of Table 4 in **Paper V**. The corresponding table for the pavilion can be found in **Paper IV**.

Building	Year	RMSE of temperature [°C]					RMSE of RH [% RH]					RMSE of RH moving mean of 7 days [% RH]				
		S0	S1	S2	S3	S4	S0	S1	S2	S3	S4	S0	S1	S2	S3	S4
Sisimiut																
$HT_{sis1[W]}$	2018	0.5	4.4	5.7	8.7	8.8	1.0	8.5	10.6	5.6	9.8	0.8	5.7	9.8	5.1	8.0
$HT_{sis1[W]}$	2021	0.5	4.7	6.2	8.2	8.5	0.9	9.7	8.9	6.5	13.3	0.5	7.5	8.1	5.7	11.9
$HT_{sis2[SE]}$	2021	0.3	2.5	1.0	5.5	5.4	1.1	13.0	9.1	22.3	20.1	0.4	11.6	4.4	22.2	16.0
$CON_{sis[SSE]}$	2020	0.7	2.4	7.1	-	-	1.3	4.3	19.2	-	-	0.9	3.3	10.8	-	-
$CON_{sis[SSE]}$	2021	0.7	2.4	7.2	-	-	1.2	4.0	18.4	-	-	0.8	2.9	9.2	-	-
$CON_{sis[SSE]}$	2022	0.7	2.9	6.2	-	-	1.3	4.5	18.4	-	-	0.8	2.8	10.8	-	-
Nuuk																
$HT_{Nuuk1[NW]}$	2021	0.7	4.0	5.4	5.3	5.5	4.9	8.4	14.5	10.6	17.0	0.8	4.6	10.6	9.3	10.5
$HT_{Nuuk1[SE]}$	2021	1.3	5.8	7.6	3.3	3.5	4.5	7.1	15.1	7.1	14.3	0.8	3.3	13.6	5.6	9.2
$HT_{Nuuk1[NW]}$	2022	0.5	5.1	6.9	1.4	1.4	1.6	6.9	14.3	5.9	13.1	0.7	2.1	12.5	5.1	9.4
$HT_{Nuuk2[NW]}$	2021	0.9	4.4	6.6	4.6	4.7	5.6	12.0	20.0	14.5	20.4	3.8	9.6	18.6	13.6	17.8
$CON_{Nuuk[SSW]}$	2022	0.5	4.5	5.4	5.9	-	1.9	9.3	18.2	-	-	1.0	8.5	12.3	-	-

The largest error for the residential buildings presented in **Paper V** was 8.8 °C for $HT_{sis1[W]}$ in 2018, as shown in Table 5.2. Generally, the differences were most significant near the exterior climate. Still, the differences exceeded the 5 °C limit at the internal side of the vapour barrier (s1) for HT_{Nuuk1}. The detailed drawings of the constructions are shown in Figure 4.6. Regarding low temperatures, the critical point is on the inner side of the insulation layers, s1 (see Figure 4.5 and Figure 4.6), because of the increased risk of high relative humidity and discomfort related to cold surfaces.

In the pavilion, only Unit C (a half-timber construction) exceeded the limit for RMSE of relative humidity for a 7-day moving mean. Unit D (a half-timber construction with cellulose insulation) was the only unit that never exceeded the relative humidity limit (based on **Paper IV** results). Figure 5.6 shows the graphs comparing measured and simulated data for these units. The error in Unit C was caused by higher measured relative humidity than simulated, and the opposite applied for Unit D. This indicates potential moisture problems in Unit C, emphasised by the high vapour content, v, at s1. However, the measurements didn't reach the critical levels of RH and temperatures (85 % at 10 °C) (Brandt *et al.*, 2023). Both constructions had vapour barriers, while only Unit C had a wind barrier, as illustrated in Figure 4.5 and Figure 5.6.

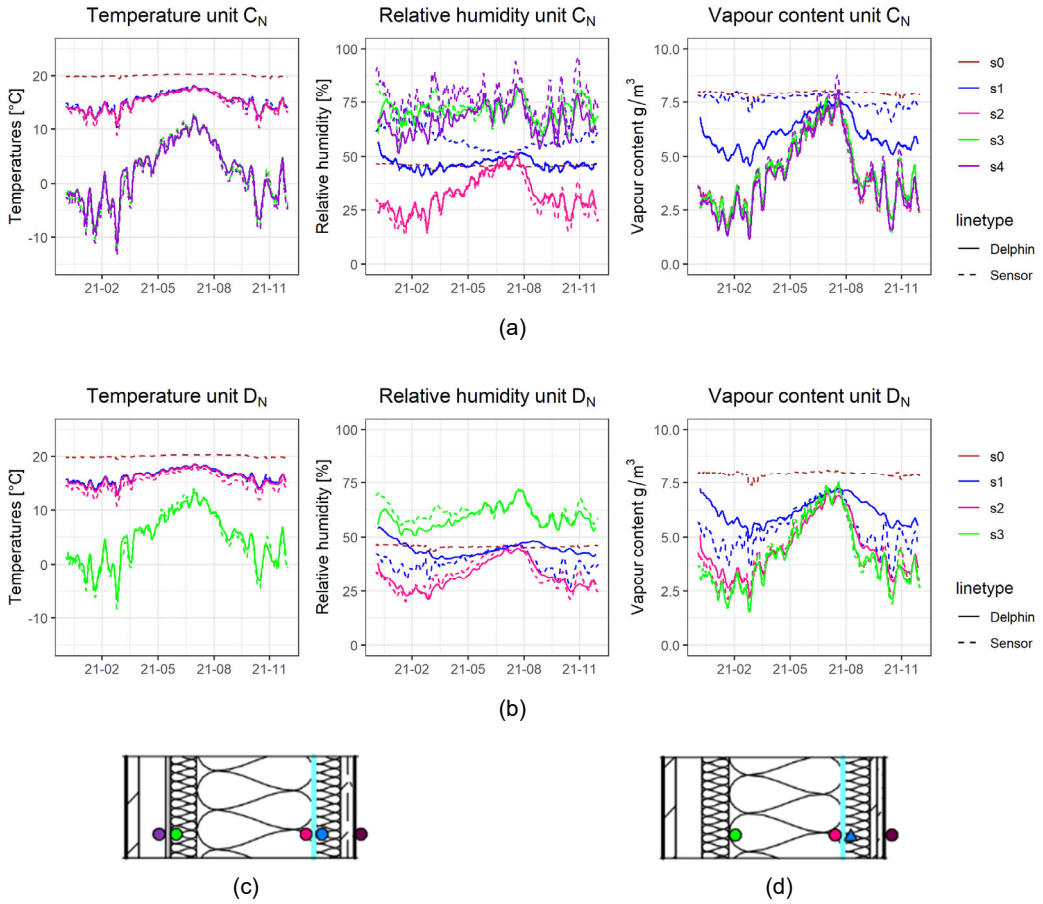

Figure 5.6. Measured and simulated conditions in the pavilion (a) Unit C and (b) Unit D. The construction of Unit C is illustrated in (c), and the construction of Unit D is illustrated in (d).

5.2.2 Investigation of a concrete construction, CONNuuk

Even though the RMSE presented in Table 5.2 was within the accepted range for CON_{Nuuk}, it was found in **Paper I** (Friis, Møller and Lading, 2021) that the measured temperatures between the concrete and insulation (s1) were significantly lower than simulated. The study was conducted because of multiple complaints from the residents. A previous study investigated the extent of the issues with a number of tests (Lading and Møller, 2019). Many problems were identified, but **Paper I** focused on the recognised cold wall surface. The conclusion was that the low temperatures corresponded to a wall, where the insulation had a thermal conductivity, λ, of 0.3 W/(m²·K) instead of the declared 0.033 W/(m²·K). In **Paper V,** it was evaluated in context with the other residential buildings. Figure 5.7 presents the measured data and the two independent Delphin simulations created with different weather data, which are presented in Table 4.4. The graph shows that the temperature at s1 was significantly lower than anticipated based on the simulations.

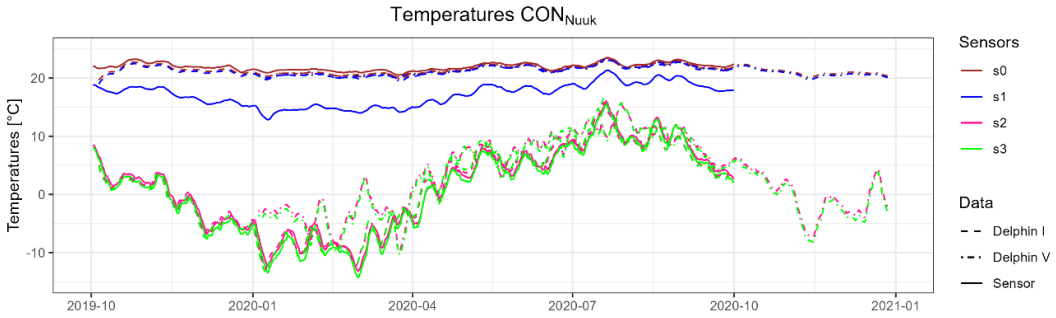

Figure 5.7. Measured temperatures from CON_{Nuuk} along with Delphin results from the models presented in **Paper I** and **Paper V**. The Delphin models in the two papers were developed independently and with different weather data. Thus, they are not identical.

In **Paper I,** the reason for these low temperatures was identified with pictures from the building site of CON_{Nuuk}. The pictures showed that the insulation material was not implemented correctly, see Figure 5.8.b. It was later found that this was also the case for CON_{sis}. See Figure 5.8.c, which is designed with the same insulation product.

(a) Illustration of wind flow dynamics (Credit: Eva Møller)

(b) Photo of insulation from CON_{nuuk} (Credit: Peter Barfoed)

(c) Photo of insulation in CON_{sis} (Credit: ABC project)

Figure 5.8. Details of the insulation in the concrete constructions in Nuuk and Sisimiut.

The insulation material in the concrete buildings is firm mineral wool with soft edges, which can be pressed together to ensure tight connections between the batts. If applied on a smooth, airtight surface, e.g., concrete, wind cannot penetrate the insulation layer, which, in theory, makes a wind membrane redundant. Thus, CON_{Nuuk} and CON_{sis} did not contain wind barriers, as illustrated in the sectional drawings in Figure 4.6.

Photos (b) and (c) in Figure 5.8 illustrate some examples of inadequate insulation installation in the two different concrete structures without wind barriers in Nuuk and Sisimiut, respectively. Photo (b) shows a gap between the concrete and the insulation and cracks in the uneven insulation surface. Photo c shows holes and inconsistencies, but foremost, an example of the insulation being installed in the wrong direction.

Uneven insulation layers create space for wind to penetrate the material and flow behind the insulation layer (see Figure 5.8.a). The case of CON_{Nuuk} is presented in **Paper I**.

Consequently, based on the photographic material, the low temperatures at the external concrete surfaces in the concrete structures are likely due to the insulation being attached unevenly.

In **Paper V**, it was found that simulation models of other constructions performed worse than or equal to CON_{Nuuk} when comparing measured and simulated data. This included $HT_{Nuuk1[SE]}$, $HT_{Nuuk1[NW]}$, $HT_{Nuuk2[W]}$, and $HT_{sis1[W]}$. Figure 5.9 presents the temperature differences between the measured and simulated data for these constructions at s1, except for $HT_{sis1[W]}$, which is excluded due to large amounts of missing data. The graphs show that the measured temperatures close to the indoor climate (s1) are generally lower than the modelled values, especially during winter. Results for HT_{Nuuk1} are represented for two directions (southeast and northwest), of which the model performance was worst for the northwest. During spring, $HT_{Nuuk1[NW]}$ was the most problematic construction.

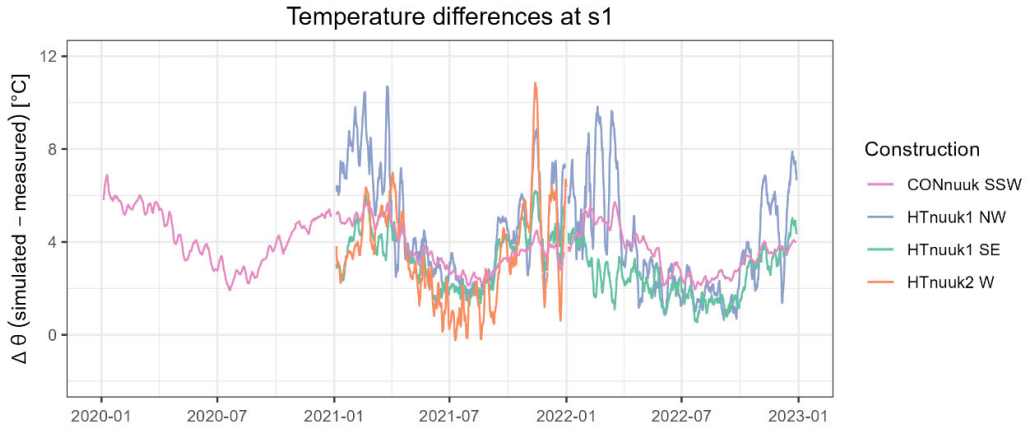

Figure 5.9. Visualisation of the temperature differences closest to the interior climate, s1, for selected constructions. The difference is calculated as simulated minus the measured temperatures.

All half-timber constructions (HT) were equipped with wind barrier boards, but based on the errors and graph assessments, the wind barriers did not perform equally well. In general, the wind barriers appeared to be less efficient on west-facing façades. This can either be due to the dominant wind direction or merely that the western constructions were poorly constructed. Considered in relation to the wind tendencies in Nuuk, where the most dominant wind directions are north, northeast, and south (World Weather, 2023), it is most likely a coincidence. In Sisimiut, however, west is the second most dominant wind direction, following east (World weather, 2023).

The only construction type that performed acceptably with respect to the inner layers in all scenarios was CLT. Both CLT constructions (see Figure 4.6) had a wind barrier, but the wind barrier was placed on the surface of the wood and would most likely not hinder cooling due to wind penetrating the insulation.

5.2.3 Mould growth indexes

The mould growth indexes were assessed for all measured data in the pavilion and the monitored residential houses. The results exceeding a mould index of 0 are presented

in Figure 5.10, based on **Paper IV** and **Paper V**. The constructions were not visually assessed. From the graphs in Figure 5.10, it is learned that the mould indexes are highest in the external layers, and there were no cases where the accepted limit of 2 was exceeded on the interior side of the wind barrier.

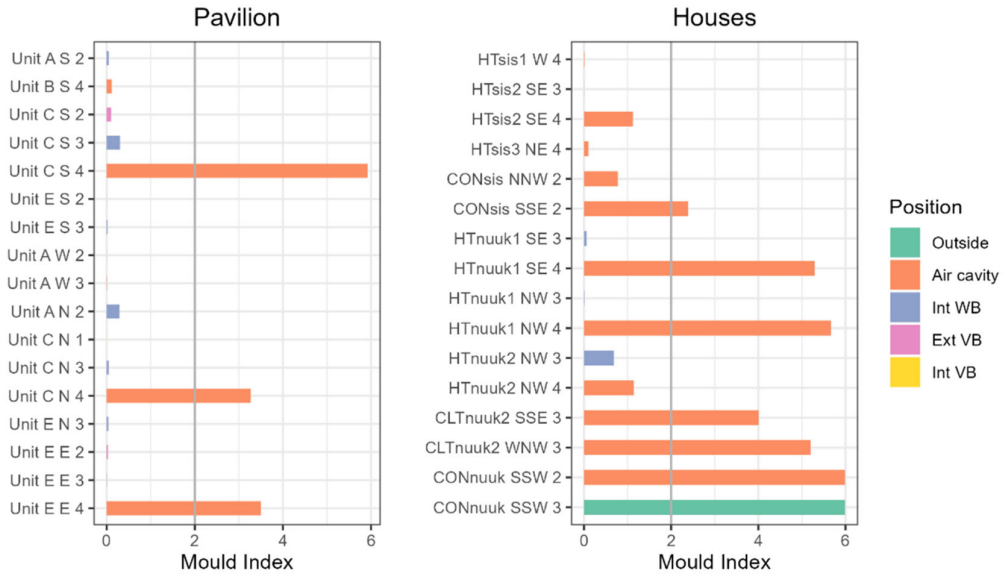

Figure 5.10. Mould growth indexes above 0 for (a) the pavilion and (b) houses.

As described in Section 4.4, the mould growth indexes in the Delphin models were analysed for different combinations of barriers. The results are presented in Table 5.3 and show that the wind barrier has minimal impact on the risk of mould growth. The analysis was performed with very sensitive material properties as described in Section 4.4.2, with additional analysis accounting for materials that are medium-resistant to mould growth (see values with asterisks (*) in Table 5.3). Comparing these results shows that the material choices significantly affect the theoretical risk of mould growth.

Table 5.3. Mould growth indexes for the models of the three selected constructions with varying presence of membranes. To make the indexes comparable, the duration of the data used to calculate the index was the same for the measured and modelled data. The values in parentheses correspond to the indexes of the measured data. Values exceeding the accepted index of 2 are shown in red. The table replicates Table 5 in **Paper V**. Results obtained with "medium resistant" sensitivity class due to the absence of wood are marked with asterisks (*) followed by the respective mould index. HT_{Nuuk1} is a half-timbered steel construction. VB is short for vapour barrier, and WB is short for wind barrier.

	Wind barrier		+	-	-	+
	Vapour barrier		-	+	-	+
	Position		**Test 1**	**Test 2**	**Test 3**	**Test 4**
$HT_{Nuuk1[SE]}$	Int VB	1	0.0	0.0	0.0	0.0 (0.0)
	Ext VB	2	-	0.0	-	0.0 (0.0)
	Int WB	3	3.8*0.0	-	-	3.7*0.0 (0.1)
	Air cavity	4	5.4	5.4	5.4	5.4 (5.3)
$CON_{Nuuk[SSW]}$	Int VB	1	0.0	0.0	0.0 (0.0)	0.0
	Ext VB	1x	-	0.0	-	0.0
	Int WB	2i	0.04*0.0	-	-	0.1*0.0
	Air cavity	2	5.3*0.0	5.4*0.0	5.4*0.0 (6.0)	5.3*0.0
	Outside	3	6.0*0.0	6.0*0.0	6.0*0.0 (6.0)	6.0*0.0
$CLT_{Nuuk2[ESE]}$	Int VB	1i	-	0.0	-	0.0
	Ext VB/Int WB	1	0.0 (0.0)	0.0	0.0	0.0
	Ext WB	2	0.0 (0.0)	-	-	0.0
	Air cavity	3	0.1*0.0 (4.0)	0.1*0.0	0.0	0.1*0.0

As described in Table 4.4, the mould indexes in the pavilion were also investigated for alternative interior conditions of 70 % RH and 80 % RH. None of these scenarios changed the mould growth risks in the façade construction units.

6 Discussion of main findings

In this section, the hypotheses and research questions posed in Section 3 will be discussed. This discussion is based on the main findings from Chapter 5 and the methods presented in the appended papers. The discussions of the two defined hypotheses will start by focusing on the research questions. This is followed by a general discussion of each specific hypothesis and the related uncertainties. Table 3.1 provides an overview of how each paper relates to a specific research question.

6.1 Hypothesis 1

The first hypothesis is: “Mould problems in Greenlandic wall constructions are caused by faulty design”. It is discussed here based on the results from **Papers I**, **IV**, and **V**.

6.1.1 Are wind barriers essential? (RQ 1.1)

A wind barrier’s main purpose is to prevent air from penetrating the insulation and other materials, which would otherwise lead to cooling of the wall construction and, consequently, cold interior surfaces. A wind barrier can also reduce the significance of leaks, in turn reducing heat loss, draught, and discomfort. For these reasons, the temperatures in the wall constructions are a good indicator of the importance or need for a wind barrier in a specific construction.

Because relative humidity depends on temperature and is a critical parameter for the risk of mould growth, the mould index can be used as an additional parameter to identify the significance of a wind barrier. Additionally, a wind barrier can reduce heat losses caused by leaks and cracks, which tend to occur in CLT constructions due to wood shrinkage (Time *et al.*, 2023). In CLT_{Nuuk1} and CLT_{Nuuk2}, however, the wind barrier was applied to protect the CLT elements during construction.

6.1.1.1 Temperature

All constructions investigated in this thesis are designed with either a wind barrier or a design that, in theory, makes a wind barrier redundant. In the investigation of the pavilion studied in **Paper I**, there were no issues with the temperatures, according to the RMSEs. In the monitored residential houses, however, there were multiple cases where the temperatures were lower than expected from the simulations in the construction layers close to the interior climate (at s1).

The investigation of CON_{Nuuk}, presented in Section 5.2.2, indicates that the presence of wind barriers can be essential to ensure airtightness in cases where the buildability of the design is questionable. This precautionary measure will increase the construction robustness regarding imperfections. The photos in Figure 5.8 showed that the insulation was not installed correctly. Further, the Delphin simulations indicate that the façades could perform adequately if the insulation was applied correctly or assisted with a wind barrier.

The half-timber facades were, however, also found to underperform despite the presence of wind barriers. The reason is unknown, but it might be due to the application of the

wind barriers not being tight. The membranes must also be applied correctly to improve the quality of the façades. Another explanation can be that the applied materials were of different kinds or worse quality than assumed based on the technical material during the production of the models in Delphin.

6.1.1.2 Mould growth index

The mould growth indexes were analysed for both the pavilion (**Paper IV**) and the monitored residential houses (**Paper V**). The same tendency was observed for mould growth as for the temperatures, i.e., no identified issues in the pavilion. Neither did the increase of internal moisture load from 50 % RH to 70 and 85 % RH, respectively, cause any problems. However, some potential issues in the residential houses were detected.

The mould indexes for different combinations of wind barriers showed that the wind barrier neither caused nor prevented mould growth in the evaluated constructions. Thus, no evidence indicates that a wind barrier is essential to avoid mould growth in wall constructions. However, wind barriers can affect the temperature throughout the whole facade. The results illustrated in Figure 5.9 demonstrate that even with an implemented wind barrier, some constructions still exhibit unexpectedly low temperatures in the internal layers, indicating increased heat losses. The fact that the measured temperatures were closer to the modelled values in the meticulously constructed test pavilion highlights the demand for quality awareness. Therefore, in practice, implementing a wind barrier may be a cost-effective precautionary measure due to the great importance of tightness.

When analysing the results in Table 5.3, it is essential to consider that the data were collected for relatively short periods, especially considering the investigation of mould growth. Furthermore, leaks might occur in the CLT elements due to the wood drying out and shrinking (Time *et al.*, 2023). Leaks can cause temperature changes and thus have an indirect impact on both RH and mould growth.

All results from WUFI Mould Index VTT must be evaluated with the awareness that the Delphin simulation assumes that the wall constructions are perfectly constructed. In practice, wall constructions tend to have imperfections or faults, and thus, a membrane might have a larger effect. The results emphasise that a wind barrier has minimal impact on the mould growth index.

6.1.1.3 Pre- and post-sensor calibration

As described in Section 4.2.3, the hygrothermal sensors used in the field studies were not calibrated as part of the research project. They were not calibrated before the studies because the product data sheets described that they were pre-calibrated. Neither were they calibrated later, as the experiments are not considered finished, and the sensors are embedded in the constructions. Despite the complexity and time demand for extracting the installed sensors, it is recommended to perform this calibration once the sensors are no longer needed. Information about drifting sensors can provide valuable data. For future studies, it is recommended to calibrate the sensors before the study to obtain a higher accuracy of the measurement data.

6.1.1.4 Ventilated air cavities and snow accumulation

Air change rates in air cavities are challenging to quantify and were not measured in this study. Instead, a constant air change value was used for the individual constructions. As described in Section 4.3.4, the significance of the ventilation rate was low. However, accumulated snow at the lower opening of an air cavity can hinder the airflow and reduce or completely stop the air change rate in the air cavity periodically based on the seasons. The consequences of this can be investigated with the models presented in this study.

6.1.2 Are vapour barriers essential? (RQ 1.2)

The function of the vapour barrier is to avoid hygrothermal conditions for mould growth and condensation. Thus, when evaluating the need for vapour barriers, the relative humidity and risk of mould growth are of interest. The importance of the vapour barriers is investigated in **Papers IV** and **V**.

As described in Section 2.6.3, RMSE is sensitive to outliers. Since relative humidity changes more rapidly during short time periods than temperature, the RMSE was calculated for both individual time steps and 7-day moving mean values. The reason was to identify if the overall tendency was satisfactory. The acceptable RMSE value for both evaluations of relative humidity was set to 10 %.

The graphs of the measured relative humidity compared to the simulated expectations are shown in Figure 5.6. The graphs show that the errors are not consequently caused by too high humidity levels, as for Unit C_N, but also by lower levels, as for Unit D_N. As presented in Figure 5.10, the mould growth indexes were not critical at the internal layers in the facades despite the high levels of relative humidity in the measurements compared to the expected values. As presented in Table 4.4 from **Paper V**, the significance of wind and vapour barriers was tested for three selected houses. As for the wind barriers, the vapour barriers did not significantly reduce or increase the risk of mould growth.

Considering these observations, the vapour barrier is not considered essential for buildings in the Arctic climate. However, it may increase the robustness, defined in Section 2.5.3, of the façade due to increased possibilities for sufficient airtightness.

6.1.3 How important is buildability? (Research question 1.3)

The case of CON_{Nuuk}, presented in Section 5.2.2, is an example of a building project where buildability was essential to the performance of the façade. In this case, the buildability of correctly implementing the insulation was poor, resulting in low temperatures in the construction and, consequently, complaints from the residents. The character of the errors presented in Figure 5.8 indicates that some workers were unaware of the importance of correctly installing this type of insulation.

Furthermore, the presence of wind barriers discussed in Section 6.1.1 was found to be relevant to buildability, as such membranes can reduce the consequences of poor construction. That is, however, only if implemented correctly. The results presented in Table 5.2 illustrated that the wind barriers performed better in the pavilion than in the façades of the residential buildings, emphasising the importance of the buildability of this building material.

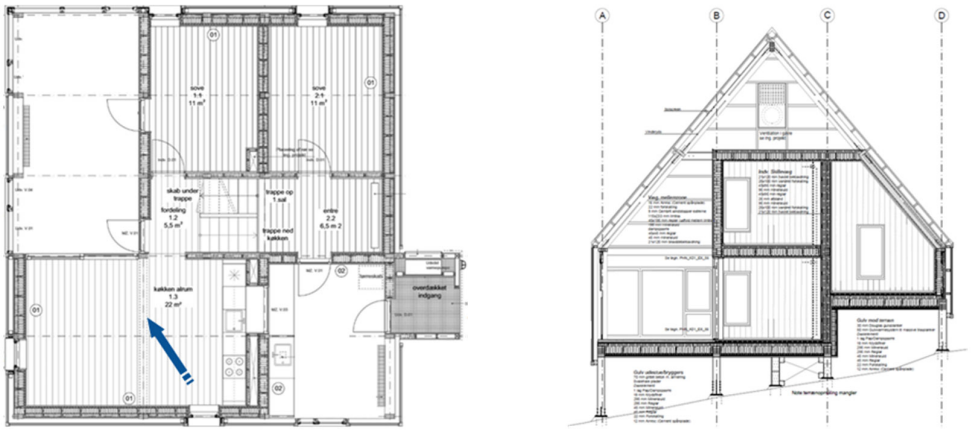

(a) (b)

(c)

Figure 6.1. (a) Horizontal and (b) Vertical detail drawing of the test house in Nuuk. White floor areas identify unheated semi-indoor zones. (c) Illustrates the concept of the unheated semi-indoor zone. The viewpoint of the rendered photo is illustrated by the blue arrow in drawing (a).

As described in Section 2.4.3, the ABC project included a test house, which was assessed independently from this thesis. However, the assessments contain additional examples of insufficient buildability for the Greenlandic circumstances:

- The concept of the test house was to create a “glass tent” with wooden boxes inside to create unheated semi-indoor zones to enjoy from spring to fall (see Figure 2.5 and Figure 6.1). The original idea was to construct the glass encasing first and, subsequently, construct the living spaces sheltered from the weather. However, this was not possible in practice. Instead, it was necessary to build the living areas first using cranes and special tools, which are not commonly found in Greenland, thus delaying the process.
- The timber construction was designed with specially designed braces, which got lost in the building process. The follow-up assessment determined that the construction process would have been more straightforward and less delayed if standard braces had been used.

- The glass was replaced with polycarbonate sheets to reduce the thermal transmittance. Since the chosen polycarbonate sheets were not completely transparent, adding windows was necessary.
- There were issues in getting workers qualified to install the flashings between the windows and the polycarbonate sheets and balance the ventilation system once the building was inhabitable.

Consequently, the design issues caused a need for implementing more advanced designs and products than originally intended. The main learnings from the preliminary study were concerned with 1) the design process and 2) the importance of actually ensuring the possibility of practically conducting and completing the building in Greenlandic conditions (Møller and Lading, 2021).

The building performance was assessed in 2021 by Slyngborg (2021). The assessment included thermographic photos taken during winter and a comparison of measured data with results from a dynamic simulation model in IDA ICE (EQUA, 2018). The middle zone was very exposed to overheating, which also impacted the inner zone. The inner rooms experienced 1175 to 3413 hours of overheating in the IDA ICE model, corresponding to up to 40 % of the year (Slyngborg, 2021).

At the same time, multiple thermal bridges and air leaks were identified in the construction. Especially in the bedroom in the NNE corner, where the surface temperature was measured to be -16 °C, see Figure 6.2. At the time of the measurement, the ambient temperature outside was -20 °C with a wind speed of 2 m/s. Additional - although less critical - thermal bridges were also found. Multiple attempts were made to eliminate one of these thermal bridges, but the result remained unsatisfactory.

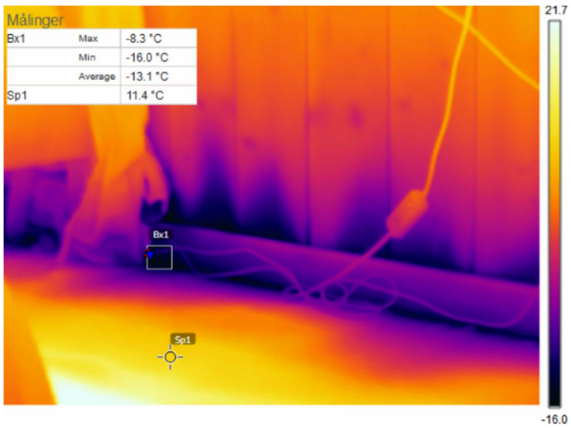

Figure 6.2. Thermographic picture of the most critical corner (NNE) identified in the test house.

Despite these findings, the estimated annual energy demand based on the simulation (128 kWh/m^2) was comparable with the actual energy consumption of 138 kWh/m^2 in 2021. The relative humidity in the building was measured to be in the range of 25-27 %, which is very dry. From the test house, it was learned that design solutions and labour quality are essential to the final performance of a construction.

Based on these cases, buildability should be considered essential. In existing literature, specific recommendations on how to achieve a high level of buildability are presented (Lam, Wong and Chan, 2006). Among the recommendations are:

- Thorough investigations of site and ground prior to design
- Coordination and project planning
- Standardised designs, repetition, and simplicity of the solutions

For a Greenlandic context, additional precautions might be beneficial, e.g., Design solutions that require a minimum of special tools, proper quality assurance to ensure that the labour is performed as instructed and increased focus on language barriers. If new methods are implemented, there must be a focus on the challenges related to new technologies or methods that are being implemented. For example, in the CON_{Nuuk} building, the concrete element factory was unable to meet the required tolerances defined by the insulation manufacturer. This could lead to potential errors, regardless of the quality of the performed construction work.

Based on this, buildability is considered essential to ensure suitable constructions for the harsh Greenlandic climate.

6.1.4 Discussion of Hypothesis 1

"*Mould problems in Greenlandic wall constructions are caused by faulty design*".

Three construction types were investigated to evaluate this hypothesis. The methods used for these investigations included experimental studies of a pavilion with controlled interior conditions and inhabited houses where the interior conditions were affected by user behaviour. Additionally, simulations were made of the hygrothermal conditions and the risk of mould growth. The applied methods have some limitations, which first and foremost relate to the limitation of the investigated constructions. It would have been desirable to collect data from more buildings. For example, there were only two examples of concrete constructions, which were both located in Nuuk. As these had more indications of problems with cooling than alternative constructions, it would be interesting to obtain more data from this construction type at different locations. In addition, data from a similar construction with an implemented wind barrier would be valuable. Furthermore, there were limitations of the hygrothermal models. Particularly, the models would have been more reliable if the material properties of the implemented products had been available. It would also have been valuable to visit all the building sites during construction to capture explanatory pictures like the ones presented in Figure 5.8. Such pictures are essential in identifying possible reasons for unexpected hygrothermal conditions.

The investigations of the research questions prove that all the investigated constructions can function adequately in Greenland. Thus, Hypothesis 1 is rejected. The most important factors for achieving robust building façades are buildability and high labour quality. If the construction is well-designed and constructed regarding airtightness, implementing wind- and vapour barriers is less significant. However, the membranes can improve the robustness of the façade.

6.2 Hypothesis 2

This hypothesis is discussed based on **Paper I-V,** as shown in Table 3.1. The formulation of the hypothesis was: “Optimal wall construction designs depend on the location in Greenland.”

6.2.1 Does the climate decisively affect façade performance? (RQ 2.1)

The term “climate” covers many parameters. Often, temperature is central, which in **Paper II** and **Paper III** is the only parameter accounted for when determining the optimal insulation thickness described in Section 4.1. The weather parameters considered during the field studies, described in Section 4.3.3, were much more comprehensive, both in terms of using hourly values instead of yearly values and in the number of included parameters. While all the investigated parameters have some impact on the performance of a building (e.g., heat loss and risk of mould growth), the extent of the influence varies. For example, rain is of the least significance due to the ventilated air cavity limiting the moisture transport from the façade cladding to the core part of the construction and the interior climate. In contrast, wind speed is of great importance for buildings with leaks, as increased airflow through the leaks and cracks increases heat losses. Pressure impacts the ACH in the air cavity, but as described in Section 2.6.6 and Section 4.3.4, this parameter is often estimated and thus associated with high uncertainties.

During this study, the outdoor temperature was included in two ways: As a series of data functioning as boundary conditions for hygrothermal simulations and as an approximate value, HDD, used to estimate the heat loss through a façade.

First, temperature development, which is fundamental for the hygrothermal simulations, was central to **Paper I**, **Paper IV**, and **Paper V**. Temperature is presented along with RH for multiple Greenlandic locations in Figure 6.3. The graphs show that the most northern considered location, Ilulissat, has the largest temperature span, as it is coldest during winter and warmest during summer. The large temperature difference is emphasised by the occurrence of midnight sun and polar night north of the Arctic Circle. Qaqortoq, the southernmost location, has the least temperature variation over the year. During summer, relative humidity is highest in Qaqortoq and lowest in Ilulissat. The statistical two-sided Wilcoxon tests were performed with a confidence interval of 95 %. They revealed that the five climates are generally significantly different, with some exceptions.

The tested parameters were temperature, RH, wind speed, and global radiation. In terms of temperature, Nuuk and Tasiilaq were not significantly different, and for humidity, Nuuk, Sisimiut, and Qaqortoq were generally found to be comparable. In terms of wind speed, Ilulissat was insignificantly different from Tasiilaq and Qaqortoq, while Nuuk was comparable to Ilulissat and Qaqortoq in terms of solar radiation. The geographic locations are visualised in Figure 2.2.

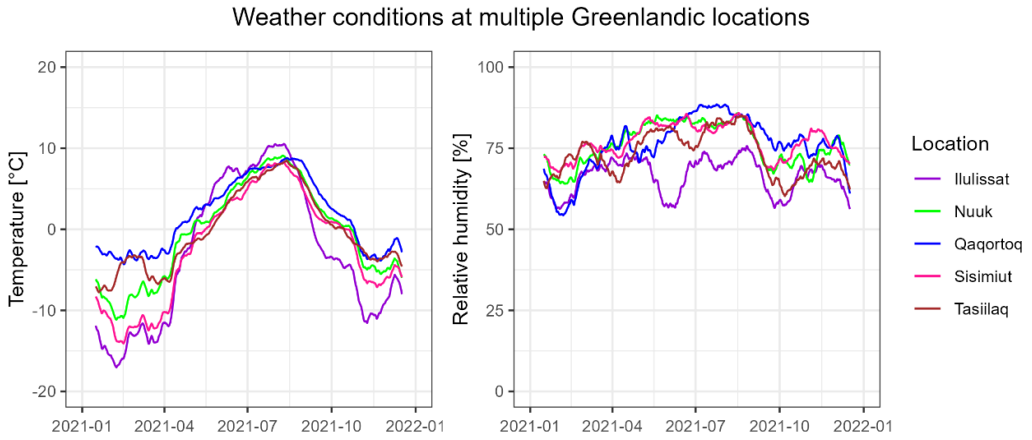

Figure 6.3. Temperature and relative humidity for one year (2021) at multiple Greenlandic locations. The graphs are shown for moving mean values of 7 days.

Another way to consider temperature is using heating degree days (HDD), introduced in Section 2.6.4. This measure is simpler to consider as it is a single value unless climate change is considered. HHD is used both in **Paper II** and **Paper III** and is a fundamental parameter in the ITO tool, as it can be used to estimate the yearly heat loss of a building. Table 2.1 contains the calculated HDD for Copenhagen and multiple Greenlandic locations.

It is well known that climate change increases temperatures globally. A general temperature increase of 0.4 °C/10 years equal to the RCP8.5 scenario (Meredith et al., 2019) will lead to higher relative temperature differences between the Greenlandic towns. There have been many attempts to quantify this temperature rise in Greenland at RCP8.5, where 0.4 °C is conservative compared to other sources, suggesting approximately 1.2 °C (Brown *et al.*, 2017). Besides temperature changes, there are many theories about other weather phenomena that can occur due to changes in the sea currents, e.g., melting sea ice.

As the climate across Greenland differs significantly, it is of interest to know if this has a significant impact on simulation results. In **Paper IV**, the same units as previously investigated were simulated using weather conditions for five different locations. Two of the locations, Ilulissat and Sisimiut, experienced relative humidity levels close to 100 %. A Wilcoxon test was made on the pavilion units to identify if the results were significantly different due to the different weather conditions. According to the Wilcoxon test, the hygrothermal simulations were found to be significantly different, with exceptions for some locations in terms of relative humidity. Thus, from a statistical perspective, the climate does decisively affect the hygrothermal behaviour of the façades. However, from the assessments of the mould growth risks of selected constructions in alternative locations, it is found that the consequences regarding mould growth are minimal. See **Paper IV**.

6.2.2 Is the difference between towns and settlements impactful? (RQ 2.2)

In Greenland, the term “town” has been used to identify inhabited areas with administrative connections to the 18 original municipalities, which were restructured in 2009. Thus, the definition of “town” is not necessarily reserved for areas with a certain number of people (Hendriksen, 2015). In this discussion, the definition provided by Asiaq is applied. Asiaq defines 17 towns, of which the smallest is Ittoqqortoormiit, with 354 inhabitants. The largest settlement is Kangerlussuaq, with 475 residents (Statistics Greenland, 2022). However, in general, towns are larger than settlements. The following discussion is not based on measured data, as all test facilities were located in towns (Nuuk and Sisimiut).

The population size of towns and settlements can be fundamental for the suitability of a specific construction in multiple ways. For instance, settlements are less likely to have the same infrastructure and facilities as towns, e.g., roads and (large) vehicles (Statistics Greenland, 2022), accessibility to machines such as cranes, and production facilities such as the concrete element factories presented in Section 2.6.7. The infrastructure can be a challenge for acquiring building materials, as the sea freezes during winter north of Sisimiut – this is, however, regardless of the town/settlement definition. The population size is also a strong indicator of the likelihood of the availability of advanced or specific skilled labour. The test house, presented in Section 2.4.3 and further discussed in Section 6.1.3, is a good example of buildability being an issue even in the largest and most resourceful towns in Greenland. Finally, energy production is partly defined by population size. Maintaining and expanding renewable energy sources, such as hydropower plants, solar panels, and wind turbines, is more profitable in towns with many buildings and people. In contrast, in areas where the energy demand is smaller, such investments are less economically sound – especially due to the low oil prices in Greenland (Nukissiorfiit, 2020).

The investigation of optimal insulation thicknesses in **Paper II** found that the optimal insulation thickness was highly dependent on the energy sources used to supply heating. Thus, the building location is a very important factor in the choice of insulation thickness. The many varying parameters and their potentially large impact indicate that the suitability of a building is significantly different for towns and settlements; however, the exact definition is of little importance compared to the resources and facilities available. For future studies, the assessment of the optimal insulation thickness could include economic aspects as well as considerations of thermal comfort.

6.2.3 How does location influence sustainability? (RQ 2.3)

A location’s impact on sustainability is partly defined by its size, which was discussed for research question 2.2 in Section 6.2.2. However, there are more aspects to examine when considering sustainability and disregarding the definition of the inhabited area.

As described in Section 6.2.1, the number of heating degree days is an indicator of the heat demand. This means that a high number of HDD leads to either increased heat loss or increased material consumption in the form of additional insulation to reduce heat losses. The ITO tool was created to evaluate the optimal compromise between heat loss and insulation production.

The environmental impact of the insulation also depends on transportation. Greenland is 2670 km long (Statistics Greenland, 2022), resulting in large variations in shipping distances depending on the end destination for the materials. However, in **Paper II** and **Paper III**, it was found that the impact from transportation was insignificant to the calculation of optimal insulation thickness in terms of reduced $CO_{2\text{-eq}}$. Additionally, Ryberg et al. (2021) concluded that transportation was insignificant when deciding on which construction type to build.

In **Paper II** and **Paper III**, the energy mix was found to have the most significant impact on the sustainability profile of wall constructions. Because of the island operation of Greenland, the energy mix varies greatly from location to location, as presented in Section 2.6.4. In Section 5.1, it was found that the optimal insulation thickness is achieved with less insulation in Nuuk than in Copenhagen due to Nuuk's access to hydropower. Thus, the answer to the research question is that location influences sustainability on multiple parameters.

An indirect parameter emphasising this conclusion is the accessibility to skilled labour. As described in the discussion of research question 2.1, skilled labour is generally more accessible in larger communities (Abrahamsen, 2019). Thus, buildability is even more central to sustainability in smaller communities, as poor construction usually leads to increased energy consumption, reduced service life, and increased resource demands for maintenance and reparation.

6.2.4 Discussion of Hypothesis 2

"*Optimal wall construction designs depend on the location in Greenland*".

The answer to Hypothesis 2, whether the location has a strong impact on the suitability of a construction, is complex. Based on the discussion of the three related research questions, it is evident that most of the parameters defining the suitability of a building are location dependent. This means that constructing complex buildings in areas with smaller populations are more likely to have errors and that a high emission factor of the heating supply results in significant environmental consequences. An overview of the parameters which influence suitability are shown in Figure 6.4. The fact that private sustainable energy sources can affect the energy mix is neglected.

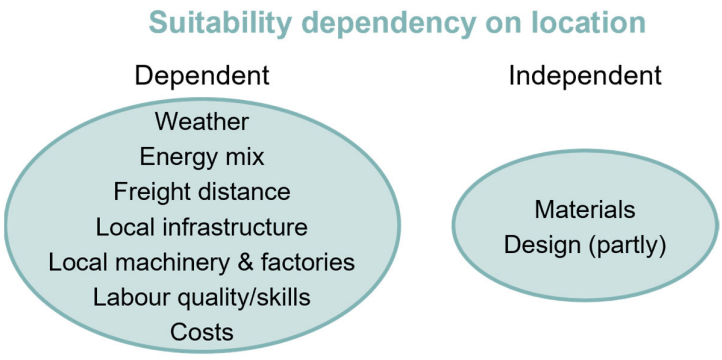

Figure 6.4. The locations influence on suitability.

7 Conclusion

The present study aimed to reduce the knowledge gap regarding optimised wall constructions in the Arctic climate with a focus on Greenland. Part of the reason for choosing Greenland is that the conditions are either comparable or more severe than most Arctic regions when considering infrastructure, energy sources, material resources, labour quality, and economy. Greenland is, however, less challenged by the melting permafrost than other Arctic regions, e.g., Svalbard, though this was not central to this study. The following sections present the conclusions of the initial hypotheses and the associated research questions. The chapter ends with a discussion of additional perspectives, ideas, and recommendations for future work.

7.1 Hypothesis 1

Hypothesis 1 stated, “Mould problems in Greenlandic wall constructions are caused by faulty design”. It was supported by three research questions. The following conclusions are based on the discussions in Section 6.1.

7.1.1 Are wind barriers essential?

The results revealed that wind barriers are not a necessity for constructing a decent façade for Greenlandic conditions. The mould growth indexes from the simulations of the monitored residential buildings (**paper V**), presented in Table 5.3, showed that the presence of a wind barrier would not change the risk of mould. It was, however, in a theoretical context, as the simulations only reflect a situation with correctly applied materials. The results from the two concrete structures, CON_{Nuuk} and CON_{sis}, showed that excluding wind barriers might have consequences in practice. While implementing a wind barrier is not essential, it might make the construction more robust toward imperfections.

7.1.2 Are vapour barriers essential?

The conclusion regarding the use of a vapour barrier is the same as for the wind barrier: it is not essential. No mould issues were found to be caused or reduced by using a vapour barrier.

7.1.3 How important is buildability?

Of the three elements (wind barrier, vapour barrier, and buildability) investigated to answer the research questions for Hypothesis 1, buildability was the most essential. Poor buildability was found to have significant consequences for the indoor climate, e.g., thermal discomfort in CON_{Nuuk}, heat losses, and a negative environmental impact related to repairing a finished building.

7.1.4 Conclusions for Hypothesis 1

As none of the three construction types (CLT, concrete, and half-timber) were found to be generally problematic in the Arctic climate, the hypothesis must be rejected from a theoretical perspective. However, from a practical perspective, some of the constructions are less buildable, resulting in decreased robustness.

Implementation of membranes can increase the robustness, and none of the results indicated that the implementation of the membranes causes harm to the construction. Therefore, membranes may be considered a precautionary measure.

7.2 Hypothesis 2

Hypothesis 2 stated, “Optimal wall construction designs depend on the location in Greenland”. It was investigated through three research questions, which were discussed in Section 6.2 based on the results from the appended papers.

7.2.1 Does the climate decisively affect façade performance?

The climates were found to be significantly different for the individual locations, and the temperature differences are expected to increase with climate change. However, the performance of the constructions was found to be acceptable regardless of the location. Therefore, the answer to this question is no.

7.2.2 Is the difference between towns and settlements impactful?

The definition of what constitutes a town versus a settlement is made purely from an administrative point of view, and does not account for population size, location, or facilities. Thus, the distinction between towns and settlements is not useful in this context. However, if categorising communities as large and small populations, the answer is yes. High complexity and resource-demanding constructions are more likely to be unsuccessful in small communities. This is due to several factors, including a lack of specialised labour skills, tools, and factories (e.g., for producing concrete elements). It is also likely that energy production is more sustainable in areas with high population densities as in these places it is often economically attractive to utilize renewable energy sources such as hydropower.

A parameter to consider for future work is the wind load in various community sizes. Buildings can protect each other from wind and thus reduce the heat loss or consequences related to leaks.

7.2.3 How does location influence sustainability?

The location is of great importance to the sustainability potential. Foremost because the energy factor varies significantly depending on the energy source of the location. In **Paper II**, heating was found to be the major contributor to GHG emissions. Considering the proven significance of buildability in research question 1.3, the risk of increased environmental consequences emphasises the importance of skilled labour, of which the availability depends on the location.

7.2.4 Conclusions for Hypothesis 2

Based on the discussions and conclusions of the research questions, location can be considered essential to suitability. The reason is not the climate conditions but rather the available facilities, resources, and expertise in the different towns and settlements. Thus, it is recommended to thoroughly investigate the available competencies and resources when building at new locations, as the island operation of Greenland makes it uncertain that a building or its related construction processes are suitable for all destinations.

7.3 Perspectives and future work

7.3.1 Additional data assessment

This study only investigated part of the data collected from the test pavilion; specifically, there are unassessed data from the roof constructions that are of interest (see Section 4.2.1). These data can provide information about essential elements and considerations when constructing horizontal building envelope elements in the Arctic. Additionally, there are sensors installed in other monitored residential buildings, which were not assessed in this study due to reduced accessibility to the buildings or lack of coherent data. Furthermore, new buildings have recently been added to the monitoring program. They are relevant to assess when sufficient data has been collected. It is recommended to work with data of at least one year. These additional data from residential buildings can be used to expand the assessments of the current study or for other purposes, such as evaluating the consequences of user behaviour on the hygrothermal conditions in the façades. Additionally, it is recommended to assess the accuracy of the sensors when the measurements are finished.

7.3.2 Identify what buildability is in a Greenlandic context

It was concluded that buildability is essential for the final quality of a building in Greenland. However, this study did not identify exactly how to achieve it. In the discussion of this topic in Section 6.1.3, some suggestions were provided. However, it is recommended to do an extensive study to formulate specific recommendations, e.g., by monitoring current approaches and communication culture and interviewing involved workers and specialists. Such an investigation must, however, be planned thoroughly. A concern is that a questionnaire or interview might not reflect the issues, e.g., if the craftsmen are not aware that the work was conducted inadequately.

References

Abdul Hamid, A., Arfvidsson, J. and Harderup, L.-E. (2022) 'Assessment on the Impact of Interior Insulation on Exterior Walls in Three Swedish Buildings', *2022 Buildings XV International Conference*, pp. 258–267.

Abrahamsen, M.R. (2019) *Urbanization in Greenland exploring the motivating factors of why people move to Nuuk*

AHDR, 2015 (2015) *Arctic Human Development Report . Regional Processes and Global Linkages : edited by Larsen & Fondahl*, *Copenhagen: Nordisk Ministerråd*. Available at: https://www.uarctic.org/news/2015/2/new-report-arctic-human-development-report-volume-ii-published/.

Andersen, J. (1976) 'Selvbyggeri i Grønland', *Tidsskriftet Grønland*. Available at: http://www.tidsskriftetgronland.dk/archive/1976-5-Artikel01.txt.

Andersen, R. (2021) *Impacts of energy renovations on the indoor environment in Greenlandic apartments*. Technical University of Denmark

Arctic Building and Construction (2018) *Evaluering af Arktisk Byggeskik - Projektbeskrivelse*

Arctic Building and Construction (2022) *Delprojekter*. Available at: https://abc-byg.dtu.dk/del-projekter (Accessed: 14 April 2023).

Arctic Centre University of Lapland (2023a) *Definitions of the Arctic*. Available at: https://www.arcticcentre.org/EN/arcticregion/Maps/definitions (Accessed: 30 March 2023).

Arctic Centre University of Lapland (2023b) *The Arctic Region*. Available at: https://www.arcticcentre.org/EN/arcticregion (Accessed: 13 March 2023).

Arctic Portal (2016) *Arctic 10°C Isotherm*. Available at: https://arcticportal.org/maps/download/arctic-definitions/2419-arctic-10-c-isotherm (Accessed: 14 April 2023).

Asiaq (2023) *About Asiaq*. Available at: https://www.asiaq-greenlandsurvey.gl/about-us/ (Accessed: 28 February 2023).

Baumklimatik-Dresden (2022) *DELPHIN*. Available at: http://bauklimatik-dresden.de/delphin/index.php (Accessed: 23 January 2021).

Brandt, E. *et al.* (2023) *SBI-anvisning 277, Fugt i bygninger - teori, beregning og undersøgelse*. 1. BUILD. Available at: https://build-dk.proxy.findit.cvt.dk/anvisninger/Pages/277-277-Fugt-1.aspx#/4-Kritiske-fugtforhold (Accessed: 14 April 2023).

Brown, R. *et al.* (2017) *Snow, Water, Ice and Permafrost in the Arctic (SWIPA)*, *Arctic Monitoring and Assessment Programme*. Available at: https://www.amap.no/documents/doc/snow-water-ice-and-permafrost-in-the-arctic-swipa-2017/1610.

Brozovsky, J., Nocente, A. and Rüther, P. (2023) 'Modelling and validation of hygrothermal conditions in the air gap behind wood cladding and BIPV in the building envelope', *Building and Environment*, 228(November 2022), p. 109917. doi:10.1016/j.buildenv.2022.109917.

Bygge og Anlægsstyrelsen (1995) 'Forskrifter for beregning af bygningers varmetab'

BygInfo (2019) *Lovgivning*. Available at: http://www.byginfo.gl/lovgivning/ (Accessed: 4 April 2023).

Cembrit (2017) *Cembrit Multi Force*. Available at: https://www.cembrit.dk/download/SDK/montagevejledninger/montagevejledning-cembrit-multi-force (Accessed: 31 January 2023).

Cembrit (2018) *Cembrit Windstopper*. Available at: https://www.cembrit.com/download/CHDK/datasheets/cembrit-windstopper-basic-datasheet.
Defo, M., Lacasse, M. and Laouadi, A. (2022) 'A comparison of hygrothermal simulation results derived from four simulation tools', *Journal of Building Physics*, 45(4), pp. 432–456. doi:10.1177/1744259120988760.
Departementet for Boliger og Infrastruktur (2019a) 'Fremtidens Boliger - Siunissami inissiat', p. 40.
Departementet for Boliger og Infrastruktur (2019b) 'Redegørelse af Grønlandske Byggematerialer'
Direktoratet for Boliger og Infrastruktur (2006) 'Bygningsreglement 2006', p. 158.
DMI (2020) *Vejrarkiv*. Available at: https://www.dmi.dk/vejrarkiv/ (Accessed: 16 December 2020).
Ecoinvent (2022) *Ecoinvent Database*. Available at: https://ecoinvent.org/the-ecoinvent-database/ (Accessed: 4 February 2022).
Engelbrechtsen, K. and Jørgensen, M.R. (2023) *Silamiut – Grønlands forhistorie*. Available at: https://silamiut.iatuagaq.iserasuaat.gl/?id=178 (Accessed: 30 March 2023).
EQUA (2018) 'IDA ICE Getting started', (January).
Erbs, D.G., Klein, S.A. and Duffie, J.A. (1982) 'Estimation of the diffuse radiation fraction for hourly, daily and monthly-average global radiation', *Solar Energy*, 28(4), pp. 293–302. doi:10.1016/0038-092X(82)90302-4.
European Centre for Medium-Range Weather Forecasts (2022) *ERA5 | ECMWF*. Available at: https://www.ecmwf.int/en/forecasts/datasets/reanalysis-datasets/era5 (Accessed: 17 January 2023).
Fraunhofer IBP (2018) *WUFI*. Available at: https://wufi.de/en/ (Accessed: 24 March 2023).
Fraunhofer Institute for Building Physics (2022) *WUFI® Mould Index VTT*. Available at: https://wufi.de/en/2017/03/31/wufi-mould-index-vtt/ (Accessed: 26 January 2023).
Friis, N.K. (2022) 'Insulation Thickness Optimizer, ITO'. doi:10.11583/DTU.19672470.
Friis, N.K., Gaarder, J.E. and Møller, E.B. (2022) 'A Tool for Calculating the Building Insulation Thickness for Lowest CO2 Emissions—A Greenlandic Example', *Buildings*, 12(8), p. 1178. doi:10.3390/buildings12081178.
Friis, N.K., Møller, E.B. and Lading, T. (2021) 'Can collected hygrothermal data illustrate observed thermal problems of the façade? - A case study from Greenland', *Journal of Physics: Conference Series*, 2069(1). doi:10.1088/1742-6596/2069/1/012071.
Friis, N.K., Møller, E.B. and Lading, T. (2023a) 'Hygrothermal assessment of external walls in Arctic climates: Field measurements and simulations of a test facility', *Building and Environment*, 238(February), p. 110347. doi:10.1016/j.buildenv.2023.110347.
Friis, N.K., Møller, E.B. and Lading, T. (2023b) 'Hygrothermal conditions in the facades of residential buildings in Nuuk and Sisimiut', *Building and Environment*, 243, p. 110686. doi:10.1016/j.buildenv.2023.110686.
Gaarder, J.E. *et al.* (2023) 'Optimization of thermal insulation thickness pertaining to embodied and operational GHG emissions in cold climates – Future and present cases', *Building and Environment*, 234. doi:10.1016/j.buildenv.2023.110187.
GEUS (2023) *Menneskenes land ved isfjorden*, *Geological Survey of Denmark and Greenland*. Available at: https://www.geus.dk/udforsk-geologien/viden-om/viden-om-ilulissat-isfjord/menneskenes-land-ved-isfjorden (Accessed: 14

April 2023).
Ghazaryan, T. and Tariku, F. (2021) 'Hygrothermal performance assessment of split insulated cork wall assemblies under various moisture load conditions', *Journal of Physics: Conference Series*, 2069(1), p. 012031. doi:10.1088/1742-6596/2069/1/012031.
Google (2022) *Google Maps*. Available at: https://www.google.com/maps (Accessed: 4 November 2021).
Greenland National Museum (2016) *Lidt om Grønlands bygningskultur*. Available at: https://issuu.com/natmus.gl/docs/gr__nlandsk_byggeskik_/1.
Grønlands Statistik (2021) *Summerede graddageværdier [END1SUM]*. Available at: https://bank.stat.gl/pxweb/da/Greenland/Greenland__EN__EN30/ENX1SUM.px/ (Accessed: 3 November 2021).
Grydehøj, A. (2014) 'Constructing a centre on the periphery: Urbanization and urban design in the Island city of Nuuk, Greenland', *Island Studies Journal*, 9(2), pp. 205–222. doi:10.24043/isj.302.
Guldborgsund Forsyning (2021) *Graddage*. Available at: https://www.guldborgsundforsyning.dk/graddage/ (Accessed: 19 October 2021).
Hejazi, B. *et al.* (2019) 'Hygrothermal Simulations Comparative Study: Assessment of Different Materials Using WUFI and DELPHIN Software', in, pp. 4674–4681. doi:10.26868/25222708.2019.211033.
Hendriksen, K. (2015) *Grønlands bygder*
Hendriksen, K. (2016) 'Greenland island infrastructures – energy challenges to the fishing industry'. Available at: https://orbit.dtu.dk/en/publications/greenland-island-infrastructures--energy-challenges-to-the-fishing-industry(3d24af13-de3c-407f-9b33-a8103b696053).html.
HOFOR (2022) *Miljødeklaration for fjernvarme*. Available at: https://www.hofor.dk/baeredygtige-byer/beregn-co2/miljoedeklarationer/miljoedeklaration-for-fjernvarme/ (Accessed: 19 October 2021).
Huerto-Cardenas, H.E. *et al.* (2020) 'Validation of dynamic hygrothermal simulation models for historical buildings: State of the art, research challenges and recommendations', *Building and Environment*, 180(June), p. 107081. doi:10.1016/j.buildenv.2020.107081.
Huijbregts, M.A.J. *et al.* (2017) 'ReCiPe2016: a harmonised life cycle impact assessment method at midpoint and endpoint level', *International Journal of Life Cycle Assessment*, 22(2), pp. 138–147. doi:10.1007/s11367-016-1246-y.
Hukka, A. and Viitanen, H.A. (1999) 'A mathematical model of mould growth on wooden material', *Wood Science and Technology*, 33(6), pp. 475–485. doi:10.1007/s002260050131.
IAPP's committee (2002) *Byggeriets effektivisering*
Innovative Sensor Technology (no date) 'HYT 221 Digital Humidity and Temperature Module', p. 3.
Institut for Menneskerettigheder (2020) *Retten til bolig - status i Grønland*
ISO (2012) *ISO 13788, Hygrothermal performance of building components and building elements – Internal surface temperature to avoid critical surface humidity and interstitial condensation – Calculation methods*. second edi
ISO (2019) 'ISO 22111, Bases for design of structures - General requirements'
Karlsson, F. and Moshfegh, B. (2013) *A Low-Energy Building Project in Sweden - the Lindås Pilot Project*, *Sustainability, Energy and Architecture: Case Studies in Realizing Green Buildings*. Elsevier. doi:10.1016/B978-0-12-397269-9.00012-8.

Klepeis, N.E. *et al.* (2001) 'The National Human Activity Pattern Survey (NHAPS): A resource for assessing exposure to environmental pollutants', *Journal of Exposure Analysis and Environmental Epidemiology*, 11(3), pp. 231–252. doi:10.1038/sj.jea.7500165.

Kommuneqarfik Sermersooq (2021) *19.000 indbyggere i Nuuk*. Available at: https://sermersooq.gl/da/2021/09/19-000-indbyggere-i-nuuk/ (Accessed: 24 February 2022).

Kotol, M. (2012) 'Survey of occupant behaviour, energy use and indoor air quality in Greenlandic dwellings', *Proceedings at the 5th International Building Physics Conference (IBPC 2012), Kyoto, Japan, 7.* [Preprint]

Kotol, M. *et al.* (2014) 'Indoor environment in bedrooms in 79 Greenlandic households', *Building and Environment*, 81, pp. 29–36. doi:10.1016/j.buildenv.2014.05.016.

Kragh, J. and Svendsen, S. (2004) *Anvisning Beregning af bygningers varmebehov i Grønland*

Kukk, V. *et al.* (2022) 'Designing highly insulated cross-laminated timber external walls in terms of hygrothermal performance: Field measurements and simulations', *Building and Environment*, 212(November 2021), p. 108805. doi:10.1016/j.buildenv.2022.108805.

Kumar, A. *et al.* (2018) '5 Hydropower'. Available at: https://www.ipcc.ch/site/assets/uploads/2018/03/Chapter-5-Hydropower-1.pdf (Accessed: 18 February 2022).

Lading, T. (2015) 'Barriers and drivers for energy- efficient homes in Greenland'

Lading, T. and Møller, E.B. (2019) 'Evaluering af Unaaq 13-19 BYG R-407 , 2019', *BYG R-407*, p. 54. Available at: https://abc-byg.dtu.dk/-/media/Centre/ABC-BYG/web2-0/relaterede-projekter/BYG-R-407-2019_Unaaq-13-19.ashx?la=da&hash=0D84FD3B1CB48490F2D59A159B14C68D16E21246.

Lam, P.T.I., Wong, F.W.H. and Chan, A.P.C. (2006) 'Contributions of designers to improving buildability and constructability', *Design Studies*, 27(4), pp. 457–479. doi:10.1016/j.destud.2005.10.003.

Larsson, L. *et al.* (2021) 'Curing building related illnesses by using an emissions barrier', *Journal of Physics: Conference Series*, 2069(1), pp. 1–3. doi:10.1088/1742-6596/2069/1/012241.

Lindsey, R. and Dahlman, L. (2021) *Climate Change: Global Temperature*. Available at: https://www.climate.gov/news-features/understanding-climate/climate-change-global-temperature (Accessed: 3 November 2021).

Luc, K.M., Kotol, M. and Lading, T. (2016) 'Energy-efficient Building in Greenland: Investigation of the Energy Consumption and Indoor Climate', *Procedia Engineering*, 146, pp. 166–173. doi:10.1016/j.proeng.2016.06.368.

Månhardt, G. *et al.* (2021) 'Moisture safety in ventilated cathedral roofs', *Journal of Physics: Conference Series*, 2069(1), p. 012018. doi:10.1088/1742-6596/2069/1/012018.

Marott Brandt, J. (2021) 'Arktisk Byggeri - En vejledende og kritisk undersøgelse'

Møller, E.B. and Lading, T. (2020) 'Current building strategies in Greenland', *E3S Web of Conferences*, 172. doi:10.1051/e3sconf/202017219004.

Møller, E.B. and Lading, T. (2021) 'Preliminary assessment of the building design of a new test house in Nuuk, Greenland', *Journal of Physics: Conference Series*, 2069(1), pp. 1–4. doi:10.1088/1742-6596/2069/1/012228.

Mukhopadhyaya, P. *et al.* (2007) 'Hygrothermal properties of exterior claddings, sheathing boards, membranes, and insulation materials for building envelope design', *Thermal Performance of the Exterior Envelopes of Whole Buildings*, (1), pp. 1–13.

Naalakkersuisut (2012) *Vores fremtid - dit og mit ansvar - på vej mod 2025*. Available at: https://www.ft.dk/samling/20121/almdel/gru/bilag/16/1200391.pdf.
Naalakkersuisut - Government of Greenland (2021) 'BR21 Høringsudgave', (13).
Nordatlantens Brygge (2020) *Blok P, The final tribute*. Available at: https://www.nordatlantens.dk/en/exhibitions/blok-p-in-nuuk/#_ftnref1 (Accessed: 14 April 2023).
Nordisk Samarbejde (2020) *Bolig i Grønland*. Available at: https://www.norden.org/da/info-norden/bolig-i-groenland (Accessed: 14 April 2023).
Nukissiorfiit (2020) *Årsregnskab 2020*. Available at: https://nukissiorfiit.gl/media/06032524-3bb3-4622-8cd7-f65c523d4446/7bEfjw/docs/Nukissiorfiit_Årsrapport_2020_dk.pdf (Accessed: 20 November 2021).
Nukissiorfiit (2022) *Nukissiorfiit Årsregnskab 2021*. Available at: https://nukissiorfiit.gl/media/ef1e98ef-1172-4a60-8c89-a260bea938d7/9fRguA/docs/Nukissiorfiit_årsregnskab_21_DK_web.pdf (Accessed: 2 February 2023).
Ojanen, T. *et al.* (2010) 'Mold Growth Modeling of Building Structures Using Sensitivity Classes of Materials', *ASHRAE Buildings XI Conference, Dec. 5-9, 2010 Cleawater Beach, Florida* [Preprint]
One Click LCA (2021) *Life Cycle Stages*. Available at: https://oneclicklca.zendesk.com (Accessed: 3 November 2021).
Orgill, J.F. and Hollands, K.G.T. (1977) 'Correlation equation for hourly diffuse radiation on a horizontal surface', *Solar Energy*, 19(4), pp. 357–359. doi:10.1016/0038-092X(77)90006-8.
Ottosen, L.M. (2006) 'Lavenergihuset i sisimiut', pp. 1–2.
Patursson, T. and Sode, T.R. (2020) *Indeklimaets betydning for helbredet*, *Videncentret Bolius*. Available at: https://www.bolius.dk/indeklimaets-betydning-for-helbredet-17406 (Accessed: 24 March 2023).
Rahiminejad, M. and Khovalyg, D. (2021) 'Review on ventilation rates in the ventilated air-spaces behind common wall assemblies with external cladding', *Building and Environment*, 190, p. 107538. doi:10.1016/j.buildenv.2020.107538.
Ryberg, M.W. *et al.* (2021) 'Comparative life cycle assessment of four buildings in Greenland', *Building and Environment*, 204. doi:10.1016/j.buildenv.2021.108130.
Ryberg, M.W. *et al.* (2022) 'Life-cycle assessment of construction errors on buildings in Greenland', *IOP Conference Series: Earth and Environmental Science*, 1085(1), p. 66DUMMY. doi:10.1088/1755-1315/1085/1/012064.
Schwalm, C.R., Glendon, S. and Duffy, P.B. (2020) 'RCP8.5 tracks cumulative CO 2 emissions', *Proceedings of the National Academy of Sciences*, 117(33), pp. 19656–19657. doi:10.1073/pnas.2007117117.
Sermitsiaq (2020) 'Ny byggemetode vinder frem', *Sermitsiaq.AG*. Available at: https://sermitsiaq.ag/node/222889 (Accessed: 16 March 2023).
Sermitsiaq AG (2010) '810.000 kroner for en byggegrund i Nuuk', *Sermitsiaq AG*. Available at: https://sermitsiaq.ag/node/76429.
SimaPro (2022) *LCA software for informed-change makers*. Available at: https://simapro.com/ (Accessed: 24 February 2022).
Slyngborg, A. (2021) *Study of Energy Performance and Optimization for Buildings in Greenland A Case Study of Prøvehuset in Nuuk for Potential Purposes*
Statens Byggeforskningsinstitut (2017) 'SBI-anvisning 258 om bygningsreglement 2015', p. 438. Available at: https://build.dk/anvisninger/Pages/258-Anvisning-om-

Bygningsreglement-2015-2.aspx.
Statistics Greenland (2010) *Dwellings by ownership and place [BOE004]*. Available at: https://bank.stat.gl/pxweb/en/Greenland/Greenland__BO__BO99/BOX004.px/chart/chartViewColumnStacked100/ (Accessed: 14 April 2023).
Statistics Greenland (2017) *Byggeomkostningsindekset pr. 1. juli 2017*
Statistics Greenland (2021) *Actual energy consumption [ENE1ACT]*. Available at: https://bank.stat.gl/pxweb/en/Greenland/Greenland__EN__EN20/ENX1ACT.px/ (Accessed: 3 April 2023).
Statistics Greenland (2022) 'Greenland in Figures 2022'. Edited by N. Kleemann, p. 36. Available at: //stat.gl/publ/en/GF/2022/pdf/Greenland in Figures 2022.pdf.
Steenholdt, P. (2019) 'Håndværker om nedrivning af Blok 1 i Nuuk: Det var alt for tidligt', *KNR*. Available at: https://knr.gl/da/nyheder/25-december-håndværker-om-nedrivning-af-blok-1-i-nuuk-det-var-alt-tidligt (Accessed: 14 April 2023).
Svendsen, S. and Kragh, J. (2004) 'Lavenergihus i Sisimiut Beregnet varmebehov Rapport R-103 BYG · DTU'
Technical University of Denmark (2022) *Om projektet - ABC - Arctic Building and Construction*. Available at: https://abc-byg.dtu.dk/om-projektet (Accessed: 5 May 2022).
Time, B. *et al*. (2023) 'Moisture safety strategy for construction of CLT structures in a coastal Nordic climate', in *Nordic Symposium on Building Physics*. Available at: https://prod-aaudxp-cms-001-app.azurewebsites.net/media/0r0k03eh/393_nsb2023_scientificpaper_cameraready.pdf.
Vadstrup, S. and Schultz-Lorentzen, H. (1994) 'Bevar Grønlands bygningskultur og bygningshistorie'. Det Grønlandske Selskab
Vladykova, P. *et al.* (2012) 'Low-Energy House in Arctic Climate: Five Years of Experience', *Journal of Cold Regions Engineering*, 26(3), pp. 79–100. doi:10.1061/(ASCE)CR.1943-5495.0000040.
Vogelsang, S., Fechner, H. and Nicolai, A. (2013) *Delphin 6 Material File Specification, Version 6.0*. Available at: https://nbn-resolving.org/urn:nbn:de:bsz:14-qucosa-126274.
Wang, R., Ge, H. and Baril, D. (2020) 'Moisture-safe attic design in extremely cold climate: Hygrothermal simulations', *Building and Environment*, 182(July), p. 107166. doi:10.1016/j.buildenv.2020.107166.
World weather (2023) *Weather archive in Sisimiut*. Available at: https://world-weather.info/archive/greenland/sisimiut/ (Accessed: 22 April 2023).
World Weather (2023) *Weather archive in Nuuk*. Available at: https://world-weather.info/archive/greenland/nuuk/#t2 (Accessed: 22 April 2023).

Part II

Papers

I. Can Collected Hygrothermal Data Illustrate Observed Thermal Problems of the Façade? - A Case Study from Greenland

Naja K. Friis, Eva B. Møller, and Tove Lading

Journal of Physics: Conference Series 2069 012071 (2021)
doi: 10.1088/1742-6596/2069/1/012071

I

Can collected hygrothermal data illustrate observed thermal problems of the façade? – A case study from Greenland

N K Friis[1], **E B Møller**[1] **and T Lading**[1]

[1]Technical University of Denmark, Department of Civil Engineering, Brovej, Building 118, 2800 Kgs. Lyngby

Corrosponding author: nfri@byg.dtu.dk

Abstract. Buildings are more vulnerable to faults in design and construction, when exposed to the extreme Greenlandic climate, however, most new materials and designs have not been tested for Arctic conditions. Thus even minor errors can result in failures like mould growth, discomfort, and unnecessary heat loss. Rekognizing the source of the error can be difficult, yet valuable. But how can it be identified whether the error lies in the design or quality of workmanship? This paper describes a case study from Nuuk, Greenland, where a new mineral wool insulation system was implemented. Residents were complaining about draft and cold areas. An investigation revealed that inaccurate use of the system caused several problems. Simulations of the exterior wall performance were conducted and compared to measurements. This paper discusses whether these measurements and simulations support the identified issues, and therefore if this kind of general surveillance of exterior walls can be used to determine the total performance of an exterior wall. The paper concludes that the collected data can support the issues of the complaints, and that the fundamental reasons for the problems are the design, the precision of the casted concrete and the lack of a wind barrier protecting the insulation.

1. Introduction

The arctic climate is harsh due to a combination of cold temperatures, precipitation, and strong winds. In the case study, located in Nuuk, Greenland, temperatures within a year span from -18.9 °C to 18.4 °C with mean -0.4 °C and median 0.8 °C. 12 % of the year (42 days), the temperatures are below -10 °C. In 27 % of that time the wind speeds were 8 m/s or more. The weather conditions are therefore more challenging than the typical climate in Europe for which many constructions are developed originally.

Before introducing new building materials and methods to the marked, these are usually tested under controlled conditions, but the practical aspects are difficult to test or assess before introducing it to reality, where the conditions are no longer controlled. Sometimes, this results in inexpedient situations, where mistakes or unforeseen challenges result in a product or design, which does not comply with the expectations. This scenario occurred in a multi storey building in Nuuk, where a new insulation material of mineral wool was introduced to the construction sector in Greenland. The residents of the buildings started complaining about draft, cold floors and walls and general discomfort in the apartments. Often complaints like these are treated by measuring the indoor temperature over some time to determine if the residents' complaints are justified. In this case, the owner chose a more thorough investigation to pinpoint the problems and determine the cause. The investigation was performed in February 2019, almost 2 years after the building was finished. Because the insulation system was new, the building had been chosen as a case study in another project and the façade was therefore already equipped with

sensors. As the sensors were placed before the first winter, the location was chosen randomly and was therefore not necessarily placed in one of the apartments with most complaints.

This paper aims to investigate if the observations from the inspection and the collected data tells the same story. Will the data from the sensors reveal the observed thermal issue and can this kind of surveillance be used to determine how a wall performs? The scope considers only the thermal quality of the insulation system and how it is installed. General issues of the building, such as thermal bridges, leaks and ventilation humidity content or risk of mould were relevant [2] but not reported here.

2. The investigated structure

The case study encompassed four identical three-storey buildings, each with 12 apartments, placed in a weather exposed area in Nuuk, Greenland. Usually, exterior walls in Greenlandic multi storey buildings consist of a wooden structure with insulation and a vapour barrier on the internal side and a wind barrier on the external side, which is finished with a ventilated cavity and external cladding. The insulation is thereby protected against precipitation and wind penetration, ensuring high performance. In this case, the vapour barrier also acts as an air barrier, ensuring a tight construction with limited air leaks. The term "wind barrier" describes a membrane, with the purpose of protecting the construction from cold winds [3].

In this specific case, the wall was a heavy structure of in-situ casted concrete with an external layer of very firm mineral wool (λ=0.033 and ρ=80 kg/m^3). The insulation was followed by an air cavity and an external cladding of a composite material. In theory, the design concept of insulation being applied tightly to the concrete makes a wind barrier redundant, as the wind needs space to create convection and the concrete acts as an air barrier. The insulation mats had two flexible zones (two adjacent sides of the mat) so the mats could be pressed tightly together without gaps between them. Figure 1 illustrates the construction along with green dots indicating the placement of the installed sensors.

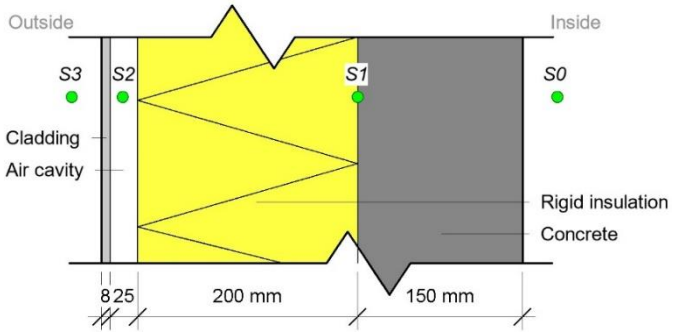

Figure 1. Detail of the new wall insulations system in Greenland. Composition of the investigated wall and green dots indicating the sensor locations. All dimensions are given in mm.

3. Methods and materials

This section will introduce the construction of the exterior wall, and the three methods applied in the investigation of the building: An inspection, data collection including assessment of data and finally, simulations conducted in Delphin.

3.1. Inspection and photos

The inspection was performed February 27th 2019, a sunny day with outdoor temperature of -4°C and no wind. It included measurements of indoor temperature and relative humidity, thermography to identify cold areas, smoke sticks to identify air flows and visual observations. Four apartments were inspected from the inside. The exterior wall of all four buildings was visually inspected from the outside. Furthermore, the evaluation also included photos from prior visits at the construction site and interviews with residents and managers.

I

3.2. Data from sensors.

The hygrothermal performance of a south facing façade of one of the apartments has been monitored since September 2018, by four sensors (see Figure 1) measuring temperature and relative humidity every hour. Sensor S0 measured the conditions in the apartment. S1 measured the conditions between the concrete wall and the insulation, while S2 was placed in the air cavity and S3 measured the conditions outside the building. S3 was placed in a box, sheltered from direct sunlight and precipitation. The sensors are of type "HYT 221" from Innovative Sensor Technology [4], and can measure relative humidity and temperature digitally with an accuracy of ±1.8% RH at +23°C (in the range 0% RH to +90% RH) and ±0.2K (in the range 0°C to +60°C).

3.3. Weather data

Asiaq and DMI, governmental meteorological institutions located in Greenland and Denmark respectively, provided weather data for Nuuk. The weather station of Asiaq is located at 64.183333 N and 51.730833 V. The data included date, time, relative humidity, precipitation, wind direction, wind speed, air pressure, air temperature, and incoming short-wave radiation. The latter is also called "global radiation" and includes all short-wave radiation measured on a horizontal plane placed in 2 m height.

3.4. Simulations

Dynamic 1D simulations with DELPHIN 6.1.0, developed by Baumklimatik-Dresden [5], were conducted to get an indication of the theoretical expectations. The chosen materials and the relevant properties are presented in Table 1. The materials were chosen from the Delphin database, as no material properties were measured in this study. The insulation material, however, is defined for the specific product applied. The exact air flow in the cavity could not be defined due to insufficient data. Instead the air flow is considered constant, with a value of 250 h^{-1} based on literature [6].

Table 1. Properties of materials used in Delphin.

Material	Density ρ [kg/m^3]	Heat capacity cp [J/kgK]	Thermal conductivity λ [W/mK]	Water vapour resistance factor μ [-]	Air change rate ACH [h^{-1}]	ID
Concrete	2400	900	2.100	110	-	56
Insulation	80	840	0.033	1	-	645
Ventilated air cavity	1.3	1.050	0.067	1	250	15
Cladding	1158.7	1.188	0.313	26	-	654

The internal boundary conditions for the Delphin model included relative humidity and temperature, which were obtained from the sensor S0 as hourly values. The external boundary conditions included 7 parameters: Temperature, relative humidity, horizontal rain, wind direction, wind velocity, diffuse radiation, and direct radiation. These were obtained from the weather data from Asiaq (see Section 3.3. However, the files only provided global radiation; sum of direct, diffuse, and reflected short-wave radiation, while Delphin uses direct and diffuse radiation. Reflected short-wave radiation is neglected.

The fractions of direct and diffuse radiation can be estimated from the Global radiation. It is an extensive method based on time and location, which is used to define the extra-terrestrial radiation. From this and the global radiation, the hourly clearness index, K_t, is calculated indicating the clearness of the atmosphere. Finally K_t is used in the "Orgill & Hollands" method resulting in the diffuse radiation, leaving only a simple calculation for defining the direct radiation too [7].

The output files were defined as points in the model. S1 and S2 were placed according to the sensors in reality (presented in Figure 1). The initial conditions in the model were defined to be 15°C and 80% relative humidity. The simulation was performed for 1 year, equal to 8,760 measure points, which was chosen based on the intention of having as few missing values as possible, while complying with Delphin's default settings of managing maximum a year. The chosen period begins 2019-10-02 at 1 pm.

Despite the careful choice of the presented period, there are lacking some values in the included data. Especially, wind direction and wind speed have some holes. Delphin demands input for every hour, why the holes must be filled with suitable values.

The missing values for air pressure were replaced with the mean value, while temperature and relative humidity were defined as a mean of the two values prior and the following values. For precipitation 0 was chosen to fill the gaps. Filling the gaps of radiation was more circumstantial. In cases missing single data, the surrounding values of the specific day were interpolated, and when a whole day was missing it was filled by a mean of the previous day and the following day, respecting the respective hours. The issue of wind direction and wind speed was challenging as these values come and go within hours, there is no way to estimate the missing values, however, the missing values were filled in with mean values unless, it was a only few in a row, which could be solved by interpolation.

4. Results and analysis

This section presents the results and analysis of the described methods.

4.1. Inspection and photos

The inspection revealed different issues, of which most could be logically explained by visiting the building and performing simple measurements. The main issues considered at the inspection were draft, cold floors, air flow between the apartments, and cold walls, of which the latter is of highest interest in this paper. The thermography revealed thermal bridges and cold floors, but no specific cold wall surfaces. Fortunately, a look on the pictures from the construction period, could reveal that the new type of insulation was not installed according to the instructions from the manufacturer. This has led to gaps between the insulation pieces. Furthermore, the product sheet demands a very smooth surface, leaving a tolerance of the concrete surface of only ±2 mm, which is basically unrealistic for in-situ casted concrete with the technology and facilities available in Greenland.

As there is no wind barrier between the insulation and the free space of the air cavity, there is risk of cold air blowing through the gaps between the batts to the concrete wall where the risk of another unintentional air cavity was identified (Figure 2), caused by the irregularities of the concrete. When the air has entered the cavity, it can flow along the concrete walls and potentially cool it down depending on the season. This phenomenon compromises the insulating properties of the insulation. In short, the tolerances are not kept, and thus the design works different than intended. If a wind barrier had been implemented in the design, the consequences might have been reduced considerably.

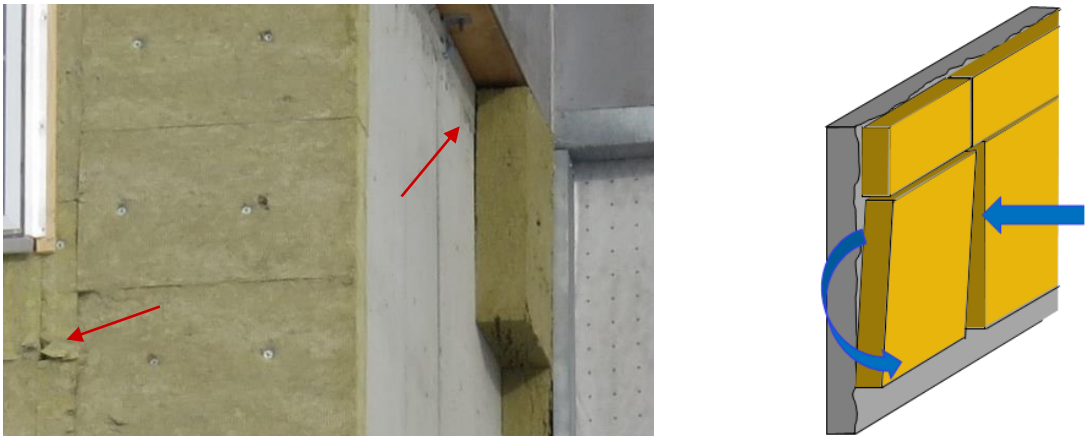

Figure 2. Illustrations of how wind can penetrate the insulation layer due to gaps between insulation mats and uneven concrete surfaces. Left: Photo taken during construction. Right: graphic illustration, which may exaggerate the situation.

4.2. Data from sensors and simulations

According to the data from the sensors, the temperatures at S2 and S3 follow each other closely despite the big instabilities. This is no surprise, as S2 is placed in fresh air as S3, with the only difference, that the air flow is usually reduced in an air cavity like this. This means that direct solar radiation might heat up the air in the cavity to be slightly warmer than outside. However, in practice, S3 is placed in a box as well, meaning that the conditions are quite similar for the two sensors. Furthermore, S0 is the foundation of the input data to the indoor climate, which leaves S1 as the main point of interest for this section.

Figure 3 illustrates the measured (black line) and simulated temperatures at S1. The orange line is based on the simulation with original λ-value of the insulation (0.033 W/mK). Apparently, the insulation is reduced due to convection. To illustrate the size of the reduction, simulation-scenarios with higher lambda values were performed although this represents conductivity, a different transport mechanism than convection. The average deviance of the annual mean of the sensor data for S1 and the simulated data for the original value of λ=0.033 W/mK is -4.1°C, calculated by formula (1). The deviance decreases to -3.0°C at λ=0.1 W/mK and -0.6°C at λ=0.3 W/mK. The simulated scenarios are chosen in an attempt to approach the measured data.

$$deviance = \frac{\sum T_{sensor}}{8760} - \frac{\sum T_{simulation}}{8760} \quad (1)$$

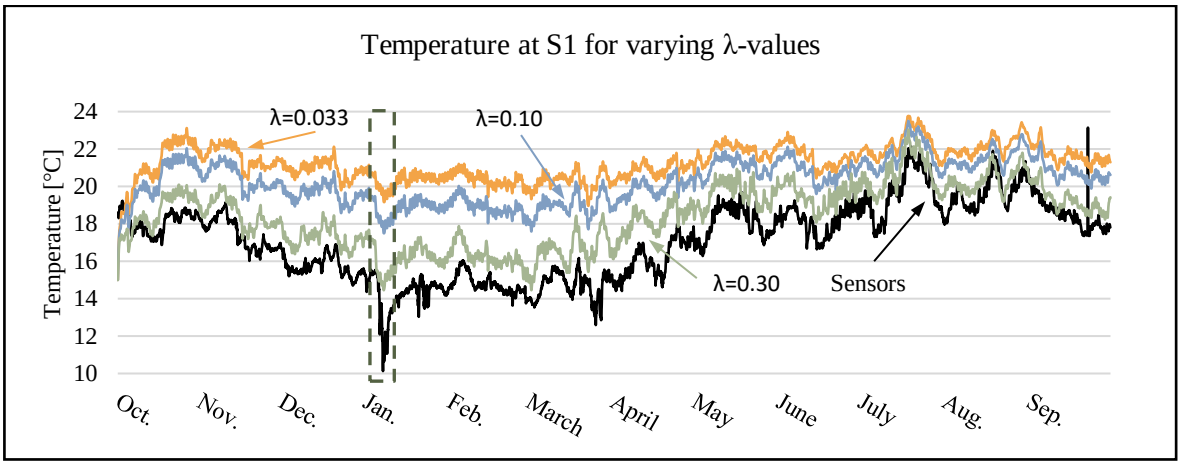

Figure 3. The difference between measured and simulated data, including two variants of insulation, in a 1-year period from 02-10-2019. The box marks the area shown in Figure 4.

The January peak towards 10°C, marked with the dash line box in Figure 3, became of interest. Therefore, it was investigated how the weather conditions were at that time, especially if the wind conditions were of importance as suspected. The peak is appearing at 1 PM, and there is some solar radiation, however it should be considered as very cloudy to no sun (global radiation of 25 W/m^2).

In Figure 4, a short period of time, surrounding the event, is presented. The black line indicates the temperature measured by the sensor and the grey shadow indicates the wind speed, which is high at this point. However, it is not higher than at other times, where the temperature is affected less. The air temperature might be the reason, being low at the time. One last aspect is the orientation of the wind, which is presented as a factor of how critical it is. Due to the orientation of the wall, the most critical wind directions are from south, spanning from SW to SE, while the least critical directions are between E and W. However, there is a potential risk from wind coming from the last two spans, as the wind in these directions might hit the corners. The factors given are 8 for risky, 4 for potential risk and 0 for no risk, meaning that there is a potential risk to the wind direction in this case.

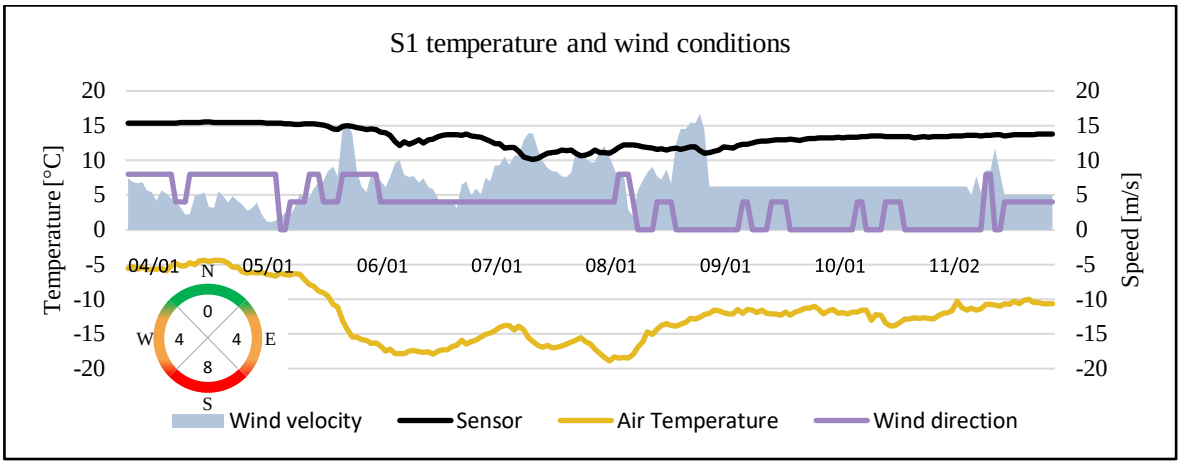

Figure 4. A graph presenting the measured temperatures at S1 along with the weather conditions.

The tendency in Figure 5 is that the temperature deviance increases with higher wind speed, while there is a general deviance of 3-4 °C, even with low wind speeds. However, the coefficient of determination (R^2) is very small, and contrary to what was expected, the tendency is similar for wind from north and south. It might be caused by wind entering at the corners creating turbulence, where the local wind speed and direction is different from what was observed at the weather station. The gap between the insulation mats is permanent and will probably contribute more to the cooling of the concrete wall than if it was only forced convection through mineral wool.

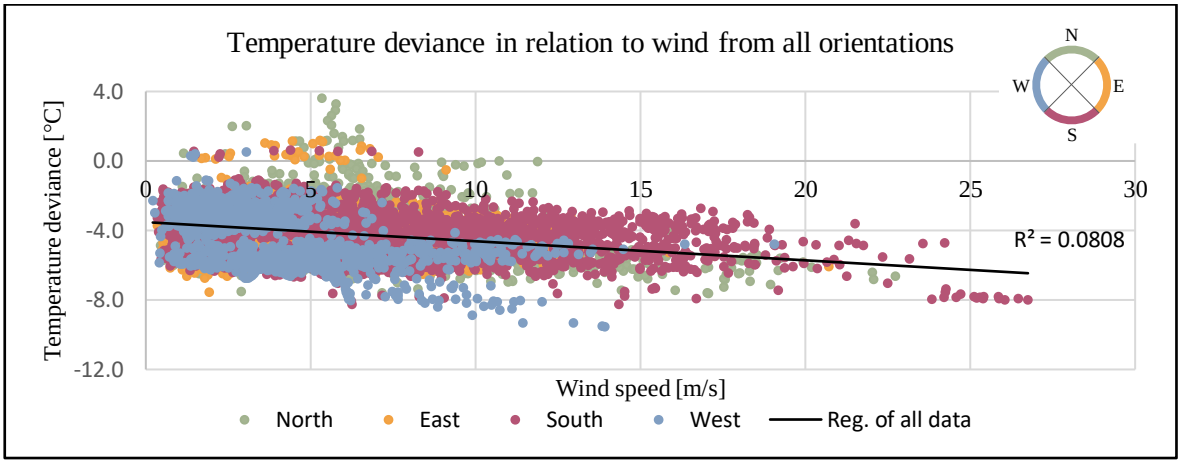

Figure 5. Temperature deviance as a function of wind speed in the four directions

5. Discussion

This study is based on measurements as well as simulations. Both parts contain uncertainties that must be addressed. Furthermore, the implications and the general relevance of the study must be discussed.

5.1. Uncertainties for inspection and measurements

The inspection was performed during wind still and relatively warm conditions, which was not ideal conditions to look for issues expected to be more significant under cold windy conditions. Therefore, the inspection itself was less useful compared to photos from the construction phase and interviews. The investigation showed that the complaints were not caused by unrealistic expectations from the residents.

Although the sensors were calibrated prior to installation, there is always a risk of them losing the calibration. As the measured temperatures in general were lower than in the simulations, this could be a part of an explanation. Additionally, the installation of the sensors is done by cutting out pieces of the

wall to insert the sensors in the respective layers. If the pieces are not put back properly, this might cause uncertainties – especially in relation to cold winds. There was extra focus on this during installation.

5.2. Uncertainty in simulations

Many elements are included in simulations. The inputs are based on measurements from the sensors, which are already at risk of uncertainties, and from weather data, for which the same counts. In general, there were some missing data – especially in the weather data. It was attempted restored, but it is impossible to predict weather into this level of detail. Additionally, the properties of the materials used in the construction are estimated not measured. The simulation was simplified; as a 1D simulation although the construction included a ventilated air gap, and the ventilation was estimated as a constant air change rate. A sensitivity analysis of the air flow has been performed and shows that increasing the airflow by 100% (to 500 h^{-1}) leads to a maximum temperature change of 0.07 °C. Thus, the simplification is acceptable. It was tested how different ways to interpret the global radiance of the weather files would influence the differences between measured and simulated temperature. This is shown in Figure 6. In the same figure it is shown how the wind speed has an effect on the temperature difference.

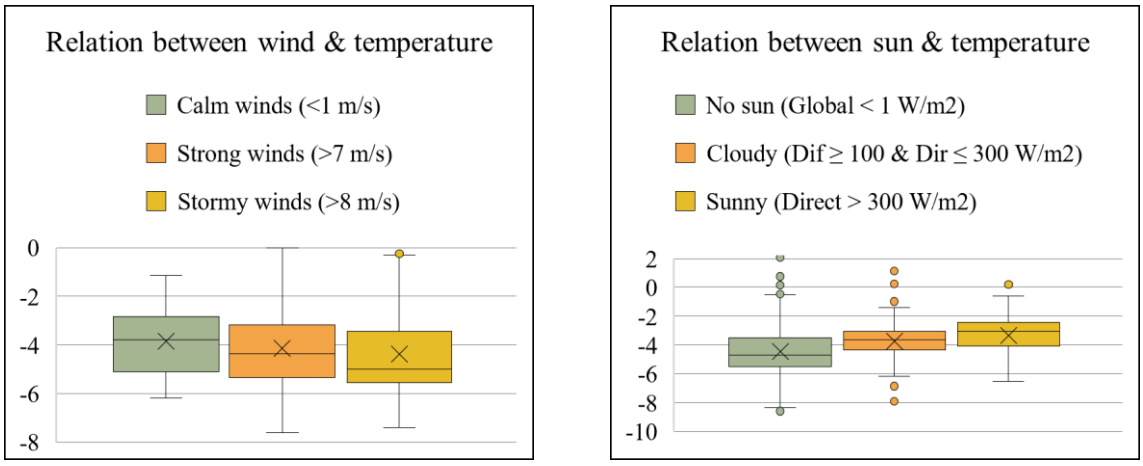

Figure 6. Box plots showing how the temperature difference between measured and simulated temperature, depending on how the wind speed has an influence (left) and how global radiation from the weather files is interpreted (right).

The simplifications cannot alone account for the differences in measured and simulated temperature, the wind speed also seems to have an effect. If the measurements are correct, there must be a fault in the construction.

5.3. Reduced insulation effect

The inspection, the photos from the construction process, the dialogues with the residents and the measurements all indicate reduced effect of the insulation, possibly by faulty use of a new insulation product. It is not surprising, that faulty installation reduces the insulation effect and that was not the main goal of this analysis. The aim was to investigate if general measurements could reveal this kind of faults where it was expected to be a patchy issue, scattered around the external walls rather than an even distribution of cold air entering the construction. Thus, the probability that the sensors were placed exactly in one of these areas was considered very limited. Still, the results of the analysis suggest that the sensors detected this issue. Whether this is luck or due to the issue being widespread could probably be defined by a new inspection at a time with suitable weather conditions. But it seemed that the insulation effect was reduced by a factor 10, as the temperatures resembled simulated temperatures with a material of a λ-value 10 times higher than the expected. This might have been reduced considerably if there had been a wind barrier. Enhancing airtightness of the insulation layer itself seems less realistic.

In principle, the issue is caused by faulty application of the material, but it can be argued that the dissatisfactory workmanship is rooted in bad design decisions. It must be expected that state of the art technologies for the location of any construction are respected in a design phase. If the general tolerances of in-situ casted concrete in Greenland had been considered, the choice might have been different, resulting in buildings of higher quality.

5.4. General perspective

If it is pure luck that the sensor was placed in an area with the problem, it does not necessarily reduce the potentials of measuring the conditions through a wall, though the measurements might not be able to stand alone. This counts in two ways. First, if the sensors provide data, with no unexpected twists, it might not mean that the building is designed and or constructed optimally. Second, collecting the measurements from different houses might tell more about the construction sector in Arctic climate and about the individual houses, than stand-alone examples as the one presented here. Therefore, several other buildings with the same construction are monitored over several years.

6. Conclusion and future work

In four buildings in Nuuk there had been complaints about thermal comfort. The insulation system used in these buildings was new to the Arctic and did not contain a wind barrier. The buildings were investigated through an inspection with simple measurements and interviews, photos taken during the construction phase and long-time measurements of temperature behind the insulation. The most likely reason for the cold walls were discovered to be convection though gaps in the insulation due to no wind barrier. This was mainly discovered through the photographs from the construction phase but supported by the other findings. Although the problem was expected only to occur as isolated incidents at the exterior wall it could be detected by long-time measurements as well. It could be a coincidence that the sensor was placed in an area with this problem, however, in this case the collected data could support the observed problems. The reason for the issues seems to build on insufficient design decisions, making it challenging for the workers to apply the product correctly. This case proves the combination of the unforgiving arctic climate, uneven concrete surfaces, and lack of wind barriers to be bad.

It is the intention to work more with this topic in the nearest future, why more data is currently being collected for further analysis and investigation. Hopefully, it can lead to general recommendations for how to build in Arctic climate.

Acknowledgments

The monitoring of the buildings is a part of the ABC-project (Arctic Building and Construction). A project financially supported by DTU, Knud Højgaards Fond, A. P. Møllers Fond, Naalakkersuisut and Kommuneqarfik Sermersooq.

References

[1] Lading T and Møller B 2019 *Evaluering af Unaaq 13-19 Byg R-407* (Denmark) p 54
[2] Langmans J, Klein R, De Paepe M, and Roels S, *Potential of wind barriers to assure airtightness of wood-frame low energy constructions, Energy Build.*, vol. 42, no. 12, p. 2376–2385, 2010, doi: 10.1016/j.enbuild.2010.08.021.
[3] Innovative Sensor Technology *HYT 221 Digital Humidity and Temperature Module Optimal for all general purpose humidity applications* p 3
[4] Baumklimatik-Dresden *DELPHIN* Available: http://bauklimatik-dresden.de/delphin/index.php. [Accessed: 23-Jan-2021].
[5] Langmans J and Roels S 2015 *Experimental analysis of cavity ventilation behind rainscreen cladding systems: A comparison of four measuring techniques, Build. Environ.*, vol. 87, pp. 177–192, doi: 10.1016/j.buildenv.2015.01.030.
[6] Duffie J and Beckmann W 1980 *Solar Engineering of Thermal Processes* p 919

II. A Tool for Calculating the Building Insulation Thickness for Lowest CO_2 Emissions - A Greenlandic Example

Naja K. Friis, Jørn Emil Gaarder, and Eva B. Møller

Buildings, 12(8) (2022)
doi:10.3390/buildings12081178

II

buildings

MDPI

Article

A Tool for Calculating the Building Insulation Thickness for Lowest CO_2 Emissions—A Greenlandic Example

II

Naja Kastrup Friis [1,*], Jørn Emil Gaarder [2] and Eva Birgit Møller [1]

[1] Department of Civil and Mechanical Engineering, Technical University of Denmark, Brovej 118, 2800 Lyngby, Denmark
[2] Department of Civil and Environmental Engineering, Norwegian University of Science and Technology, Høgskoleringen 7B, 7033 Trondheim, Norway
* Correspondence: nfri@byg.dtu.dk

Abstract: Increased insulation reduces the energy needed during operations, but this may be less than the energy required for the extra insulation material. If so, there must be an optimal insulation thickness. This paper describes the development of a tool to determine the optimal insulation thickness, including what parameters are decisive, and presents some results along with a discussion of the success criteria and limitations. To make these considerations manageable for regular practitioners, only the transmission heat loss through walls is calculated. Although the tool is universal, Greenland is used as an example, because of its extreme climatic conditions. The tool includes climate change, 10 locations and 8 insulation materials. It focuses on greenhouse gas emissions, considers oil and district heating as heating sources, and evaluates four different climate change scenarios expressed in terms of heating degree days. The system is sensitive to insulation materials with high CO_2 emissions and heating sources with high emission factors. This is also the case where climate change has the highest impact on the insulation thickness. Using the basic criterion, emitting a minimum of $CO_{2\text{-eq}}$, the Insulation Thickness Optimizer (ITO), generally identifies higher insulation thicknesses as optimal than are currently seen in practice and in most building regulations.

Keywords: arctic; insulation thickness and materials; LCA; façade; energy mix; climate change

Citation: Friis, N.K.; Gaarder, J.E.; Møller, E.B. A Tool for Calculating the Building Insulation Thickness for Lowest CO_2 Emissions—A Greenlandic Example. *Buildings* **2022**, *12*, 1178. https://doi.org/10.3390/buildings12081178

Academic Editor: Xi Chen

Received: 11 July 2022
Accepted: 4 August 2022
Published: 6 August 2022

1. Introduction

To achieve a high-quality building, many aspects must be considered. The relative importance of the different aspects has changed over time, and in recent years the environmental footprint of a building has become increasingly relevant, due to the urgent need to reduce global warming. The layer of insulation in a building envelope has two purposes, ensuring a comfortable indoor climate, and reducing heat loss and thus saving both energy and money. The manufacturing and transportation of insulation materials are both energy-demanding processes, and the reduction in heat loss per mm of insulation decreases with the increase in the insulation thickness. Therefore, there must be an optimum CO_2-oriented insulation thickness. The focus of this research is on the insulation of wall constructions. In a Norwegian study, the operational emissions of $CO_{2\text{-eq}}$ have been identified as being much more sensitive to the insulation thickness in walls than in roofs or floors in a conventionally shaped house [1].

Most of the building regulations stipulate a maximum U-value for each part of a building, which must be met along with the demands on the overall energy consumption of the building. In the current Greenlandic building regulations from 2006 [2], the dimensioning energy demand of a building distinguishes between the areas north and south of the Arctic Circle, but, otherwise, the regulations do not account for the climatic and energy production conditions of each town and settlement. From a comfort and health point of view, this makes sense. However, the energy sources may differ considerably, from hydropower to oil, so that the same heat loss in two different locations can have different environmental

impacts, based on the emitted Greenhouse Gases (GHG). An open-source Excel tool has been developed to simplify the process of defining the optimal insulation thickness based on multiple parameters, including insulation material, location and heating method. The tool is named "ITO", which stands for "Insulation Thickness Optimizer".

Insulation is a never-ending hot topic, including material development and comparison, optimal thicknesses, correct placement in the construction and emerging issues such as mold and rot. The volume of literature within this field is immense. However, defining the optimal insulation thickness for a location of interest can be completed in many ways, as there are many available indicators and parameters that can be used in this analysis. In particular, an economic benchmark is popular, defining the payback period, after which the investment in the insulation becomes beneficial compared to the cost savings due to the reduction in heat loss. One of the studies working from this perspective was that of Ozel [3], who showed that the thermal conductivity (R) of a construction without insulation leads to an increased optimal insulation thickness and energy savings, while the payback period of the insulation decreases. The location of the study was Turkey, which is reflected in the recommended optimal insulation thickness of only 2.0–8.2 cm, depending on the scenario. Another study with a similar approach was Iranian and concluded that a maximum of 4 cm is the optimal insulation thickness (Rosti et al., 2020) [4]. In [4], the authors attributed the outcome to cheap electricity prices and claimed that the energy policies or pricing mechanisms should be adjusted to encourage the proper insulation of buildings, so as to ensure reduced heat loss and GHG emissions.

The new tool, ITO, introduced in this paper uses CO_2 emission as a benchmark for an optimal insulation thickness. This approach has been used in other studies. For example, the three Turkish papers [5–7] all used a Life Cycle Assessment (LCA) method to analyze a fictive brick-wall case. They all reached different conclusions on the optimal insulation thicknesses for the individual cases, which makes it difficult to compare the results. However, these papers demonstrated an obvious interest in the dynamics between the insulation thicknesses, energy savings, emission reduction and, in many cases, economic aspects. This indicates the value of a simple tool, such as ITO, which can automatically make such calculations. In its present form, ITO does not consider Life Cycle Costs (LCC) because the values of the materials and energy resources change continuously, but it will eventually be possible to replace all of the environmental inputs with economic inputs to achieve an output based on the economic considerations instead of the climate impact. A recent study from 2021 by Dylewski et al. [8] considered energy consumption for both the heating and cooling in the search for an optimal insulation thickness. The benchmark was a metacriterion including both the economic and ecological aspects with equally weighted importance. In addition, Janusz Adamczyk et al. [9], and Spanodimitriou et al. [10] considered both the economic and ecological perspectives, however Adamczyk et al. used HDD and Spanodimitriou et al. performed simulations and included considerations regarding the wall orientations. The latter study concluded that the best results were achieved for an east–west orientation of the building, compared to a north–south oriented building. This decision could save up to 13.6% energy. The Greek paper (Axaopoulos et al. 2019) considered the wall orientation as a variable parameter when defining the optimal insulation thickness [11]. Dynamic simulations were performed of a system with different orientations. The paper considered four different climate zones, with varying Heating Degree Days (HDD) and U-value regulations, and concluded that the south-facing walls should have less insulation, while the north-facing walls should have more insulation. A study by Ounis, S. et al. [12] changed the focus from the specific insulation material and investigated the needed U-value in different countries instead. A full map of Europe, excluding Greenland, was presented and the recommended U-value for Denmark was concluded to be 0.12 W/m^2 K, based on $HDD_{20\ ^\circ C}$ and $CDD_{24\ ^\circ C}$.

Regardless of whether the focus is on the LCC or LCA, the climate plays a role, and as the service life of buildings is long, climate change may be expected to affect the results. This is something that none of the presented papers considers when defining the optimal

insulation thickness. The rising temperatures will lead to lower HDD and consequently, the heat loss of the construction will be reduced. This might result in a decrease in the optimal insulation, regardless of the focus. ITO can evaluate three climate scenarios, as well as constant HDD. The user can easily adjust the temperature change for each scenario, but the tool has three initial settings, based on the information from the Intergovernmental Panel on Climate Change (IPCC), which is currently developing the sixth report on climate change, investigating the extent of global warming [13]. It has already been concluded that climate change is experienced in every region of the globe.

ITO is intended to be a simple tool that a building designer can use to determine the optimal insulation thickness in a given situation. A thorough determination of the optimal insulation thickness is very demanding, and, for most buildings, it is unlikely to be performed, especially in single-family houses in Greenland. With ITO, the issue can more easily be considered and contribute to more sustainable decision-making, as it delivers an indication of the optimal insulation thickness.

The present paper describes the development of ITO. In Section 2, Method, the fundamental equations, assumptions and considerations are presented. The section ends with a presentation of the input and output parameters of the tool, details about the considered insulation materials and a definition of a wall construction, which is used as a case during the article. In Section 3, Results, some of the outputs produced by ITO are presented for five chosen destinations. The section includes both the simple results considering the insulation alone and the results for insulation implemented in the case of a wall construction. The results are analyzed in Section 4, Analysis, which consists of three parts; a sensitivity analysis testing the robustness of the tool; an investigation of the impact of emissions from elements, which are defined to be beyond the system boundary; and finally, an analysis of the results when changing the definition of "optimal insulation thickness" to be less strict. Some of the content from the previous sections is discussed in Section 5, Discussion, followed by a conclusion, which is the final part of this article.

2. Method

The tool was developed in Microsoft Excel, together with user-friendly guidelines. It is intended to be used for decision-making both by the building industry and by individual building owners. The tool is based on standard methodologies and equations for thermal matters, and LCA, and uses data from the literature and available databases.

2.1. System

When trying to define the optimal insulation thickness, d_{opt}, it is necessary to define the success criteria. The first aspect of this is deciding on which parameter the balance should depend. There are three obvious possibilities, energy (kWh), greenhouse gas emissions (kg $CO_{2\text{-eq}}$) and monetary cost. As ITO is intended to promote better decisions in terms of sustainability, the benchmark parameter was chosen to be GHG emissions. This parameter takes into account the fact that different energy sources have different climatic impacts.

Figure 1 illustrates the product system for the insulation. The yellow boxes are processes that contribute to the emissions arising from the insulating material ($E_{material}$ (kg $CO_{2\text{-eq}}/m^3$)), while the green box denotes the emissions related to the resulting heat losses, E_{heat}. Equation (1) clarifies the relation between the yellow boxes and quantifies the total GHG emissions for 1 m^3 insulation, $E_{material}$. The indices refer to the yellow boxes in Figure 1:

$$E_{material} = E_{prod} + E_{freight} + E_{waste} + E_{freight,waste} \quad (1)$$

In theory, the best insulation thickness is found when the reduction in the greenhouse gas emissions (GHG), achieved by the insulation, equals the emitted GHG caused by the production and handling of the insulation. This can be expressed very simply by $\Delta E_{heat} = E_{material}$, where ΔE_{heat} is the emission difference relating to the reduced heat loss through the wall caused by the insulation. In practice, however, this criterion is challenged because the reduced heat loss cannot be calculated without defining a starting point, which

II

would require a definition of the additional construction layers of the wall. In the tool, this will be an option but not a necessity. Furthermore, there might be situations where this equation is never fulfilled with a realistic thickness. Therefore, d_{opt} is defined to be the thickness, d, with minimum emissions, E, which is described as $E(d_{opt})$ in Equation (2):

$$E(d_{opt}) = Min(E_{material}(d) + E_{heat}(d)) \quad (2)$$

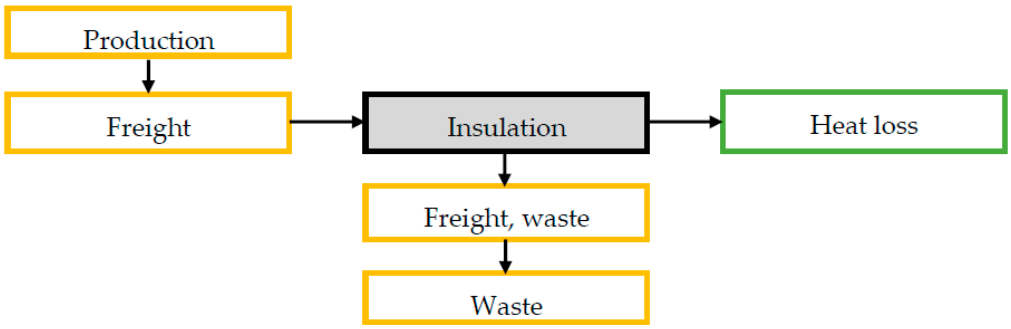

Figure 1. Flow chart of the product system for the insulation material (gray box). The colors indicate whether the process results in emissions related to the material, $E_{material}$, (yellow) or the resulting heat loss, E_{heat}, (green).

The tool calculates the emissions for each stage for 1 m^3 insulation material and cumulates them. The sum of E_{heat} and $E_{material}$ for 1 m^2 wall is then calculated in a list with increasing insulation thicknesses, starting from 5 mm. In this list, the minimum level of $CO_{2\text{-eq}}$ emissions can be identified along with the corresponding thickness. Because of this approach, all of the equations regarding emissions are given for 1 m^3 of material.

2.2. Life Cycle Stages

To calculate the total material emissions ($E_{material}$) it is necessary to consider all of the aspects of its life cycle. There are multiple phases to LCA. Figure 2 illustrates the many phases, which elaborate on the yellow boxes in Figure 1. Four of the boxes are hatched to show that they are not considered by the tool. A5, "installation into buildings" and C1, "deconstruction and demolition" are disregarded, because their contribution to the system is small and quantifying them would involve too many assumptions without changing the outcome significantly. The operation stage of the insulation, B1-7, is not included as it is expected that the material will last as long as the building itself, meaning that no repairs or replacement of the insulation material will be necessary. The maintenance of the entire wall is assumed to be independent of the insulation thickness. Furthermore, the operation of the insulation does not require fuel or other resources, which B1-7 also accounts for. The last stage, D "Benefits and loads beyond the system boundary," is usually given in the product datasheet, but the impacts depend on the current state of the art, which is why including it in such a long-time perspective could be misleading. The value of D can both be positive and negative. The negative values are possible because D accounts for any heat gained from incineration, or an amount of insulation produced with less raw materials due to recycling. Furthermore, Stage D depends on the perspective and method of the product datasheet, which is not always transparent, and is thus difficult to compare. In some of the datasheets, the saved energy from Stage D exceeds the emissions from the other phases, indicating that the more material consumption the greater the sustainability, which can never be the case. Due to the uncertainties of these data, D is not considered in the tool.

Life cycle stages of the insulation										
Production stage			Construction process stage		Operation stage	End-of-Life stage				Benefits and loads beyond the system boundary
Raw material supply	Transport	Manufacturing	Transport to building site	Installation into building	Maintenance, Repair, etc.	Deconstruction/ demolition	Transport	Dsiposal	Waste processing	Reuse, recovery, recycling
A1	A2	A3	A4	A5	B1-7	C1	C2	C3	C4	D

Figure 2. Life cycle stages of the insulation as described in EN 25978:2012 [14]. The hatched boxes are disregarded in the tool. The text in "Raw material supply" refers to Supplementary Materials.

2.2.1. Production and Operation Stage

The emissions from the production stage ($E_{A1\text{-}3}$) are given in the product datasheets for each material. For the pre-coded materials, the free software "LCAbyg 5" [15] is used to find these data, and the ITO shows the exact sources. The sources used in the ITO give A1-3 in kg $CO_{2\text{-eq}}/m^3$, but it may vary for the different datasheets. During production and transportation, there will be a waste fraction ($W_{material}$). How much is uncertain, but this value is usually between 2 and 10% at the factory. As the material may have to be transported a long way from the factory to the building site, it is recommended to set the value at the high end of this span or even slightly above. Equation (3) calculates the emissions caused by producing 1 m^3 insulation, E_{prod}:

$$E_{prod} = E_{A1-3} \cdot (1 + W_{material}) \quad (3)$$

2.2.2. Construction Stage

The emissions caused by A4 "Transport to the building site", are based on the production country given in the product datasheet and the location of the building site. It is assumed that there are three transportation methods: truck; boat and plane. It is unusual to transport building materials by plane, but the option is implemented for certain cases. All of the materials listed in the tool are produced in Europe. It is assumed that all of the materials are produced somewhere in the middle of the selected country. If the building site is placed in Copenhagen, it is assumed that the materials are taken by truck directly from the factory. For the Greenlandic destinations, it is assumed that the insulation is transported by truck to an industrialized harbor in the same country and then shipped to the specific harbor of the destination. Royal Arctic Line has an exclusive concession with the Greenlandic government, covering all of the sea cargo in Greenland, both internally and externally [16]. According to the Royal Arctic Line webpage, all of the transportation out of Greenland passes through Reykjavik and ends in Aalborg harbor [16]. Based on this, the distances, D, in km for each mode of transportation are estimated by using the measurement tool in Google Maps [17]. The transportation emissions are from Ecoinvent 3, consequential unit [18] processed in SimaPro version 9.2.0.2 [19] and the method used is ReCiPe 2016 Midpoint (H) [20]. The chosen process for boat transportation emits E_{boat} = 0.00959 kg CO_2/tkm, the truck emits E_{truck} = 0.167 kg CO_2/tkm and the plane emits E_{plane} = 0.436 kg CO_2/tkm. Equation (4) assumes that half of the wasted material, $W_{material}$, will be transported all of the way to the building site. This is a rough estimation that some of the waste will occur at the building site. ρ is the density of the insulation in kg/m^3.

$$E_{freight} = \frac{\rho}{1000} \cdot \left(1 + \frac{W_{material}}{2}\right) \cdot \left(E_{boat} \cdot D_{boat} + E_{truck} \cdot D_{truck} + E_{plane} \cdot D_{plane}\right) \quad (4)$$

II

2.2.3. End of Life Stage and Benefits and Loads beyond the System Boundary

The End-of-Life (EoL), for a material has multiple options, such as landfill, incineration, recycling and reuse. Currently, the options for reuse and recycling are very limited in Greenland, which is why most of the waste materials end up in landfills. If the location can facilitate incineration, it will most likely be the preferred solution. It is planned that the incinerators in Nuuk and Sisimiut should be modernized by 2023, making it possible in these two locations to incinerate the content of the dumps and the waste of all the other settlements and cities [21]. To reuse or recycle the waste, it is necessary to transport the waste materials to other countries, e.g., Denmark or Germany. Whether or not this emits less GHG is case dependent, but generally, recycling or reuse through other countries is unlikely. Based on this information, it was decided to make default settings for incineration and landfill for each location, while recycling is left as a possible manually selected option for those cases in which detailed information is available.

EoL, covering C2-C4 in Figure 2, is often given in the product datasheet, but the transportation, C2, is highly dependent on the location of the building site and must be evaluated based on the Greenlandic conditions. In ITO, it is assumed that all of the waste is transported by boat to either Nuuk or Sisimiut and incinerated. ITO assumes that it is moved to the nearest of the two, however that might be different in practice. If the material is landfilled, it is assumed to be taken by truck across the city. The equation for $E_{freight,waste}$ is the same as for $E_{freight}$, presented in Equation (4). The equation for E_{waste} is presented in Equation (5), where $W_{material}$ is the unitless waste factor and E_{C3} and E_{C4} are the EoL-stages presented in Figure 1, given in kg $CO_{2\text{-eq}}/m^3$:

$$E_{waste} = (1 + W_{material}) \cdot (E_{C3} + E_{C4}) \quad (5)$$

2.3. Heat Loss and Emissions

The tool considers heat loss in two scenarios: an individual layer of insulation material, $Scen_{ins}$, and a full wall construction, $Scen_{wall}$. The first mentioned is simple to apply, as it does not require any information beyond the system presented in Figure 2. The result of this method is unreliable from a practical perspective but can be used to identify the correlations between the choices of inputs. $Scen_{wall}$ demands more initial knowledge about the whole wall construction, which will provide more accurate definitions of the optimal insulation thickness and the correlating GHG emissions. Working with the second scenario and considering the whole wall, it is important to be aware that it does not consider the emissions related to the additional construction materials used to build the wall.

The heat loss through a wall can be calculated with varying precision, ranging from complicated simulations to simple estimations. To facilitate the regular practitioner, the priority, in this case, was to keep the tool simple and quick to use, with few demands on software. Therefore, the heat loss calculations are based on Heating Degree Days (HDD), a method that can be performed in Excel or any other spreadsheet. This compromises the accuracy of the results, however, it will indicate an optimization that will not be prioritized if the process is too demanding of time and money.

E_{heat} is an expression for the emissions related to the heat loss of the insulation or wall, depending on the approach. It is calculated by Equation (6), where E_{factor} is the emission factor, quantifying the amount of kg $CO_{2\text{-eq}}$ per kWh heat:

$$E_{heat} = Q \cdot E_{factor} \quad (6)$$

The heat loss caused by transmission (Q) depends on the heat conductivity, λ (W/mK), and on the insulating material and its thickness (d (m)). As a simplification, only thermal conductivity is considered, and only a simple wall. The doors, windows, thermal bridges, etc. are disregarded. The climate plays an active role, as shown in Equation (7), where *HDD* is the Heating Degree Days (K days/year))for the location, (U (W/m^2 K)) is the heat transmission coefficient of the insulation material and *ESL* is the Estimated Service Life (year). *ESL* is an independent variable, which can be set from 10 to 110 years, while

60 years is the most common value used for dimensioning. Equation (7) calculates Q for 1 m^2 wall (kWh/m^2):

$$Q = U \cdot ESL \cdot HDD \cdot (1 + W_{dist}) \cdot \frac{24}{1000} = \frac{1}{d/\lambda} \cdot ESL \cdot HDD \cdot (1 + W_{dist}) \cdot \frac{24}{1000} \quad (7)$$

W_{dist} is the heat loss caused by the distribution of heat. This is usually 2–10% for district heating [22], and in the low end for local heating with e.g., oil. By default, this tool provides two options for heating, but in specific cases with in-depth knowledge about the heating, the factors can be changed accordingly. The two default options are local heating with oil and district heating (dh). The emission factors relating to the heating source (E_{factor}) are individual for the district heating at each location. Usually, district heating in Greenland consists of incineration, hydropower and the burning of oil. Table 1 shows the emission factors for the default locations in the tool. If the building is heated solely by oil, the emission factor is defined to be 0.335 kg $CO_{2\text{-eq}}$/kWh. Not all of the towns and settlements in Greenland have access to district heating, but the default towns in ITO do have.

Table 1. HDD and E_{factor} related to district heating for each location represented in the tool [23]. * indicates alternative calculation methods for HDD.

Location	HDD	E_{factor}
	(K/a)	(kg $CO_{2\text{-eq}}$/kWh)
Copenhagen	2500	0.0499
Qaqortoq	6210	0.218
Paamiut	6740	0.19
Nuuk	7080	0.009
Maniitsoq	6820	0.176
Sisimiut	7570	0.161
Aasiaat	7970	0.207
Qasigiannguit	7740	0.136
Uummannaq *	7908	0.002
Qaanaaq	9580	0.107

The default locations in the tool represent a variety of cities in Greenland, where Nuuk is the absolute largest with 19,000 inhabitants [24] and Qaanaaq is the smallest with 619 residents [25]. The second largest is Sisimiut, with more than 6000 inhabitants [26]. There are gaps in the list of the cities, because of missing information about *HDD* and $E_{factors}$. With sufficient information, the tool can be edited to cover any desired location. The heat loss through the wall is calculated by using *HDD*, instead of the usual dimensional indoor and outdoor temperatures. Heating degree days, *HDD*, is a measure for the difference of 1 K between the indoor mean temperature of 17 °C and the external average temperature over 24 h [27]. In Denmark, the heating season spans from May to October, and the months are considered individually; the average sum of *HDD* in the heating season over 5 years results in 2500 degree days, which is implemented in the tool [27]. In Greenland, it is common to heat residential buildings all of the year, which is why an average of the latest 5 years of *HDD* is used for the individual locations. The heating degree days are provided by Grønlands Statistikbank [28]. For Uummannaq, the source did not include *HDD* for the last 5 years. Thus, the implemented value is for 2020 alone. The degree days for all of the locations are given in Table 1.

The total emissions of 1 m^2 insulation (E_d) with a given thickness of insulation (d) can be calculated by Equation (8):

$$E_d = E_{material} \cdot d + E_{heat(d)} \quad (8)$$

II

2.4. Climate Change

Climate change will lead to extensive changes all over the world, but especially in the Arctic, where the temperature is rising more rapidly than elsewhere [29]. As climate change is a future circumstance, the exact development is unknown. Thus, the Intergovernmental Panel on Climate Change (IPCC) has developed different scenarios called the Representative Concentration Pathways (RCP). The original four RCPs are RCP2.6, RCP4.5, RCP6 and RCP8.5. The numbers describe the radiative forcing values range in 2100 with the unit W/m^2. For each RCP there are multiple predictions about how the individual scenario will affect the temperatures in the future, and the low RCPs lead to lower temperature differences.

The tool, ITO, considers three climate scenarios for a period of up to 110 years besides a constant scenario. The first and most "conservative" scenario predicts a change of 0.2 °C/10 years. This is based on the data showing that the Earth's surface temperature has generally risen by 0.18 °C/10 years since 1981 [29]. This development is between RCP1.9 and RCP2.6, of which the latter is likely to keep the temperature rise below 1.5 °C, and thus fulfil the Paris Agreement. The second scenario predicts 0.4 °C/10 years based on the median-predicted temperature rise for RPC8.5, which is a scenario with high GHG emissions. This scenario is called "moderate", however, it is currently at the high end of the expectations of experts. The last and most "extreme" scenario is 2.7 °C/10 years. This is based on IPCC claiming that the surface temperatures during winter in the central Arctic were 6 °C higher in 2016 and 2018 compared to the average of 1981–2010 [30]. The 2.7 °C/10 years is calculated as a 6 °C temperature increase over 22 years (the middle year of each interval 1995 and 2017). The default scenarios are set to investigate how climate change might reduce the need for insulation, but they can be adjusted as desired in the tool.

The climate development is simplified by identifying the change in the heating degree days (HDD_{change}) for every 10th year caused by the temperature change (T_{change}). Equation (9) shows the calculation completed for every period of 10 years:

$$HDD_{change} = \frac{\left(HDD - \left(HDD - T_{change} \cdot 365\right)\right)}{HDD} \quad (9)$$

The change is implemented by calculating the heating degree days for every period. Based on the information about the ESL of the building, the tool cumulates the total HDD for the lifetime of the building.

2.5. Inputs and Outputs

The developed tool, ITO, can be found in the repository [31]. In the present paper, the main features are presented. ITO requires a list of inputs, of which some are very straightforward, while others are important but uncertain information. The tool was developed to make it possible to use it with limited information, or if desired, with a higher level of detail or accuracy, by user-defining the inputs. As stated in Section 2.3., the tool evaluates two setups: the insulation as a stand-alone scenario, $Scen_{ins}$; and a full wall, $Scen_{wall}$, which considers the secondary construction materials. Due to the analysis described later in Section 4.2., it was decided to add "$Scen_{slab}$", a scenario accounting for the emissions related to the slabs, roof and foundation. The reason is that thicker walls demand larger slabs. The $Scen_{slab}$ can be combined with both $Scen_{ins}$ and $Scen_{wall}$. Table 2 lists the necessary information needed for each setup.

Table 2. Introduction to the necessary inputs for $Scen_{ins}$ as well as the mandatory information for $Scen_{wall}$ and $Scen_{slab}$. The * marks an additional option called "User-defined".

	Parameter	Type	Range	Unit	Note
Insulation only	Town	Dropdown menu	10 options *	-	See Table 1
	Heat loss by distribution	Manually	0–100	%	Usually 2–10%
	Insulation type	Dropdown menu	8 options *	-	Defines λ, ρ and production country
	Est. material waste	Manually	0–100	%	Usually 2–10%
	Waste handling	Dropdown menu	2 options	-	Landfill or Incineration
	Est. Service Life	Dropdown menu	11 options	year	10–110 years in 10-year intervals
	Temperature increase	Manually	0–10	°C/10 years	Optional
Full wall	λ for add. layers	Manually	-	W/mK	
	Thicknesses of add. layers	Manually	-	m	
Incl. slab	Floor height	Manually	-	m	From slab to slab
	Nr. Of slabs per floor	Manually	-	-	Decreases with number of floors
	Slab type	Dropdown menu	3 options *	-	Defines $E_{A1–3}$ for the slab construction

The tool considers two heating sources, and the system automatically presents the results for both of the options, so it is not an input parameter.

Table 3 shows all of the materials that were considered and their properties. It is assumed that the environmental impact of landfilling will be 0.01364 kg $CO_{2\text{-eq}}$ per kg material [32] and identical for all of the materials.

Table 3. Presentation of materials included in the tool. Descriptions of Life Cycle Stages are presented in Figure 2.

Type	λ	ρ	A1-3	$C3_{inc}$	$C4_{inc}$	$C4_{land}$	Sum_{inc}	Sum_{land}	Prod.
	(W/mK)	(kg/m^3)			(kg $CO_{2\text{-eq}}$)				(–)
Cellular glass	0.041	115.00	151.80	0.00	1.57	1.57	153.37	153.37	Belgium
Cellulose fiber, batts	0.041	80.00	−19.99	176.10	0.00	1.09	156.11	−18.90	Germany
Cellulose fiber, loose	0.039	45.00	−73.37	99.08	0.00	0.61	25.71	−72.76	Germany
EPS 18 kg/m^3	0.040	18.00	52.50	59.50	0.00	0.25	112.00	52.75	Germany
EPS 22.7 kg/m^3	0.035	22.70	59.50	0.00	75.20	0.31	134.70	59.81	Germany
Mineral wool, batts	0.034	30.00	40.31	0.72	0.40	0.41	41.43	40.71	Germany
Mineral wool, loose	0.034	50.00	64.02	1.25	0.69	0.68	65.96	64.71	Germany
Wooden fiber	0.036	51.70	−61.11	85.10	0.00	0.71	23.99	−60.40	France

To present and analyze the functionality and results of the full wall, $Scen_{wall}$, it is necessary to predefine a wall. It is very common to build with ventilated walls in Greenland. To make sure that the wall is representative of the construction sector, a composition assessed in a previous study will be used. The wall was first presented in [33] and is a heavy construction, as described in Table 4. The wall contains a ventilated cavity, and according to the Danish Standard DS 418 [34], the R-value of the cavity and the following external layers can be replaced by the internal heat transmission factor, R_{si}, for the same construction. In this case, the R_{si} is 0.130 m^2 K/W. The external standard for R_{se} is 0.040 m^2 K/W.

Table 4. Definition of the specific wall applied to $Scen_{wall}$ cases.

Material	Thickness	Thermal Conductivity	Thermal Resistance
	d (mm)	λ (W/mK)	R (m^2 K/W)
R_{si}			0.130
Concrete	150	2.100	0.071
Insulation	Variable	Variable	d/λ
Ventilated air cavity	25		0.13
Cladding	8		
R_{se}	-		

The outputs of the tool consist of both intermediate results, covering the balance of emissions for 1 m^3 of insulation and a final recommendation of an optimal thickness of insulation for both oil and district heating. The latter is supported by graphs.

3. Results

Table 5 shows the results produced by ITO for five of the available ten cities and all of the eight materials. The five cities are Copenhagen, Nuuk, Sisimiut, Aasiaat and Qaanaaq, ordered with the most southern location first and the most northern location last. This also means that the number of heating degree days increases from Copenhagen to Qaanaaq. The parentheses after the location name shows the emission factor for the district heating at that location. Today, the Greenlandic requirements for the maximum U-values are 0.30 W/m^2 K and 0.20 W/m^2 K for heavy and light wall constructions, respectively [2]. These demands can usually be met with 200 mm of insulation. However, it is expected that the new regulations will be implemented soon, and the requirements are expected to be tightened to 0.15 W/m^2 K for all of the wall types [35]. This can typically be fulfilled with approximately 250 mm of insulation. E_{d25} represents the total amount of emissions for 250 mm of insulation for comparison with the optimal insulation thickness. The results in Table 5 are for $Scen_{ins}$, which excludes the additional wall structure and only considers the insulation.

Table 5. $Scen_{ins}$ results produced by ITO for chosen locations with constant climate. The secondary pre-sets are production and heat waste of 5%, ESL of 60 years, and incineration as waste handling.

	CPH (0.0499)			**Nuuk (0.009)**			**Sisimiut (0.161)**			**Aasiaat (0.207)**			**Qaanaaq (0.107)**		
	d_{opt} (m)	**E_{opt}** (kg $CO_{2\text{-eq}}$)	**E_{d25}**	**d_{opt}** (m)	**E_{opt}** (kg $CO_{2\text{-eq}}$)	**E_{d25}**	**d_{opt}** (m)	**E_{opt}** (kg $CO_{2\text{-eq}}$)	**E_{d25}**	**d_{opt}** (m)	**E_{opt}** (kg $CO_{2\text{-eq}}$)	**E_{d25}**	**d_{opt}** (m)	**E_{opt}** (kg $CO_{2\text{-eq}}$)	**E_{d25}**
Cellular glass	0.21	76.9	78.01	0.16	53.6	59.77	0.68	234.4	360.60	0.79	272.5	472.78	0.62	216.9	310.96
Cellulose fiber, batts	0.21	76.4	77.45	0.15	54.3	61.07	0.67	237.8	361.87	0.78	276.6	474.06	0.61	219.4	311.99
Cellulose fiber, loose	0.46	33.3	39.89	0.34	23.5	24.50	1.47	102.8	310.60	1.71	119.5	417.33	1.32	96.0	262.94
EPS 18 kg/m^3	0.26	62.0	61.99	0.18	44.2	46.37	0.80	193.4	339.79	0.93	225.0	449.27	0.73	177.7	290.71
EPS 22.7 kg/m^3	0.22	63.6	64.22	0.16	45.4	50.52	0.68	198.5	307.26	0.79	230.9	403.05	0.62	182.5	264.36
Mineral wool, batts	0.37	36.5	39.31	0.27	25.9	25.95	1.16	113.4	275.36	1.35	131.8	368.41	1.06	104.9	233.75
Mineral wool, loose	0.29	46.2	46.74	0.21	32.8	33.26	0.92	143.4	282.69	1.07	166.8	375.74	0.83	132.7	241.22
Wooden fiber	0.42	33.8	38.5	0.34	21.6	22.55	1.47	94.5	286.65	1.72	109.9	385.17	1.32	88.6	242.73

The results in Table 5 show that the cities with low emission factors, such as Nuuk, require less insulation. The maximum thickness for minimum GHG emissions is 1.72 m, which is extremely high (Wooden fibers in Aasiaat). This is also the combination with the most emissions at $E_{d25.}$ The thinnest optimal insulation thickness is found for Cellulose fiber batts in Nuuk, and the least emissions to achieve d_{opt} is found for Wooden fiber in Nuuk. This combination also had the lowest E_{d25}. Most of the scenarios lead to thicker insulation layers than are usually needed to fulfil the current and future building regulations. Regardless of the building location, choosing Cellular glass, Cellulose fiber batts or EPS 22.7 kg/m^3 lead to the thinnest layers of insulation. The Loose cellulose fiber and Wooden fiber lead to the thickest, optimal insulation thicknesses. For all of the locations, except Copenhagen, the Wooden fiber emits less CO_2 to obtain the optimal insulation thickness than the Cellulose fiber. It is worth noting that the optimal insulation thickness is greater for Copenhagen than for Nuuk, which indicates the importance of the emissions related to heating. Cellulose fiber batt is the best overall regarding d_{opt} but also the worst overall regarding E_{opt}. The opposite counts for Wooden fiber, which is the best overall regarding E_{opt} and almost the worst regarding d_{opt}, only exceeded by Loose cellulose fiber.

The main purpose of the four graphs in Figure 3 is to compare the climate scenarios and the scenario $Scen_{ins}$ with $Scen_{wall}$. A comparison of (a) and (c) shows that the additional layers of the wall have a very limited impact on the optimal insulation thickness, less than 3 mm thickness difference, in these cases. This is explained by (b) and (d), showing that the flow of the correlation between the emissions and the insulation thickness barely changes. This means that the optimum does not move either. However, the y-axes are very different, resulting in much lower total emissions at d_{opt} in cases with thin insulation layers.

The thicker the d_{opt}, the less change in the emissions for the two scenarios. If, however, the chosen thickness is thinner than the d_{opt}, the additional layers will be significant in identifying the total emissions of CO_2. All of the graphs in Figure 3 show that the buildings heated by oil generally require thicker insulation than those heated with district heating. The energy mix in Sisimiut emits more GHG than the mix in Nuuk, and the city has a higher level of heating degree days during a year. Thus, thicker insulation is necessary for the buildings in Sisimiut than in Nuuk to achieve a minimum of GHG. Finally, Figure 3 shows that global warming, considered with the three climate scenarios, causes minimal changes in the optimal insulation thickness when the E_{factor} is small e.g., when district heating consisting mainly of hydropower is used. The figure also shows that the tool demands very thick layers of insulation when the goal is to fulfil Equation (2). In the next section, it will be discussed how the criteria can be modified. In the following sections, only a constant climate will be considered.

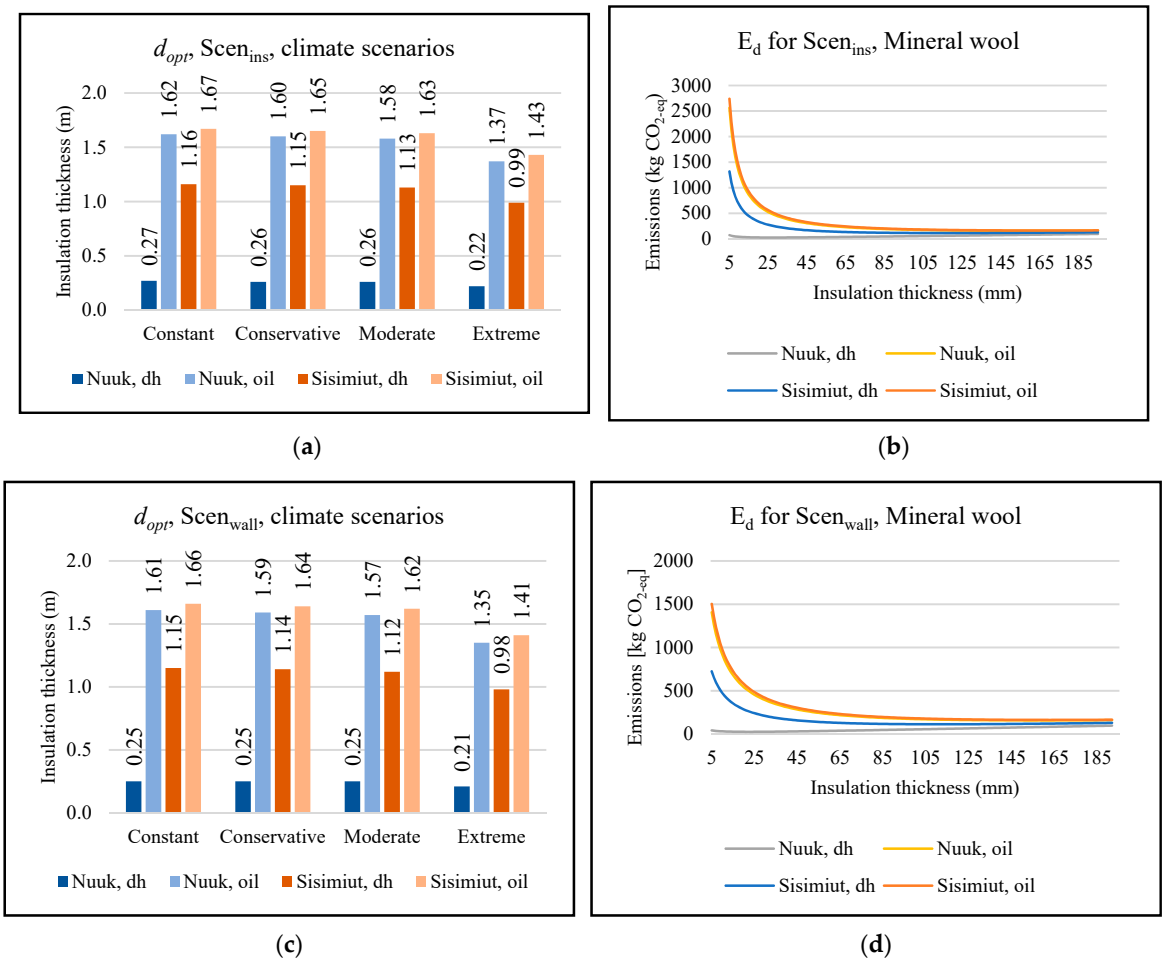

Figure 3. Graphs presenting some results from ITO. (**a**,**b**) are for Scen$_{ins}$, while graphs (**c**,**d**) are for Scen$_{wall}$. (**a**,**d**) consider climate scenarios for dh and oil heating in Nuuk and Sisimiut, while (**b**) and (**d**) presents the development of emissions at different thicknesses for mineral wool in Nuuk and Sisimiut with constant climate. ESL = 60 years.

Figure 4 shows that transportation generally is of less importance in the bigger picture. Based on the inputs in the emission factors for transportation presented in Section 2.2. that is because of the transportation method. If planes were chosen instead of trucks and boats, then the distance would have a bigger impact. The graphs also indicate that the impact of transportation has a bigger share of the total emissions when the waste ends as landfill, because it has fewer related emissions than incineration.

II

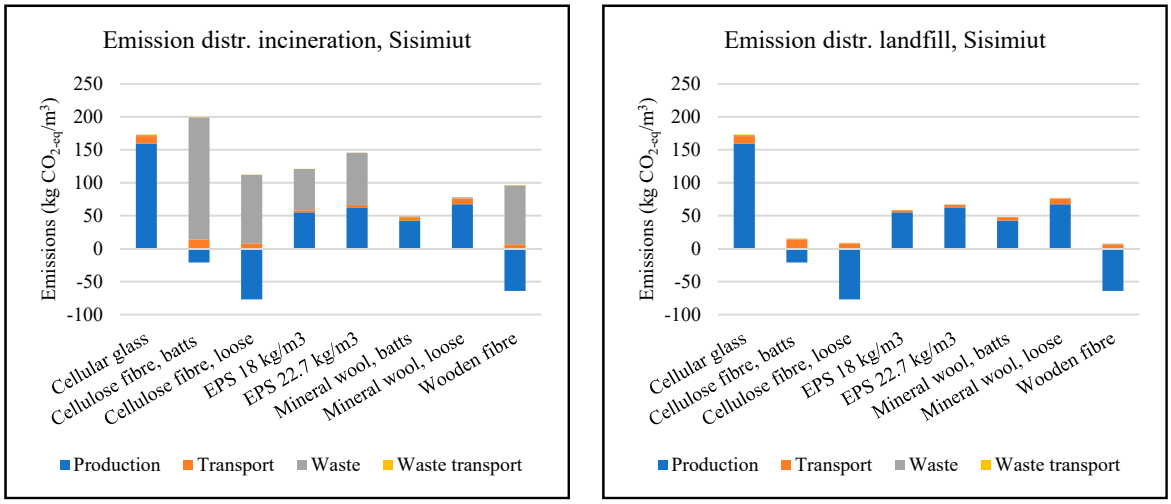

(**a**) (**b**)

Figure 4. $CO_{2\text{-eq}}$ emissions from the different phases of 1 m^3 insulation material. (**a**) is for incineration and (**b**) is for landfill. See Table 3 for specific data on each material.

From the graphs, it can be seen that the Cellulose fiber batts and Cellular glass are the costliest to produce in terms of $CO_{2\text{-eq}}$ when incinerated. When using landfills, the Cellular glass performs worst, while the production of the Cellulose fiber and Wooden fiber reduces the CO_2 by binding it to the material. ITO neglects the heat recovery possibilities of incineration.

4. Analysis

4.1. Sensitivity Analysis

As ITO considers a great deal of information, it is relevant to evaluate the sensitivity of the output to each of the inputs. A sensitivity analysis was performed by adding and subtracting 10% to each input and quantifying the changes in the output. The method was applied for both $Scen_{ins}$ and $Scen_{wall}$. As the changes in the input parameters are in percentages, some of them will have the same impact on the results, due to the equations presented, e.g., due to Equations (6) and (7), changing either *ESL*, *U*, E_{factor} or *HDD* with a specific factor will lead to the same changes in the outputs. The sensitivity of the parameters is expected to be different for each location, which is why 3 of the 10 cities were chosen as the representatives. The representative cities selected were Qaqortoq, Nuuk and Qasigiannguit, as they are placed south of, near and north of the Arctic Circle. Additionally, they all have different E_{factor}. Each type of material is only represented in one form (as batts if that is an option), leading to assessments of five materials: Cellular glass; Cellulose fibers (batts); EPS (22.7 kg/m^3); Mineral wool (batts) and Wooden fibers. The initial conditions for the analysis are *ESL* = 60 years, waste handling = "Incineration", $W_{material}$ = 5%, W_{dist} = 5%. The analysis was performed for both district heating and oil. It was quite an extensive analysis, so only the most relevant and informative results are highlighted and discussed.

The considered parameters were λ, *ESL*, *D* and $E_{A1\text{-}3}$ as shown in Figure 5. When analyzing the diagrams for each material at all of the three locations focusing only on E_{opt}, the results are very similar for both dh and oil. Thus, Qaqortoq represents all of the three locations in Figure 5, allowing a simple comparison of the sensitivity of E_{opt} for each material for both $Scen_{ins}$ and $Scen_{wall}$. This is shown in Figure 5a,b, respectively. Figure 5 illustrates that the sensitivity is very similar for all of the materials except the Wooden fiber, which is more sensitive to changes in the production stage, $E_{A1\text{-}3}$, than the other materials. Comparing (a) with (b) reveals that the transportation distance, *D*, causes more sensitivity for $Scen_{wall}$ than $Scen_{ins}$. The transportation distance, *D*, is also the only parameter change causing similar changes in the output for $Scen_{wall}$.

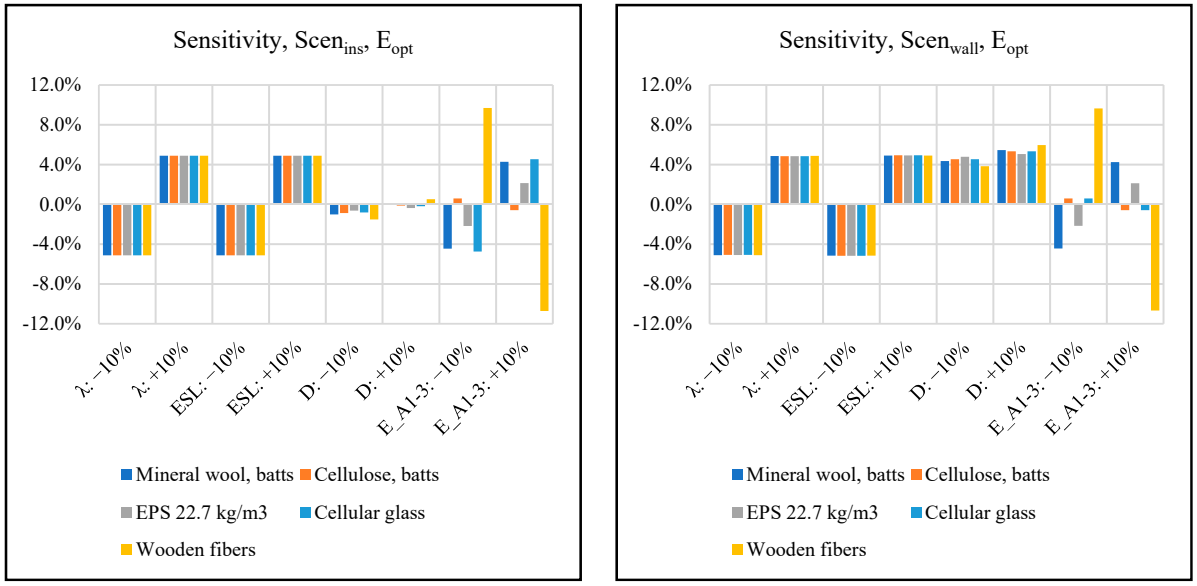

(**a**) (**b**)

Figure 5. Sensitivity analysis of E_{opt} for all materials. (**a**) is for Scen$_{ins}$, and (**b**) is for Scen$_{wall}$ as described in Table 4. The results are nearly identical for the three cities, but these are specifically for Qaqortoq with district heating.

The d_{opt} for Wooden fibers reacts differently than for all the of the materials. herefore, there are two different figures: Figure 6a is for the Wooden fibers only, and Figure 6b is for the rest of the materials represented by EPS. Figure 6a shows the difference between the sensitivities of d_{opt} for Wooden fibers for Qaqortoq, which represents all of the considered locations. Figure 6b differentiates between the Wooden fibers and the rest of the materials, which react similarly. The d_{opt} is more sensitive to the location than E_{opt}, which is why Nuuk is shown separately, while Qaqortoq represents the other cities in Figure 6b. All of the materials are less sensitive for Scen$_{ins}$ than for full walls. In Figure 6, Scen$_{ins}$ is described as "ins" and Scen$_{wall}$ is described as "wall".

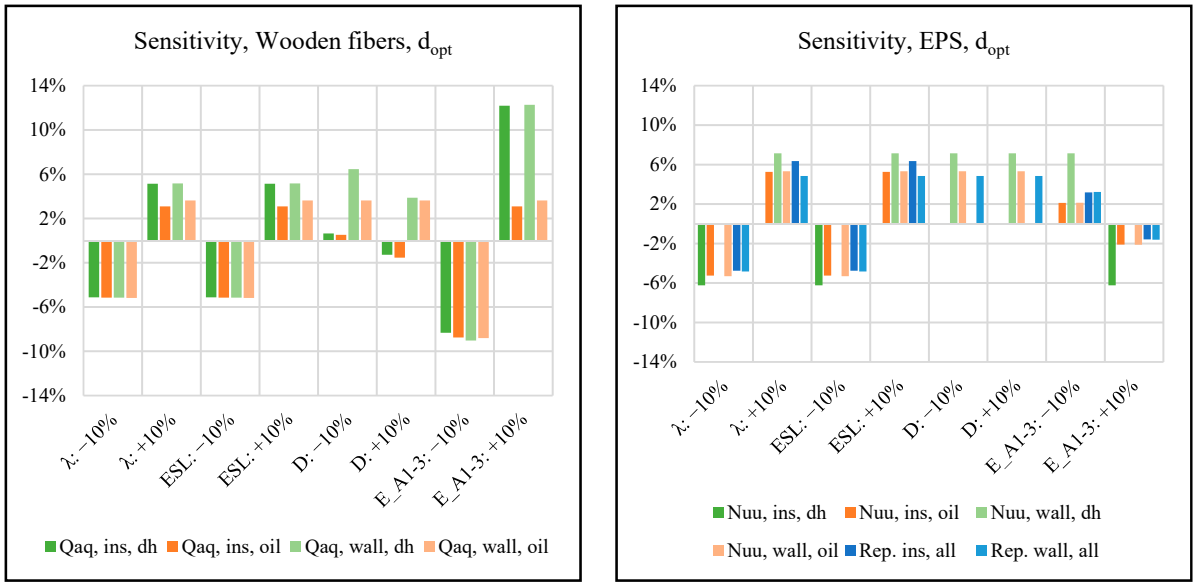

(**a**) (**b**)

Figure 6. (**a**) is for Wooden fibers in Qaqortoq representing all cities, and (**b**) is for EPS representing all materials. Qaqortoq represents all cities except Nuuk.

II

4.2. Impacts beyond the System Boundary

Discussing the optimal insulation thickness while focusing on a limited number of parameters will affect the other conditions outside the defined system boundary, see Figure 1. One obvious effect is that thicker walls demand larger roofs and slabs. A short, simplified assessment of this impact is conducted, considering three material scenarios of the slab. The emissions for 1 m^2 (E_{slab_sqrm}) of each type of considered slab are: (A) concrete box girder ($E_{slab\_sqrm\_A}$ = 42.11 kg $CO_{2\text{-eq}}/m^2$); (B) in situ casted concrete ($E_{slab\_sqrm\_B}$ = 87.58 kg $CO_{2\text{-eq}}/m^2$) or (C) wooden elements ($E_{slab\_sqrm\_C}$ = 24.22 kg $CO_{2\text{-eq}}/m^2$). It is assumed that the floor height, h, is 3 m. The number of slabs per floor, n, will, as the worst-case scenario, be n = 2, representing the floor and roof. In practice, this would be less for multistorey buildings. The assessment does not differ between slabs, roofs and foundations, and does not account for corners, doors or windows. Equation (10) indicates how the share (S) of the emission contribution of the slabs (E_{slab}) can be calculated:

$$S_{E,slab} = \frac{E_{slab}}{E_{slab} + E_{wall}} = \frac{E_{slab\_sqrm} \cdot n \cdot d_{opt}}{E_{slab\_sqrm} \cdot n \cdot d_{opt} + E_{opt} \cdot h} \quad (10)$$

The results of Equation (10) considering slab B on $Scen_{ins}$ show that the emissions related to the slabs, E_{slabs}, can be of significant importance. For the Wooden fibers in Aasiaat, the slabs account for 73%, which is the highest amount identified. The average importance for each material is highest in Aasiaat, but for all of the three slab types, 10% is the lowest average share. For Slab C, however, the share is much smaller, due to the lower emissions of the slab. Changing this parameter only leads to a share of 43% for the Wooden fibers in Aasiaat. Since it can be of great importance, it was decided to expand the tool to be able to handle this information. The input parameters required to benefit from this are shown in Table 2.

The graphs in Figure 7 show how d_{opt} is reduced, when the slabs are considered as part of the system. Both graphs are for $Scen_{ins}$.

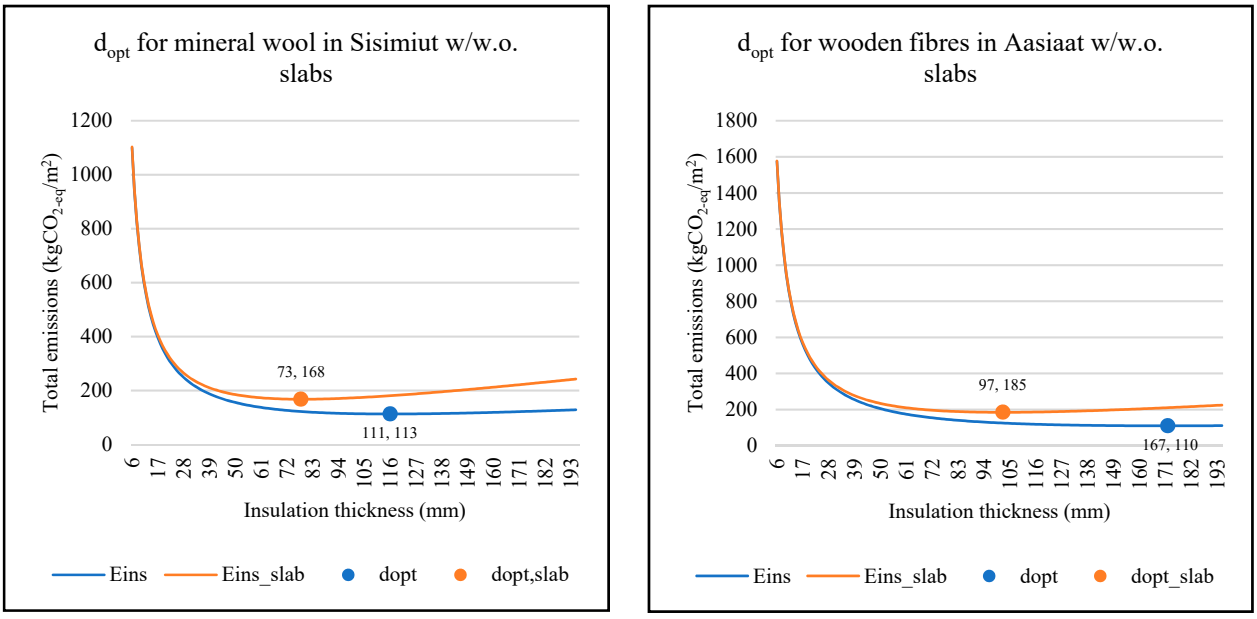

(**a**) (**b**)

Figure 7. Graphs comparing dopt for two cases with and without slabs. (**a**) is for mineral wool in Sisimiut and (**b**) is for Wooden fibers in Aasiaat. The format of the point labels is "d_{opt}; E_{opt}". The pre-sets are: h = 3, n = 2, incineration, ESL = 60 years, $W_{material}$ = 5% and W_{heat} = 5%. The considered slab type is in situ casted concrete (Type B).

The reduction of d_{opt} in (a) corresponds to 34.2% and in (b) it corresponds to 41.9%. If the corresponding calculations were completed for $Scen_{wall}$, it would result in a reduction of 18.2% for setup (a), and for setup (b) the reduction would be 13.9%, meaning that if the full wall construction is considered, the impact of the slabs will be of less significance.

4.3. Alternative Definitions of "Optimal Thickness"

The success criteria in Equation (2), which defines that d_{opt} is the thickness where a minimum of GHG is emitted, generally leads to some very thick walls, as may be seen in Table 5. This definition is therefore challenged in this section, in an attempt to define other criteria which might be more realistic. Figure 3b,d illustrate that each centimeter reduces the heat less than the last, meaning that accepting the emissions to be 10% more than for d_{opt} will reduce the thickness by at least 10%. This criterion is named $Crit_{\%}$ and was tested as one alternative way to define d_{opt}. Here, $Crit_{\%}$ was tested for 5% and 10%, but the acceptance factor can be defined as desired.

Another way to define the d_{opt} is to consider the slope of the curves in Figure 3b,d and define an angle of the tangent to the curve, indicating that the next centimeter of insulation will save too little heat to be recommendable. In theory, the initial success criterion from Equation (2) defines the angle, α, to be 0°, meaning that the tangent is horizontal. This criterion is named $Crit_{\alpha}$, and here it is tested to be $-20°$ and $-45°$.

The challenge of both of the alternatives is to define the factors of success. Regardless, both of the criterion compromise the ambition to reduce the emissions of GHG as much as possible. Figure 8 shows how these two interpretations of d_{opt} change the outcomes.

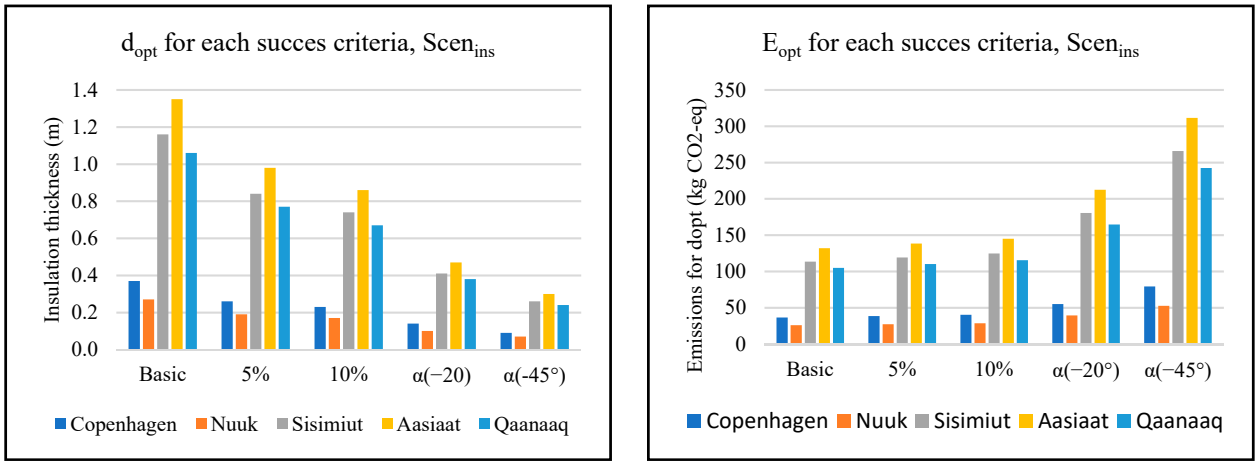

(**a**) (**b**)

Figure 8. Thickness (**a**) and emissions (**b**) for different success criteria for $Scen_{ins}$ with Mineral wool batts and district heating.

5. Discussion

The tool has some obvious limitations. First, it does not consider possible moisture issues in the wall construction. The reason is partly that it demands information about each material included in the wall composition, and partly that it was not the purpose of the tool. If one wants to use the tool for that purpose as well, it is an option to implement a Glaser scheme or similar in a spreadsheet that uses the information from the pre-coded data. In addition, the tool represents oil and district heating, while many households in Greenland use only or partly electric heating. This is not included in the standard tool because of limited sources to indicate the use of energy.

In Table 1, the E_{factor} for Uummannaq stands out with the factor of 2 g $CO_{2\text{-eq}}$/kWh, while the second-lowest factor is for Nuuk (9 g $CO_{2\text{-eq}}$/kWh) and the third-lowest is for Copenhagen (49.9 g $CO_{2\text{-eq}}$/kWh). The reason for such low energy factors in Greenland is claimed to be hydropower, but Uummannaq has questionable low emission factors because

hydropower usually emits 4 to 14 g $CO_{2\text{-eq}}$/kWh. It has even been estimated to be up to 150 g $CO_{2\text{-eq}}$/kWh for reservoir hydropower, which is usually used in Greenland [36]. The source for the emission factors is Nukissiorfiit, which is the company that provides energy and water to most of Greenland and is thus the best informed on this topic. The question is whether it is important enough for them to carry out research and investigations, quantifying the actual E_{factor} for each location in Greenland. The point of this discussion is not to question the honesty of Nukissiorfiit and the intentions of informing others about the sustainability of the energy production, but to create awareness of the difficulties and costs in quantifying such information, especially when fewer than 1000 people are affected. In general, more information and data on energy in Greenland would be valuable for future research.

Another uncertainty of the tool is the estimation of the produced material waste and heat waste. Both were set to 5% for the results presented in this study, but in practice, the waste of insulation material will depend on the type of insulation and its handling, while the waste of heat will depend on the heating source and the type and quality of the installation. This means, that the values are likely to be different for each case. The impact of these waste fractions on the optimal insulation thickness is, however, very small, which is indicated in Figure 7. For the Mineral wool in Qaqortoq, the d_{opt} for district heating increased by 5.8% when both $W_{material}$ and W_{heat} were increased from 5% to 15%. The emissions caused by freight of the material ($E_{freight}$) also depends on $W_{material}$, and Equation (4) shows that it is estimated that half of the material waste is transported to the building site. By this, it is not assumed that damaged insulation is distributed to construction sites, but that some of the waste is caused by the transportation, handling, errors during construction and inevitable leftovers from reshaping the material to fit the construction. This assumption is very rough, as the quantification of waste in the construction sector is extremely challenging and influenced by uncertainties. The sensitivity analysis in Figures 5 and 6 show that the emissions contribution from transportation is very small, especially when considering $Scen_{ins}$.

Another limitation to the system is the uncertain definition of "optimal insulation thickness". The user must decide what the boundaries should be for the specific case. It is also an option to use all of the three success criteria presented in Figure 8, to provide a more holistic and nuanced basis for the decision. In Dylewski et al. [8], the research resulted in a metacriterion considering both the ecological and economic perspectives, while weighing them equally. The challenge in implementing the economy in such a simple tool as ITO is that it requires a lot of the user, in terms of researching current market values. This would likely hinder part of the target group from using the tool.

The benchmark for ITO, regarding the optimal insulation thickness, is $CO_{2\text{-eq}}$. This is a fundamental premise of the tool, and, as previously described, there are many aspects to consider. The most applied criteria are $CO_{2\text{-eq}}$ and economic value, while some of the studies combine these. However, there are many other parameters to consider. The three fundamental parts of sustainability are ecology, economy and people. In none of the literature presented in Section 1, are the people considered in more than a comment. This neglects comfort and safety. It is very common to consider ecology and economy as equally important—even in certification systems, such as DGNB [37]. In studies that only consider ecology, it is most common to include $CO_{2\text{-eq}}$ as the only parameter, however, there are many other LCA impact factors to include, such as acidification and ecotoxicity of water and ground, usage of water and the reduction in mineral resources. Including these parameters complicates the reading of the results, and the GHG in the form of $CO_{2\text{-eq}}$ is a very well communicated, or even branded, measure, which most people can relate to. There is great reason to discuss whether this justifies the simplification, however, in a tool such as ITO, the users' understanding of the results is essential, for the product to matter.

As shown in Figure 4, incinerating the waste material emits more $CO_{2\text{-eq}}/m^3$ material than landfill. This condition can lead one to think that it is best to landfill the building

waste, but as sustainability is about much more than greenhouse gases, this is not the conclusion that should be drawn from the figure.

As described in Section 2.4, environmental development is considered, although the future conditions are uncertain. The temperature changes are being investigated thoroughly by scientists in different organizations, such as the IPCC. However, other weather phenomena may occur due to the changes in the global flow of heat and water. The impact of these possible phenomena is impossible to predict, and ITO does not consider the climate beyond the temperatures expressed by HDD. This can be considered both a strength and a weakness of the system, as it makes the system more robust to use despite uncertainties, but may exclude relevant factors. The predictions for temperature change vary both in methods and results, but the three climate scenarios included in this paper are based on acknowledged literature. As presented in Figure 3, comparing the optimal insulation thickness for the current climate scenario with the extreme climate scenario results in only minor differences compared to the differences related to the emission factors of the locations. The proportions of climate change are uncertain and have a relatively low impact. In contrast, the energy sources have lower uncertainty and relatively high impact, due to major differences between the emission factors. For reference, the emission factor varies by a factor of 37 comparing oil and the district heating in Nuuk (consisting mainly of hydropower), while the HDD differs up to a factor of 4.4 caused by extreme climate change (for Copenhagen over 110 years). However, the energy source may change during the lifetime of the building.

ITO is designed to minimize GHG emissions, but there are many aspects to consider hen constructing a house, as was stated in the Introduction. Section 4.2 focuses on one of them, but it is still based on the GHG emissions, while the other impacts also have important roles to play. Examples of this are comfort and buildability. The tool does not consider the practical difficulties in installing extremely thick insulation layers, which might lead to errors and problems in the construction phase. The level of comfort in a building depends on many different factors, but those that might affect the validity of an ITO analysis are comfort and daylight. In some cases, the minimum emission of GHG may be achieved with very thin layers of insulation, which might lead to cold walls during winter. Some of the results tabulated in the Results section exceeded one meter of insulation, which is far more than the 150–250 mm typically required by building regulations. This will create shadows around the windows, and therefore allow less light and heat to enter the building. Adequate light has been shown to be essential for comfort [38], and reduced heat gain from the sun will lead to an increased demand for heating. This could be interesting to consider in the calculation but would probably require too much information about the architectural design of the building, orientation, and the window types for this to be useful in practice. The additional layers of insulation also cause reduced heat gain during sunny seasons, which can impact the need for heating and cooling. In other research, such as Ozel et al. [3] and Axaopoulos et al. [11], this was considered. Since ITO does not consider the need for cooling, this heat gain is less significant, however the results can be considered a worst case on this perspective.

Figure 3 showed that the optimal insulation thickness was nearly independent of the additional wall layers. This might be due to the very thick optimal insulation layers demanded by the harsh Arctic climate. In other climates, the U-value of the uninsulated wall may have a higher impact e.g., Dylewski et al. [8] found that the optimal U-value would be independent of the uninsulated wall. The source, Ounis et al. [12], concluded that the optimal U-value in Denmark was 0.12 W/m^2 K based on $HDD_{20\ ^\circ C}$ and $CDD_{24\ ^\circ C}$, which led to 4348 HDD. The U-value is lower than the current building regulations that demand 0.3 W/m^2 K, and more HDD than accounted for in this study (2500). The difference is caused by the benchmark temperature when defining the days with heating demand, which was 17 °C in this study and 20 °C in the Ounis et al. study. Furthermore, the heating season might have been neglected in the other study. This is mentioned to bring

awareness of the importance of the definitions and the challenges in comparing the results of different studies.

II

6. Conclusions

The new tool, ITO, can determine the optimal insulation thickness in walls, if this is defined as the thickness that minimizes greenhouse gas emissions. The tool uses several simplifications on how to determine energy loss, as it only considers thermal conductivity through 1 m^2 wall without doors, windows, thermal bridges, etc. However, it is easy to use, and a sensitivity analysis shows that it results in reliable outputs.

The present paper clarifies the importance of insulation thickness, showing that the emissions from this parameter of the design can vary considerably, depending on the material, heating source and building location, which affects both the heating degree days and the freight distance. The output of the two scenarios, $Scen_{ins}$, which only considers the insulation, and $Scen_{wall}$, which considers a predefined wall with multiple layers, were very similar. However, there is a significant difference between the scenarios for very thin layers of insulation, as the first centimeters of material reduce the heat loss more than the last.

The optimal insulation thickness, d_{opt}, was found to be very HDD-dependent, while the emissions from the transport of the insulating material had limited impact, even when the distances are considerable. The sensitivity of the transportation distance, D, was found to be more vulnerable for $Scen_{wall}$ than for $Scen_{ins}$.

The system can be sensitive to processes taking place outside the system boundaries, especially when the emission factor of heat or the heating degree days is high. Different climate-change scenarios were investigated, but they caused minimal changes to the optimal insulation thickness when the E_{factor} was small, e.g., when district heating mainly consisting of hydropower was used. The difference in the HDD was less dependent on the climate change scenario than the location.

The tool illustrates the importance of green energy and well-considered building design. If the energy source has low CO_2 emission, the optimal insulation thickness may be thinner in a cold climate than it would be in a more moderate climate with an energy source that emits more CO_2.

Supplementary Materials: The following supporting information can be downloaded at: Doi: https://doi.org/10.11583/DTU.19672470.

Author Contributions: Conceptualization, N.K.F., J.E.G. and E.B.M.; methodology, N.K.F., J.E.G., E.B.M.; software, N.K.F.; validation, N.K.F., E.B.M.; formal analysis, N.K.F.; investigation, N.K.F.; X.; writing original draft preparation, N.K.F.; writing—review and editing, N.K.F., E.B.M., J.E.G.; visualization, N.K.F.; supervision, E.B.M. All authors have read and agreed to the published version of the manuscript.

Funding: This research was funded by the Government of Greenland, Kommuneqarfik Sermasooq, Knud Højgaards Fond, and Kerrn-Jespersens Fond.

Data Availability Statement: The tool, ITO, is available at DTU Data [31].

Acknowledgments: The authors would like to thank the Arctic Building and Construction project for funding this collaboration [39].

Conflicts of Interest: The authors declare no conflict of interest.

References

1. Totland, M.; Kvande, T.; Bohne, R.A. The effect of insulation thickness on lifetime CO_2 emissions. In *IOP Conference Series: Earth and Environmental Science*; IOP Publishing: Bristol, UK, 2019; Volume 323. [CrossRef]
2. Direktoratet for Boliger og Infrastruktur. *Bygningsreglement 2006* **2006**, 158. ISBN 87-991296-0-4. Available online: http://www.byginfo.gl/media/1131/br2006dk.pdf (accessed on 15 February 2022).
3. Ozel, M. Thermal performance and optimum insulation thickness of building walls with different structure materials. *Appl. Therm. Eng.* **2011**, *31*, 3854–3863. [CrossRef]

4. Rosti, B.; Omidvar, A.; Monghasemi, N. Optimal insulation thickness of common classic and modern exterior walls in different climate zones of Iran. *J. Build. Eng.* **2020**, *27*, 100954. [CrossRef]
5. Dombayci, Ö.A.; Ozturk, H.K.; Atalay, Ö.; Acar, Ş.G.; Ulu, E.Y. The Impact of Optimum Insulation Thickness of External Walls to Energy Saving and Emissions of CO2 and SO2 for Turkey Different Climate Regions. *Energy Power Eng.* **2016**, *8*, 327–348. [CrossRef]
6. Aktemur, C.; Bilgin, F.; Tunçkol, S. Optimisation on the thermal insulation layer thickness in buildings with environmental analysis: An updated comprehensive study for Turkey's all provinces. *J. Therm. Eng.* **2021**, *7*, 1239–1256. [CrossRef]
7. Akyüz, M.K. The effect of optimum insulation thickness on energy saving and global warming potential. *Türk Doğa Ve Fen Derg.* **2020**, *9*, 18–23.
8. Dylewski, R.; Adamczyk, J. Optimum Thickness of Thermal Insulation with Both Economic and Ecological Costs of Heating and Cooling. *Energies* **2021**, *14*, 3835. [CrossRef]
9. Dylewski, R.; Adamczyk, J. Impact of the Degree Days of the Heating Period on Economically and Ecologically Optimal Thermal Insulation Thickness. *Energies* **2021**, *14*, 97. [CrossRef]
10. Spanodimitriou, Y.; Ciampi, G.; Scorpio, M.; Mokhtari, N.; Teimoorzadeh, A.; Laffi, R.; Sibilio, S. Passive Strategies for Building Retrofitting: Performances Analysis and Incentive Policies for the Iranian Scenario. *Energies* **2022**, *15*, 1628. [CrossRef]
11. Axaopoulos, I.; Axaopoulos, P.; Gelegenis, J.; Fylladitakis, E.D. Optimum external wall insulation thickness considering the annual CO_2 emissions. *J. Build. Phys.* **2019**, *42*, 527–544. [CrossRef]
12. Ounis, S.; Aste, N.; Butera, F.M.; del Pero, C.; Leonforte, F.; Adhikari, R.S. Optimal Balance between Heating, Cooling and Environmental Impacts: A Method for Appropriate Assessment of Building Envelope's U-Value. *Energies* **2022**, *15*, 3570. [CrossRef]
13. IPCC. Climate Change Widespread, Rapid, and Intensifying. 2021. Available online: https://www.ipcc.ch/2021/08/09/ar6-wg1-20210809-pr/ (accessed on 1 February 2022).
14. Danish Standards. EN 15978:2012 Sustainability of construction works – Assessment of environmental performance of buildings – Calculation. 2012; 64.
15. SBI. LCAbyg. 2021. Available online: https://www.lcabyg.dk (accessed on 4 November 2021).
16. Royal Arctic Line. Home. Available online: https://www.royalarcticline.com (accessed on 4 January 2022).
17. Google. Google Maps. Available online: https://www.google.com/maps (accessed on 4 November 2021).
18. Ecoinvent Database—Ecoinvent. Available online: https://ecoinvent.org/the-ecoinvent-database/ (accessed on 24 February 2022).
19. SimaPro. LCA Software for Informed-Change Makers. 2022. Available online: https://simapro.com/ (accessed on 24 February 2022).
20. Huijbregts, M.A.; Steinmann, Z.J.; Elshout, P.M.; Stam, G.; Verones, F.; Vieira, M.; Zijp, M.; Hollander, A.; van Zelm, R. ReCiPe2016: A harmonised life cycle impact assessment method at midpoint and endpoint level. *Int. J. Life Cycle Assess.* **2017**, *22*, 138–147. [CrossRef]
21. KNR. Nyt Affaldsselskab vil Fjerne Lossepladserne i Grønland. Available online: https://knr.gl/da/nyheder/nyt-affaldsselskab-vil-fjerne-lossepladserne-i-gr\T1\onland (accessed on 3 December 2021).
22. Nukissiorfiit Fjernvarme. 2020. Available online: https://nukissiorfiit.gl/da/Produkter/Varme/Fjernvarme (accessed on 22 February 2022).
23. Nukissiorfiit. Årsregnskab 2020. 2020. Available online: https://nukissiorfiit.gl/media/06032524-3bb3-4622-8cd7-f65c523d4446/7bEfjw/docs/Nukissiorfiit_%C3%85rsrapport_2020_dk.pdf (accessed on 20 November 2021).
24. Kommuneqarfik Sermersooq. 19.000 indbyggere i Nuuk—Kommuneqarfik Sermersooq. 2021. Available online: https://sermersooq.gl/da/2021/09/19-000-indbyggere-i-nuuk/ (accessed on 24 February 2022).
25. Avannaata Kommunia. Fakta om Kommunen. 2021. Available online: https://www.avannaata.gl/emner/om_kommunen/fakta-om-kommunen?sc_lang=da (accessed on 24 February 2022).
26. Qeqqatta Kommunia. Sisimiut. 2021. Available online: https://www.qeqqata.gl/emner/om_kommunen/byer_bygder/sisimiut?sc_lang=da (accessed on 24 February 2022).
27. Guldborgsund Forsyning. Graddage. Available online: https://www.guldborgsundforsyning.dk/graddage/ (accessed on 19 October 2021).
28. Grønlands Statistik. Summerede Graddageværdier [END1SUM]. 2020. Available online: https://bank.stat.gl/pxweb/da/Greenland/Greenland__EN__EN30/ENX1SUM.px/ (accessed on 3 November 2021).
29. Lindsey, R.; Dahlman, L. Climate Change: Global Temperature. 2021. Available online: https://www.climate.gov/news-features/understanding-climate/climate-change-global-temperature (accessed on 3 November 2021).
30. Meredith, M.; Sommerkorn, M.; Cassotta, S.; Derksen, C.; Ekaykin, A.; Hollowed, A.; Kofinas, G.; Mackintosh, A.; Melbourne-Thomas, J.; Muelbert, M.M.C.; et al. Polar regions. *IPCC Spec. Rep. Ocean Cryosph. A Chang. Clim.* **2019**, 203–320. [CrossRef]
31. Friis, N.K. Insulation Thickness Optimizer, ITO. 2022. [CrossRef]
32. Ökobaudat. Process Data Set: Construction Rubble Landfill. 2018. Available online: https://www.oekobaudat.de/OEKOBAU.DAT/datasetdetail/process.xhtml?uuid=b7cacb37-7945-4518-be5a-bf7df7edf5c2&version=20.19.120 (accessed on 10 November 2021).

33. Friis, N.K.; Møller, E.B.; Lading, T. Can collected hygrothermal data illustrate observed thermal problems of the façade?—A case study from Greenland. *J. Phys. Conf. Ser.* **2021**, *2069*, 012071. [CrossRef]
34. Danish Standards. DS418, Calculation of Heat Loss from Buildings. 2020; ISBN 978-87-571-2458-3.
35. Naalakkersuisut-Government of Greenland. BR21 Høringsudgave, no. 13, 2021.
36. Kumar, A.; Schei, T.; Ahenkorah, A.; Caceres, R.R.; Devernay, J.; Freitas, M.; Hall, D.; Branche, E.; Burkhardt, J.; Descloux, S.; et al. 5 Hydropower. 2018. Available online: https://www.ipcc.ch/site/assets/uploads/2018/03/Chapter-5-Hydropower-1.pdf (accessed on 20 November 2021).
37. Green Building Council Denmark and DGNB. Guide til DGNB. *Green Build. Counc. Den.* **2021**, 54. Available online: https://dk-gbc.dk/publikation/guide-til-dgnb-for-bygninger (accessed on 21 March 2022).
38. Boyce, P.; Hunter, C.; Howlett, O. The Benefits of Daylight through Windows. 2003, p. 88. Available online: https://www.lrc.rpi.edu/programs/daylighting/pdf/DaylightBenefits.pdf (accessed on 15 February 2022).
39. Technical University of Denmark. Om Projektet-ABC-Arctic Building and Construction. Available online: https://abc-byg.dtu.dk/om-projektet (accessed on 5 May 2022).

III. Optimisation of Thermal Insulation Thickness Pertaining to Embodied and Operational GHG Emissions in Cold climates – Future and Present

Jørn Emil Gaarder, **Naja K. Friis**, Ingrid S. Larsen,
Berit Time, and Eva B. Møller

Building and Environment, 234 (November 2022)
doi:10.1016/j.buildenv.2023.110187

III

Building and Environment 234 (2023) 110187

Contents lists available at ScienceDirect

Building and Environment

journal homepage: www.elsevier.com/locate/buildenv

Optimization of thermal insulation thickness pertaining to embodied and operational GHG emissions in cold climates – Future and present cases

Jørn Emil Gaarder [a,*], Naja Kastrup Friis [b], Ingrid Sølverud Larsen [a], Berit Time [c], Eva B. Møller [b], Tore Kvande [a]

[a] Norwegian University of Technology and Science (NTNU), Trondheim, Norway
[b] Technical University of Denmark (DTU), Kgs, Lyngby, Denmark
[c] SNTEF Community, Trondheim, Norway

ARTICLE INFO

Keywords:
Building
Operational emissions
Embodied emissions
Energy emission factor
Climate change
Energy use

ABSTRACT

Determining the optimal insulation thickness is useful for designing zero-emission buildings (ZEB) to minimize the environmental impacts. The energy required to heat buildings in cold climates is relatively high. Substantial reductions in the total energy usage of a building can be achieved by reducing the U-value of the external surfaces. Increasing the insulation thickness reduces the operational CO_2 emissions, although simultaneously increases the embodied CO_2 emissions from materials. To mitigate climate change, Norway and Denmark are trending towards stricter regulations to limit energy use in buildings. However, these countries have no current regulations in the building codes for limit embodied CO_2 emissions from materials. This study analyzes the influence of the energy emission factor and future climate change (scenarios?) on the optimal insulation thickness. We used three independent models for case studies in Greenland and Norway. The differences between the case studies highlight the influence of model parameter choices, such as indoor climate, energy emission factor and material emissions, whereas the similarities may be used to analyze the problem from a broader perspective. The results show that optimal insulation thickness calculations are most valuable for case studies in which the energy emission factor is low. Considering energy emission factors above 25–30 g CO_2eq/kWh, operational emissions dominated the calculation results in all case studies.

1. Introduction

Globally, buildings are responsible for 40% of the total energy consumption and 25% of the greenhouse gas (GHG) emissions [1]. In Norway, one-third of the consumed energy is used for direct heating of buildings [2]. In cold climates, sufficient thermal insulation of buildings to reduce heat loss is important and this is reflected in both Norwegian and Danish building codes. Regulations for the energy performance of buildings have been tightened over the past decades in both Norway and Denmark [3]; Bygningsreglementet 2018), thereby reducing GHG emissions from buildings. Although the Greenlandic building codes have yet to be updated based on the Danish building codes of 2018. However, the environmental impacts of the materials used to insulate buildings have not yet been considered in the building codes. As the insulation layers become thicker, the embodied emissions increase, and operational emissions decrease. Earlier studies have found that the influence of operational emissions in buildings tend to outweigh the influence of embodied emissions in the Norwegian climate [4]. However, the results are sensitive to the energy emission factor of the heating source used to calculate operational emissions. The energy emission factor describes the GHG emissions resulting from power production to heat the building.

The past decade has yielded significant research findings relating to how future climate changes will impact energy use in buildings [5], and significant efforts have been made to reduce global emission rates. For example, the ongoing decarbonization of the European power sector has the ambitious aim of reducing GHG emissions by 90% between 2010 and 2050 [6], which will lower the energy emissions significantly. Temperature measurements of the climate in Norway conducted by the Norwegian Meteorological Institute (MET) since 1900 indicate a steady increase in average temperature starting from 1985 [7]. This trend is expected to continue, with the rate of increase dependent on future global emission rates [8]; 2022).

Most research concerning optimization of thermal insulation relates

* Corresponding author.
E-mail address: jorn.e.gaarder@ntnu.no (J.E. Gaarder).

https://doi.org/10.1016/j.buildenv.2023.110187
Received 9 November 2022; Received in revised form 3 March 2023; Accepted 5 March 2023
Available online 9 March 2023

the issue to warmer climates, predominantly emphasizing energy use for cooling or moderate heating [9]. The building practice in warm regions (i.e. Turkey and Morocco) has traditionally neglected the need for thermal insulation, thus motivating research for lowering either cost or GHG-emissions through optimal insulation strategies [10–13]. These studies conclude that optimal insulation thicknesses are in the range of 5–20 cm, depending on the insulation material, climate and energy emission factors used [9].

It is becoming more important to address the issue in cold-climates as well, as changes in the climate are expected to occur more rapidly in arctic regions, compared to most other places on Earth [14]. Few studies have considered the consequences for the built environment in cold regions, or subsequently formulated appropriate adaptation measures [5]. High energy demands for heating and high energy emission factors in these regions, has led to an approach of "the more the better" within the practical range of insulation thicknesses [4]. This conclusion may change as the energy emission factors are likely to decrease in the future, due to the focus on green energy production in Europe [6].

This study analyzed how energy emission factors and future temperature changes affect the optimal strategies for limiting emissions from buildings in cold climates by examining three different models, each calculating four cases with varying climates and energy emission factors. The climates considered by the models were classified according to the Köppen climate classification [15] as subarctic continental (group Dfc) and arctic (group E). Subarctic continental climates are characterized by the coldest month averaging below 0 °C and 1–3 months averaging above 10 °C, whereas arctic climates are characterized by no month averaging above 10 °C. In addition to considering the Norwegian climate, this study also includes case studies of the Greenland climate. Greenland, being an island-based community, have challenges regarding centralized infrastructure. This leads to unique combinations of energy sources in each location, thus affecting the energy emission factors.

Future climate change and energy emission factors are highly complex subjects, as both depend on global socioeconomic developments, introducing high levels of uncertainty into the models. Due to the complexity, this study analyzed the problem using three independently constructed models for calculating the optimal insulation thicknesses. Models 1 and 2 were simplified to consider an insulated outer wall segment of 1 m^2. Thus, some of the complexities introduced by using a full-scale building model are omitted. Model 3 considers a full-scale building to verify the results from the first two models. The purpose of this study is to see how changes in climate and energy emission parameters influence the total emissions from energy and material use. The research questions explored are as follows.

1. How will future climate changes influence the optimal thermal insulation thickness in cold climates?
2. How will future changes in the energy emission factors used for heating influence the optimal insulation thickness?

A theoretical framework focused on climate modeling, energy performance, energy emission factors, and Life-Cycle Analysis (LCA) of building materials is presented in section 2. Three models were established for calculating operational and embodied emissions. The results of each model are presented in section 4, along with a sensitivity analysis that identifies the robustness of each method. A discussion of the impacts is presented in section 5. None of the models address the second-order benefits or disadvantages of a given insulation thickness (e.g., construction practicality, indoor comfort levels, or changes in floor area), as they are strictly focused on the emission intensities of different insulation thicknesses. Further, the models use input for material emissions using standard LCA methodology, documented through European Product Declarations (EPD). The impact of more holistic methods for determining the carbon footprints of materials emerging, such as the PEF method (EU 2013), are outside the scope of this paper. Because the models rely on pre-documented EPDs for determining the material emissions, the embodied emissions in materials are unchanged in the future scenarios considered.

2. Theoretical framework

2.1. Future climate scenarios

The climate is changing rapidly because of the increased concentration of GHGs in the atmosphere (IPCC 2022). This has consequences for the built environment and how buildings are designed [16]. An increase in GHGs in the atmosphere captures more thermal radiation, causing the global average temperature to rise. In the fifth assessment report from the International Panel on Climate Change (IPCC), different scenarios based on projections of emission rates were categorized by Representative Concentration Pathways (RCPs), which describe radiative forcing from GHG concentrations in the atmosphere. As defined in the IPCC report, the four RCPs used for climate modeling are RCP 2.6, RCP 4.5, RCP 6, and RCP 8.5. The IPCC released a new assessment report in 2021/2022 with updated scenarios. As the case studies described in this study were conducted before the release of the sixth assessment report, future climate scenarios were used as outlined in the fifth assessment report.

The RCP 8.5 scenario, described as "business as usual" in the IPCC report and assuming negligible intervention to curtail GHG emissions, could lead to a global increase in average temperature of 2.6–4.8 °C by 2100. The emission curve in RCP 8.5 closely agrees with the historical total cumulative CO_2 emissions from 2005 to 2020 (within 1%), and is often used for near-to-mid-term assessments [17]. However, the RCP 8.5 scenario is not in agreement with the sub 2 °C goal outlined in the Paris Agreement [18]. Comparing the RCP 8.5 scenario with historical conditions is useful because these two scenarios may represent the outer boundaries of the optimal insulation strategy.

2.2. Energy performance

The U-value describes the amount of heat transported through the construction per unit area and per unit temperature difference and is defined in Equation (1).

$$U = \left(\sum_{0}^{i=n} R_i \right)^{-1} \quad \left[\mathrm{W} / \left(\mathrm{m^2 K} \right) \right] \tag{1}$$

where R_i is the heat resistance of layer i (m^2K/W). The U-value does not decrease linearly with increasing insulation thickness because it is inversely related to the heat resistance, as illustrated in Fig. 1. Thus, increasing the insulation thickness to reduce operational emissions yields diminishing returns.

Neglecting solar irradiation and heating from internal loads, such as lighting and equipment, the conductive heat loss through a 1 m^2 outer wall can be balanced by considering the outdoor temperature at which occupants specifically use energy for heating the building [19]. proposed the use of $T_{out,\ crit} = 10$ °C because internal heating loads generated by occupants, hot water use, lighting, and equipment tend to match the heating demand above this temperature. Earlier studies have found that the variability of average indoor temperature for single-family homes was dominated by occupant behavior including comfort level, energy-saving behavior, and use of equipment [20,21]. The average indoor temperature measured by Ref. [20] was found to have a normal distribution with an average of 21.5 °C and a standard deviation of 1.3 °C.

2.3. Energy emission factor

To compare the embodied carbon emissions from the production of materials to the operational emissions from heating, the two categories

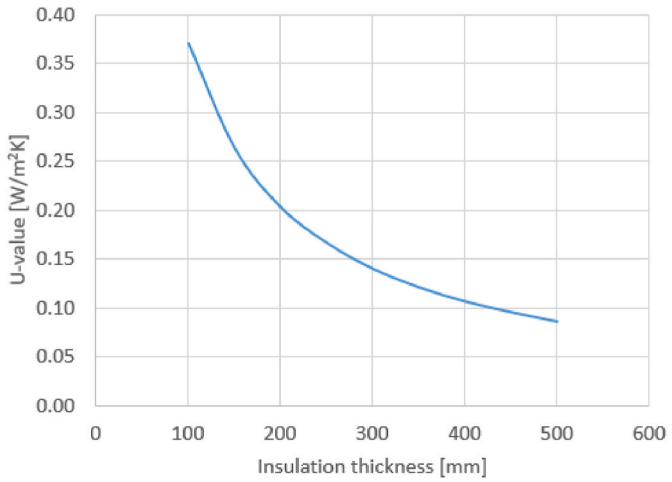

Fig. 1. U-value as a function of insulation thickness for a typical Norwegian wooden framework wall with ventilated outer cladding(36 mm thick wooden studs c/c 600 mm, wooden frame estimated to be 13% of total wall area, and. The insulation material heat conductivity is 0.034 W/(mK)).

must be converted into comparable functional units, i.e., the carbon footprint per functional unit. Emissions from energy use is described by the energy emission factor in units of gCO_2eq/kWh [22]. The Norwegian Standard NS 3720:2018 [23], which describes methods for GHG emission calculations for building designs, allows the use of two different scenarios related to the system boundaries. Firstly, the average emission rate from the Norwegian energy consumption mix over the last three years and secondly, the average emission rate from the European energy consumption mix over the last three years. Examining Norway in a closed system using the Norwegian energy mix is logical, e.g., Scenario 1; however, the global energy grid is interconnected between countries, and consuming an additional 1 kWh of electric energy in Norway may lead to either increased imports or decreased exports of 1 kWh of energy, both of which create a need to generate an additional 1 kWh outside of Norway. This is not the case in Greenland, as there are no imports or exports of energy. As there is no central grid connecting different cities in Greenland, each location is an isolated case with a clearly defined energy mix, giving high confidence to energy emission factor estimations. The various sources of energy used for heating buildings in different locations in Greenland include district heating from combustible sources, hydropower, and direct local heating from oil and gas [24].

The Norwegian energy mix is 95% hydropower [25] which is a very low-carbon intensity power source even by renewable energy standards [26]. The average emission factor for the Norwegian energy mix for the period 2015–2075 was set to 18 gCO_2/kWh in NS 3720:2018. The average European energy factor for the same period was set to 136 gCO_2/kWh, with 43% generated from combustible sources in 2015 [23]. The two major sources of hydropower emissions are activities related to the construction of dams and power stations, as well as methane emissions from the anaerobic decomposition of flooded organic matter. A meta-analysis by Ref. [26] comparing 12 studies on emission factors from hydropower reported calculated emission factors of 2–20 gCO_2/kWh. In comparison, the same study reported calculated emission factors for oil and natural gas in the range of 380–1000 gCO_2/kWh, and coal emission factors up to 1300 gCO_2/kWh [26]. A careful consideration of the energy mix used in the calculations is important as it affects calculated energy emission factors which are crucial in operational emission calculations.

Using a future scenario for the development of renewable energy sources in Europe, a Norwegian Research Center on Zero Emission Buildings (FME ZEB) proposed calculating emission factors by assuming a 90% reduction in GHG emissions in the power sector in 2050 compared to 2010, as per the European Union's (EU's) Roadmap Towards 2050 [6,27]. By first determining the service life of buildings in the LCA calculations, the average emission factor over the building lifetime can be calculated and used as a design value, as illustrated in Fig. 2.

The FME ZEB method considered an average European energy mix, which is substantially more carbon intensive than the Norwegian energy mix, and thus yields a higher emission rate per kWh. A study on energy emission factors proposed an energy emission factor of 132 g/kWh based on results from the FME ZEB [28]. However, this number is continuously changing as this method is based on the energy emission factor throughout the lifetime of a building. Assuming a building lifetime of 60 years, Fig. 2 shows the development of the design energy emission factor recommended by the FME ZEB depending on the year of construction. The energy emission factor for the year 2010 were estimated by the FME ZEBto be 361 gCO_2/kWh, with a linear decline towards 31 gCO_2/kWh in 2050 and reaching 0 by extrapolation in 2054 [27]. Therefore, this model is unrealistic for long-term energy emission factor estimations such as the future scenarios considered in this study (2071–2100).

In cooperation with Statistics Norway (SSB), the Norwegian Water Resources and Energy Directorate (NVE) calculated the emission factor to be 17 g CO_2eq/kWh for actual delivered electrical energy in Norway in 2019, based on hourly measurements of net import/export and energy consumption [29].

The NVE calculations only consider the direct emissions from the energy carrier used to generate energy and disregards the emissions from infrastructure (i.e., creating power plants and maintaining the power grid) and energy carrier harvest (i.e., procuring fossil and nuclear fuels). As import/export has a significant impact on the Norwegian energy mix, the energy emission factor for energy design in Norway must be carefully considered. An overview of the energy emission factors based on the sources discussed in this study is presented in Table 1.

3. Methods

3.1. Introduction to the case methodology

The estimated service life (ESL) was set to 60 years for all cases in accordance with the FME ZEB guidelines for life cycle assessments [30] assuming no need for maintenance or material exchange. When changing the insulation thickness in the models. Secondary effects, such as decreased floor area, are not considered. The analysis was performed using glass wool as a thermal insulation material. The global warming potential (GWP) for the insulation products considered in each model is presented in Table 2, along with the pertinent details required for the energy emission calculations. In all building models, the GWP included the production process from cradle-to-gate (A1-A3), transportation to the building site (A4), and transportation and the process of waste handling (C2–C3).

The geographical positions of the four locations studied in the three models are shown in Fig. 3. For each model, four calculation cases have been assessed, designated A-D. Cases designated A and B are calculated with the relevant low-end energy emission factor alternative for the location, with historic and future climate respectively. Cases C and D are equal to A and B in every respect, only calculated with the relevant high-end energy emission factor.

The total emissions over the service life time as a function of insulation thickness, $M_{tot}(t)$, are calculated for all models according to the definition given in Equation (2).

$$M_{tot}(t) = \left(\sum_{60\ yr} (f_e \bullet E_{heat}(t)) \right) + M_{mat}(t) \quad (2)$$

, where f_e is the energy emission factor, $E_{heat}(t)$ is the yearly energy use for heating as a function of insulation thickness and $M_{mat}(t)$ is the ma-

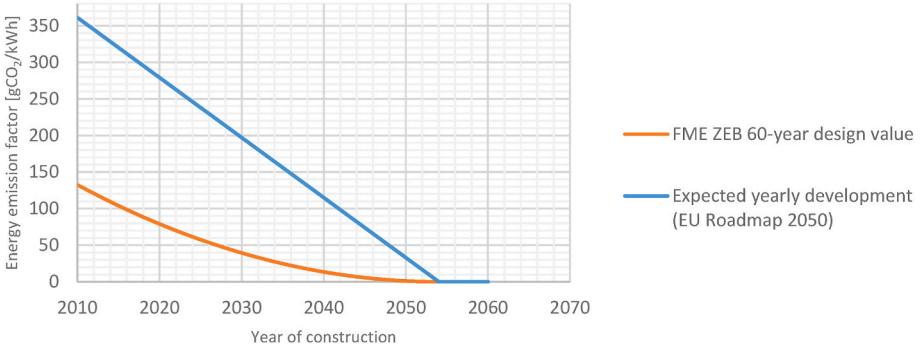

Fig. 2. Development of design energy emission factor for grid electricity [27], based on the development of energy emissions in the European energy market.

Table 1
Energy emission factors reported by the sources discussed in this chapter.

Source	Energy grid	Recommended energy emission factor [gCO_2/kWh]	Description
Norwegian Standard (NS3720:2018) [23]	Norway	18	Estimated average Norwegian energy mix in building lifetime (2015–2075)
Norwegian Standard (NS3720:2018) [23]	Norway	136	Estimated average European energy mix in building lifetime (2015–2075)
FME ZEB [28]	Norway	132	Estimated average European energy mix based on future development of renewable energies from 2010 to 2050 (reported in an article from 2014, based on construction year 2010)
FME ZEB [28]	Norway	74	Updated estimated average European energy mix based on the future development of renewable energies from 2010 to 2050 (calculated for construction year 2021)
Norwegian Water Resources and Energy Directorate [29]	Norway	17	Calculated actual average energy emission factor for delivered energy in Norway in 2019, including only direct emissions from energy carriers
Departement for Landbrug, Selvforsyning, Energi og Miljø [24]	Greenland	9	Electrical heating from 100% hydropower (location: Nuuk)
Departement for Landbrug, Selvforsyning, Energi og Miljø [24]	Greenland	207	Electrical heating from combustible energy sources (location: Aasiaat)

terial emissions as a function of insulation thickness.

3.2. Case 1: subarctic continental climate (unit-level model, Norway)

The first case study of a typical single-family home in the district of Ydalir, Elverum, Norway. Ydalir has been used as a pilot project in the FME ZEB research center, which emphasizes studying collective emissions for a neighborhood, both embodied and operational. Approximately 1000 residential living units with passive-house standards or higher will be developed in the district over the next 15–20 years [32].

The model for calculating operational and embodied emissions was restricted to 1 m^2 of a representative outer wall with insulation thicknesses of 100–500 mm. Based on historical conditions and a future climate scenario (RCP 8.5), the energy performance and resulting emissions were calculated for the case study.

The U-value is calculated based on a typical Norwegian wooden framework wall. The wall is composed of glass wool insulation with heat conductivity equal to 0.034 W/(mK) placed in a wooden framework with an inner cladding of 12.5 mm gypsum board, and ventilated wooden outer cladding with a 9 mm gypsum board wind barrier. Assuming a stud width of 36 mm and c/c 600 mm studding in a single-family home with a ceiling height of 2.4 m the wood-to-insulation ratio per area is 13%, in accordance with the tables provided by SINTEF in Byggforskserien 471.401 [33].

The model compares operational emissions in two different climates: one based on historical weather data and the other based on a future climate scenario. MET has weather stations throughout the country that continually register weather data. Weather data from Rena, 35 km north of Elverum, were used to create weather files with hourly temperature data. The basis for the historical reference year is temperature measurements in the period 1961–1990, and the future scenario (2071–2100) is a downscaling of a regional climate model based on the RCP 8.5.

Weather files were generated by MET and median, maximum, and minimum temperatures, as well as standard deviations for each month were recorded for each period. A 366-day year series, with maximum and minimum temperature values, was generated by random drawing with a normal distribution over each month as a constraint. Three repetitive years were generated, and the hourly values generated by spline interpolation before the first and last years were removed to eliminate noise from the series. Energy calculations for ten runs of both historical and future scenarios were performed, and the results are shown as the average of the ten runs.

The heating strategy assumed in Model 1 was based on the critical outdoor temperature. The critical outdoor temperature, below which energy is used specifically for heating, is set to 10 °C in accordance with the recommendations of [19]. The indoor temperature was set to 21 °C in close agreement with the average measured indoor dwelling temperature in a comprehensive survey by Refs. [19,20]. The yearly energy use for heating, $E_{heat}(t)$, in Model 1 is calculated according to Equation (3).

$$E_{heat}(t) = U(t) \bullet \sum_{n=1}^{8760} \left((T_{in} - T_{out}(n)) \bullet 1hr \right) \quad (3)$$

Table 2
Parameters and ID of each model.

Case	Model type[a]	ID	Location	Climate	Indoor temp [C°]	Average HDD[b] [(K • d)/a]	Energy emission factor [kg CO_2eq/kWh]	Insulation material GWP [kg CO_2eq/(m^2K/W)m^2]
Model 1	Local	1.A	Elverum (NO)	1961–1990	21.5	6637	0.017	0.8
		1.B	Elverum (NO)	2071-2100 (RCP 8.5)	21.5	4995	0.017	0.8
		1.C	Elverum (NO)	1961–1990	21.5	6637	0.132	0.8
		1.D	Elverum (NO)	2071-2100 (RCP 8.5)	21.5	4995	0.132	0.8
Model2	Local	2.A	Nuuk (GL)	1996–2000	19	7200	0.009	1.0
		2.B	Nuuk (GL)	2021–2040 (RCP 8.5)	19	6950	0.009	1.0
		2.C	Aasiaat (GL)	1996–2000	19	8150	0.207	1.0
		2.D	Aasiaat (GL)	2021–2040 (RCP 8.5)	19	7900	0.207	1.0
Model 3	BES	3.A	Oslo (NO)	1961–1990	19	4088	0.017	0.5
		3.B	Oslo (NO)	2071-2100 (RCP 8.5)	19	3016	0.017	0.5
		3.C	Oslo (NO)	1961–1990	19	4088	0.132	0.5
		3.D	Oslo (NO)	2071-2100 (RCP 8.5)	19	3016	0.132	0.5

[a] Local model: values calculated for 1 m^2 wall, BES model: values calculated on a building level.
[b] HDD = Heating Degree Days. The HDD for Models 1 and 3 are calculated for comparison purposes only, as neither model uses HDD as an explicit input value.

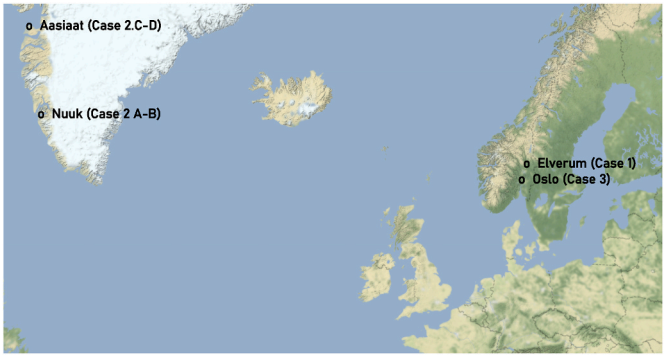

Fig. 3. Geographical locations included in the study [31].

, where $U(t)$ is the U-value of the wall with insulation thickness t in W/(m^2K), T_{in} is the indoor temperature (21 °C) and $T_{out}(n)$ is the outdoor temperature in hour n. All hourly values where $T_{out} > 10°C$ were omitted.

The resulting operational emissions were calculated according to Equation (2) using energy emission factors of 17 gCO_2eq/kWh for the measured Norwegian energy consumption mix in 2019 [29] and 132 gCO_2eq/kWh for the European mix for construction year 2010 according to the method proposed by the research center FME ZEB [27].

Based on the environmental impacts of glass wool insulation reported in the European Product Declarations (EPD) review by Ref. [34] and a control comparison against 5 EPDs found in the database provided by EPD Norway, the median value is used (0.8 kg CO_2eq/(m^2K/W)m^2). For wood materials, the average environmental impact from the four studied EPDs found in the EPD-Norway database (EPD-Norway 2022) was used (106 kg CO_{2eq}/m^3). As proposed by NS 3720:2018, the biogenic carbon storage of wood was set to zero [23]. The calculations included emissions from the production, transport, construction, maintenance, and demolition stages. Benefits beyond the system boundaries, such as the reusing of materials, were not considered. Furthermore, changes in future energy emission factors were not considered in the calculation of material emissions.

3.3. Case 2: arctic climates (Greenland, unit-level model)

The model for the Greenland case is based on the insulation thickness optimizer tool ITO, which was described and analyzed in an earlier study [35]. Considering the optimal insulation thickness in Greenland, the conditions varied for each town. The model for calculating operational and embodied emissions was restricted to a 1 m^2 wall. The wall consisted of 150 mm of concrete, insulation, a ventilated air cavity, and cladding. Construction represents a typical wall for residential buildings in Greenland. Without insulation, the wall exhibited an R-value of 0.331 m^2K/W.

The calculations for ITO were based on heating degree days (HDD). The HDD for the historical climate dataset is based on five-year-average data from 1996 to 2000, provided by the Danish public institution Statistikbanken (2022). According to Ref. [36]; following the RCP 8.5 pathway is equal to a future change in HDD of −400 K°d over the next 40 years in Greenland, leading to an average temperature decrease of 10 HDD/year. The tool distributes the temperature change evenly over the ESL of the building, which is a simplification as research shows that changes occur more rapidly over time.

The analysis was conducted at two locations, Nuuk and Aasiaat. Nuuk is the largest city in Greenland, with approximately 19,000 inhabitants, and has a very low emission factor of only 9 g/kWh owing to the availability of local hydropower [24]. Additionally, Nuuk is located south of the polar circle, making the climate less extreme than that in many other parts of Greenland. There is no central electrical grid in Greenland between different urban areas, making the energy emission factors of the different areas independent. Aasiaat is a much smaller town with approximately 3000 inhabitants, and the emission factor of heating energy was calculated to be 207 g/kWh, as the energy mix in Aasiaat is based on combustible energy sources [24]. Aasiaat is located north of the polar circle, thereby causing a higher heating demand (see Table 2).

The analysis was based on the EPD from the LCAbyg database (LCAbyg 2022). The EPD for glass wool is suitable for façade construction (Ökobaudat 2022) and is given as 1.0 kg CO_2eq/(m^2K/W)m^2. The density was 46.25 kg/m^3 and the lambda value was 0.034 W/(mK). The EPD contributes to stages, A1-3, C3, and C4, while transportation is

based on distances from the production country to the respective location of the building.

3.4. Case 3: subarctic continental climate (Norway, global model)

The boundary of the model in Case 3 is expanded to encompass the entire building, using a building energy simulation model (BES). For Cases 1 and 2, the model calculates changes in operational and embodied emissions as a function of the thermal insulation thickness of the wall but is summed up at the building level. As Case 3 is a full-scale model of a building, the energy calculations consider excess heat from electrical equipment and heat loss through ventilation when calculating the energy demand for heating, and is therefore valuable as a validation for the necessary assumptions of heating strategies in the unit-level models for Cases 1 and 2. To ensure that the embodied emissions of materials outside the wall boundaries are fixed for varying wall thicknesses, the model assumes that the outer dimensions of the building are fixed rather than the inner floor area.

The building in the model is a prefabricated detached single-family house designed by Norgeshus, called Trend 2 (see Fig. 4), which is representative of a typical Norwegian single-family dwelling and satisfies the Norwegian Building Code. The full set of schematics, including a full list of materials and quantities, were made available to the authors by the contractor. The total heated floor area is 129.4 m^2 over two stories. For a full set of details on the building in this case study, see Totland [4] and Andenæs, Kvande, and Bohne [37]. To calculate the energy demand, SIMIEN, which is a commercial Norwegian simulation program for calculating energy consumption and power requirements in buildings, was used. SIMIEN simulates energy need based on the Norwegian Standard NS 3130: Calculation of energy performance of buildings (Standard-Norge 2014). Standard input values from NS 3130 were used in all instances except where data specific to Trend 2 was obtained. The central parameters of the BES are listed in Table 3.

The embodied emissions from the materials used were calculated using OneClick-LCA software, and the standard values of environmental impacts proposed by the program were used for all materials except thermal insulation. The materials in the considered wall includes ventilated outer wooden cladding, wooden fiber wind barrier, thermal insulation in a wooden framework, PE vapor barrier and wooden fiber inner cladding. The environmental impact of the thermal insulation is chosen based on an EPD of a specific type of Norwegian-produced soft glass wool, Glava Proff 34, with a lambda value of 0.034 W/(mK, and an environmental impact calculated to 0.5 kg CO_2eq/(m^2K/W)m^2 (EPD-Norway 2022).

Operational emissions for two climate scenarios were compared: one based on 30-year average historical measurements (normal period 1961–1990) and the other based on future climate projections using RCP 8.5. Climate data was provided by the MET using the same methods as in Case 1 to generate the weather data. The chosen geographical location for Case 3 was Oslo, Norway, which has a normal inland Norwegian climate.

Fig. 4. Architectural rendition of the prefabricated detached single-family house used for the energy calculations in Case 3 (Illustration used with permission by Norgeshus).

Table 3
Central parameters of the building energy simulation model used in Case 3.

Parameter	Value
U-value external wall	0,086–0371 W/(m^2K)
U-value ground floor	0,09 W/(m^2K)
U-value roof	0,14 W/(m^2K)
U-value windows	0,81 W/(m^2K)
Airtightness, n50	0,9 h^{-1}
Normalized thermal bridge value	0,05 W/(m^2K)
Normalized internal heat capacity	51 Wh/(m^2K)
Set-point temperature, heating	19 °C
Ventilation heat recovery efficiency	85%
Specific fan power, SFP	1,10 kw/(m^3/s)
Ventilation	1,20 m^3/(m^2h)
Excess heat from lighting, equipment, occupants	5,25 W/m^2
Solar factor, windows, SF	0,33
Installed effect, heating	80 W/m^2
Operational schedule, ventilation	24 h
Operational schedule, heating	16 h

4. Results

This section presents the results from the three cases as well as a sensitivity analysis for unit-level Models 1 and 2. A sensitivity analysis was performed by changing the input parameters to ±10% and evaluating the changes in the model outputs.

4.1. Case 1: subarctic continental climate (Norway, unit-level model)

4.1.1. Model results

The energy performance calculations estimated a 22% reduction in the energy needed for heating in the RCP 8.5 future scenario (2071–2100) compared to the historical scenario (1961–1990). Operational emissions from the heat loss through a 1 m^2 wall were calculated based on the emission factors for the Norwegian energy mix in isolation in 2017 (17 g CO_2eq/kwh) and the energy mix for the interconnected power grid with import/export to Europe, proposed by the FME ZEB in 2010 (132 g CO_2eq/kwh). The embodied emissions for each insulation thickness and the corresponding operational emissions were added and presented as a function of insulation thickness. The results for Case 1.A – 1.D, are shown in Fig. 5.

According to this model, the optimal insulation thickness for the RCP 8.5 future scenario was reduced by 75 mm compared to the historical scenario (from approximately 475 mm to approximately 400 mm), assuming an energy emission factor of 17 g CO_2eq/kWh. As the chosen insulation thickness approached the optimum value, the impact of the change on total emissions was reduced. Increasing or reducing the insulation thickness by 100 mm from the optimum value resulted in a 3.5% increase in the total CO_2 emissions. The total emissions were more sensitive to changes in insulation thickness on the left side of the optimum, owing to the nonlinear nature of the U-value as a function of insulation thickness, as illustrated in Fig. 1.

4.1.2. Sensitivity analysis

To determine how the changes in each parameter influenced the model results, a sensitivity analysis was performed. The analyzed parameters were the insulation lambda-value, HDD, energy emissions, and material emissions, as these were the most critical parameters. The HDD expresses the difference between the outdoor and indoor climates used in the model, which was separated into two different input parameters in

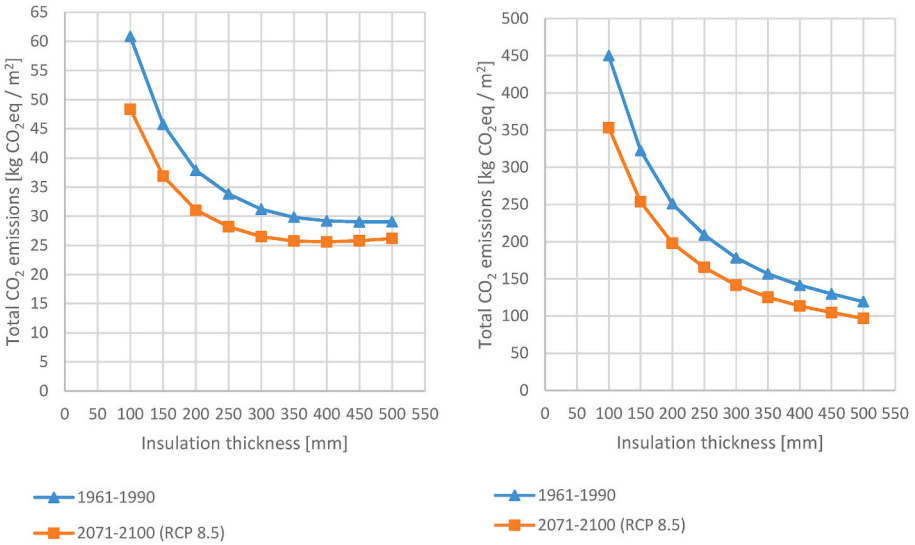

Fig. 5. Comparison of calculated future and historical CO_2 emissions for Case 1, using 17 g CO_2eq/kWh (a) and 132 g CO_2eq/kWh (b) as energy emission factors. Note the different scales on the y-axes.

the model of Case 1. Hence, the HDD is calculated for the sensitivity analysis only. This was a critical parameter because of the uncertainty in future climate change and occupant behavior. Energy emissions also had high uncertainty, owing to both future developments in energy generation and the calculation of the energy emission factor. The latter was especially true in the Norwegian context because the locally produced energy mix had a significantly lower emission factor than the interconnected energy mix of Europe. The results of the sensitivity analysis are shown in Fig. 6.

The parameter with the highest influence on the model in each of the four cases was the energy emissions. This was also the parameter with the highest variability, as the energy emissions for different cases could vary by a factor of 10, based on the building source of heating energy. The high impact of this parameter was also expressed by the effect of material emissions on the results for different energy emission factors. For an energy emission factor of 17 g CO_2/kWh, a 10% change in material emissions yielded a 3% change in model outputs (total emissions), whereas for an energy emission factor of 132 g CO_2/kWh, the same change in material emissions yielded almost no change. This was because the absolute material emissions were much lower than the absolute operational emissions for the high-energy emission factors. A 10% reduction in parameter values yielded approximately the same result as a 10% increase because the parameters were either linearly connected to the model result or approximately.

4.2. Case 2: arctic climates (Greenland, unit-level model)

4.2.1. Model results

The future and historic climates in Case 2 were closer to each other than for Cases 1 and 3, as the historical climate was based on measurements from 1981 to 2000, and the future climate was based on a climate model for 2021–2040. The chosen climate scenario had a very low influence on the model results compared to the Norwegian cases where the climates are 110 years apart. However, the energy emission factor was more pronounced in the Greenlandic cases, as the energy emission factor for Nuuk was based on 100% locally produced

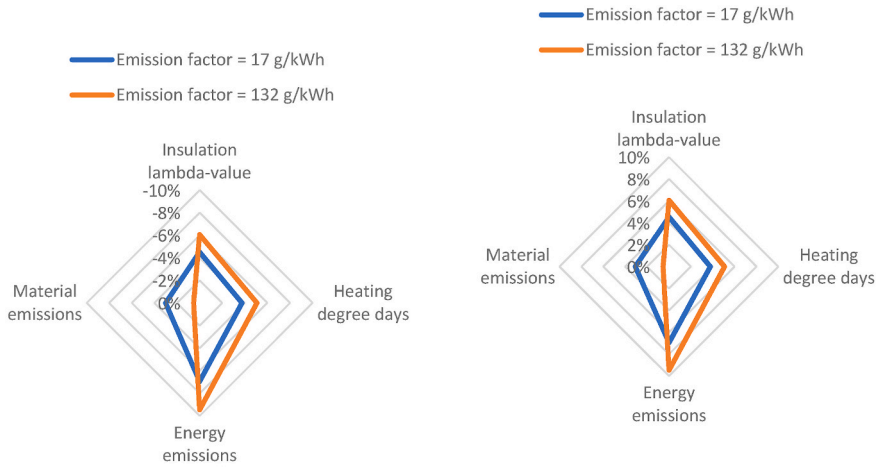

Fig. 6. Sensitivity analysis for the model used in Case 1, using wall insulation thickness d = 300 mm. Each parameter is changed by 10% with all other parameters fixed, and the change in model outputs is expressed as a percentage of change from the base case.

hydropower, and the energy emission factor for Aasiaat was based on district heating from combustible energy sources. The results of the Greenland model are shown in Fig. 7.

Climate change factors caused larger absolute changes in Aasiaat than in Nuuk; however, the percentage of change was the opposite. The low-emitting energy mix in Nuuk made the impact of reduced HDD very small, and the nearness in the two climate cases (1996–2000 and 2021–2040) resulted in climate parameters having a very low impact on the overall results. The optimal insulation thickness for Nuuk was 250 mm, whereas that of Aasiaat was outside the calculated area. This illustrated the high impact of energy emission factors on such calculations and underlines the importance of carefully considering this parameter.

III

4.2.2. Sensitivity analysis

The sensitivity analysis in Fig. 8 shows that the model for Aasiaat was more sensitive to positive changes than to negative changes. In both diagrams, the model for Aasiaat had low sensitivity to changes in emissions related to the production of insulation material. For Nuuk, the model showed approximately equal sensitivity to all parameters, although it was slightly more sensitive to negative changes than to positive changes, which is the opposite of Aasiaat.

Owing to the equation for calculating the heat loss through construction, a sensitivity analysis for the estimated service life was equivalent to the analysis of the HDD. Multiplying the HDD with a given factor yielded the same result in the model output as multiplying the estimated service life with the same factor. Therefore, the sensitivity analysis of the estimated service life was omitted.

An identical analysis was conducted for 30% changes, which led to similar trends but with greater sensitivity. This analysis was performed for an insulation layer of 300 mm which is beyond the optimal insulation thickness for Nuuk and may be responsible for its generally low sensitivity. The Nuuk case study is more sensitive to changes in the energy emission factor than the Aasiaat case study. Lower operational emissions make the contribution from embodied emissions more significant. For the other three parameters, the Aasiaat case study was more sensitive than the Nuuk case study, which was caused by the significance of the energy emission factor. When the energy emission factor was high, the operational emissions were more dependent on the climate and insulation quality.

4.3. Case 3: subarctic continental climate (Norway, global model)

4.3.1. Model results

The energy emission factors for Case 3 were the same as those for Case 1, as both case studies were situated in Norway, and both assumed the building was heated with 100% electrical energy and no locally-produced energy. The method of determining future climate conditions was also similar; however, Case 3 was based on the Oslo climate, whereas Case 1 was based on the Elverum climate, with the latter being slightly colder on average (see Table 2). The model results for Case 3 are shown in Fig. 9.

The model outputs from the global model in Case 3 displayed similar behavior to the model outputs in Case 1, but with less pronounced effects of changing insulation thicknesses. This is because the Case 3 models considers more effects, such as ventilation systems and passive heating through electrical equipment. In addition, the material emissions of the wall in Case 3 included outer and inner claddings. For an energy emission factor of 17 g CO_2/kWh, the optimal insulation thickness in Case 3 was calculated to be approximately 350 mm for the future case and approximately 300 mm for the historical case, in agreement with the results from the unit-level model in Case 1. For both Cases 1 and 2, when the energy emission factor was high, the optimal insulation thickness was outside the thickness range calculated by the model.

4.4. Summary of results

Table 4 summarizes the results from all calculated cases. The results for each case have been normalized for comparison purposes, by calculating the ratio of embodied and operational emissions of each insulation thickness relative to the embodied and operational emissions of insulation thickness 300 mm.

Models 1 and 2 are unit-level studies of the emission balance of a 1 m^2 wall. The internal energy loads from lighting and equipment and other effects must be estimated for the energy calculations. Therefore, a comparison of the findings from Models 1 and 2 to those of a similar study using a BES model (Model 3) should be performed to verify the validity of the assumptions. The climate scenarios and energy emission factors of Models 1 and 3 were the most similar and the results show similar trends for the optimal insulation thicknesses. Both show an optimum thickness of approximately 300–400 mm for the historic climate scenario with an energy emission factor 17 gCO_2eq/kWh, and both show

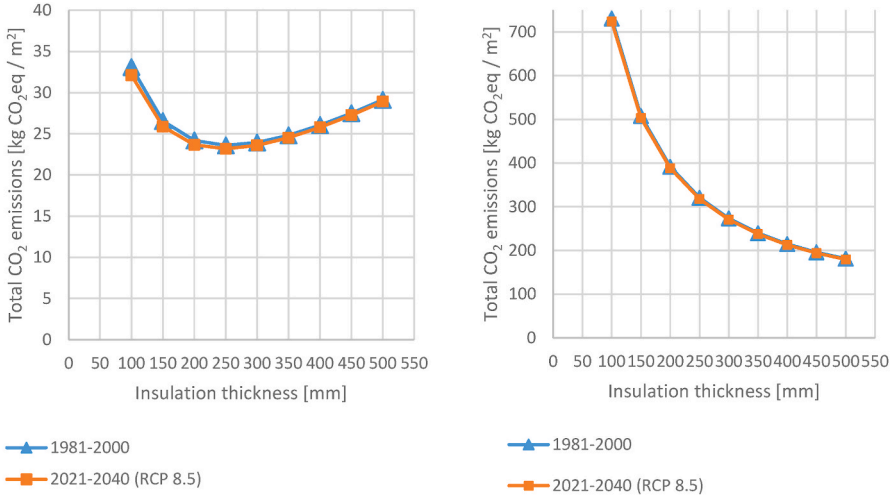

Fig. 7. Comparison of calculated future and historic CO_2 emissions for the two locations in Case 2. Nuuk's energy emission factor is 9 g CO_2eq/kWh (a) and Aasiaat's 207 g CO_2eq/kWh (b). Note the different scales on the y-axes.

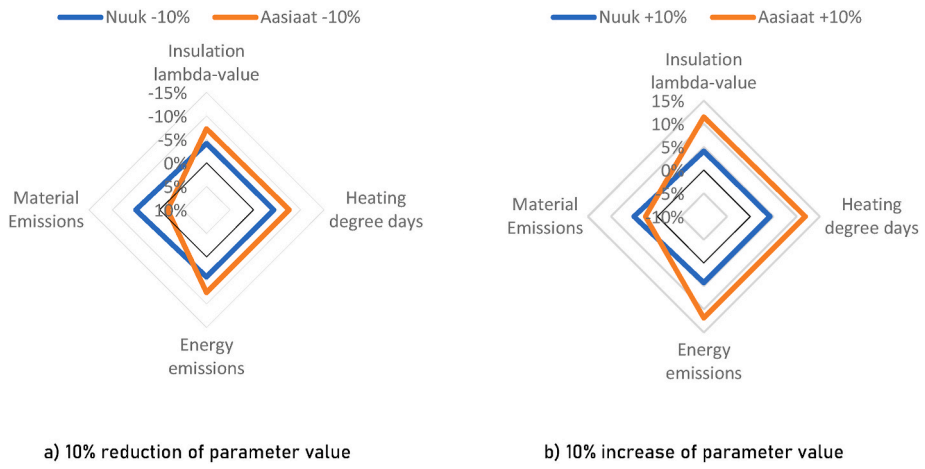

a) 10% reduction of parameter value b) 10% increase of parameter value

Fig. 8. Sensitivity analysis for the model used in Case 2, using wall insulation thickness d = 300 mm.

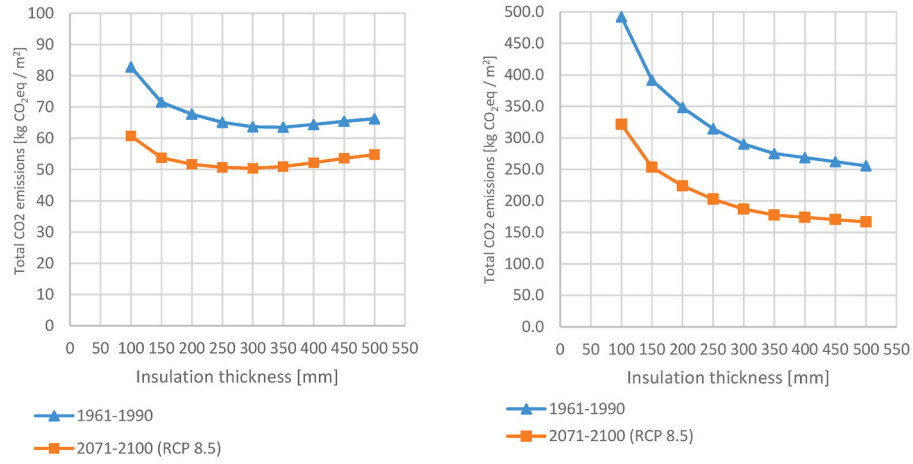

a) Emission factor = 17 g CO_2eq/kWh (Case 3.A and 3.B) b) Emission factor = 132 g CO_2eq/kWh (Case 3.C and 3.D)

Fig. 9. Comparison of calculated future and historic CO_2 emissions for Case 3, using 17 g CO_2eq/kWh (a) and 132 g CO_2eq/kWh (b) as energy emission factors. Note the different scales on the y-axes.

Table 4
Calculated ratio of embodied and operational emissions over 60 years for insulation thicknesses 100–500 mm for all cases, relative to t = 300.

T [mm]	The ratio of total emissions for a wall construction with insulation thickness t, relative to t = 300 mm											
	1.A	1.B	1.C	1.D	2.A	2.B	2.C	2.D	3.A	3.B	3.C	3.D
100	1.95	1.82	2.53	2.50	1.38	1.36	2.67	2.67	1.30	1.21	1.70	1.72
150	1.47	1.39	1.81	1.79	1.11	1.10	1.86	1.86	1.12	1.07	1.35	1.35
200	1.21	1.17	1.41	1.40	1.01	1.00	1.43	1.43	1.06	1.03	1.20	1.20
250	1.08	1.06	1.17	1.17	0.99	0.98	1.17	1.17	1.02	1.01	1.08	1.08
300	**1.00**	**1.00**	**1.00**	**1.00**	**1.00**	**1.00**	**1.00**	**1.00**	**1.00**	**1.00**	**1.00**	**1.00**
350	0.96	0.97	0.88	0.88	1.04	1.04	0.88	0.88	1.00	1.01	0.95	0.95
400	0.94	0.97	0.79	0.80	1.09	1.09	0.79	0.79	1.01	1.04	0.93	0.93
450	0.93	0.97	0.73	0.74	1.15	1.16	0.72	0.72	1.02	1.06	0.90	0.91
500	0.93	0.99	0.67	0.68	1.22	1.23	0.66	0.66	1.04	1.09	0.88	0.89

a reduction in the optimum thickness of approximately 75–100 mm for the future climate scenario. Furthermore, the models displayed similar behavior regarding the impacts of both climate and emission parameters. Note that the absolute values calculated by the two models are on different scales: Model 1 reports emissions per m^2 wall, and Model 3 reports emissions for the total wall area.

The most significant difference between Models 1 and 2, the two unit-level models, is the choice of the future climate scenario. Model 2 imposes gradually developing climate change for the future scenario, and Model 1 assumes a static climate. The comparably lower impact of climate change in Model 2 illustrates the sensitivity of these models to methodological choices.

5. Discussion

5.1. Assessment of optimal insulation thickness

Calculations of optimal insulation thicknesses in cold climates are

most useful for low energy emission factors, as the combination of high energy emission factor and cold climate results in high operational emissions. For energy emission factors above 25–30 gCO_2eq/kWh, more insulation will always yield lower total emissions over the building lifespan within the practical range of insulation thicknesses assessed in this study (100–500 mm). A comparable study by Raimundo et al. [38] reached the same conclusion for cold climates and high energy emission factors. Raimundo et al. calculated and compared results from 5 different climate zones using a similar methodology as this study and concluded that for the climate of Reykjavik (HDD = 5670 Kd/a) an energy emission factor of 144 gCO_2eq/kWh yielded insulation thicknesses above 400 mm even when using EPS as insulation material, which has a lower environmental impact than the glass wools used in this study. When using high energy emission factors, even studies of milder climates such as Ireland, with HDD in the range of 2–3000 Kd/a and energy emission factors 205–437 gCO_2eq/kWh, yields insulation thicknesses higher than the highest calculated insulation thickness (>250 mm) when optimizing for environmental impact [39]. The total emissions will be lower for a decreasing energy emission factor, but the sensitivity of the total emissions to deviations from the optimum value will increase. Therefore, building projects with emission reduction ambitions should not neglect calculating the optimal insulation thickness if the energy source for heating the building has a low emission factor.

5.2. Influence of climate parameters on the model results

An assessment of how future climate change influences the optimal insulation thickness can only be made after defining the energy emission factor, as this parameter will change the model's response to climate change. The results from Cases 1 and 3 are discussed using the energy emission factor suggested by the NVE (17 g CO_2eq/kWh). Greenland is self-sufficient on a national scale and also on a local scale, as the infrastructure in Greenland does not allow for an intercity exchange of energy. Nuuk is currently self-sufficient, with 100% of the electrical energy generated by hydropower, whereas Aasiaat relies on locally generated power from fossil fuel sources [24]. To compare the high and low emission factors in the discussion of how climate parameters impact the results, these are assumed to remain unchanged in future climate change scenarios.

RCP 8.5 is used as the future scenario in all three cases. When conducting studies comparing a historical scenario to only one future scenario, the worst-case scenario provides valuable insights, as the two curves comprise the outer limits of the probable outcome space. The temporal spacing of the two scenarios was approximately 100 years for Cases 1 and 3 (1961–1990 and 2071–2100). For assumed emission rates equal to or lower than the assumptions in scenario RCP 8.5, the total emissions over 60 years for a given insulation thickness will therefore be somewhere between the two curves according to these models.

The future scenario used for Greenland has a relatively small impact on total emissions compared to the future scenario used for Norway. This is partly because the future scenario in Case 2 is calculated over a shorter period (40 years) and because the model for future development in Case 2 is different from Cases 1 and 3. Cases 1 and 3 were calculated for (a) a static historical climate and (b) a static future climate, while Case 2 was calculated for (a) a static historical climate and (b) gradually changing future climate. Consequently, the Norwegian cases are based on climates 110 years apart, whereas the Greenlandic cases operates only 40 years apart. The effect can be observed by comparing the HDD for the different cases in Table 2, where the calculated HDD for both Norwegian case studies decreased by approximately 25% in the climate change scenario, and the same number was 3–4% in the Greenland climate change scenarios. The difference between the methods in the Greenland and Norwegian cases highlights an important fact: Choosing the appropriate model for the future scenario considering its intended use is vital, as there is a significant difference in the impact of climate change on a building built in 2071 compared to the impact on a building built today.

The difference between the indoor and outdoor temperatures is the deciding factor for the heating demand, as there is no principal difference between increasing outdoor temperature through climate change and decreasing indoor temperature through occupant behavior. Assessing how these two thermal conditions develop in relation to each other, and how much uncertainty is connected to the prediction of both becomes important. Case 1 assumes an indoor temperature of 21.5 °C and Cases 2 and 3 assume an indoor temperature of 19 °C. Both are viable options within the normal indoor temperature range during the heating season. However, there is still a 2.5 °difference between them, analogous to changes in the outdoor temperature resulting from decades of climate change in the RCP 8.5 scenario. The uncertainty of indoor temperatures due to occupant behavior is frequently highlighted as a critical parameter, by i.e. Galimshina et al., who in an earlier study evaluated the method-related and future-related uncertainties in calculations of LCA-optimized building renovation [40]. Occupant heating strategy preferences may change over time because of increased environmental awareness or an increased focus on thermal comfort. Both future climate and occupant behavior changes will affect future heating demand. The development of these two important input parameters has both a high uncertainty and a high impact on the results. Total emissions from heating energy use and insulation material production should be carefully considered and include multiplecombinations of indoor and outdoor climates to highlight the range of possible outcomes. This conclusion is also reached by Ylmen et al. [41], who developed a method for optimal insulation thickness calculation through the use of parametric analysis. Ylmen et al. showed that by considering parametric uncertainties, fewer design solutions are rejected in comparison with using point estimates. Calculating a range of values for critical parameters mitigates the problem of rejecting promising solutions based on low quality data. Further, it provides a means of addressing and evaluating subjective choices present in life cycle studies of building design [41].

5.3. Influence of the energy emission factor on model results

Fig. 10 shows the annual development of the calculated total CO_2 emissions for Case 1 with insulation thicknesses of 200, 300, and 400 mm based on the energy emission factor recommended by FME ZEB [27]. Future climate change was assumed to be a linear development from a historical climate (1990) to a future climate (2071). The estimated lifetime of the building used in the calculations was 60 years, and the energy emission factor was a function of the construction year, assuming the development illustrated in Fig. 2.

The total CO_2 emissions are highly dependent on the chosen emission factor for the energy mix, which is consistent with the results of similar studies [42,43]. Using the factor proposed by the FME ZEB, which declines linearly towards zero in 2054, the insulation thickness with respect to CO_2 emissions becomes arbitrary by approximately 2040 for the model in Case 1 (Fig. 10). After 2040, the results will be dominated by embodied emissions from the materials, and an increase in insulation thickness will yield an increase in total CO_2 emissions. A study on retrofitting building stock in England conducted by Li and Densley Tingley [44] found that adding insulation to walls with relatively low pre-retrofit U-valueled to an increase in total CO_2 emissions over the building life-time when considering an energy emission factor declining towards near-zero in 2050. It is however important to note the distinct differences in the studied climates, as the study by Li and Densley Tingley was conducted using English climate, using HDD = 2183 Kd/a in 2023 with a linear decline towards 1419 Kd/a in 2050. The heating demand in the climates investigated in this study are considerably higher, thus giving higher influence to operational emissions for the considered range of insulation thickness (100–500 mm).The rapid decline of the energy emission factor towards zero in 2050 may underestimate future operational emissions, as even renewable sources of

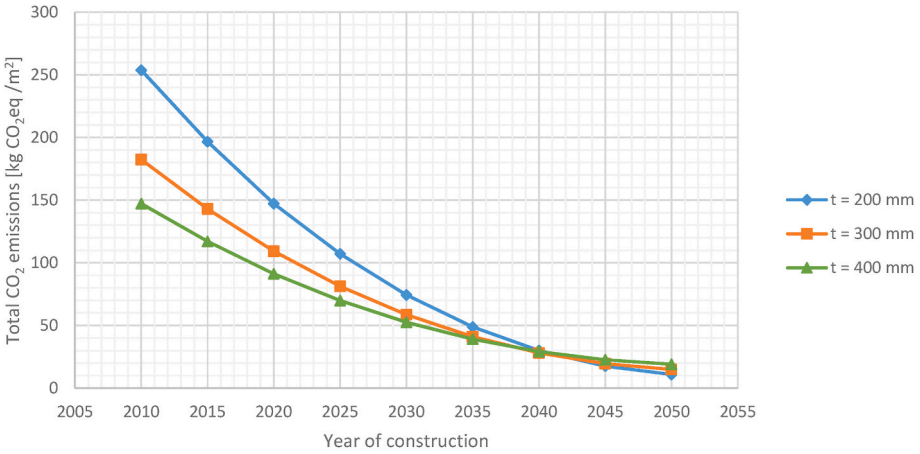

Fig. 10. Development of total CO_2 emissions for construction years between 2010 and 2050 using the model from Case 1 and using FME ZEB energy emission factor updated year by year.

energy will produce emissions because of infrastructure development [26]. This method of calculating the energy emission factor is not suitable to assess the development of future conditions in 2071–2100 as it assumes zero operational emissions. But it illustrates the high-impact energy emission factors have in studies such as this, and further highlights the need for considering multiple calculation cases due to future uncertainties, as confirmed by similar studies [39,41,45]When the considerations by the FME ZEB were performed in 2010–2012 the energy mix in Europe was dominated by emissions from the burning of oil, coal, and gas [28]. However, this will not be the case in the future if the EU goal of a 90% reduction in GHG emissions in the power sector by 2050 are realized. Future emissions from the power sector in Europe in 20–30 years are more likely to be comparable to the emissions of the Norwegian power sector today, as proposed by Ref. [46] when describing a method for the temporal development of emission intensities in LCA analysis [26]. found that sector-specific emission rates from renewable sources still exceed zero, but are highly variable when considering infrastructure and secondary effects. When the EU grid is dominated by renewable sources, infrastructure and secondary effects become more prevalent in the estimation of energy emission factors.

To assess the influence of the energy emission factor, the optimal insulation thickness as a function of the energy-emission factor was calculated for all cases, as shown in Fig. 11. When using energy emission factors exceeding 25–30 kgCO_2eq/kWh, the total emissions are dominated by operational emissions, resulting in an increasing gradient of the curves for higher insulation thicknesses. Because the calculation points are based on the optimum thicknesses the curves displayed in Fig. 11 do not express the consequences of deviating from the optimum thickness. Small deviations from the optimum will not yield significant changes in total emissions. Together with the inherent uncertainties involved in the parameters of such models (i.e., future energy emission factors, future climate, occupant heating behaviors, and material emissions), such calculations should not be performed to find a precise optimum, but rather to see the general development of optimal insulation thickness within a value range of energy emission factors.

As more green energy becomes available, the energy emission factor is expected to decrease [6]. However, the rate of development is difficult to predict in the short term, and increasingly complex in the long term. For interconnected grids, such as in Cases 1 and 3, the rate of development depends on socio-economic development and policy-making on an international scale. The evaluation of a single deterministic value will conceal high levels of uncertainty in the results. However, the uncertainty of this factor decreases dramatically if the energy for heating is dominated by locally produced renewable heat and energy sources, such

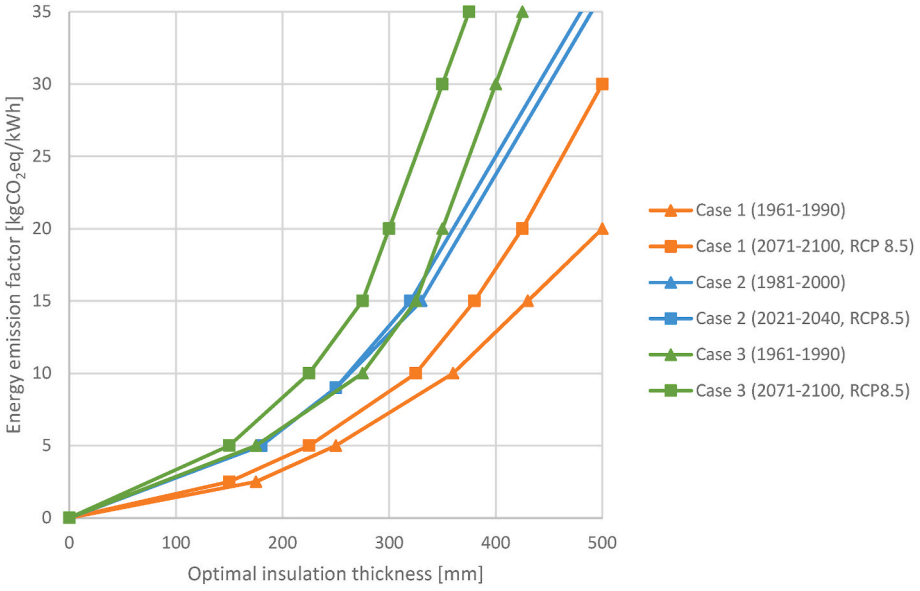

Fig. 11. Comparison of calculated future and historic optimal insulation thickness for all cases, as a function of the energy emission factor.

as in Cases 2A and 2B.

For the lower energy emission factor scenarios considered in Cases 1 and 3, the shift from the future to the historical scenario in the minima was approximately 50–75 mm. However, missing the optimum by ± 100 mm will have a limited impact on total CO_2 emissions. For Case 1, by increasing or decreasing the insulation thickness by 100 mm from the optimum value, the total emissions increased by less than 5%. The Greenlandic case of Nuuk, with an even lower energy emission factor, is more sensitive around the optimum value, and choosing an optimal insulation thickness outside the range of ±50 mm from the optimum value will have a significant impact on the total emissions. While this result indicates that the precision of the calculations is more important for lower-energy emission factors, low-energy emission factors also lead to low total emissions. This indicates that the absolute difference in total emissions will not be as dramatic in the lower range of emission factors.

The evaluation of reduced grid emission factors due to future development is more complex than evaluating emission factors from locally produced green energy, as material emissions also rely on the development of the grid energy emission factor. Embodied emissions are influenced by the types of energy sources available owing to the production and transportation of materials requiring energy. Further complicating the relationship between embodied and operational emissions, reduced emissions in the construction phase (from embodied emissions) have a greater impact on future climate change than an equal reduction in emissions over a 60-year lifespan (from operational emissions). Assessing the value relationship between these two parameters is outside the scope of this study; however, further study of this relationship should be made considering the total emissions from the heating demand of buildings.

6. Conclusions

This study assessed how future climate and energy emission factor changes in cold climates influence the selection of optimal insulation thickness of walls. A comparison of the three case study models for such calculations yielded the following conclusions.

Climate change will reduce the optimal insulation thickness for Norwegian inland climates by 75–100 mm towards 2071–2100, compared to the situation in 1961–1990 considering scenario RCP 8.5, an energy emission factor of 17 g CO_2eq/kWh, and glass-wool insulation. However, occupant behavior has a significant impact on the calculations as this determines the indoor climate. Multiple combinations of indoor and outdoor climates should be considered by calculating a range of optimal insulation thicknesses before finalizing the insulation thickness. These factors have both high impact and high uncertainty.

In cold climates, optimal insulation thickness calculations are most valuable for cases with low energy emission factors. When considering energy emission factors above 25–30 g CO_2eq/kWh, the total emissions from insulation and heating energy use were dominated by operational emissions for all the considered cases due to the high energy demand for heating. Furthermore, the energy emission factor significantly impacts the calculated optimal insulation thickness and should be carefully chosen. Case 1 demonstrated that, given an energy conversion factor of 17 g CO_2eq/kWh, insulation thicknesses within 100 mm from the optimum thickness increased the total CO_2 emissions by less than 5%. Given an energy emission factor under 10 g CO_2eq/kWh, deviation from the optimum will have a more significant impact on the total emissions.

The results from all three cases highlight the energy emission factor as the dominant influencing factor in climates with high energy demands for heating. Considering the applicability of the results to other Nordic countries, the relative difference in climate seems not to be the determining factor. If the building is self-sufficient in locally produced energy from i.e. solar panels, calculations of optimal insulation thickness may prove valuable regardless of location in the arctic and sub-arctic climate zones. If however, the building relies on grid electricity for heating with an energy emission factor above 25–30 g CO_2eq/kWh, the conclusion found by previous studies remains: "The more insulation the better".

Funding

This research was funded by the Research Council of Norway (grant number: 237859) and the Arctic Building and Construction Project, DTU (www.arctic.dtu.dk).

CRediT authorship contribution statement

Jørn Emil Gaarder: Writing – review & editing, Writing – original draft, Visualization, Methodology, Formal analysis, Conceptualization. **Naja Kastrup Friis:** Writing – review & editing, Writing – original draft, Visualization, Methodology, Formal analysis. **Ingrid Sølverud Larsen:** Visualization, Methodology, Formal analysis. **Berit Time:** Writing – review & editing, Supervision, Funding acquisition. **Eva B. Møller:** Writing – review & editing, Supervision, Funding acquisition. **Tore Kvande:** Writing – review & editing, Supervision, Methodology, Funding acquisition, Conceptualization.

Declaration of competing interest

The authors declare that they have no known competing financial interests or personal relationships that could have appeared to influence the work reported in this paper.

Data availability

Data will be made available on request.

Acknowledgements

The authors gratefully acknowledge the financial support from the Research Council of Norway and several partners associated with the Center for Research-based Innovation 'Klima 2050' (Grant No.237859) (see www.klima2050.no).

References

[1] Y.L. Li, M.Y. Han, S.Y. Liu, G.Q. Chen, 'Energy consumption and greenhouse gas emissions by buildings: a multi-scale perspective, Build. Environ. 151 (2019) 240–250.
[2] Ingrid H. Magnussen, Kartlegging og vurdering av potensial for effektivisering av oppvarming og kjøling i Norge, in: Teknisk Rapport, 2020.
[3] DiBK, Byggteknisk Forskrift TEK 17', *Direktoratet For Byggkvalitet*. EPD-Norway, 2017, 2022, https://www.epd-norge.no.
[4] Marie Totland, Tore Kvande, Rolf André Bohne, The effect of insulation thickness on lifetime CO2 emissions, in: IOP Conference Series: Earth and Environmental Science, IOP Publishing, 2019, 012033.
[5] A.E. Stagrum, T. Kvande, A. Engebø, E. Andenæs, J. Lohne, Climate implication and adaptation measures for energy use in buildings–a scoping review, in: IOP Conference Series: Earth and Environmental Science, IOP Publishing, 2019, 012035.
[6] Susanne Langsdorf, 'EU Energy Policy: from the ECSC to the Energy Roadmap 2050, Green European Foundation, Brussels, 2011.
[7] MeteorologiskInstitutt, 'Klima fra 1900 til i dag', Meteorologisk Institutt, 2021. https://www.met.no/vaer-og-klima/klima-siste-150-ar. (Accessed 18 May 2021). Accessed.
[8] IPCC, Climate change 2014 synthesis report, in: R.K. Pachauri, L. Meyer (Eds.), International Panel of Climate Change, Climate Change 2022: Impacts, Adaptation and Vulnerability, 2014, 2022, http://ipcc.ch.
[9] Omer Kaynakli, A review of the economical and optimum thermal insulation thickness for building applications, Renew. Sustain. Energy Rev. 16 (2012) 415–425.
[10] Ali Bolatürk, Determination of Optimum Insulation Thickness for Building Walls with Respect to Various Fuels and Climate Zones in Turkey, *Applied Thermal Engineering* Bygningsreglementet, 2006, p. BR18, 2018, (Bolig- og Planstyrelsen).
[11] Al-Khawaja, J. Mohammed, Determination and selecting the optimum thickness of insulation for buildings in hot countries by accounting for solar radiation, Appl. Therm. Eng. 24 (2004) 2601–2610.
[12] Jinghua Yu, Changzhi Yang, Liwei Tian, Dan Liao, A Study on Optimum Insulation Thickness of External Walls in Hot Summer and Cold Winter Zone of China, *Applied Energy* Ökobaudat, 2009, 2022, https://www.oekobaudat.de.

[13] Rachida Idchabani, Khyad Ahmed, Mohamed El Ganaoui, Optimizing Insulation Thickness of External Walls in Cold Region of Morocco Based on Life Cycle Cost Analysis, Energy Procedia, 2017.
[14] Susan Joy Hassol, Robert W. Corell, Arctic Climate Impact Assessment', *Avoiding Dangerous Climate Change*, 2006, p. 205.
[15] Wladimir Köppen, 'Das geographische system der Klimate, Handbuch der klimatologie 46 (1936).
[16] Anna Eknes Stagrum, Erlend Andenæs, Tore Kvande, Jardar Lohne, Climate change adaptation measures for buildings—a scoping review, Sustainability 12 (2020) 1721.
[17] Christopher R. Schwalm, Glendon Spencer, Philip B. Duffy, 'RCP8. 5 tracks cumulative CO2 emissions, Proc. Natl. Acad. Sci. USA 117 (2020) 19656–19657.
[18] Jr Pielke, Matthew G Burgess Roger, Justin Ritchie, 'Most Plausible 2005-2040 Emissions Scenarios Project Less than 2.5 Degrees C of Warming by 2100, 2021.
[19] Karl-Erik Westergren, Hans Högberg, Norlén Urban, Monitoring energy consumption in single-family houses, Energy Build. 29 (1999) 247–257.
[20] Trine Dyrstad Pettersen, 'Variation of energy consumption in dwellings due to climate, building and inhabitants, Energy Build. 21 (1994) 209–218.
[21] Goune Kang, Hunhee Cho, Dongyoun Lee, Dynamic lifecycle assessment in building construction projects: focusing on embodied emissions, Sustainability 11 (2019) 3724.
[22] Benedikte Wrålsen, Reyn O'Born, Christofer Skaar, 'Life cycle assessment of an ambitious renovation of a Norwegian apartment building to nZEB standard, Energy Build. 177 (2018) 197–206.
[23] Standard-Norge, NS 3720:2018 Metode for klimagassberegninger for bygninger, Statistikbanken. 2022, https://www.dst.dk, 2018.
[24] Nukissiorfiit. Årsregnskap, 2020.
[25] SSB, 'Produksjon, Import, Eksport Og Forbruk Av Elektrisk Kraft, GWh, 2021. https://www.ssb.no/energi-og-industri/energi/statistikk/elektrisitet. (Accessed 12 May 2021).
[26] Roberto Turconi, Alessio Boldrin, Thomas Astrup, 'Life cycle assessment (LCA) of electricity generation technologies: overview, comparability and limitations, Renew. Sustain. Energy Rev. 28 (2013) 555–565.
[27] Inger Andresen, Kristian M. Lien, Thomas Berker, Igor Sartori, Birgit Risholt, Greenhouse Gas Balances in Zero Emissions Buildings - Electricity Conversion Factors Revisited, SINTEF Academic Press, 2017.
[28] Ingeborg Graabak, , Bjørn Harald Bakken, Nicolai Feilberg, 'Zero emission building and conversion factors between electricity consumption and emissions of greenhouse gases in a long term perspective, Environmental and Climate Technologies 13 (2014) 12–19.
[29] Astrid Stavseng, 'Hvor kommer strømmen fra? The Norwegian Water Resources and Energy Directorate (NVE), 2020. https://www.nve.no/energiforsyning/kraftproduksjon/hvor-kommer-strommen-fra/. (Accessed 12 May 2021). Accessed.
[30] Fufa, Selamawit Mamo, Reidun Dahl Schlanbusch, Kari Sørnes, Marianne Rose Inman, Inger Andresen, A Norwegian ZEB Definition Guideline, SINTEF Academic Press, 2016.
[31] openstreetmap.org: an open source map generator, accessed in 2022.
[32] C. Lausselet, K.M. Lund, H. Brattebø, 'LCA and Scenario Analysis of a Norwegian Net-Zero GHG Emission Neighbourhood: the Importance of Mobility and Surplus Energy from PV Technologies', *Building And Environment*, vol. 189, 2021, 107528. LCAbyg. 2022, https://www.lcabyg.dk.
[33] Peter G. Schild, 471.401 - U-verdier. Vegger over terreng med bindingsverk av tre med gjennomgående stendere, in: SINTEF Byggforskserien, SINTEF Community, 2012. https://byggforsk.no.
[34] Callum Hill, Andrew Norton, Janka Dibdiakova, A comparison of the environmental impacts of different categories of insulation materials, Energy Build. 162 (2018) 12–20.
[35] Naja Kastrup Friis, Gaarder, Jørn Emil, Eva Birgit Møller, Tool for calculating the building insulation thickness for lowest CO2 emissions – A greenlandic example, Buildings 12 (2022) 1178.
[36] Adrien Deroubaix, Inga Labuhn, Marie Camredon, Benjamin Gaubert, Paul-Arthur Monerie, Max Popp, Johanna Ramarohetra, Yohan Ruprich-Robert, Levi G. Silvers, Guillaume Siour, 'Large uncertainties in trends of energy demand for heating and cooling under climate change, Nat. Commun. 12 (2021) 1–8.
[37] Erlend Andenæs, Tore Kvande, Rolf André Bohne, Footprints of failure: quantifying carbon impacts of roof leakages in a single-family residential building, in: IOP Conference Series: Earth and Environmental Science, IOP Publishing, 2020, 042053.
[38] António M. Raimundo, Afonso M. Sousa, A. Virgílio, M. Oliveira, Assessment of energy, environmental and economic costs of buildings' thermal insulation–influence of type of use and climate, Buildings 13 (2023) 279.
[39] Rakshit D. Muddu, D.M. Gowda, Anthony James Robinson, Aimee Byrne, Optimisation of retrofit wall insulation: an Irish case study, Energy Build. 235 (2021), 110720.
[40] Alina Galimshina, Maliki Moustapha, Hollberg Alexander, Pierryves Padey, Sébastien Lasvaux, Sudret Bruno, Guillaume Habert, 'What is the optimal robust environmental and cost-effective solution for building renovation? Not the usual one, Energy Build. 251 (2021), 111329.
[41] Peter Ylmén, Kristina Mjörnell, Johanna Berlin, Jesper Arfvidsson, 'Approach to manage parameter and choice uncertainty in life cycle optimisation of building design: case study of optimal insulation thickness, Build. Environ. 191 (2021), 107544.
[42] Shu Su, Xiaodong Li, Yimin Zhu, Borong Lin, Dynamic LCA framework for environmental impact assessment of buildings, Energy Build. 149 (2017) 310–320.
[43] Eirik Resch, Inger Andresen, Francesco Cherubini, Helge Brattebø, Estimating dynamic climate change effects of material use in buildings—timing, uncertainty, and emission sources, Build. Environ. 187 (2021), 107399.
[44] X. Li, D Densley Tingley, 'A whole life, national approach to optimize the thickness of wall insulation, Renew. Sustain. Energy Rev. 174 (2023), 113137.
[45] Farshid Shadram, Shimantika Bhattacharjee, Sofia Lidelöw, Jani Mukkavaara, Thomas Olofsson, 'Exploring the trade-off in life cycle energy of building retrofit through optimization, Appl. Energy 269 (2020), 115083.
[46] Eirik Resch, Inger Andresen, Eivind Selvig, Marianne Wiik, Lars G. Tellnes, Stoknes Stein, FutureBuilt ZERO Metodebeskrivelse, SINTEF Academic Press, 2020.

III

IV. Hygrothermal Assessment of External Walls in Arctic Climates: Field Measurements and Simulations of a Test Facility

Naja K. Friis, Eva B. Møller, and Tove Lading

Buildings and Environment (2023)
doi: 10.1016/j.buildenv.2023.110347

IV

Building and Environment 238 (2023) 110347

Contents lists available at ScienceDirect

Building and Environment

journal homepage: www.elsevier.com/locate/buildenv

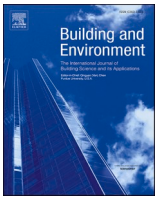

Hygrothermal assessment of external walls in Arctic climates: Field measurements and simulations of a test facility

Naja Kastrup Friis *, Eva B. Møller, Tove Lading

Technical University of Denmark, Brovej 118, 2800, Kgs. Lyngby, Denmark

IV

ARTICLE INFO

Keywords:
Hygrothermal simulations
Arctic climate
Test facility
Façade constructions
Ventilated air cavity
Mould index

ABSTRACT

The Greenlandic building sector is under pressure due to ever-changing building trends and a building shortage. Regrettably, there have only been made small efforts to investigate the performance of the existing buildings, and few resources have been dedicated to learning from previous attempts. Consequently, the available information and research are insufficient to ensure the construction of robust and well-functioning buildings. This knowledge gap motivated the ABC project, which had the goal of collecting and sharing information about optimal building practices in Greenland. As a part of the ABC project, this study aimed to determine which building practice is the most suitable for Greenlandic conditions. To this end, several real-time experiments were created, including a test pavilion in Nuuk consisting of five different wall constructions oriented towards north and south. This article presents the measured data from this pavilion. The performance of each construction type was compared with each other and to simulations performed in the hygrothermal analysis software Delphin. Furthermore, the robustness of the facades was tested by performing simulations with weather data for different towns in Greenland, including quantification of mould growth risk using the Viitanen model. It was found that the facades were unevenly affected by orientation. Nevertheless, none of the constructions could be labelled unsuitable for the Arctic climate as the assessments revealed no risk of mould growth. Additionally, reanalysis weather data from ERA5 was found to be suitable for performing hygrothermal simulations. It was also found that Nuuk is a favourable location for future test facilities.

1. Introduction

1.1. Changing building styles

The Greenlandic construction industry is relatively new and, to a high degree, affected by other cultures, especially Danish traditions. This has resulted in rapidly changing building traditions. E.g. according to Møller and Lading [1], the Greenlandic building style has fundamentally changed multiple times since the 1950s. Originally, the tendency was to build small Norwegian-style standard houses of 1–2 storeys, but over time concrete buildings up to four storeys became more common. The most recent tendency has been to build groups of identical multistorey buildings (up to seven storeys) with ventilated air cavities in the façade construction. The main drivers for the changing building style are typically economical and political [2]. Meanwhile, the research on the performance of each building style has been very limited, with the majority of research being performed within the last ten years. Consequently, new construction types have been implemented without validated experiences and sufficient technical knowledge to justify the design choices. To overcome this knowledge gap, several long-term experiments of different construction types were performed within the Arctic Building and Construction (ABC) Project [3]. These experiments were carried out at different locations on the west coast of Greenland, including a test pavilion located in Nuuk, which provided the data used in this article. The overall goal of the ABC project was to identify current challenges and present possible solutions to improve the quality of future constructions in Arctic climates, with a primary focus on the Greenlandic industry and society.

1.2. Indoor climate, mould, and renovation

While the literature concerning construction practices in Greenland is limited, there has been significant research on the indoor climate, especially focusing on moisture and mould. Poor indoor climate can cause discomforts such as headaches, asthma, eczema, coughing, and irritation of mucous membranes [4]. Additionally, diseases like

* Corresponding author.
E-mail address: nfri@dtu.dk (N.K. Friis).

https://doi.org/10.1016/j.buildenv.2023.110347
Received 8 February 2023; Received in revised form 20 April 2023; Accepted 21 April 2023
Available online 22 April 2023

tuberculosis thrive better in poor indoor climates and appear 20 times as often in Greenland compared to the rest of the Nordic countries [5]. According to Kotol [6], the indoor environment often suffers due to a lack of ventilation in the kitchen and bathrooms, as well as drying of clothes indoors during winter and not using the kitchen hood during cooking. Thus, attempts have been made to increase public awareness of the issues [7]. Regardless of the reason, a poor indoor climate can affect the building envelope and cause condensation in the construction, potentially leading to rot and a reduction of the building life span. Helgason [8] presented several examples of severe moisture problems, including high humidity in a bathroom ruining the building façade, disintegrating wind barriers due to driving rain, and mould issues caused by implementing moist or mouldy building materials into new constructions. Despite moisture and mould issues, the indoor relative humidity (RH) in Greenlandic buildings is generally low. A study from 2014 performed in Sisimiut found that the average RH in 79 bedrooms were 42% and 26% during summer and winter, respectively. The average indoor night temperature was 22 °C [9].

IV

Water is another considerable risk factor in façade constructions. Both regarding the risk of mould, but also due to thaw-freeze processes, which can cause leaks or expansion of cracks. Nevertheless, this study focuses on mould as the main failure mechanism since wood decay caused by other fungi starts at higher moisture levels, and frost damage is less likely.

Wind is another risk factor, e.g., Lading and Møller [10] reported of a concrete construction where the lack of wind barrier combined with poor labour quality resulted in colder surfaces than expected [11]. The discussion presented in Ref. [11] emphasised the need for solutions without unnecessarily complex solutions. This was also emphasised by de Place when surveying moisture-related challenges in the Greenlandic building sector [12].

Simultaneously with the aforementioned issues, there has been a massive building shortage. For example, in 2019, there were 2000 people on waiting lists for housing, and 10.000 new residents are expected in Nuuk during the next ten years [13]. In addition to the economic infrastructure causing bottlenecks in the construction of new buildings [14], there is a need for increasing the service life of future constructions to meet expected needs, as well as a strategy for maintaining the existing building mass. According to a recent article in the Greenlandic newspaper Sermitsiaq, the Greenlandic self-government has put aside 1.5 billion DKK in the national budget to renovate existing buildings [15]. While this is a decent start, lector Tove Lading from DTU pointed out that it is too unambitious, considering that more buildings will decay during the renovation period.

1.3. Sustainability

While sustainability in the construction sector is a hot topic globally, the literature within this field concerning Greenlandic conditions is minimal. Morten Ryberg et al. [16] conducted a comparative sustainability study of four buildings in Greenland, representing the current construction methods. Specifically, the study considered a CLT construction, a concrete construction, a timber frame construction, and a renovation case. The study concluded that renovating old buildings was the most environmentally friendly option. Due to the limited local resources in Greenland, most building materials must be transported long distances, which contributes to the environmental impact. However, according to an Icelandic study [17], the impact of long-distance overseas transport of building materials is negligible within most sustainability impact groups. The exceptions are acidification and eutrophication, where transportation contributes 25% and 31%, respectively. Friis et al. [18] also found that transportation is insignificant to the level of CO_2 emissions when considering various types of insulation. Besides smaller sustainability projects, the Green Building Council Denmark [19] has recently DGNB-certified a residential building in Nuuk [20]. The German certification system, DGNB, aims to improve and quantify the social, economic and environmental performance of buildings [21]. According to Leif Hansen Bygherrerådgivning [22], the certification requirements have been adjusted to Greenlandic conditions in order to make the certification criteria “ambitious but fair”. Some adjustments were necessary due to the climatic conditions, e.g., the demand of planted trees was revised as they cannot grow north of the tree line, and the allowed energy consumption per square meter was increased to match the available technical solutions and harsh climate. Furthermore, as all land in Greenland is public, the DGNB requirements for parking lots and gardens have been adjusted. The ambitions of DGNB stand in stark contrast to the current Greenlandic building regulation from 2006 [23], which is currently under revision.

1.4. Aim and research questions

Due to the limited research on the hygrothermal conditions of façade constructions in Greenland, this study aims to evaluate current construction methods and identify possible unfavourable construction tendencies in a Greenlandic context. The study is based on experimental data from a test pavilion in Nuuk, which included five different construction types. A test pavilion, i.e., an experimental test facility consisting of a container with a controlled indoor climate, was chosen to minimise uncertainties compared to conducting measurements in existing buildings. As the pavilion was constructed meticulously in a lab facility at the Technical University of Denmark (DTU), the data represents the performance of the technical design solutions concerning the climate without accounting for poor workmanship or building errors. Consequently, the test pavilion does not necessarily represent similar conditions as construction made on-site locally in Greenland. The collected data for each construction type are compared with each other and with the results of hygrothermal Delphin simulations to evaluate if the conditions behave as intended and expected. With the fitted hygrothermal models, it is possible to analyse the behaviour of the various construction types in different climates. The present study seeks to answer the following research questions.

1) Are any of the considered construction types unsuitable for the Arctic climate in Nuuk?
2) How robust are the constructions to the climatic conditions in other regions of Greenland?
3) Which parameters are essential to the robustness of the façade construction?

2. Methods

This study is based on experimental data from the test pavilion in Nuuk and hygrothermal simulations produced using the software Delphin. Delphin is a Coupled Heat, Air, Moisture and Pollutant Simulation for Building Envelope Systems (CHAMPS-BES) simulation tool, which has been verified by Nicolai et al. [24]. This section first introduces the pavilion, the different integrated constructions, and descriptions of how the data were analysed, compared, and assessed. This is followed by a thorough description of the hygrothermal simulation method. Finally, the investigation of the risk of mould growth using the Viitanen model implemented in WUFI VTT [25] is described. The process flow of this study, from data collection to analysis, is presented in Fig. 1.

2.1. The test pavilion

The experimental test facility was a closed pavilion similar to a container located in Nuuk. More specifically, the pavilion consisted of a small building with a single room with a controlled indoor climate of 20 °C air temperature and 50% relative humidity. As presented in Section 1.2, the relative humidity indoors is typically much lower in Greenland, while the temperature is representative. The high indoor relative humidity was chosen as a worst-case scenario. The outer walls

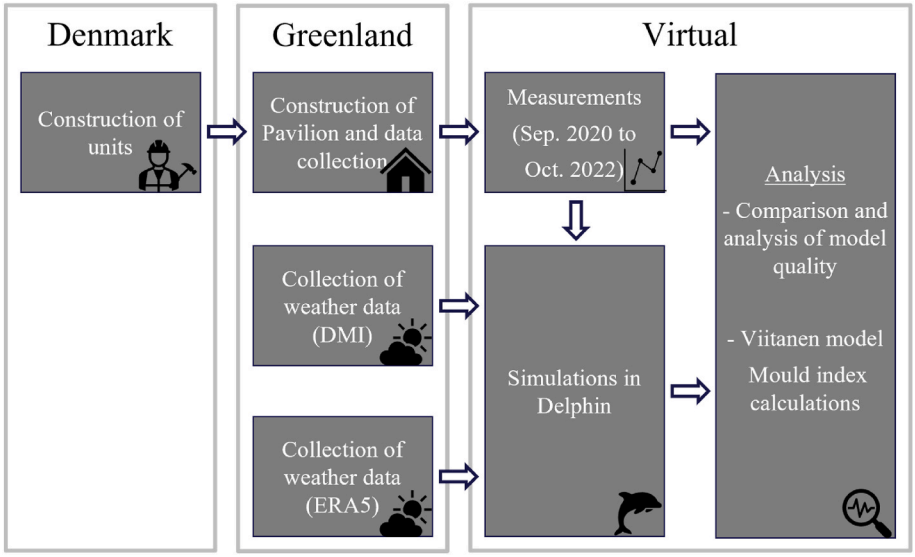

Fig. 1. Relation between collected data and applied methods during this study.

consisted of five differently designed façade elements, which for the remainder of this paper are referred to as "units". The orientation of the pavilion and the placement of the five different units (A-E) are shown in Fig. 2. All units were produced in two or three replicates, with the individual units facing different directions. The gables were constructed using units A and E. Data from the roof and floor units were also logged, although this article only focuses on the wall constructions. The pavilion was oriented at an angle of 40° from north (see Fig. 2). This means that what is referred to as the "northern side" in this study is actually offset 5° from north-east. The entrance door was placed in the western gable, A_W.

2.2. Construction of the pavilion units

All the constructions were designed to replicate existing facade types found in the construction industry in Greenland. All units had a ventilated air gap behind a cladding of watertight plywood.

Details of the thermal transmittance of the walls, the material types, and material thicknesses are given in Fig. 3 and Table 1. In Unit B, fibre cement boards were used to replicate concrete to ensure the buildability of the test pavilion. The materials were not identical regarding hygrothermal properties, but considering the large span of properties for different concrete products, it was considered an acceptable approximation.

Several temperature and relative humidity sensors were installed within each unit. The specific number of sensors installed was dependent on the construction type and the number of material layers. As a minimum, measurements were made on each side of the vapour barrier and behind the wind barrier. As the air gap, cladding, and U-value were approximately the same in all units, the conditions in the air gaps were only measured in one unit for each orientation. The conditions in the air cavity were measured in Units C_N, C_S, A_W, and E_E. The location of the sensors in each unit is shown in Fig. 3, where the dots and triangles represent the sensors. Dots indicate sensors that are available in all orientations of that unit, while triangles mark sensors that are only available in one orientation. The colours of the sensors correspond to the lines in the graphs in Section 3. The sensors used in the test facility are of

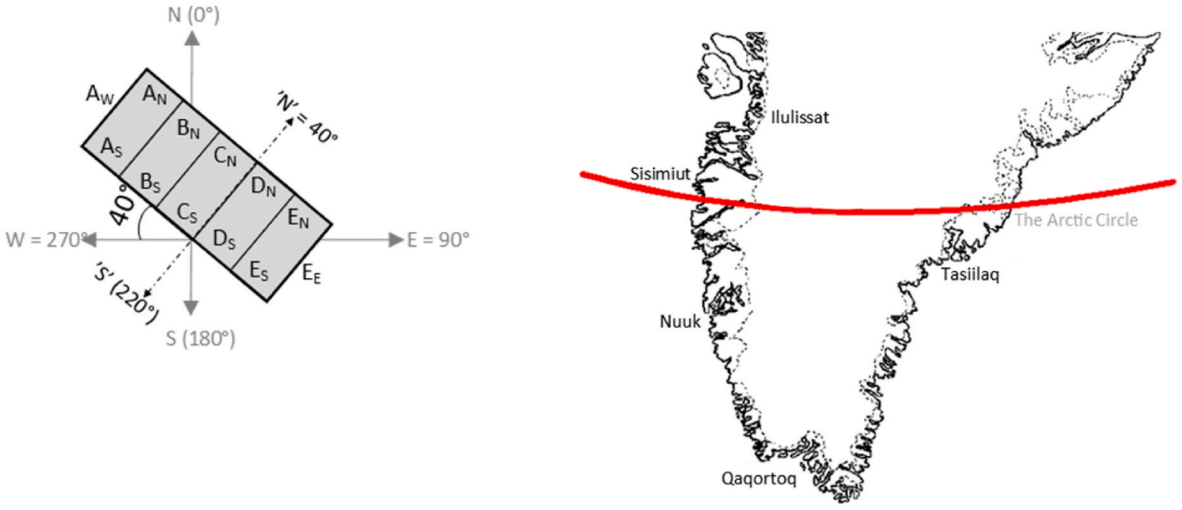

Fig. 2. a) Orientation and division of the wall units of the test pavilion. b) Geographic overview of the considered cities in Greenland (adapted from BR2006 [23]).

IV

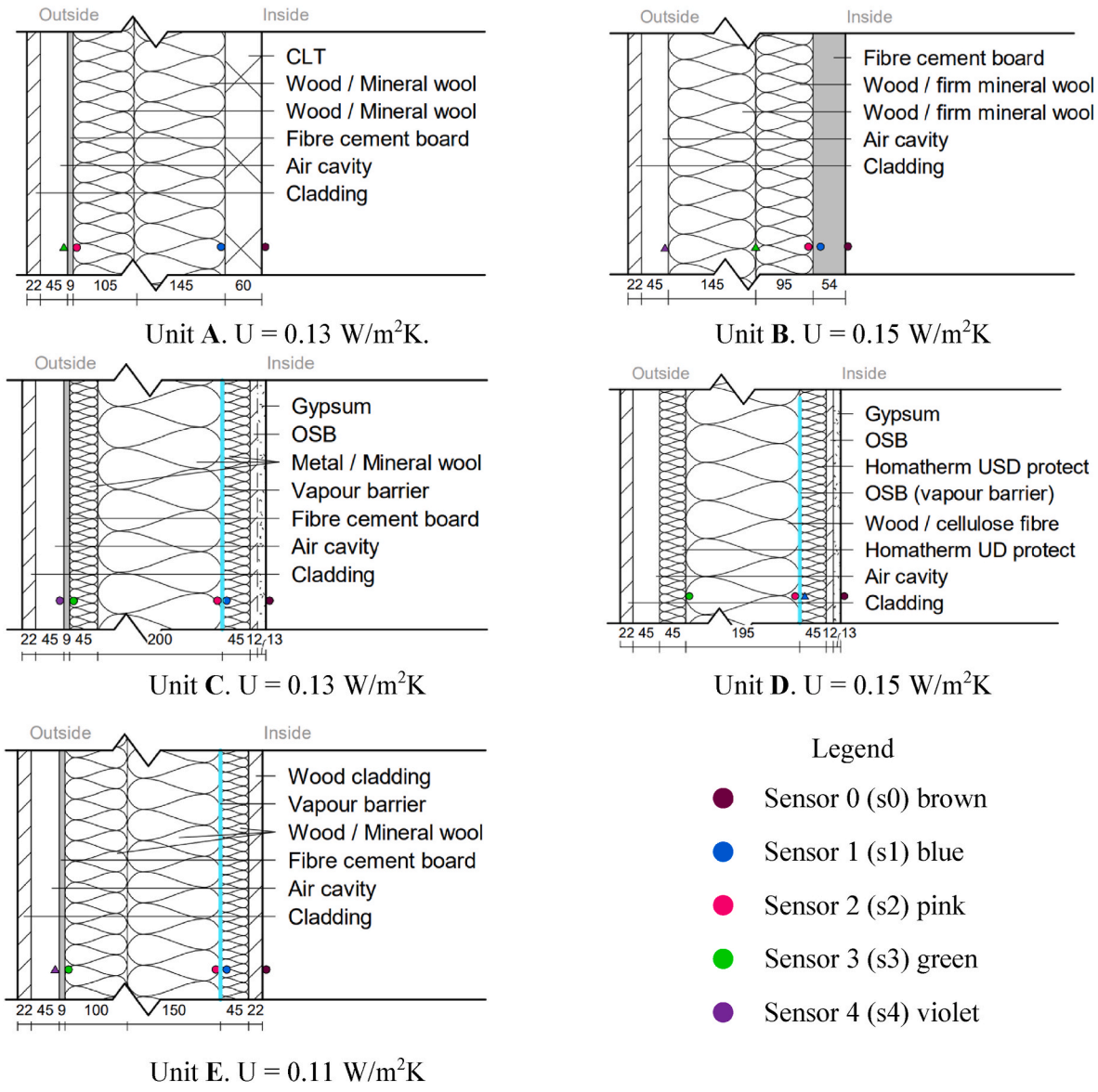

Fig. 3. Details of the construction of each unit and placement of the sensors. Sensor locations are either represented as dots (multiple orientations) or triangles (single orientation). The sensor colour corresponds to the lines in the graphs in Section 3. The sensors are named s0 to s4, starting from the interior side of the wall. (For interpretation of the references to colour in this figure legend, the reader is referred to the Web version of this article.)

Table 1
Material properties applied in Delphin. Asterisks (*) indicate calibration and grey values are from the Delphin database.

Material	λ	μ	ρ	Cp	A_w	W_{sat}	W_{80}	$K_{l,eff}$	A	B	C	D	E
	W/mK	–	kg/m^3	J/kgK	kg/m^{2}s^{½}	kg/m^3	kg/m^3	s					
Mineral Wool (731)	0.035	1.5*	67	840	0	900	0.1	0	x				x
Fibre cement board (265)	0.24 [38]	20 [39]*	1424 [38]	900 [40]	0.01	419.0	40.0	0	x	x	x		x
Air cavity (17)	0.222	0.25	1.3	1050	0	1000	0	0	x	x	x	x	x
Cladding, external (279)	0.067 [41]	80	500 [41]	1880 [42]	480.2	215	0	–	x	x	x	x	x
CLT (626)	0.12	73	425	1245	0.0024	590.2	72.6	9.5e^{-10}	x				
Firm mineral wool (731)	0.04*	1.5*	85 [38]	1030 [43]	0	900	0.1	0		x			
Gypsum (599)	0.14*	20*	745.1	1826	0.18	574.9	8.8	6.6e^{-11}			x	x	
OSB (650)	0.13	165	595	1500	0	847	95.7	–			x	x	
Mineral wool/metal (731)	0.042*	1	67	840	0	900	0.1	0			x		
PE-foil (174)	0.32*	100.000	1500	2100	0	0	0	0			x		x
Homatherm USD (580)	0.042 [44]	3 [44]	190 [44]	2100 [44]	0.56	780	6.3	3.5e^{-6}				x	
Cellulose (580)	0.048	2.05*	55.2	2500	0.56	780	6.3	3.5e^{-6}				x	
Homatherm UD (580)	0.044 [44]*	3 [44]	160 [44]	2100 [44]	0.56	780	6.3	3.5e^{-6}				x	
Wood cladding (844)	0.148	3.81	414.6	2416	0.01	718.9	76.3	–					x

the type HYT 221 from Innovative Sensor Technology [26]. The sensors are pre-calibrated and can digitally measure relative humidity from 0% to 100% and temperature from −40 °C to +125 °C. The accuracy is declared to be ±1.8% RH at 23 °C in the range 0% RH to 90% RH (no uncertainty information is specified above 90% RH, although it is expected to be higher) and ±0.2 K (in the range 0 °C to +60 °C).

2.3. Construction process of test pavilion

As the pavilion was designed and erected as a test facility, its construction was untraditional and highly meticulous. To ensure high-quality workmanship, each unit, including the sensors, was pre-assembled by skilled workers at a test facility at the Technical University of Denmark (DTU) in Denmark. Subsequently, the units were shipped to Nuuk, where they were implemented in the pavilion. It is important to note that there are a few inconsistencies in the test setup, which could affect the results. These include.

- Cut-out in fibre cement boards in Unit B to make space for a sensor.
- Inconsistent placement of the external sensor (s3/s4) in Unit B.
- Faulty measurements in sensor s1 in Unit D_S.

Except for s1 in Unit B, all sensors are placed next to an insulation layer, making room for the sensors without specific holes in the construction layers. Furthermore, at the time of writing, the sensors are still implemented in the test pavilion, which is why they have not been recalibrated after the data collection. Also, the elements have not been visually analysed for mould growth.

2.3.1. Experimental data

All of the experimental data, i.e., temperature and relative humidity measurements, are presented in graphs and compared based on the construction units. The pavilion was constructed in June 2019, and data has been logged hourly since October 29th, 2020. Based on these data, the vapour content at each sensor point was calculated. The equation for calculating the vapour content, υ (g/m^3), is given in Eq. (1) [27], where the φ is the relative humidity (−), and θ is the temperature (°C). All three parameters are analysed for all orientations and construction types and finally compared to the simulated data.

$$\begin{aligned} &\text{For } \theta \geq 0\ ^\circ\text{C}, \upsilon = \varphi \bullet \frac{610.5 \bullet e^{\frac{17.269 \bullet \theta}{237.3+\theta}}}{0.4615 \bullet (\theta + 273.15)} \left[g / m^3\right] \\ &\text{For } \theta < 0\ ^\circ\text{C}, \upsilon = \varphi \bullet \frac{610.5 \bullet e^{\frac{21.875 \bullet \theta}{265.5+\theta}}}{0.4615 \bullet (\theta + 273.15)} \end{aligned} \quad (1)$$

2.4. Hygrothermal simulations

2.4.1. Weather data

When simulating in the hygrothermal simulation program, Delphin 6.1 [28], it is necessary to set boundary conditions which highly impact the quality of the results. The air temperature and relative humidity were measured in the ceiling of the test pavilion and used as the interior boundary condition. The external boundary condition was defined using weather data sourced from Asiaq, a government-owned institute operating weather stations across Greenland [29]. The weather station, "Nuuk City" (64.183333, −51.730833) [30], was placed approximately 300 m from the pavilion (64.185879, −51.731583) [31]. The weather station measured most of the necessary parameters required for Delphin, including ambient temperature (°C), relative humidity (%), wind direction (°), wind velocity (m/s), air pressure (Pa), and rain (l/m^{2}h). Delphin can also consider long-wave counter radiation, but this parameter was not measured in Nuuk. The considered weather station measured global shortwave radiation, but Delphin requires direct and diffuse radiation. Therefore, these two parameters were calculated from the global radiation using the Orgill & Holland decomposition algorithm [32]. All parameters exhibited 430 missing data points, except air pressure, with only 225 missing observations. For air pressure, the longest period of consecutive missing data was 137 h (almost six days) and 287 h (nearly 12 days) for the remaining parameters. Due to the limited number of missing data, linear interpolation was applied for all parameters except solar radiation. For solar radiation, linear interpolation was applied for instances where data was missing for less than one day. In cases where data was missing for more than one day, the missing data were filled by substituting the missing data with data from the same time of day from the previous and following available days. The exchange coefficients for heat transmission and vapour diffusion were the same for all simulations. For the inner side of the façade constructions, the heat transmission exchange coefficient for still air was assumed to be 8 W/m^{2}K and for vapour diffusion it was 1e^{-8} s/m. Externally, the effective heat conduction exchange coefficient was 25 W/m^{2}K, while the vapour diffusion mass transfer coefficient was 7.5e^{-8} s/m. For wind driven rain, the reduction coefficient was set to 0.7, which is standard for vertical walls in Delphin, and the solar adsorption coefficient was defined to be 0.7. The initial conditions of the simulation model were defined to be 20 °C and 50% relative humidity, corresponding to the indoor climate conditions.

2.4.2. Air change rate in cavity

The airflow in the ventilated air cavity is a challenging parameter to define. Hence this parameter is often discussed in studies concerning hygrothermal conditions and simulations. According to Brozowsky et al. [33], air change rates (ACH) varying from 0 to 650 h^{-1} have been reported in the literature. Langmans and Roles [34] described four measuring techniques to identify cavity ventilation rates. Falk and Sandin [35] conducted a field study and found that the orientation of the battens in the air cavity had a significant impact on the ACH. For vertical battens, the ACH was 230–310 h^{-1}, and for horizontal battens, it was 60–70% lower. Furthermore, solar irradiance could cause the ACH to increase by a factor of three. Moreover, Girma and Tariku [36] found that narrow air cavities reduce airflow and increase heat gain. In this study, no measurements were performed to identify the air change rate. As the ACH is already affected by significant uncertainty, it was decided to assume a constant flow. Based on simulation results and considering the range of 0–650 h^{-1}, the ACH was set to 60 h^{-1}. The sensitivity of this factor is investigated in Section 3.2.4.

2.4.3. Modelling in delphin

The procedure for modelling the constructions in Delphin was to replicate each construction, as shown in Fig. 3, and define the sensor locations and the material properties as accurately as possible. Unfortunately, datasheets for the applied materials were unavailable, which is why the material properties in the Delphin models were iteratively calibrated to get the best fit between the model output and the measured data. The iterations have been conducted by changing single parameters for one or, preferably, more units and analysing the impact on the results. The chosen ranges of the parameter variation were based on literature or materials from the Delphin database. The materials used in this study are described in Table 1, including the required parameters in Delphin, which are: thermal conductivity (λ), water vapour diffusion resistance factor (μ), density (ρ), specific heat capacity (Cp), water uptake coefficient (A_w), water content at saturation (W_{sat}), water content at 80% RH (W_{80}), and liquid water conductivity at effective saturation ($K_{l,eff}$) [37]. Some of these values were based on more specific material properties, including open porosity (Θ_{por}), effective saturation (Θ_{eff}), capillary sorption value at 80% RH (Θ_{80}), capillary saturation content (Θ_{cap}), and air permeability (K_g) [37]. In Table 1, the material ID from the Delphin database is given in parentheses, and the original data are shown in grey. Modified material data are specified with their respective sources. Asterisks (*) indicate that material properties were adjusted during the model calibration and deviated from the references. The materials are identical regardless of which unit they are applied to, as

IV

only one type of each material was purchased for the test pavilion. Not all materials require all properties due to airtightness or water tightness; however, they are available in Delphin and thus reported in the table.

The simulations are run with the standard grid mesh generated by Delphin, which varies from 1 mm to 50 mm with a stretch factor of 1.3. This results in a mesh of 71–102 grid elements, depending on the specific unit. According to Ruiz et al. [45], the obtained mesh leads to very high accuracy, as a grid of 20 elements was found sufficient for walls of high complexity.

2.4.4. Evaluation method

To quantify the difference between the measured and simulated data, the Root Mean Square Error (RMSE) is introduced [46]. The RMSE quantifies the error between the simulated data and measured data (considered the truth). The equation for RMSE is presented in Eq. (2), where N is the number of datapoints, $x_{sensor,i}$ is the observed data in the respective unit and, $x_{delphin,i}$ is the simulated data in the respective unit for the $i^{'}th$ time step. RMSE is always positive, and thus it cannot describe in which direction the modelled data deviates from the measured data. The unit of the parameters x_{sensor} and $x_{delphin}$ defines the unit of the RMSE. The coefficient of variance of RMSE, CV(RMSE), is often used to compare hygrothermal measurements with simulations. The advantage is that the unit is in percentage, which is easier to interpret. In this case, the errors will depend significantly on the position of the sensor, as low values result in higher errors. Therefore, RMSE is used in this study.

$$RMSE = \sqrt{\frac{\sum_{i=1}^{N}\left(x_{delphin,i} - x_{sensor,i}\right)^2}{N}} \quad (2)$$

2.5. Model applications to various locations

To evaluate the robustness of the constructions in the climatic conditions in other regions of Greenland, the Delphin models are run with weather data from various locations to investigate how different weather conditions can be expected to affect the hygrothermal conditions of the façade constructions. The pavilion models have been simulated using weather data for Tasiilaq, Sisimiut, Ilulissat, and Qaqortoq to test the robustness of the façades. The towns are geographically located, as shown in Fig. 2. Sisimiut is chosen as it is the second largest town in Greenland, after Nuuk, and therefore holds a large building mass. Ilulissat is another relatively large town located north of Sisimiut. Qaqortoq is located south of Nuuk and thus has a higher moisture level. Tasiilaq is located on the east coast, where the climate is more extreme. All simulations were carried out using reanalysis weather data for 2021 from ERA5 provided by the European Centre for Medium-Range Weather Forecasts (ECMWF) [47]. The missing data were interpolated, and the global solar radiation was derived using the Erbs decomposition algorithm [32].

2.6. Quantifying the risk of mould growth

The robustness of a construction in the Arctic climate depends on many parameters, including the risk of mould growth, which in turn depends on the materials, temperature, and humidity. The mould index was chosen as the focus of this evaluation because the conditions for mould growth have lower limit values than wood-decaying fungi, i.e., the construction is more vulnerable to mould than wood-decaying fungi. The software WUFI Mould Index VTT 2.3 [25] was used to determine the Mould Growth Index based on the three conditions using the Viitanen model [48]. As the intention was to assess a critical scenario, the analysis was performed with a highly sensitive material for all units; pine sapwood from the WUFI material database was chosen for this purpose. The mould growth index was calculated for the sensor locations, which were considered the most critical based on the results.

3. Results and analysis

This section only presents the essential graphs produced. Additional figures can be found in the supplementary figures [49]. It should be noted that all of the presented graphs show either 7 or 30-day moving means in order to visualise the long-term trends. The moving mean period is specified in the captions of each figure. The following graphs were generated and analysed for all units and all directions.

- Temperature graphs of sensor data for all orientations of the same construction.
- Relative humidity graphs of sensor data for all orientations of the same construction.
- Temperature graphs, including sensor data and Delphin results.
- Relative humidity graphs, including sensor data and Delphin results.
- Vapour content graphs for both sensor data and Delphin results.

3.1. Evaluation of experimental data

All available data from 2020-09–29 to 2022-10-20 are shown in Fig. 4, including interpolated values. The graphs had two purposes. First, to visually check for any remarkable changes in the measurements over time, which could indicate sensor drift. Second, to illustrate the differences between the units and the orientations. Noticeably, there was a decrease in the interior relative humidity during spring 2022, which did not seem to be caused by temperature changes. Plausible explanations could be that the humidifier, controlling the indoor relative humidity, stopped working or that the water tank connected to the humidifier was empty. Besides this, small deviances in the interior climate were noticeable, caused by maintenance activities in the pavilion, such as filling the humidifier tank and ensuring continuous data logging. From Fig. 4, it can also be seen that the temperatures in the exterior layers were highest in the south-oriented directions, lowest for the northern orientation, and in between for east and west orientations. A plausible explanation of these differences is heat contribution from direct solar irradiation. This could be seen for all units except B, as the sensors were placed differently in the north and south direction. Another general observation was that none of the constructions was exposed to 100% relative humidity for longer periods of time.

Based on s1 in Unit A, it is noticeable that the temperature was lower in the western orientation than in the north and south. As there were no visible differences between the orientations in the exterior layers, this temperature difference might have been caused by improper assembly of the entrance door, which could result in thermal bridges or wind flow in the construction. Given that the relative humidity was also lower in the western orientation, this may very well be the case. The relative humidity in s1 in Unit C stands out, as it was very different for the two orientations. The relative humidity was highest for the north orientation and never overlapped with the measurements for the south orientation. The temperature was also slightly lower in the north than in the south. In Unit $E_{N,}$ there was a peak in temperature in March 2021. The peak in temperature occurred throughout all the northern units.

3.2. Comparison of measured and simulated data

3.2.1. Root Mean Square Error

The following section focuses on the year 2021. Table 2 shows the Root Mean Square Errors (RMSE) (see Eq. (2)) of the Delphin simulations. The first two sections of the table compare the original hourly data, while the last section compares the seven-day moving mean relative humidity. The latter indicates whether the model is able to capture the general tendency, despite the high RMSE caused by short-term peaks and outliers. When developing the Delphin models, the aim was to

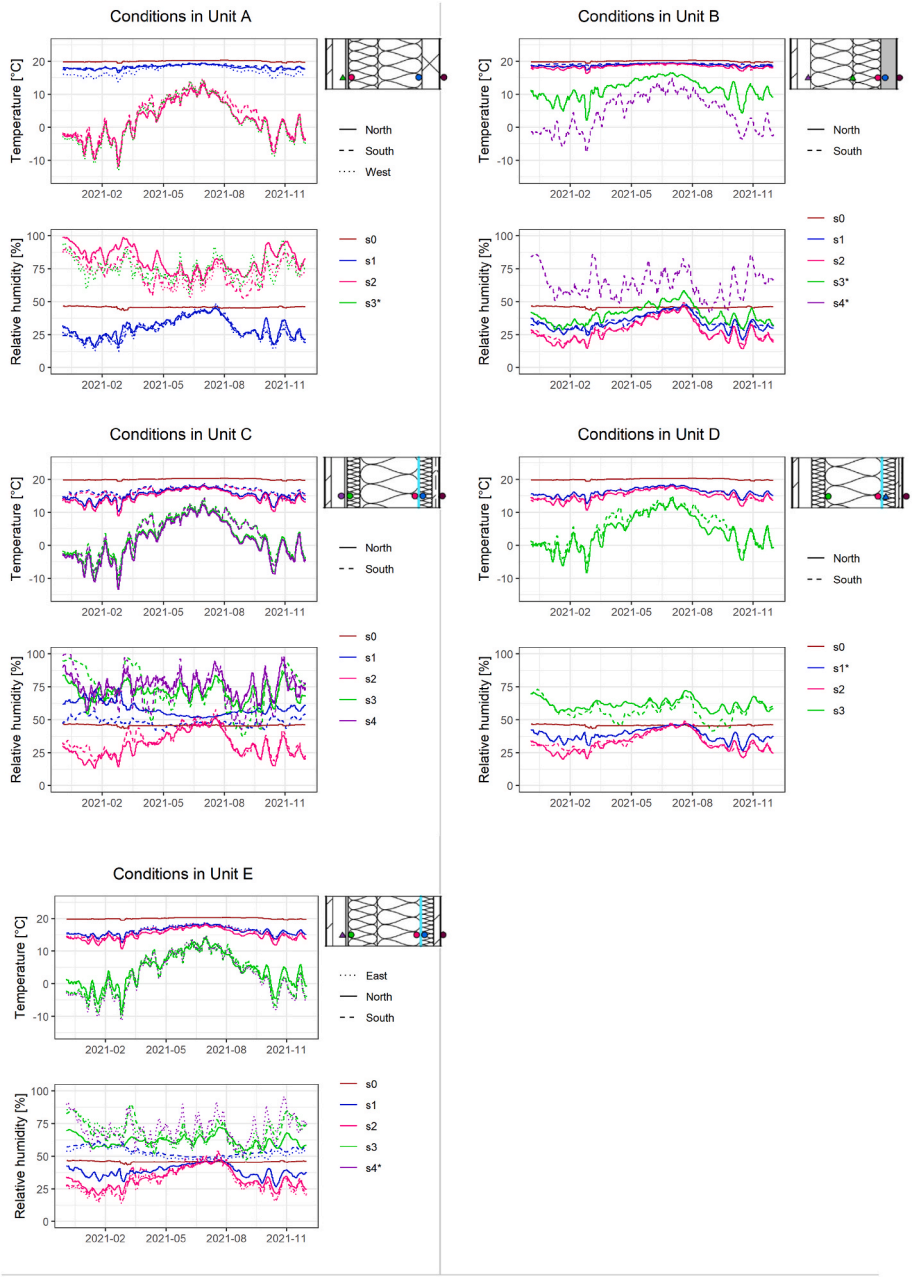

Fig. 4. Hygrothermal conditions in Units A – E (seven-day moving mean). The asterisks (*) indicate that the measurement point was only found in one direction of the unit (equal to a triangle in Fig. 3).

achieve an error of less than 5 °C for temperatures and less than 10% for relative humidity. The primary purpose of these limits was to easily identify at which sensor points the model deviated significantly from the measured data. The additional benefit was that the limits could be used as a benchmark for when the model is "good enough," as simulations can be improved infinitely without significant scientific gain. The cells exceeding the threshold limits are marked with yellow. The first table section shows that the modelled temperature was generally sufficiently accurate, as none of the RMSEs exceeded 5 °C. For relative humidity, the highest errors were found at the sensor positions closest to the exterior climate, which is to be expected due to the stable indoor climate and highly varying external climate. The sensitivity of the ACH and the vapour diffusion mass transfer coefficients are investigated in Section 3.2.4. Generally, the model for Unit D seemed to fit the best, while the model for Unit C performed the worst.

Since the measured interior climate was used as an input for Delphin, it might seem strange that there was an error at this measurement point. The reason is that the measured data is used as the room conditions, while the modelled data point corresponds to the surface conditions. Therefore, the room conditions (s0) from the Delphin output are not illustrated on the graphs throughout this section.

3.2.2. *Comparison of conditions in the air cavities*

As presented in Fig. 3, not all units had a sensor in the ventilated air cavity, but still, there was at least one representative sensor for all orientations. To identify how the orientation affected the hygrothermal conditions in the air cavity, the measurements in the ventilated air cavities are compared in Fig. 5.

The lowest temperatures were found in the northern-oriented Unit C, which can be explained by the fact that this orientation received the least amount of solar irradiation. Some of the highest relative humidity conditions were also detected in this unit. The vapour content in Unit A_W

Table 2
Root Mean Square Error of each unit comparing the Delphin models with the measured data. Yellow cells indicate that RMSE is higher than desired.

	Temperature [°C]					Relative humidity [%]					RH (7-day moving mean) [%]				
	S0	S1	S2	S3	S4	S0	S1	S2	S3	S4	S0	S1	S2	S3	S4
$A_{N(10)}$	0.3	0.5	1.9	-	-	0.9	5.6	9.4	-	-	0.8	3.9	8.0	-	-
$A_{S(1)}$	0.3	0.6	3.7	-	-	0.8	5.5	9.1	-	-	0.8	3.3	7.5	-	-
$A_{W(15)}$	0.3	0.7	3.1	3.3	-	0.9	7.3	9.0	15.6	-	0.8	4.3	7.8	8.5	-
$B_{N(11)}$	0.4	0.4	0.8	2.3	-	1.0	4.5	3.4	3.3	-	0.9	4.0	2.5	2.1	-
$B_{S(2)}$	0.4	0.4	0.8	3.2	-	0.9	5.0	3.5	-	10.6	0.9	4.6	2.4	-	5.2
$C_{N(12)}$	0.5	1.2	1.4	2.0	2.3	1.3	15.5	11.0	8.5	14.6	1.2	13.4	3.1	5.5	10.5
$C_{S(3)}$	0.5	2.2	2.1	3.8	4.2	1.2	9.4	13.5	15.0	19.9	1.2	4.2	4.4	13.6	13.7
$D_{N(13)}$	0.4	0.5	1.2	1.6	-	1.0	8.4	3.6	4.3	-	1.0	8.0	2.8	3.9	-
$D_{S(4)}$	0.4	-	1.1	2.5	-	1.0	-	3.5	5.2	-	0.9	-	2.8	4.7	-
$E_{N(14)}$	0.3	1.0	1.4	2.1	-	0.8	7.3	11.9	8.9	-	0.6	2.7	4.7	7.6	-
$E_{S(5)}$	0.3	1.3	1.7	4.1	-	0.8	6.7	13.0	9.2	-	0.6	1.2	3.8	7.7	-
$E_{E(17)}$	0.3	1.0	1.4	4.4	4.8	0.8	7.8	14.4	10.0	17.5	0.6	3.5	3.4	8.1	5.9

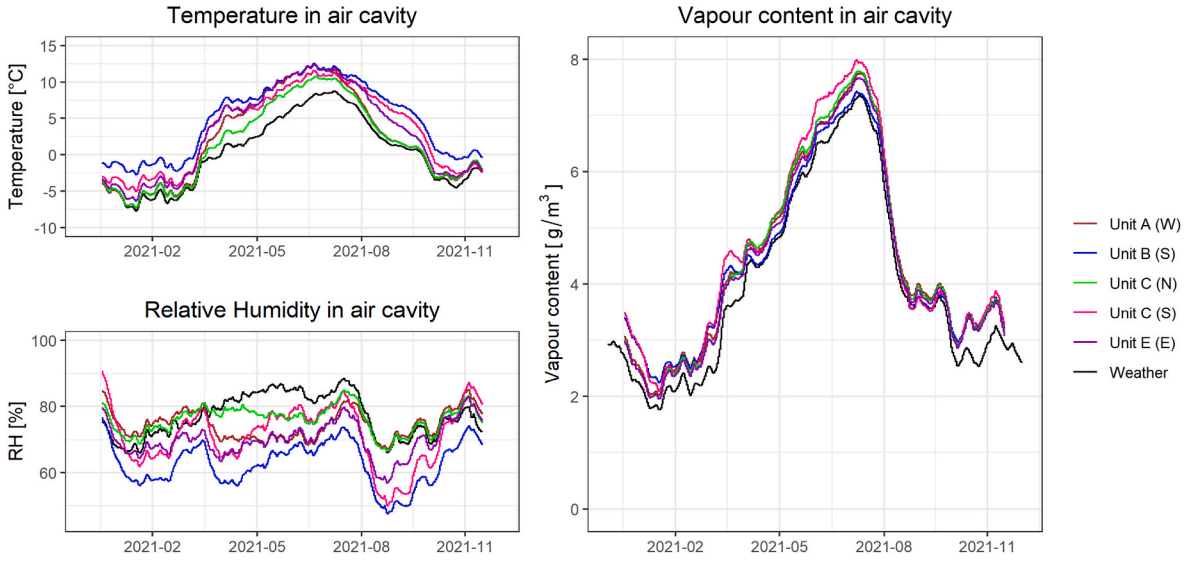

Fig. 5. Graphs for temperature, relative humidity, and vapour content in the air cavity in the year 2021. The graphs display the 30-day moving means to visualise the long-term trends.

and Unit C_N were similar, but in A_W, the temperatures were higher, and in the summer months, the RH was lower. It was expected that in each direction, the conditions in the air cavity would be very similar. However, this was not the case, as Unit B_S had higher temperatures and lower RH than Unit C_S. It did not seem to be caused by drifting of the sensors, as they were not displaced equally during the year. The temperature difference between B_S and C_S could be caused by B_S having a higher U-value (U = 0.15 W/m^{2}K) than C_S (U = 0.13 W/m^{2}K), which allowed a higher heat loss through the surface.

It was found that the vapour moisture content exceeded 10 g/m^3 at sensor point s2 for all elements with fibre cement board as the wind barrier. The vapour moisture content also exceeded 15 g/m^3 for all units except the ones facing north.

3.2.3. *Visual comparison – measurements and simulations*

To compare the simulations with the measurements, the focus will be on the sensors where the RMSE was highest. In the following section, data will be specified according to the sensor position and data origin, e.g., m_3 or d_3 corresponds to measured and simulated (Delphin) data at sensor position 3, respectively. Figs. 6–10 presents the 7-day moving means to make it easier to detect long-term trends. Based on these graphs, the following is noticed.

- The simulation of A_W generally performed worse than A_N and A_S. Unit A_W is the gable with the entrance door, which might affect the hygrothermal performance of the unit. Fig. 5 shows that the RH in the air cavity was high in this orientation compared to the other orientations, which is also shown in Fig. 6, where the RH in d_3 was lower than m_3.
- In Unit B_s, the simulated relative humidity (d_4) was higher than the measured (m_4) (see Fig. 7). As for Unit A_W, this could be traced back to the hygrothermal conditions in the air cavity, where m_4 for B_s had the lowest relative humidity.

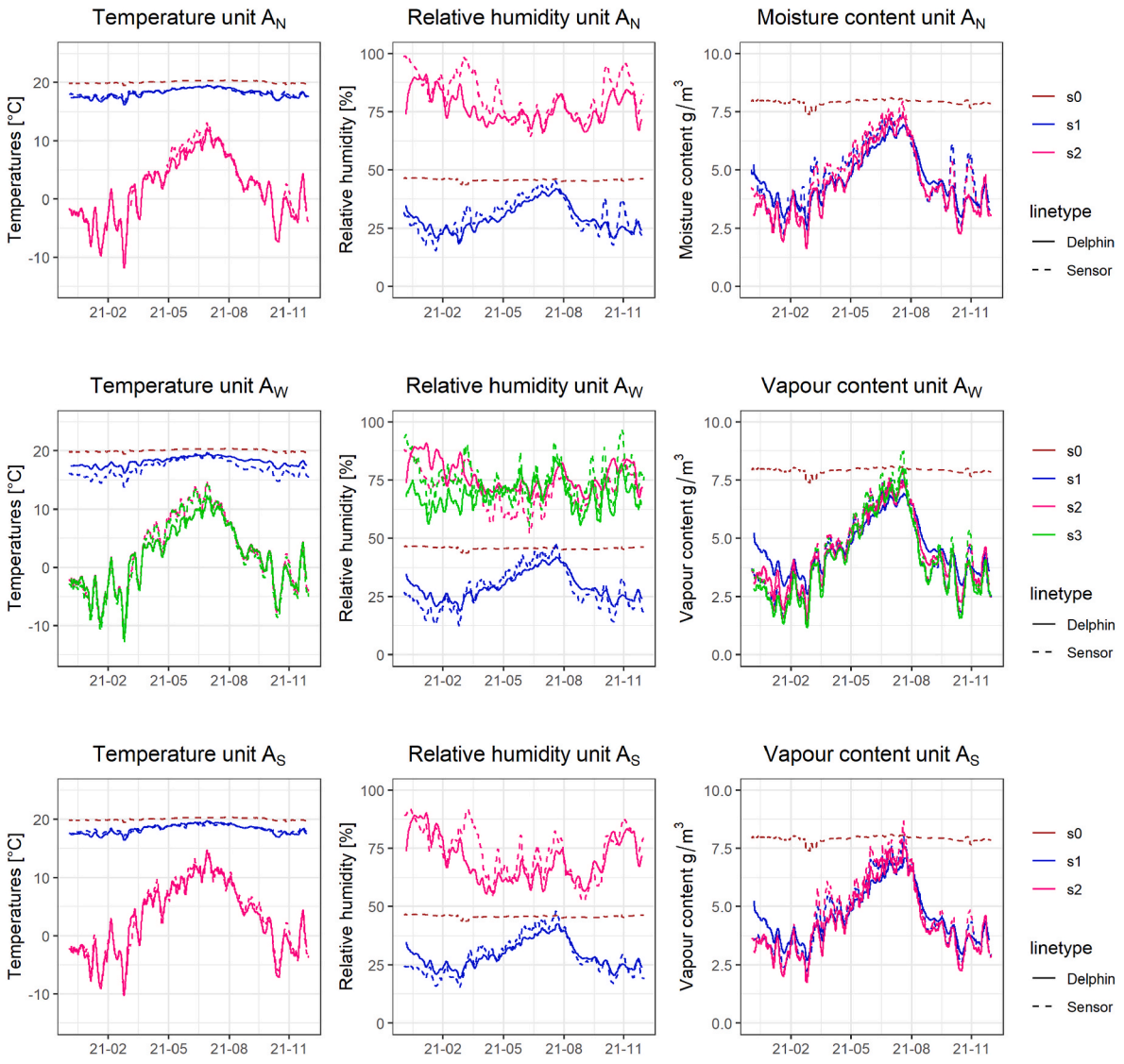

Fig. 6. Hygrothermal conditions for Unit A. Time format yy-mm.

- Both C_N and C_S had sensor points with high RMSE, even for the moving mean of RH. The measured values were very different at s1 compared to s2 and s3, e.g., the peaks were much higher in the southern direction (see Fig. 8). This difference challenged the model fitting in Delphin, as solar irradiation seemed to have a bigger impact on the orientation in the measured data than in Delphin. The high RH in m_1 in the north end (see Fig. 8) does not indicate a perforated vapour barrier, as that would cause the humidity level to align closer with the interior climate. In theory, the difference can be caused by poor sensor calibration, but as described in Section 3.1, Fig. 4 does not indicate such a situation.
- All orientations for Unit E had high RMSE for relative humidity at sensor point s2. According to the low RMSE for the moving mean values, the error occurred due to short-term spikes in the data. The RMSE for s3 in E_S was also high, where the modelled parameters from Delphin were higher than the measured (m_3). In the gable, E_E, d_4 had smaller peaks than m_4 (see Fig. 10).

All simulations are imperfect. In this specific case, the type of imperfection does not seem to be directly connected to the construction type or the orientation. Furthermore, the measurements did not indicate any severe consequences, such as frost close to the interior climate or high levels of relative humidity over long periods of time. This was also true for the simulated results.

3.2.4. *Sensitivity of flow in the air cavity*

This analysis was performed on the model for Unit B, i.e., the unit where simulations fit the measurements best according to the RMSEs presented in Table 2.

The results of the sensitivity analysis are presented in Table 3 and were calculated as the difference in the RMSE in percentage as described in Eq. (3), where $RMSE_{change}$ is the new value and $RMSE_{basic}$ is the original RMSE value. The results revealed that changes could improve the simulation model at sensor points s0 and s1, although at the expense of the precision at s2 and s3. It also showed that the air change rate, ACH, has a reduced impact on the RMSE closer to the interior climate. Also, the RMSE can be considered insensitive to the ACH, as even a reduction of 60% or a doubling of the value has an insignificant effect. The effect is only significant when the ACH is very low (less than 24 h^{-1}).

$$sensitivity = \frac{(RMSE_{change} - RMSE_{basic})}{RMSE_{basic}} \bullet 100\ [\%] \quad 3$$

As identified in Section 3.2.1, the largest RMSEs were found for the sensors in the exterior layers of the constructions. The results of the sensitivity analysis of the ACH, presented in Table 3, showed that the

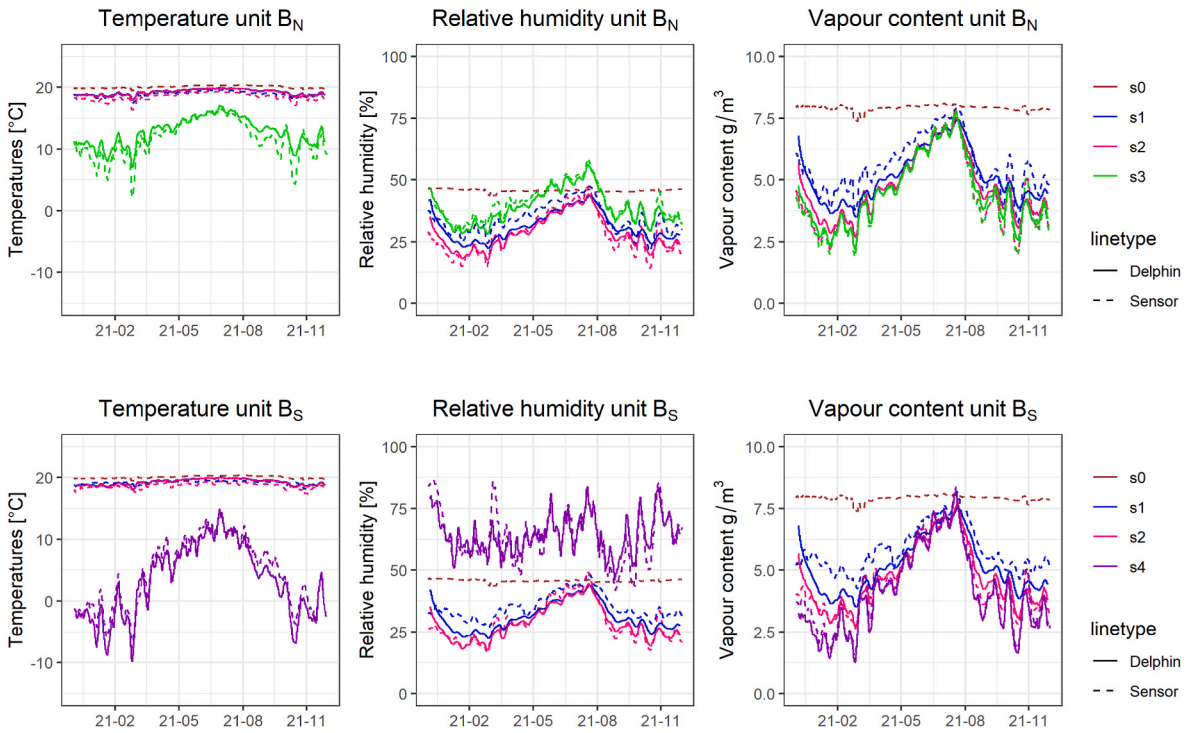

Fig. 7. Hygrothermal conditions for Unit B. Time format yy-mm.

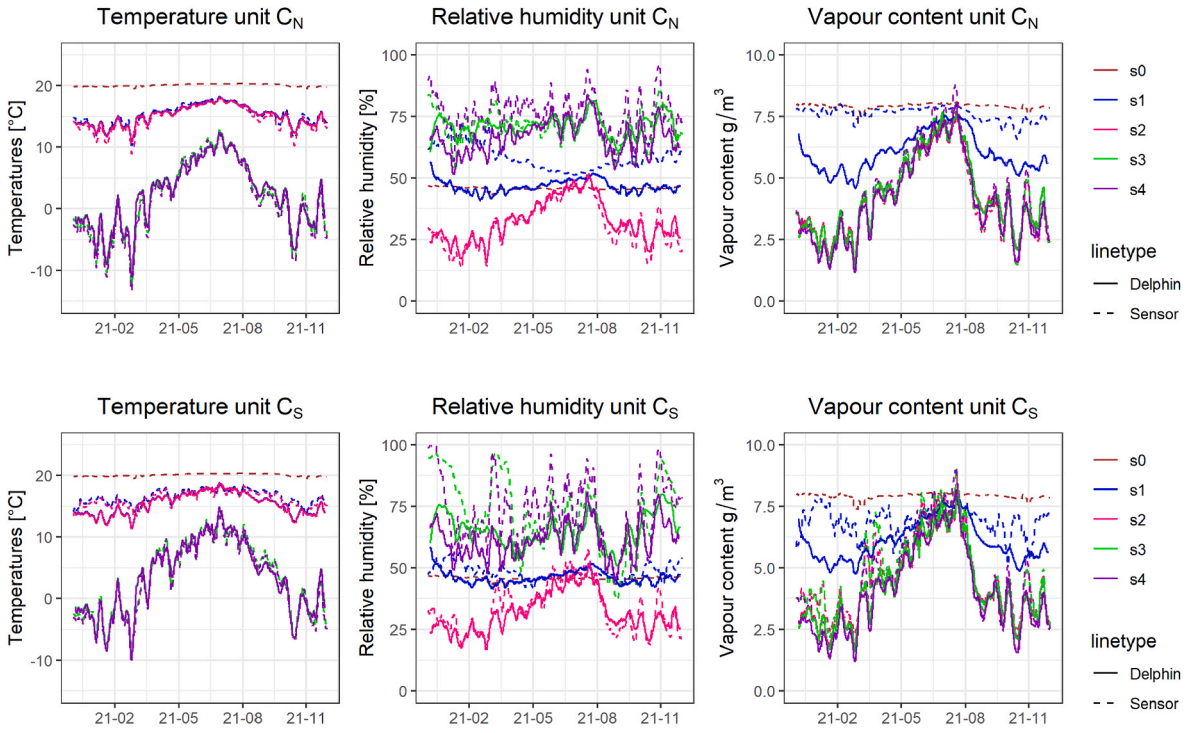

Fig. 8. Hygrothermal conditions for Unit C. Time format yy-mm.

sensitivity of the ACH was highest at the two exterior sensor locations, meaning that this parameter might contribute to the initially high errors along with the varying weather conditions. The sensitivity of the vapour diffusion mass transfer coefficient was investigated for Unit A_N based on the same methodology as for ACH. The initial value was $7.5e^{-8}$, and the tested alternative values were $7.5e^{-6}$, $7.5e^{-10}$, and $7.5e^{-12}$, causing a maximum change of 0.65% of the RMSE occurring for the temperature at sensor point s2. Therefore, the effect of changing the vapour diffusion mass transfer coefficient was considered negligible.

3.2.5. *Consequences of cut-out*

As presented in Section 2.3, there was a hole in the layer of fibre cement boards in Unit B. This was neglected in the hygrothermal simulations, but a small analysis has been conducted to investigate how this

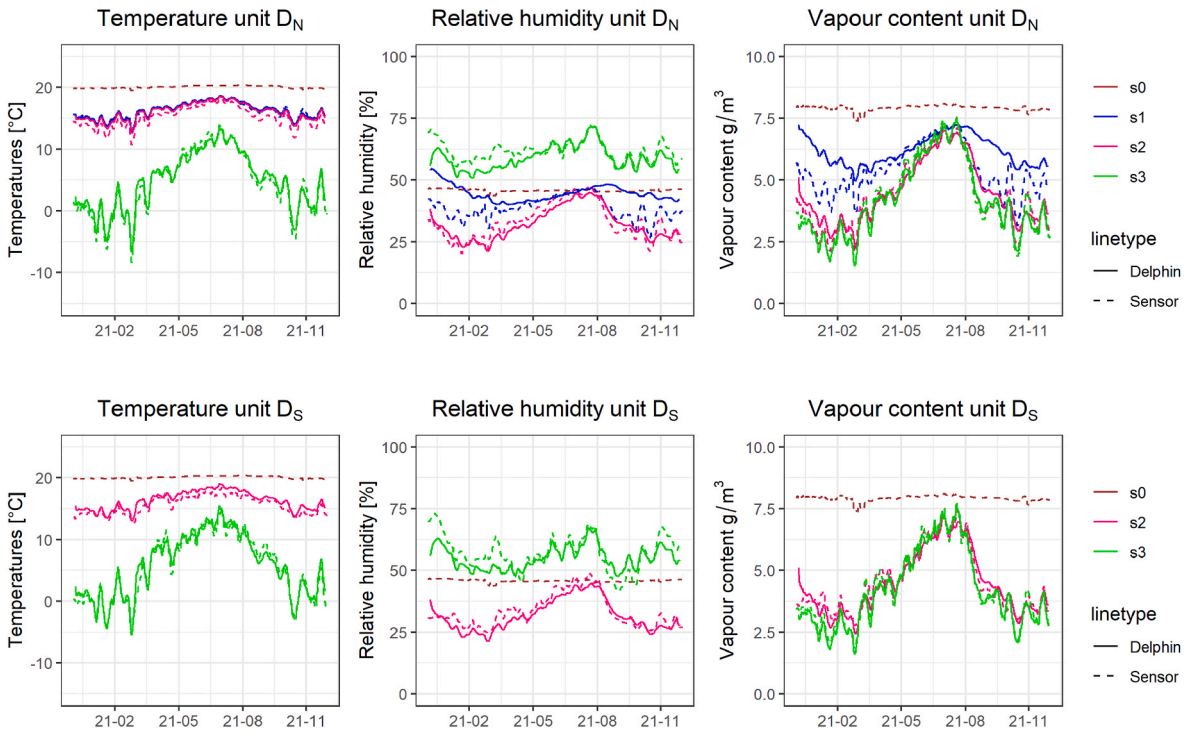

Fig. 9. Hygrothermal conditions for Unit D. Time format yy-mm.

decision affects the quality of the model. An alternative simulation model was built with a 27 mm air cavity (Delphin ID 16) with no airflow. The air gap was placed 18 mm from the interior side of the fibre cement board, which left a 9 mm board between the insulation and the sensor on the other side. The impact is small when comparing the measured values with simulations of solid boards and simulations with holes. However, the temperature is slightly higher at sensor points s1 and s2 for the cut-out simulation. The maximum temperature difference was 1.8 °C, while the mean difference was less than 0.3 °C. The comparison of the temperatures and relative humidity is presented in the repository [49].

3.3. Other climates

The temperature and relative humidity from the ERA5 reanalysis dataset for the five locations is presented in Fig. 11.

The graphs in Fig. 12 were made using a seven-day moving mean and show the hygrothermal conditions at each sensor point for all considered locations. When evaluating the results, it must be considered that the ERA5 weather data are modelled and not measured. The location had almost no influence on the temperature and minimal impact on the relative humidity at the inner layers (sensor points s1 and s2). Therefore, these are not included in Fig. 12. Neither are the graphs representing humidity levels below 75%. The absent graphs can be found in the repository [49]. At the other sensor points (s3 to s4), the highest relative humidity appears in Ilulissat and Sisimiut, followed by Nuuk.

3.4. Risk of mould growth

The constructions and locations at the highest risk of mould growth are identified from the graphs in Fig. 12. The analysis in WUFI VTT is based on the Viitanen model [48] and is made for both measured and simulated values. For all assessments, the material was defined as pine sapwood, which is very sensitive and thus represents a worst-case scenario. The upper part of Table 4 presents the results for the included sensor points analysed with the measured interior conditions from the test pavilion (constant interior conditions of approximately 50% RH and 20 °C). Because of the controlled indoor climate, an additional analysis was made to see the impact of the potentially inappropriate use of a residential building causing high indoor relative humidity. The indoor temperatures were still taken from the measured values from the pavilion, but the RH was changed to 70% and 80%. The calculated mould indexes are presented in Table 4. The mould index ranges from 0 to 6 [50], and according to Ojanen et al. [50], the infestation level is considered acceptable when the index is 2 or less for surfaces inside a construction. The mould index itself is less important as it is based on a relatively short period, but it illustrates the differences and sensitivity for different conditions.

4. Discussion

4.1. Uncertainties and limitations

The intention was to install sensors on each side of the vapour barrier and on the internal side of the wind barrier. However, due to misunderstandings, a hole was created in the fibre cement board in Unit B to make space for a sensor, even though the construction did not contain a vapour barrier. According to simulations in Delphin, this cut-out had small consequences for the hygrothermal conditions in Unit B.

Another uncertainty that caused challenges in replicating the constructions in Delphin was that there were no datasheets for the applied materials. If these data had been available or measured in the lab, the simulations might have been more precise; however, lab measurements of material parameters were not part of this study.

The lack of sensor calibration caused the last apparent uncertainty. Prior to the start of the experiments, the sensors were calibrated at the factory, but it would be valuable to calibrate them after the measuring period. Especially relative humidity sensors are known to drift over time. The data was considered reliable despite the missing calibration based on Fig. 4, which showed a continuity of the yearly cycle and no apparent sensor drift.

The weather data were another source of uncertainty. As described in Section 2.4.1, there was some missing data for each weather parameter. The most uncertain of these was global radiation, as this parameter has the highest variability, e.g., 1 h can be very sunny, while the next can be

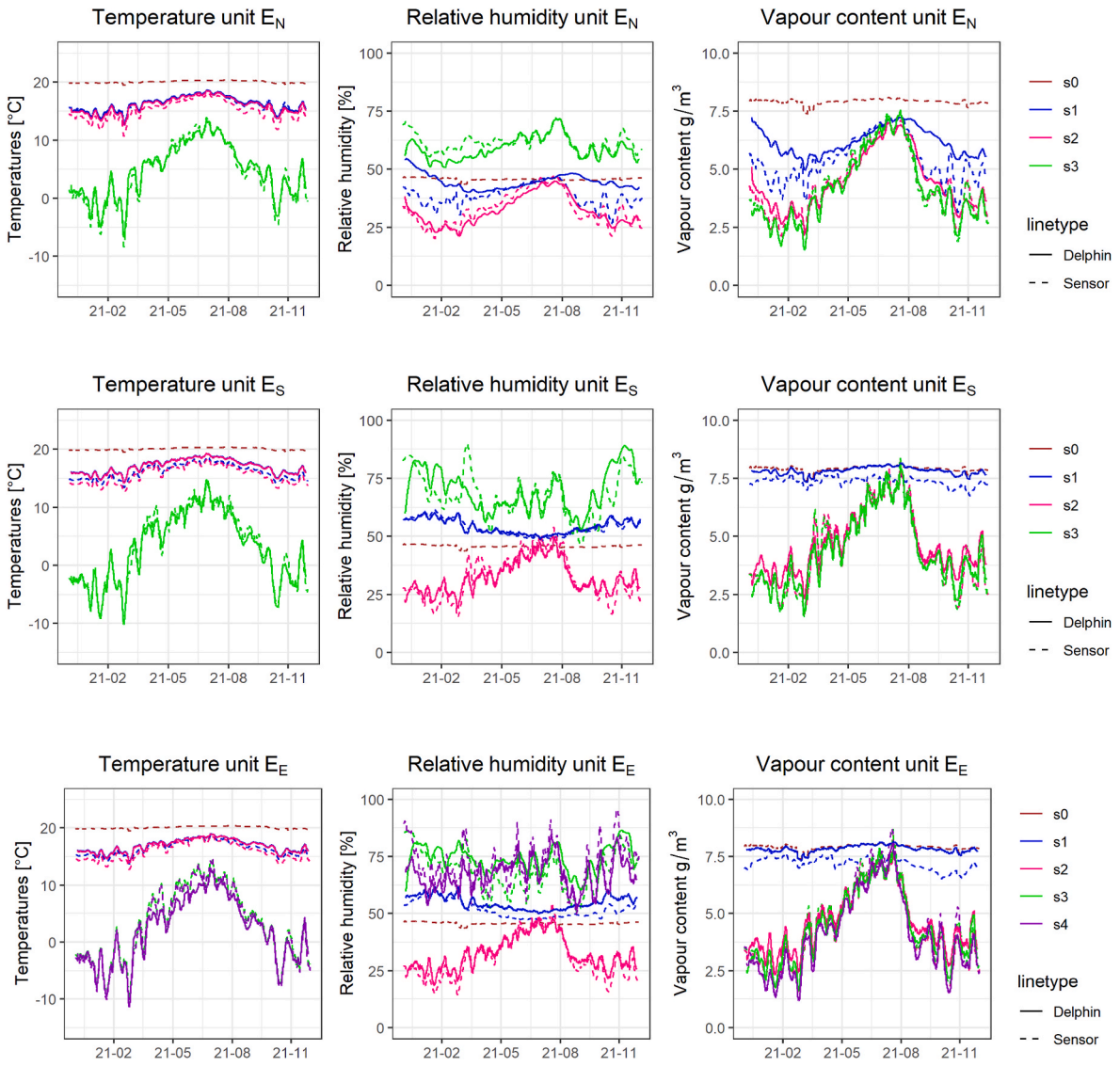

Fig. 10. Hygrothermal conditions for Unit E. Time format yy-mm.

Table 3
Sensitivity of the air change rate in the ventilated air cavity in Unit B. The results are given as the change of RMSE in percentage.

	Temperature				RH			
Change	S0	S1	S2	S3	S0	S1	S2	S3
−10%	0%	0%	0%	0%	0%	0%	1%	0%
−60%	−1%	3%	2%	3%	−1%	−5%	9%	5%
−80%	−2%	4%	2%	4%	−1%	−11%	23%	19%
10%	0%	0%	0%	0%	0%	0%	−1%	0%
100%	1%	−3%	−2%	−3%	2%	2%	−3%	−3%
500%	4%	−8%	−5%	−8%	5%	3%	−6%	−9%
1000%	6%	−11%	−6%	−10%	6%	3%	−6%	−10%

very cloudy or after sunset. This makes it very difficult to fill out the missing data with reliable values. An additional source of uncertainty for the solar radiation data is the decomposition of global radiation into direct and diffuse radiation.

Another uncertainty was caused by the air change rate, ACH, in the ventilated air cavity surrounding the test pavilion. As shown in Fig. 5, the hygrothermal conditions varied, even on the same side of the pavilion. If another facility like this should be planned or if this one was to be improved, it would be beneficial to install sensors to measure the wind speed inside the cavity; however, measuring the airflow is a challenge because the measuring equipment alters the airflow. The sensitivity analysis of the ACH showed that the airflow was insignificant, and each adjustment, whether it was negative or positive, caused both positive and negative changes in the RMSE. The surroundings of the pavilion can also affect the measurements, e.g., altering the airflows and casting shadows. This may very well have been the case as the pavilion was placed on pillars on a sloped surface and close to another test house.

As described in the introduction, user behaviour tends to play a significant role in the quality and long-term conditions of a building. This perspective cannot be evaluated by the presented test facility, as the

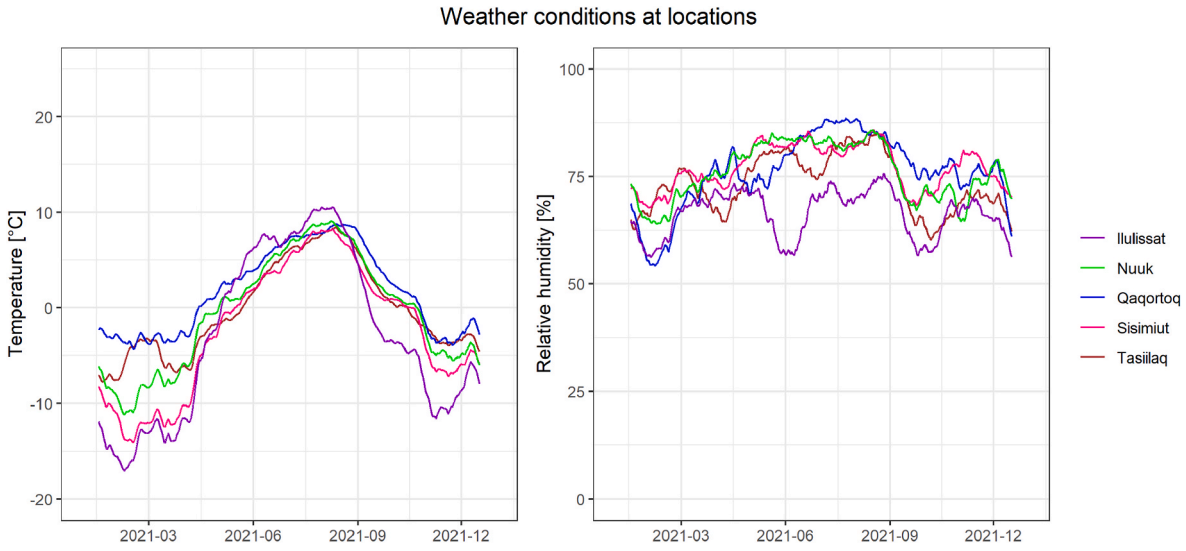

Fig. 11. Weather conditions at the five locations in 2021 (seven-day moving mean).

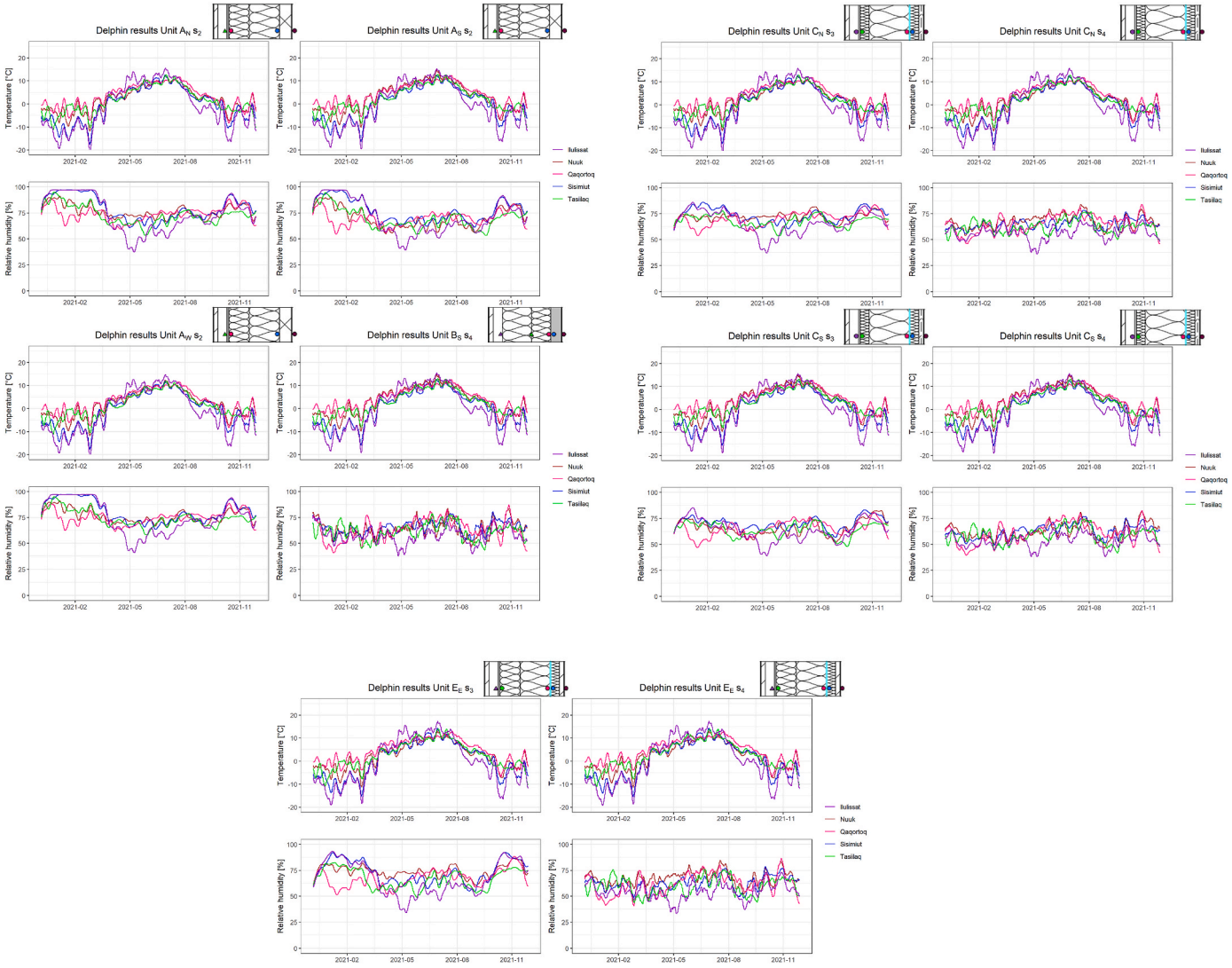

Fig. 12. Comparison of results for multiple Greenlandic locations.

Table 4
Mould index for different simulation scenarios. The interior conditions in the pavilion in Nuuk were set to 50% RH and 20 °C. The measured conditions were used for all assessments.

City	Unit	sensor	Index	Interior conditions	Note
Nuuk	C_S	3	0.00	Measured	0 for all other locations (ERA5)
Nuuk	C_S	4	0.04	Measured	
Sisimiut	A_S	2	0.00	Measured	
Sisimiut	A_N	2	0.00	Measured	
Sisimiut	A_W	2	0.00	Measured	
Ilulissat	A_S	2	0.01	Measured	
Ilulissat	A_N	2	0.02	Measured	
Ilulissat	A_W	2	0.02	Measured	
Nuuk	E_S	3	0.00	Measured	0 for all other locations (ERA5)
Nuuk	C_S	3	0.04	RH = 70%	
Nuuk	C_N	3	0.11	RH = 70%	
Nuuk	C_S	4	0.04	RH = 70%	
Nuuk	C_N	4	0.07	RH = 70%	
Nuuk	C_S	3	0.21	RH = 85%	
Nuuk	C_N	3	0.62	RH = 85%	
Nuuk	C_S	4	0.04	RH = 85%	
Nuuk	C_N	4	0.07	RH = 85%	

IV

interior climate was controlled, and the pavilion was not inhabited. This was also not the intention of this study, as the primary aim was to assess the constructions under real outdoor conditions while minimising other uncertainties. However, a few Delphin assessments were made for constant humidities of 70% and 85% and showed no risk of mould growth with an index of maximum 0.62, which is much lower than the acceptance limit of 2. This indicates that the observed mould problems in buildings with these constructions are not the result of high indoor relative humidity. Instead, it is more likely that other problems, such as leakages or thermal bridges, possibly in combination with high indoor relative humidity, may be the cause.

4.2. Evaluation of weather data

As described in Section 2.5, the simulations made for alternative locations were conducted using reanalysis weather data. Reanalysis data are considered better than Test Reference Years (TRY) as they represent conditions for a specific time, although they are not measured by rather derived from a weather model. It is relevant to evaluate how it affects the simulation quality by comparing the simulation results made with ERA5 and measured data from Asiaq. This is shown in Fig. 13, along with the data from the sensors. The results are shown for Unit E as it is representative of all units. The rest of the graphs can be found in the repository [49].

The results from Delphin generated using measured weather data (Asiaq) for Nuuk in 2021 are very similar to the results obtained with the modelled weather data (ERA5). The maximum change of RMSE for the temperatures was 0.65 °C, and for RH, it was 6.84% (41 of 48 RMSE-values are below 2.13%). This indicates that the reanalysis weather data can be used as an alternative to measured weather data for studies investigating the impact of different locations. Coincidentally, it can be observed that the modelled weather results in a better fit for RH than the measured weather.

4.3. Experiment improvement and future work

For future setups like the test pavilion presented in this study, there are some takeaways that could improve the quality and reliability of the results. From a more technical perspective, it can be recommended to install sensors in the air cavity detecting the wind speed, to improve the reliability of the hygrothermal models regardless of the software program. In future studies, it is also recommended to calibrate the sensors before and after the test program.

Furthermore, it could be considered to carry out a blower door test on the pavilion to investigate the tightness of the constructions, but with the current layout, any leaks would be hard to locate. It might, however, be possible in combination with thermography. If air tightness is a central parameter to future studies, dividing the test facility into sections should be considered.

Just like the designed models were used to test the façade constructions for robustness in other regions of Greenland, they can be used to evaluate the consequences of climate change, using predicted future weather data.

4.4. Results

Based on the results, it was not possible to determine a best or worst

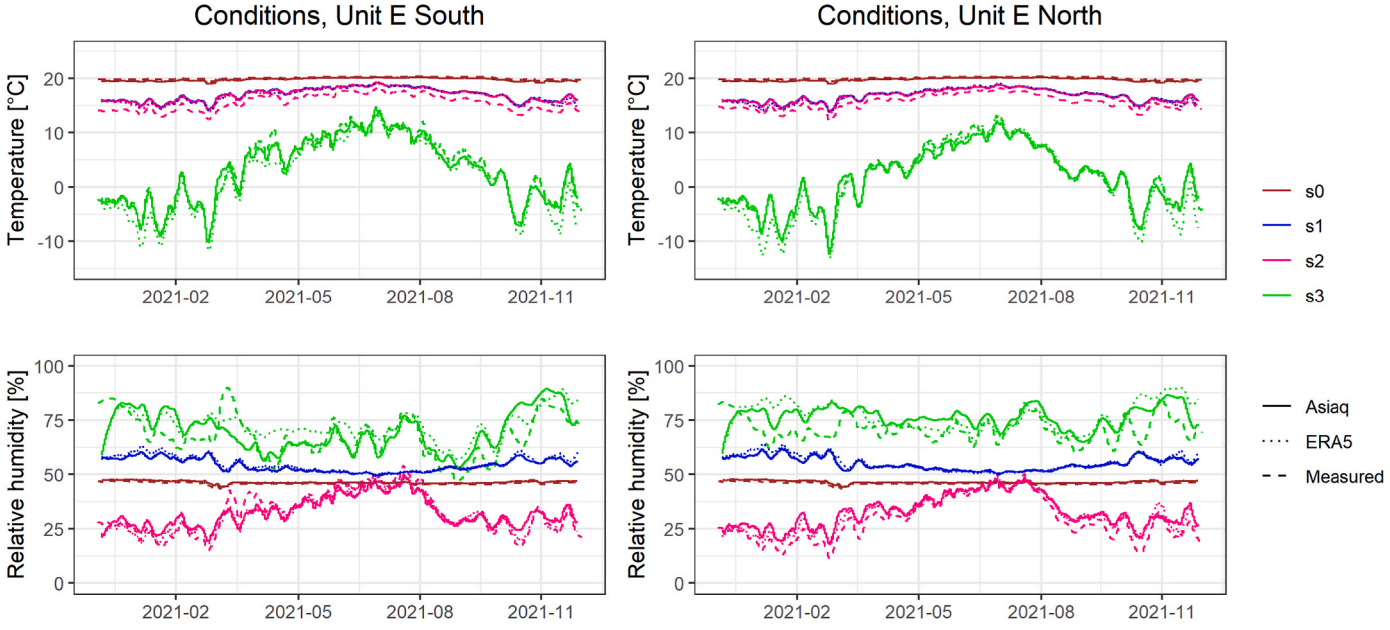

Fig. 13. Simulated and measured conditions in Unit E for different weather data sources for Nuuk.

construction for the Arctic climate. None of the constructions showed a risk of mould growth, which would have been indicated by a Mould Growth Index above 2. Still, it was possible to identify which construction types are sensitive to other things, such as orientation or location. For example, the temperature and relative humidity in the inner layers of the traditional half-timber construction (Unit C) differed for the north and south. This observation does not prove that this construction type should be avoided, but in this experiment, it either shows sensitivity to orientation, a challenge in the buildability, or an error in the sensors. As the simulations were very insensitive to the orientation in Unit C and the other units, the cause is most likely either faulty installation or sensor errors.

4.5. Location of test facilities

When constructing test facilities such as the presented pavilion, choosing a representative or worst-case location is of interest while making it as accessible and cheap as possible. Based on the results presented in Section 3.3, Nuuk is representative of most locations in Greenland. Furthermore, placing a test facility in Nuuk is advantageous as it is by far the biggest city (Nuuk has 19.000 inhabitants, second largest town has 5.500 [5]). Therefore, it has relatively easy accessibility, local technical competencies, and available weather data. Additionally, Nuuk has the largest building stock in Greenland, making the results directly applicable.

4.6. Perspectivation

4.6.1. Sustainability

Assessing which construction type performs the best could also include a sustainability study. As presented in the introduction, Ryberg et al. [16] made a comparative sustainability study in 2021, including four construction methods: concrete, CLT, timber frame, and renovation. As three of these are included in this study, it led to the following reflection. In the discussion, Ryberg et al. wrote, "*While there is a difference in the impact scores for the three new buildings, neither of the buildings outperforms the others across all midpoint impact categories.*" This means that the technical and practical aspects become even more critical to the decision regarding the construction method because flawed constructions can lead to increased heat loss and reduced lifetime, eventually compromising the sustainability performance. Exactly this is also the conclusion made by Ryberg et al. [51], who also highlight that correction of potential errors can have substantial environmental impacts.

4.6.2. Concrete constructions without wind barriers

The introduction also presented a previous study of a concrete construction without a wind barrier [11]. One of the construction types in the test pavilion was inspired by this construction; thus, it was considered suitable to discuss the findings here. The previous study found that wind penetrating the insulation layer caused the concrete to cool down. Theoretically, the wind barrier is redundant, as the combination of concrete and firm tight-fitting insulation boards should be wind-tight. Due to a combination of rough concrete surfaces and poor execution of the construction work, it did not work as planned in the case described in Ref. [11]. This resulted in poor thermal performance of the insulation, specifically the heat loss coefficient was found to be $\lambda = 0.3$ W/(m•K), while the declared value was $\lambda = 0.033$ W/(m•K). The present study found that the simulation model of Unit B, which is similar to the aforementioned concrete wall, performed reasonably, especially when compared to the other units, where the RMSE was worse (see Table 2). When making this comparison, it is essential to know that the pavilion unit was built with fibre cement boards and not concrete as in the original building. Together with a relatively small unit fitted to the size of insulation mats, the unit benefited from the smooth surface to limit wind-induced convection between the insulation and fibre cement board. However, this study demonstrates that the design is technically possible, but it does not answer whether it is suitable for Greenlandic conditions, where practical issues may make it difficult to build precisely as designed. The buildability of a solution can be dependent on location.

Furthermore, there may be additional challenges that would occur in real-life cases. E.g., unit A with CLT elements will be more exposed to moisture in a real construction process, but over time it will dry and shrink, which could lead to cracks and result in air gaps. Such air gaps can cause increased heat loss and moisture problems. This could be a topic for further investigation.

5. Conclusion

Large amounts of data have been collected from the test pavilion, which can be analysed and investigated in many ways. Currently, data has been collected for two years, starting at the end of October 2020 (data logging is still ongoing). The pavilion comprises of five construction types: CLT, concrete, steel frame with mineral wool, timber frame with cellulose insulation, and timber frame with mineral wool. These five constructions represent the current building methods in Greenland as of 2023. Despite the high ambitions, there were many uncertainties connected to the experiment, which can and should be avoided in future test facilities.

The study had three research questions; the first was whether the studied constructions were unsuitable in Nuuk, and the second if the constructions were robust enough for other regions in Greenland. The study showed that all investigated constructions could function acceptably in Nuuk and in other Greenlandic climates if built as designed and prescribed by the manufacturer. Furthermore, it showed that the conditions in the ventilated air cavity were, to some extent, depending on the surface's orientation. However, the ventilation rate had very little influence when defined within a normal range. The conditions in the air cavity had an insignificant impact on the hygrothermal conditions inside the wall.

The modelled weather data from ERA5 were found to be adequate to replace measured weather data in cases where it is desirable to study the effect of climate and measured weather data is unavailable.

The third research question was whether any parameters are essential to the robustness of the constructions. The study did not reveal any parameters that may be critical to achieving a good performance in the Arctic, as a comparison between the measured data with simulated data produced in Delphin, did not reveal any severe issues. Still, the results indicated that some of the units reacted differently to the boundary conditions than the simulations.

This leads to the conclusion that all the investigated constructions perform acceptably in theory and when meticulously executed. As other studies have shown problems with some of the constructions, these problems are expected to be due to insufficient level of detail in the design or poor quality of the labour. The design, proper instructions, and labour quality are essential to the performance of at least some constructions. Therefore, the need for supervision of the building process, and quality assurance on site are also important findings.

CRediT authorship contribution statement

Naja Kastrup Friis: Writing – review & editing, Writing – original draft, Visualization, Methodology, Formal analysis, Data curation. **Eva B. Møller:** Writing – review & editing, Supervision, Methodology, Conceptualization. **Tove Lading:** Supervision, Project administration, Funding acquisition, Conceptualization.

Declaration of competing interest

The authors declare that they have no known competing financial interests or personal relationships that could have appeared to influence

the work reported in this paper.

Data availability

Data will be made available on request.

Acknowledgements

This research was funded by DTU, DTU Byg, Grønlands Selvstyre, Kommuneqarfik Sermersooq, A.P. Møller Fond and Knud Højgaards Fond.

References

[1] E.B. Møller, T. Lading, Current building strategies in Greenland, E3S Web Conf. 172 (2020), https://doi.org/10.1051/e3sconf/202017219004.
[2] Departementet for Boliger og Infrastruktur, Redegørelse Af Grønlandske Byggematerialer, 2019.
[3] Technical University of Denmark, Om Projektet - ABC - Arctic Building and Construction, 2022 [Online]. Available: https://abc-byg.dtu.dk/om-projektet. (Accessed 5 May 2022).
[4] Indeklima - sundhedsstyrelsen [Online]. Available: https://www.sst.dk/da/Viden/Forebyggelse/Miljoe/Indeklima. (Accessed 19 November 2022).
[5] Statistics Greenland, Greenland in Figures 2022 19 (2022) 36.
[6] M. Kotol, Survey of occupant behaviour, energy use and indoor air quality in Greenlandic dwellings, in: Proc. 5th Int. Build. Phys. Conf. (IBPC 2012), 2012, p. 7. Kyoto, Japan.
[7] I.N.I. As Boligselskabet, Skimmelsvamp." [Online]. Available: http://www.byginfo.gl/media/1124/ini-as-skimmelsvamp.pdf.
[8] J. Helgason, Fugtpåvirkning Af Ydervægge I Grønland, 2017.
[9] M. Kotol, C. Rode, G. Clausen, T.R. Nielsen, Indoor environment in bedrooms in 79 Greenlandic households, Build. Environ. 81 (2014) 29–36, https://doi.org/10.1016/j.buildenv.2014.05.016.
[10] T. Lading, E.B. Møller, Evaluering af unaaq 13-19 BYG R-407 , 2019, BYG R-407 (2019) 54.
[11] N.K. Friis, E.B. Møller, T. Lading, Can collected hygrothermal data illustrate observed thermal problems of the façade? - a case study from Greenland, J. Phys. Conf. Ser. 2069 (1) (2021), https://doi.org/10.1088/1742-6596/2069/1/012071.
[12] E. Jan de Place Hansen, Moisture related challenges in the Greenlandic building sector – results from a survey, J. Phys. Conf. Ser. 2069 (1) (Nov. 2021), 012072, https://doi.org/10.1088/1742-6596/2069/1/012072.
[13] M. Rønberg, Hvordan bygger vi bæredygtigt, når der er 30 graders frost, og alt skal fragtes tusindvis af kilometer? Bygge- & Anlægsavisen, 2021.
[14] K. Seidelin Pedersen, Massiv Mangel På Boliger I Grønland, 2019 [Online]. Available: https://fagbladetboligen.dk/alle-nyheder/2019/januar/massiv-mangel-pa-boliger-i-gronland/. (Accessed 10 March 2020).
[15] J.A. Wille, Chefredaktøren Anbefaler: Halvdelen Af Alle Boliger Skal Renoveres | Sermitsiaq.AG," *Sermitsiaq*, 2022 [Online]. Available: https://sermitsiaq.ag/chefredaktoeren-anbefalerhalvdelen-boliger-renoveres. (Accessed 3 December 2022).
[16] M.W. Ryberg, P.K. Ohms, E. Møller, T. Lading, Comparative life cycle assessment of four buildings in Greenland, Build. Environ. 204 (May) (2021), https://doi.org/10.1016/j.buildenv.2021.108130.
[17] N. Emami, B. Marteinsson, J. Heinonen, Environmental impact assessment of a school building in Iceland using LCA-including the effect of long distance transport of materials, Buildings 6 (4) (2016), https://doi.org/10.3390/buildings6040046.
[18] N.K. Friis, J.E. Gaarder, E.B. Møller, A tool for calculating the building insulation thickness for lowest CO2 emissions—a Greenlandic example, Buildings 12 (8) (2022), https://doi.org/10.3390/buildings12081178.
[19] Green Building Council Denmark, Green building Council Denmark [Online]. Available: https://dk-gbc.dk/. (Accessed 21 November 2021).
[20] K. Peitersen, Bæredygtigt Byggeri Vinder Frem I Grønland, 2022. Business - Review.
[21] Green Building Council Denmark and DGNB, Guide Til DGNB, Green Build. Counc. Denmark, 2021.
[22] Iserit, in: Iserit A/S Opfører Grønlands Første Bæredygtigheds-Certificerede Byggeri I Nuuk, 2022, p. 48.
[23] Direktoratet for Boliger og Infrastruktur, Bygningsreglement, 2006, 2006.
[24] A. Nicolai, J. Grunewald, J.J. Zhang, Recent improvements in HAM simulation tools: Delphin 5/CHAMPS-BES, in: Conf. Proc. 12th Symp. Build. Phys, 2007, pp. 866–876. June 2015.
[25] Fraunhofer Institute for building physics, "WUFI® Mould Index VTT." [Online]. Available: https://wufi.de/en/2017/03/31/wufi-mould-index-vtt/. (Accessed 26 January 2023).
[26] Innovative Sensor Technology, "HYT 221 Digital Humidity and Temperature Module." p. 3.
[27] ISO, Hygrothermal Performance of Building Components and Building Elements – Internal Surface Temperature to Avoid Critical Surface Humidity and Interstitial Condensation – Calculation Methods, ISO 13788, second ed., 2012.
[28] Baumklimatik-Dresden, DELPHIN," 2022. [Online]. Available: http://bauklimatik-dresden.de/delphin/index.php. (Accessed 23 January 2021).
[29] Asiaq, About Asiaq, 2023 [Online]. Available: https://www.asiaq-greenland survey.gl/about-us/. (Accessed 28 February 2023).
[30] Asiaq, Vejret nu, Nuuk city [Online]. Available: http://vejr.asiaq.gl/#/station/Nuuk?tab=META. (Accessed 21 November 2022).
[31] Asiaq, Satellitfoto grønland beta [Online]. Available: https://asiaq.maps.arcgis.com/apps/webap/pviewer/index.html?id=6fda5f51a2824934b11058a9c4d1c34d. (Accessed 21 November 2022).
[32] J.A. Duffie, W.A. Beckman, J. McGowan, Solar engineering of thermal processes, Am. J. Phys. 53 (4) (1985) 382, https://doi.org/10.1119/1.14178, 382.
[33] J. Brozovsky, A. Nocente, P. Rüther, Modelling and validation of hygrothermal conditions in the air gap behind wood cladding and BIPV in the building envelope, Build. Environ. 228 (November 2022) (2023), 109917, https://doi.org/10.1016/j.buildenv.2022.109917.
[34] J. Langmans, S. Roels, Experimental analysis of cavity ventilation behind rainscreen cladding systems: a comparison of four measuring techniques, Build. Environ. 87 (2015) 177–192, https://doi.org/10.1016/j.buildenv.2015.01.030.
[35] J. Falk, K. Sandin, Ventilated rainscreen cladding: measurements of cavity air velocities, estimation of air change rates and evaluation of driving forces, Build. Environ. 59 (2013) 164–176, https://doi.org/10.1016/j.buildenv.2012.08.017.
[36] G.M. Girma, F. Tariku, Experimental investigation of cavity air gap depth for enhanced thermal performance of ventilated rain-screen walls, Build. Environ. 194 (2021), 107710, https://doi.org/10.1016/j.buildenv.2021.107710. October 2020.
[37] S. Vogelsang, H. Fechner, A. Nicolai, Delphin 6 Material File Specification, 2013, Version 6.0.
[38] P. Mukhopadhyaya, M.K. Kumaran, J. Lackey, N. Normandin, D. van Reenen, F. Tariku, Hygrothermal properties of exterior claddings, sheathing boards, membranes, and insulation materials for building envelope design, Therm. Perform. Exter. Envel. Whole Build. 1 (2007) 1–13.
[39] Cembrit, Cembrit windstopper [Online]. Available: https://www.cembrit.com/download/CHDK/datasheets/cembrit-windstopper-basic-datasheet, 2018.
[40] Cembrit, Cembrit multi force [Online]. Available: https://www.cembrit.dk/download/SDK/montagevejledninger/montagevejledning-cembrit-multi-force, 2017. (Accessed 31 January 2023).
[41] F. Tariku, D. van Reenen, M.K. Kumaran, J.C. Lackey, N. Normandin, Summary report from task 3 of MEWS project at the institute for research in construction – hygrothermal properties of several building materials, *Natl. Res. Counc. Canada*, no. March (2002) 71, https://doi.org/10.4224/20386076, 2002.
[42] W. Sonderegger, P. Niemz, Thermal conductivity and water vapour transmission properties ofwood-based materials, Eur. J. Wood Wood Prod. 67 (3) (2009) 313–321, https://doi.org/10.1007/s00107-008-0304-y.
[43] A./S. Rockwool Danmark, FLEXIBATTS 37." [Online]. Available: https://www.rockwool.com/dk/produkter-og-konstruktioner/produktoversigt/bygningsisolering/flexibatts-37/#Tekniskeegenskaber&sortiment. (Accessed 29 November 2022).
[44] Homatherm, Homatherm Produktkatalog, 2015 [Online]. Available: http://2a6616e28592bb9cbad5b4f0860dbb9b88ecc84a.web26.temporaryurl.org/wp-content/uploads/HOMATHERM-produktkatalog-nov-2015.pdf. (Accessed 31 January 2023).
[45] M. Ruiz, V. Masson, M. Bonhomme, S. Ginestet, Numerical method for solving coupled heat and mass transfer through walls for future integration into an urban climate model, Build. Environ. 231 (January, 2023), https://doi.org/10.1016/j.buildenv.2023.110028.
[46] R.J. Hyndman, A.B. Koehler, Another look at measures of forecast accuracy, Int. J. Forecast. 22 (4) (2006) 679–688, https://doi.org/10.1016/j.ijforecast.2006.03.001.
[47] European Centre for Medium-Range Weather Forecasts, "ERA5 | ECMWF." [Online]. Available: https://www.ecmwf.int/en/forecasts/datasets/reanalysis-datasets/era5. (Accessed 17 January 2023).
[48] A. Hukka, H.A. Viitanen, A mathematical model of mould growth on wooden material, Wood Sci. Technol. 33 (6) (1999) 475–485, https://doi.org/10.1007/s002260050131.
[49] N.K. Friis, E.B. Møller, Repository (2023), https://doi.org/10.11583/DTU.21971789.
[50] T. Ojanen, H. Viitanen, R. Peuhkuri, J. Vinha, K. Salminen, Mold Growth Modeling of Building Structures to IMPROVE the MODEL, 2010.
[51] M.W. Ryberg, T. Serrano, E. Møller, T. Lading, Life-cycle assessment of construction errors on buildings in Greenland, IOP Conf. Ser. Earth Environ. Sci. 1085 (1) (2022), https://doi.org/10.1088/1755-1315/1085/1/012064, 66DUMMY.

V. Hygrothermal Conditions in the Façades of Residential Buildings in Nuuk and Sisimiut

Naja K. Friis, Eva B. Møller, and Tove Lading

Building and Environment (2023)
doi: 10.1016/j.buildenv.2023.110686.

V

Building and Environment 243 (2023) 110686

Contents lists available at ScienceDirect

Building and Environment

journal homepage: www.elsevier.com/locate/buildenv

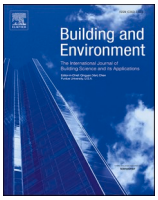

Hygrothermal conditions in the facades of residential buildings in Nuuk and Sisimiut

Naja Kastrup Friis *, Eva B. Møller, Tove Lading

Technical University of Denmark, Brovej 118, 2800, Kgs. Lyngby, Denmark

ARTICLE INFO

Keywords:
Hygrothermal simulations
Arctic climate
Measurements
Façade constructions
Mould index
Membranes

ABSTRACT

The limited documentation of the performance of previous and present building techniques in Greenland confines the basis for optimal design decisions. This study presents hygrothermal data from nine houses in Nuuk and Sisimiut, representing constructions of half-timber, concrete, and cross-laminated timber, all designed with a ventilated air cavity. The temperatures and relative humidity are monitored on the wall's inner side, in the air cavities and on each side of possible implemented wind and vapour membranes. The data are subjected to intercomparisons and compared to simulations from the hygrothermal simulation tool, Delphin. Finally, the measured and simulated data are analysed for the risk of mould growth with the Viitanen model in the free software WUFI Mould Index VTT. It is found that all construction types can function adequately under Greenlandic conditions. It is, however, recommended to be critical when excluding building elements, such as wind barriers, due to the risk of reduced performance of the façade structure. Furthermore, it is found that the mould risk is minimal inside the constructions but to some extent critical in the air cavities; however, the consequences of mould there are limited. Finally, the results are compared to other similar studies.

1. Introduction

1.1. Greenlandic history and building tradition

The construction industry in Greenland has been under rapid development in the last 150 years. Traditionally, people lived in smaller communities and settlements, and even up to the middle of the 19th century, some people lived in peat houses [1]. Originally, the Greenlandic people lived as nomads until the missionaries and the traders began to see advantages in stationary trading posts. This interference caused a change in the way of living, building, and organising society [1]. Since the development of the Greenlandic Technical Organisation (GTO) in 1950, the architectural style has been everchanging, from small wooden standard houses to multistorey concrete buildings [2]. Unfortunately, the evaluation of the implemented building methods has been irregular and inadequate, causing gaps in the knowledge regarding proper building methods in Greenland. When constantly implementing new design solutions on multiple buildings before evaluating the performance, the consequences can be costly, e.g., due to reduced service life, increased heating demand, or extended need for maintenance or renovation.

The development of the Greenlandic building industry has been a hot topic for a long time, both during the period of GTO but also since the disintegration of this organisation (which in 1987 became part of the Greenlandic home rule government under the name Nuna-tek) in 1990 [3]. An example is the report by the Directory of Buildings and Infrastructure, IAPP's, committee regarding the efficiency improvement of the building work from 2002 [4], stating that the initiatives from the prior 20–30 years were meaningful but insufficiently supported by educational and technological initiatives and active knowledge sharing. The committee concluded that the collection and dissemination of construction knowledge should be highly prioritised to improve the building processes. These issues are, however, still addressed today, 20 years later.

1.2. Aim and objectives

This study presents hygrothermal measurements from nine houses in Nuuk and Sisimiut to enable evidence-based decisions on suitable construction types in Greenland. They represent three common construction types [2]: half-timber, concrete, and cross-laminated timber (CLT). The implementation of the measuring sensors, providing the data for this

* Corresponding author.
E-mail address: nfri@dtu.dk (N.K. Friis).

https://doi.org/10.1016/j.buildenv.2023.110686
Received 9 March 2023; Received in revised form 30 July 2023; Accepted 1 August 2023
Available online 2 August 2023

study, is independent of the construction process of the buildings. This condition allows an evaluation of the robustness of the constructions, both regarding design choices and buildability. This circumstance contrasts a previous study [5], analysing the same construction types constructed under controlled conditions and exposed to constant interior climate. The present study aims to contribute to the collected and disseminated knowledge sharing as encouraged by the AIPP committee in 2002, by answering the following research questions with a focus on the three assessed construction types:

1) Does it cause hygrothermal problems not implementing wind barriers in Greenland?

This question has become relevant, as one new construction type does not use a wind barrier. The traditional building style includes a very robust wind barrier (sealed fibre cement boards). This study focuses on the wind barriers' ability to reduce air infiltration of the insulating layers rather than increasing airtightness and eliminating thermal bridges.

2) Are all the assessed constructions robust to the Arctic climate?

In general, constructions used in the Arctic are based on building methods commonly used in milder climates; in Greenland, Danish building methods have been implemented with a few adjustments to Greenlandic conditions. However, these adjustments might not make the constructions robust for an Arctic setting.

These topics are not extensively investigated for the Arctic climate; however, there are some examples of studies evaluating the need for different membranes in cold climates. E.g., Vinha [6] investigated the hygrothermal performance of exterior timber-frame walls for multiple Finnish locations, including one above the Arctic Circle (Sodankylä). It was found that for all Finnish climates, it was safe to implement plastic vapour barriers in wall constructions. Other literature focus on other northern regions. An example is Langmans [7], who studied the feasibility of exterior air barriers in building envelopes at multiple European destinations. The study found that good workmanship and adequate material choices were essential to the airtightness of the building envelope when applying exterior air barriers. The airtightness was essential, as the purpose of the membranes was to reduce leaks in the building envelope.

Despite the existing literature regarding building quality and best practices in Arctic regions, Greenland is further challenged due to insufficient infrastructure, poor economy, and limited access to skilled labour. These limitations result in a need for a specific focus on Greenlandic conditions. However, the findings for Greenland can be applied in other Arctic regions. Therefore, this article aims to collect data from different Greenlandic building technologies and assess their performance, to benefit the construction industry in the whole Arctic region.

The remainder of this article briefly introduces specific challenges and previous projects, followed by a description of the employed methodologies and the context and setup of the monitored residential houses. Lastly, the data is analysed and discussed, leading to a conclusion.

1.3. Arctic building and construction

This study is a part of the research project, Arctic Building and Construction (ABC) project, which aims to identify the issues and good practices in the current construction tendencies in Greenland [8]. The ABC project primarily relies on three Greenlandic data sources. 1) a test house that experiments with sheltered unheated areas between rain screen and insulation, creating semi-indoor zones [9], 2) a test pavilion containing the most typical Greenlandic façade constructions for new constructions [5,10] and 3) hygrothermal sensors in the façades of multiple residential buildings. This study investigates the collected data from most of the monitored residential houses and compares them with results from the test pavilion [5].

As part of the ABC project, a building insulated with a new firm mineral wool insulation type was evaluated because residents complained about thermal discomfort. Theoretically, the insulation batts should eliminate the need for wind barriers when applied tightly to a concrete construction. The material had two perpendicular soft edges (flex zones) to ensure tight connections between the batts. In practice, however, the insulation was installed incorrectly and insufficiently tight, resulting in cold walls, draught, and discomfort [11]. The building was also investigated by Friis et al. [12], showing that the thermal issues could be identified by hygrothermal sensors implemented in the façade. The findings indicated that such measurements are valuable when evaluating façade performances, and similar measurements have been utilised in this study. The building façade is further presented in Section 2.1.

1.3.1. The low-energy house in Sisimiut

In 2005, an experimental building was built in Sisimiut to investigate the performance of low-energy technologies in a Greenlandic context [13]. It was equipped with up to 350 mm of insulation, solar panels, a heat recovery system, and windows with low heat loss and high heat gain. In addition to the innovative installations and design decisions, the house was monitored regarding consumption of heat, hot water, and energy, the effect of the solar panel, room temperatures, and relative humidity in the construction. At the time of construction, the building regulation of 2006 [14], which is still valid in Greenland, was soon to be implemented, and the goal was to create a building which would consume only half of the permitted energy demand.

After five years, the performance was assessed, showing that it did not meet the initial ambitions [15], with an oil consumption of 140 kWh/m^2 compared to the calculated 80 kWh/m^2. According to Rode [15], the main issue was that the actual airtightness of 2.4 $l/(s \bullet m^2)$ was worse than the anticipated 1.5 $l/(s \bullet m^2)$. Still, Greenland has no demand for maximum leakage [14]. However, Rode et al. [16] estimated that poor airtightness alone might cause energy consumption to increase by 20%. The reduced airtightness indicates that the vapour barrier was insufficient, reducing the construction's robustness to the Arctic climate. Due to this and other identified issues, the building was renovated in 2018 and became part of the ABC project. Therefore, it is included in this study with its optimised building envelope, presented in Section 2.1.

1.3.2. Façade membranes in the Arctic

As described in Section 1.3.1, airtightness plays a significant role in the building's heat loss and, thus, its energy consumption. In many cases, the risk of cold air infiltrating the building or insulation can be minimised by implementing wind barriers and ensuring tight material connections. Moisture can also be a severe construction problem and significantly affect the indoor climate – especially when causing rot or mould. Strategic placement of vapour barriers can influence the hygrothermal performance of a building envelope [6]. Langmans [7] found that sufficient airtightness was essential to avoid moisture issues caused by forced convection. The consequences of the presence of these membranes will be investigated in this study.

1.4. Moisture and mould

The moisture content (v) in the outdoor air is often very low in Greenland during winter. According to Kotol et al., it can be less than 1 $g/kg_{dry,air}$. However, cold temperatures can cause high relative humidity (RH) [17] (65%–90% RH in Nuuk 2022 [18]). The moisture excess (Δv) is defined as the difference between the interior and exterior moisture content. Ilomets et al. [19], conducted a field study on 237 dwelling units in cold climates and found an average moisture excess value of 2.8 g/m^3 during cold periods. Furthermore, Δv was defined to be low when it was approximately 2 g/m^3 during winter. Møller and Helgason [20]

evaluated the excess moisture in several buildings on Greenland's west coast and found an average of 3.9 g/m^3. Indoors, dry air can cause static shock and discomfort, such as eye irritation, dry skin, dermatitis causing itch, dehydration, sore throat and asthma [21].

On the other hand, high humidity levels can cause an increased risk of mould growth and elevated concentrations of house-dust mites [22]. Additionally, studies show that high relative humidity increases the risk of activating latent tuberculosis [23]. Still, tuberculosis is 20 times more common in Greenland than other Northern countries [24], with higher indoor relative humidity levels. Despite the low indoor humidity levels, mould is common in Greenlandic buildings. Some building owners try to reduce the mould growth risk by educating the residents on how to use the buildings properly [25] to ensure lower relative humidity. The strong dependency between humidity, mould growth and human health [6] makes mould growth a simple performance criterion for moisture conditions in a building.

2. Methods

This article is based on data collected from 4 houses in Sisimiut and 5 in Nuuk. The collected data are subjected to intercomparisons and comparison to the results of hygrothermal simulations performed in Delphin 6.1 [26]. Furthermore, the hygrothermal conditions from measurements and simulated data are analysed for mould growth risk.

2.1. Monitored buildings

This study includes nine buildings on the west coast of Greenland. Table 1 provides an overview of them. Four were located in Sisimiut (at the Arctic Circle), while the rest were in Nuuk, 300 km south of Sisimiut. The facades were monitored with sensors (see details in Section 2.1.2) measuring the temperature and the relative humidity at different depths in the façade. As given in Table 1, each building had different amounts of data because of the independent installation of the sensors. The monitored walls are oriented inconsistently, defined in the column "Orient". "ID" is the identification number, while "Name" is introduced to ease the understanding through this article. The houses are named depending on their construction types and the location. HT identifies half-timbered façade constructions, and CON and CLT describe concrete and cross-laminated timber constructions. "Type" presents the construction type shortly, "Year" describes the construction year, and "Angle" defines the deviance between the north façade and the north orientation. "Nr" is the number of sensors, and lastly, "Delphin years" lists for which years the individual house is assessed.

The included buildings were selected to represent the current construction tendencies. However, the primary motivation for the selection was the possibility and acceptance of implementing sensors in their facades. Additionally, drawings and descriptions of the constructions were crucial. Certain juristic precautions were necessary, including compliance with GDPR restricting the sharing of additional information about the building's locations.

2.1.1. Façade constructions

The facade constructions of the nine houses presented in Table 1 are shown in Fig. 1. The number of sensors in each wall construction depends on the wind and vapour membranes implemented. In general, the sensors are placed in the air cavity, on the inner side of the wall (measuring the indoor climate) and on each side of potential vapour barriers and wind barriers. This approach results in 3–5 sensors in each wall. The sensors are coloured to match the graphs in Section 3.

House HT_{sis3} is the low-energy house in Sisimiut described in Section 1.3.1, and the detail drawing shows the façade after the renovation in 2005, as the measurements are from the following period.

In the CLT-houses, CLT_{Nuuk1} and CLT_{Nuuk2}, there are wind barriers on the exterior side of the CLT element, primarily to protect the elements from external weather conditions during construction. Kukk et al. [27] concluded that high initial moisture content in CLT panels can reduce the airtightness of CLT elements. Thus, the implemented wind barrier has two ways of contributing to the airtightness of the building, i.e., reducing the risk of cracks and reducing the airflow through leaks. The CLT is produced in Austria, but the architectural material does not define the wood species. However, it is assumed to be spruce, as this wood species is typically used in European CLT.

2.1.2. Sensors

The installed HYT 221 sensors from Innovative Sensor Technology measure temperature with an accuracy of ±0.2 K within the range of 0–60 °C and RH with an accuracy of ±1.8% from 0 to 90% RH. The expected long-term drift is 0.5% RH/year and 0.05 K/year, and the operational temperature is −40 to 125 °C and 0–100% [28]. The data sheet stated that the sensors were calibrated from the factory and therefore were not calibrated as part of this study. Because of the desire to continuously measure the hygrothermal conditions in the walls, the sensors have not yet been removed and calibrated as a final endeavour of the study.

The sensors are installed with the backside towards the membranes, while the simulations provide the conditions near the surface. Optimally, the sensing part should point towards the membrane. Fig. 2 displays two examples of the sensor installation method, which is consistent for all facades. The yellow dot in the black box indicates the sensing part.

2.2. Hygrothermal simulations

The one-dimensional hygrothermal simulations are performed in Delphin 6.1.5 [26], which simulates coupled heat, air and moisture (HAM). Studies have validated the software and shown that the results are similar and consistent to other programs, though minor discrepancies can occur [29,30]. It is necessary to know the composition of the wall structures, the material properties, and the boundary conditions to create the models. The quality of the models was evaluated with Root Mean Square Error, RMSE. The following presents the evaluation method and the relevant details.

Table 1
Presentation of buildings. * Indicates that at least half of the data for the year is missing in at least one orientation. ▪ Indicates the renovation year.

	ID	Name	Type	Year	Orient	Angle	Nr	Delphin years
Sisimiut	3	HT_{sis1}	Concrete w. wind barrier	2012	W	7°	5	2018*, 2021*
	4	CON_{sis}	Concrete wo. wind barrier	2018	NNW, SSE	−25°	3	2020, 2021, 2022
	5	HT_{sis2}	Timber frame	2010	NE, SE	−40°	5	2021, 2022
	13	HT_{sis3}	Renovated timber frame	2018▪	NE	50°	5	2021, 2022
Nuuk	7	HT_{Nuuk1}	Steel frame		SE, NW	40°	5	2021, 2022
	8	HT_{Nuuk2}	Timber and steel frames	2010	NW	40°	5	2021
	9	CLT_{Nuuk1}	Cross-laminated timber		NNW, SSE	−33°	4	2022*
	10	CON_{Nuuk}	Concrete wo. wind barrier	2015	SSW	30°	3	2020, 2021, 2022
	12	CLT_{Nuuk2}	Cross-laminated timber	2016	ESE, WNW	30°	4	2020, 2021, 2022

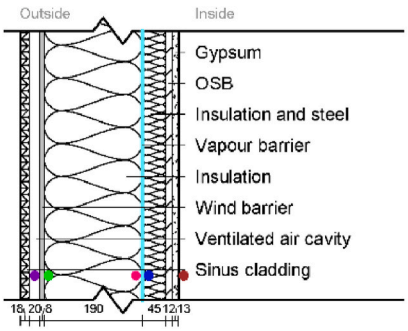

HT_{sis1}

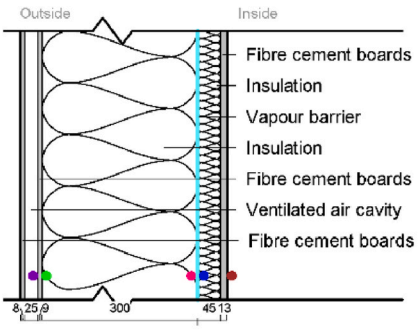

HT_{sis2}

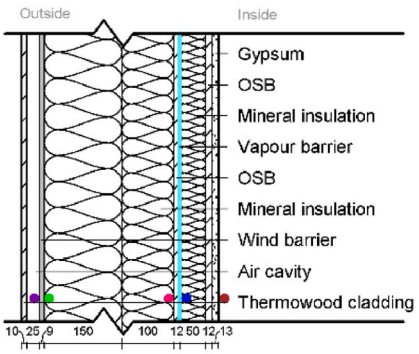

HT_{sis3}

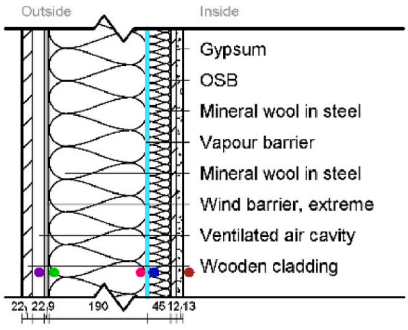

HT_{Nuuk1}

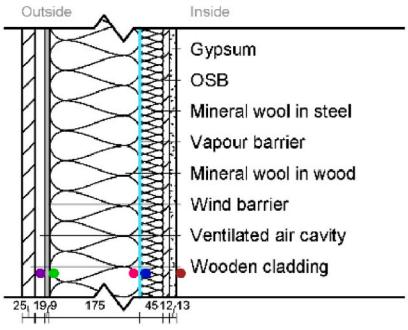

HT_{Nuuk2}

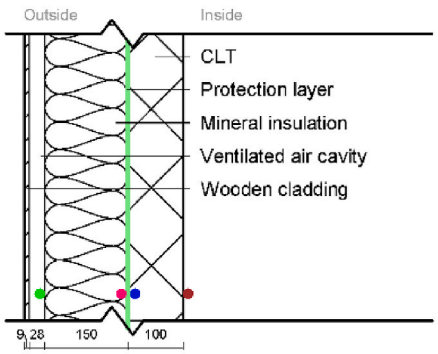

CLT_{Nuuk1}

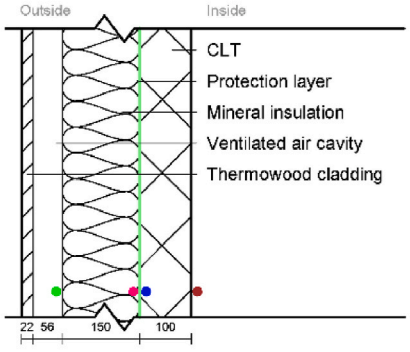

CLT_{Nuuk2}

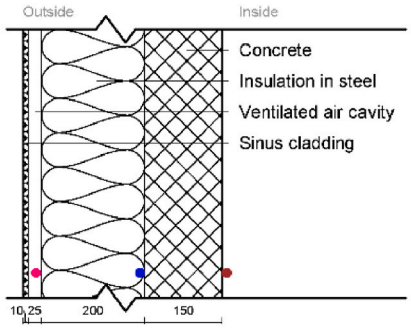

CON_{sis}

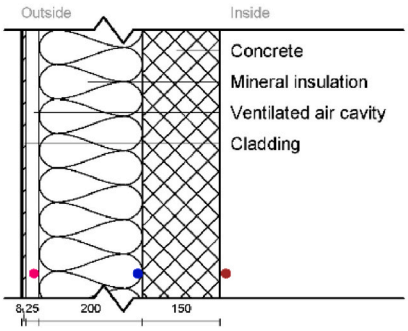

CON_{Nuuk}

Fig. 1. Cross-section drawings of the wall constructions. The dots indicate the placement of sensors, and the colours refer to the graphs in Figs. 4 and 5. (For interpretation of the references to colour in this figure legend, the reader is referred to the Web version of this article.)

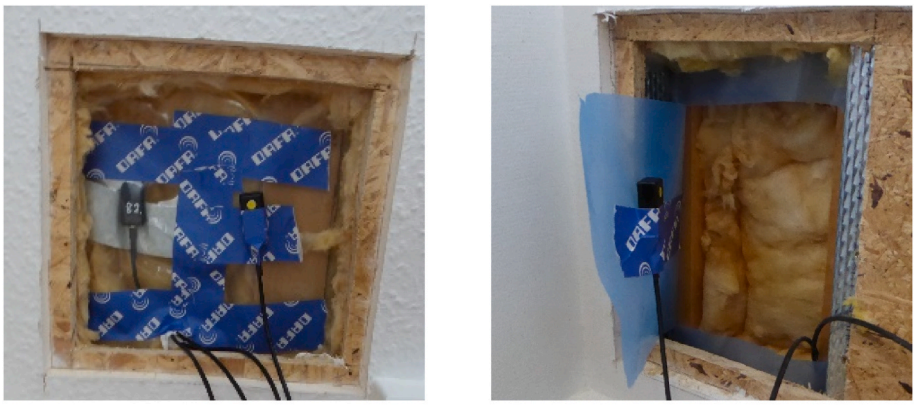

HT_{Nuuk2} HT_{sis1}

Fig. 2. Example of sensor orientation near the membrane. The yellow dot is the sensing part. The membrane to the left has no colour and is transparent. (For interpretation of the references to colour in this figure legend, the reader is referred to the Web version of this article.)

2.2.1. Evaluation method

The accuracy of the models was identified with Root Mean Square Error, RMSE. It is calculated as presented in Eq. (1) and quantifies the error between the measured data, $x_{sensor,i}$, and simulated data, $x_{delphin,i}$. N is the total amount of data points, which are individually denoted by i. The formula is applied on the temperature and relative humidity for each sensor. The aim is to reduce the RMSE by calibrating the models by iterations to achieve the lowest possible errors. The success criteria for RMSE are 5 °C for temperature and 10% RH.

$$\mathrm{RMSE} = \sqrt{\frac{\sum_{i=1}^{N}\left(x_{delphin,i} - x_{sensor,i}\right)^2}{N}} \quad [1]$$

Various evaluation methods have their advantages and disadvantages. The normalised RMSE (NRMSE) is often applied for its more straightforward interpretation as the unit is in percentage. However, normalised errors can magnify the errors for smaller values by removing the scale differences between the outputs [31,32]. In this study, this is a disadvantage since it involves temperature and humidity profiles through the walls, potentially leading to misinterpretation of the errors. Therefore, RMSE was chosen for this purpose. The disadvantages of using RMSE include its high sensitivity to outliers and the fact that error is always positive, neglecting whether the model is overestimating or underestimating [32,33].

2.2.2. Material properties

The quality of a model relies on the accuracy of the material properties. The material properties were assumed to vary as the buildings were constructed independently. The variances were defined during an iterative calibration process for each façade model. The iteration processes were based on RMSE for temperature and relative humidity.

Table 2 contains the settings for all materials for each house. Most materials were found in the Delphin database, but few were unavailable and thus defined manually. The manually defined materials were based on similar materials from the Delphin database (see respective material IDs in superscripted square brackets in Table 2) to ensure reasonable material properties regarding moisture transportation. Asterisks (*) define iterated values, while properties found in other literature and data sheets are noted with references in the specific table cell.

The exterior cladding on House HT_{sis1} and CON_{sis} are sinus-shaped metal sheets. The sectional drawings in Fig. 1 describe the curve sizes, while the material thickness is defined to be only 0.6 mm in the Delphin models. In the other houses, except House HT_{sis2}, thermowood or rough wood is applied as exterior cladding. These are problematic to define precisely due to the lack of descriptions in the available project material and the broad spectre of material properties available for these products. Thus, the material properties were adjusted by calibrating the models based on iterations.

The thermal transmittance, U-value, is calculated for each construction based on the chosen materials. Table 2 presents the essential material properties, but more detailed properties are connected to each material. These can be found in Delphin based on the material ID. The given properties, defined according to the standards in Delphin [34], include density (ρ), specific heat capacity (Cp), thermal conductivity (λ), water vapour resistance (μ), water content at saturation (W_{sat}), water content at 80% RH (W_{80}), water uptake coefficient (A_W), and liquid water conductivity at effective saturation ($K_{l,eff}$). All vapour barriers are defined to have a vapour diffusion thickness (sd) of 20.

2.2.3. Boundary conditions

The hygrothermal simulations demand hourly weather data containing temperature, relative humidity, wind direction, wind velocity, direct radiation, diffuse radiation, rain, and air pressure.

The Danish Meteorological Institute (DMI) [18] provided hourly quality-assured weather data for Nuuk. The data were free of charge but not available for Sisimiut. European Centre for Medium-Range Weather Forecasts, ECMWF, provided hourly reanalysis weather data of the relevant climate variables (ERA5) [38]. Reanalysis is a method to estimate weather conditions in a grid based on multiple surrounding weather stations. These data are also quality-assured and contain none or very few missing data. However, the data are not measured locally but are estimated for a grid structure based on available measured data.

DMI and ERA5 provide global radiation, which is then decomposed into direct and diffuse radiation using the Erbs method [39]. Missing data for solar radiation is filled in two ways. For whole days or multiple days of missing data, they are filled by interpolating the value of the same time of the day from the previous and following available day. For missing data during night-time or where the first and last hour of daylight is measured, the data are filled by interpolating the adjacent values. All other missing data are supplied by interpolation.

Fig. 3 presents selected weather parameters for all considered years. The graphs show a continuous period of missing data in 2020.

The temperature and relative humidity from the internal sensors are used to define the interior climate and are individual for each façade. Missing data are filled by linear interpolation.

For all simulations, the inner heat transmission exchange coefficient for still air was assumed to be 8 W/m^2K, while the vapour diffusion coefficient was set to $1e^{-8}$ s/m. On the exterior sides, the effective heat conduction exchange coefficient, including both convective and radiant heat conduction, was 25 W/m^2K, and the mass transfer coefficient for vapour diffusion was $5e^{-8}$ s/m. The reduction coefficients for wind-driven rain and the solar adsorption coefficient were set to 0.7, which

Table 2
Final material properties for each material in all houses. The U-values are given for each house in the grey headlines.

Material	ρ	Cp	λ	μ	W_{sat}	W_{80}	A_w	$K_{l,eff}$
	Kg/m^3	J/kgK	W/mK	–	Kg/m^3	Kg/m^3	$Kg/m^2s^{½}$	s
House HT_{sis1}. U = 0.15 W/m^2K								
Gypsum [81] 0.013 m	850	850	0.200	10	551	7.2	0.28	$6.3e^{-9}$
OSB [172] 0.012 m	630	1880	0.13	280	350	36.8	0	$8.3e^{-11}$
Insulation [730] 0.045 m	37	840	0.032	1.2*	900	0.1	0	–
Vapour barrier [174] 0.0002 m	1500	2100	0.23	100,000	0	0	0	0
Insulation [648] 0.019 m	168	840	0.040	1.7*	900	0.4	0	–
Fibre cement [265] 0.008 m	1424 [35]	900 [36]	0.24 [35]	20 [37]	419	40	0.01	0
Air cavity 40 mm [17] 0.20 m	1.3	1050	0.138	0.4	1000	0	0	0
Sinus cladding [778] 0.006 m	7700	460	25,000	–	–	–	–	–
House HT_{sis2}. U = 0.09 W/m^2K								
Fibre cement [265] 0.13 m, 0.09 m, 0.08 m	1424 [35,35]	900 [36]	0.24 [35]	20 [37]	419	40	0.01	0
Insulation [731] 0.045 m	67	840	0.035	1	900	0.1	0	–
Vapour barrier [174] 0.0002 m	1500	2100	0.23	100,000	0	0	0	0
Insulation [731] 0.03 m	67	840	0.035	1	900	0.1	0	–
Air cavity 25 mm [16] 0.25 m	1.3	1050	0.138	0.4	1000	0	0	0
House HT_{sis3}. U = 0.12 W/m^2K								
Gypsum [81] 0.013 m	850	850	0.200	10	551	7.2	0.28	$6.3e^{-9}$
OSB [172] 0.012 m, 0.012 m	630	1880	0.130	280	350	36.8	0	$8.3e^{-11}$
Insulation [730] 0.050 m	37	840	0.032	1	900	0.1	0	–
Vapour barrier [174] 0.0002 m	1500	2100	0.230	100,000	0	0	0	0
Insulation [648] 0.1 m, 0.15 m	168	840	0.040	1	900	0.4	0	–
Fibre cement [265] 0.009 m	1424 [35]	900 [36]	0.24 [35]	20 [37]	419	40	0.01	0
Air cavity 25 mm [16] 0.025 m	1.3	1050	0.138	0.4	1000	0	0	0
Thermowood [654] 0.008 m	1158.7	1188	0.313	26.40	283.6	70.9	0.01	$2.5e^{-12}$
House HT_{Nuuk1}. U = 0.15 W/m^2K								
Gypsum [81] 0.013 m	850	850	0.200	10	551	7.2	0.28	$6.3e^{-9}$
OSB [172] 0.012 m	630	1880	0.13	280	350	36.8	0	$8.3e^{-11}$
Insulation [730] 0.045 m	37	840	0.032	1	900	0.1	0	–
Vapour barrier [174] 0.0002 m	1500	2100	0.23	100,000	0	0	0	0
Insulation [648] 0.190 m	168	840	0.040	1	900	0.4	0	–
Fibre cement [265] 0.009 m	1424 [35]	900 [36]	0.24 [35]	20 [37]	419	40	0.01	0
Air cavity 25 mm [16] 0.022 m	1.3	1050	0.138	0.4	1000	0	0	0
Cladding [654] 0.022 m	1158.7	1188	0.313	26.4	283.6	70.9	0.01	$2.5e^{-12}$
House HT_{Nuuk2}. U = 0.15 W/m^2K								
Gypsum [81] 0.013 m	850	850	0.16*	10	551	7.2	0.28	$6.3e^{-9}$
OSB [172] 0.012 m	630	1880	0.13	280	350	36.8	0	$8.3e^{-11}$
Insulation [730] 0.045 m	37	840	0.032	1	900	0.1	0	–
Vapour barrier [174] 0.0002 m	1500	2100	0.23	100,000	0	0	0	0
Insulation [648] 0.175 m	168	840	0.04*	1	900	0.4	0	–
Fibre cement [265] 0.009 m	1424 [35]	900 [36]	0.24 [35]	20 [37]	419	40	0.01	0
Air cavity 40 mm [17] 0.019 m	1.3	1050	0.138	0.4	1000	0	0	0
Cladding [654] 0.025 m	1158.7	1188	0.313	26.4	283.6	70.9	0.01	$2.5e^{-12}$
House CLT_{Nuuk1}. U = 0.19 W/m^2K								
CLT [626] 0.100 m	425	1245	0.120	73	590.2	72.6	0	$9.5e^{-10}$
Wind barrier [28] 0.0001 m	1200	2000	0.145	15,000	2.5	0	0	–
Insulation [731] 0.150 m	67	840	0.035	1	900	0.1	0	–
Air cavity 40 mm [17] 0.028 m	1.3	1050	0.138	0.4	1000	0	0	0
Wood cladding [279] 0.009 m	1250	1100	0.580	80	260	59.5	0	–
House CLT_{Nuuk2}. U = 0.19 W/m^2K								
CLT [626] 0.100 m	425	1245	0.120	73	590.2	72.6	0	$9.5e^{-10}$
Wind barrier [28] 0.0001 m	1200	2000	0.145	15,000	2.5	0	0	–
Insulation [731] 0.150 m	67	840	0.035	1.7*	900	0.1	0	–
Air cavity 56 mm [16] 0.560 m	1.3	1050	0.138	0.4	1000	0	0	0
Cladding [654] 0.022 m	600*	1188	0.2*	26.4	283.6	70.9	0.01	$2.5e^{-12}$
House CON_{sis}. U = 0.17 W/m^2K								
Concrete [569] 0.150 m	2104.2	1000	2.100	76.12	219.9	102.3	0.1	$2.7e^{-10}$
Insulation [731] 0.200 m	67	840	0.035	1	900	0.1	0	–
Air cavity 25 mm [16] 0.025 m	1.3	1050	0.138	0.4	1000	0	0	0
Sinus cladding [778] 0.0006 m	7700	460	25,000	–	–	–	–	–
House CON_{Nuuk}. U = 0.17 W/m^2K								
Concrete [569] 0.150 m	2104.2	1000	2.100	76.12	219.9	102.3	0.1	$2.7e^{-10}$
Insulation [731] 0.200 m	67	840	0.035	1.7*	900	0.1	0	–
Air cavity 25 mm [16] 0.025 m	1.3	1050	0.138	0.4	1000	0	0	0
Cladding [654] 0.0008 m	1158.7	1188	0.313	26.4	283.6	70.9	0.01	$2.5e^{-12}$

is standard for vertical walls in Delphin. Additionally, the grids for simulation are defined based on the standards for Delphin, i.e., minimum 1 mm and maximum 50 mm, with a stretch factor of 1.3. The initial hygrothermal conditions are defined as 20 °C and 50% RH.

2.2.4. Ventilated air cavities

All considered wall constructions have a ventilated air cavity. The air change rate (ACH) in the cavity is problematic to quantify, both theoretically and experimentally. In a similar study, the quality of the Delphin models was found insensitive to this factor [5]; however, it does affect the RMSE in the external layers of the construction. Because of the complexity in quantifying the ACH [40–42] and the varying conditions in this study, the value was iterated within the range from 0 to 650 h^{-1} [43]. The initial setpoint is 60 h^{-1}.

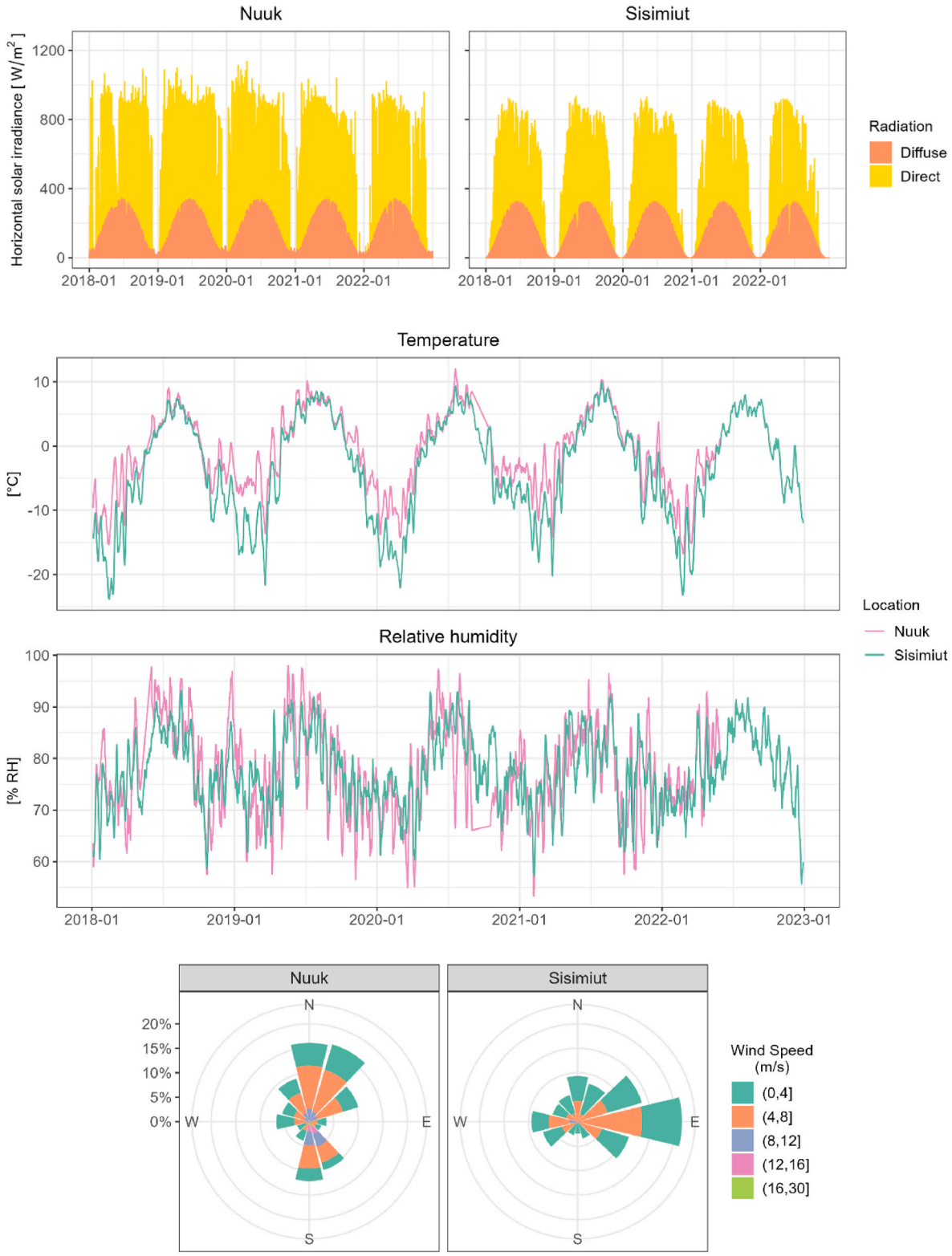

Fig. 3. Weather data for Nuuk (DMI) and Sisimiut (ERA5) for the time of sensor data from the nine houses.

2.3. Mould index and evaluation of membranes

According to SBI 277, the risk of mould growth depends on the amount of moisture, the temperature, the availability of nutrition and time. The growth risk is high for temperatures between 20 and 30 °C, and the critical level for wood is 75% RH and higher for other materials [44].

Based on the measured conditions for each sensor point, the mould growth risk was determined for all evaluated facades by using the Viitanen model [45], which is the underlying method in the software "WUFI Mould INDEX VTT 2.3" [46]. Additionally, three houses (one of each construction type) in Nuuk were picked to investigate the consequences of present and absent membranes. Four scenarios were set up and analysed:

1. Applied wind barrier but no vapour barrier.
2. Applied vapour barrier but no wind barrier.
3. No membranes.
4. Both membranes.

In the Viitanen model, the nutrition level for potential mould is defined as the sensitivity of a material. The available sensitivity classes are "very sensitive", "sensitive", "medium-resistant", or "resistant" [47]. The "very sensitive" predefined pine sapwood material was selected for the general assessments. This property reflects the worst-case scenarios, as some exposed materials are less sensitive. An additional assessment has been made to match the actual conditions for these layers.

The mould growth rates are indexed from 0 to 6, where 0 equals no growth. Indexes 1 and 2 are used for small amounts or several local colonies on a microscopic level, while indexes 3 and above are used for visually present or large amounts of microscopic mould [47]. The mould growth index inside constructions is acceptable if it is below 2. As mould growth is one of the first indications of biological deterioration, it is an excellent hygrothermal performance criterion [48].

3. Results and analysis

This section presents the most important results and visualisations from the assessments performed according to Section 2. Additional graphs and data can be found in the repository [49].

3.1. Visual assessment of measured data

The graphs in Fig. 4 present the measured data for each house as a moving mean of 7 days. The graphs are provided to give an overview of the quantity of collected data points, which varies for each building, and in some cases, for each orientation due to technical circumstances. Each orientation's interior climate is unique as the sensors are placed in different rooms. Larger versions of the graphs are presented in the repository [49].

Unfortunately, the amount of data for HT_{sis1} is minimal due to technical issues disrupting the constant logging. Despite the missing data, it was included to represent the west-oriented half-timber facades in Sisimiut. The graphs for HT_{sis1} show that the temperatures are almost identical on both sides of the wind barrier (s3 and s4), while the relative humidity decreases considerably on the inner side of this construction element.

For HT_{sis2}, there are more available data points for the SE than NE orientation. In the SE orientation, the relative humidity in the external layers is generally higher in SE than in NE. On the other hand, the temperatures are higher in the internal layers in NE to SE. However, the interior climates are very similar for both orientations.

The fact that the temperature in s2 is higher than in s1 in $HT_{sis2[SE]}$ indicates that at least one of the sensors has drifted or that the error of the sensors exceeds the temperature difference at the two measurement points. There is no obvious explanation for the warmer temperatures on the exterior of the thin vapour barrier, which has a relatively high thermal conductivity, λ.

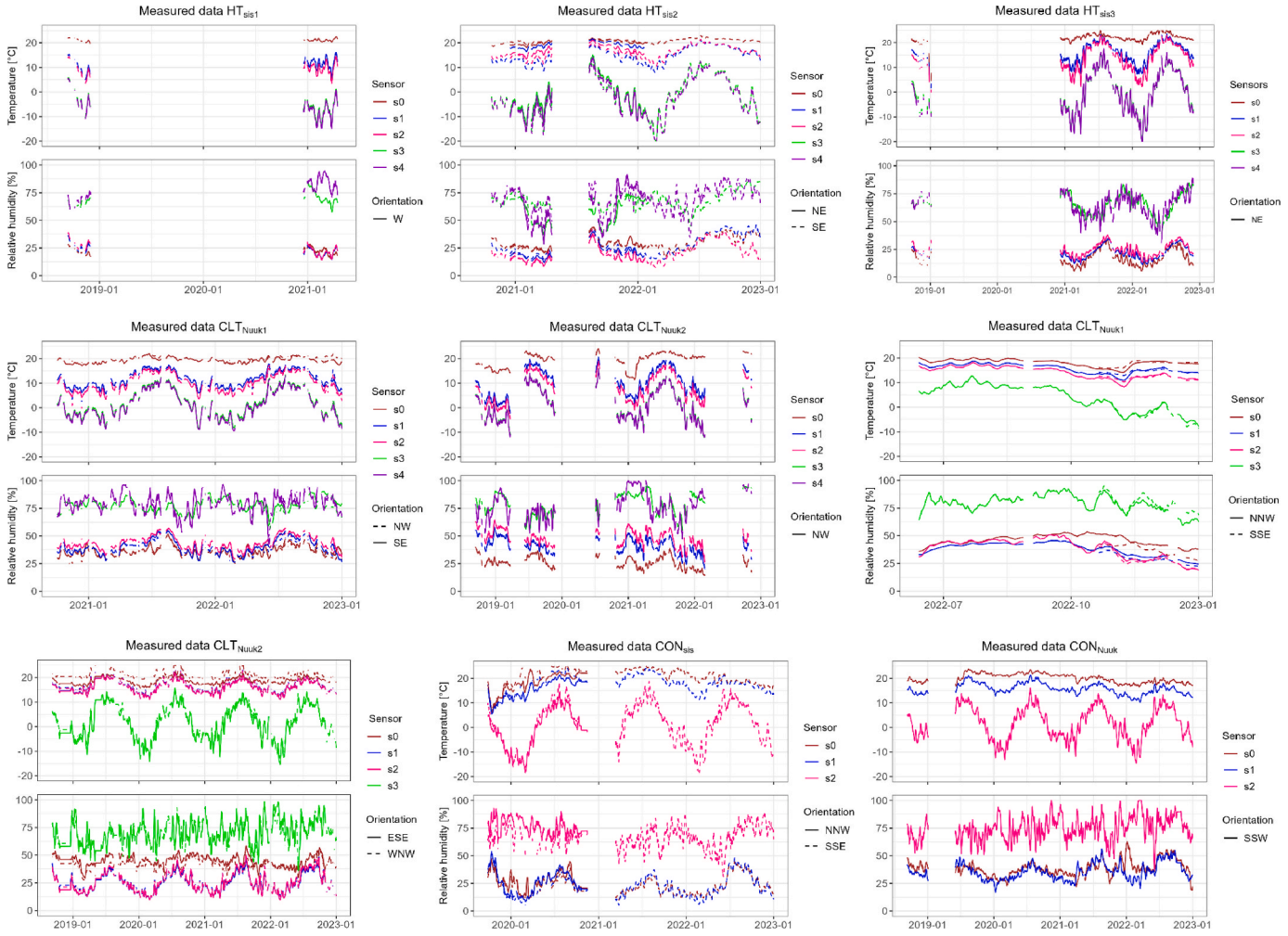

Fig. 4. Presentation of all measured data for each building, including temperature and relative humidity. All graphs are displayed for moving mean values of 7 days.

Fig. 5. Comparison of the measured hygrothermal conditions and the results of Delphin models for selected houses, orientations, and years. All graphs are displayed for moving mean values of 7 days.

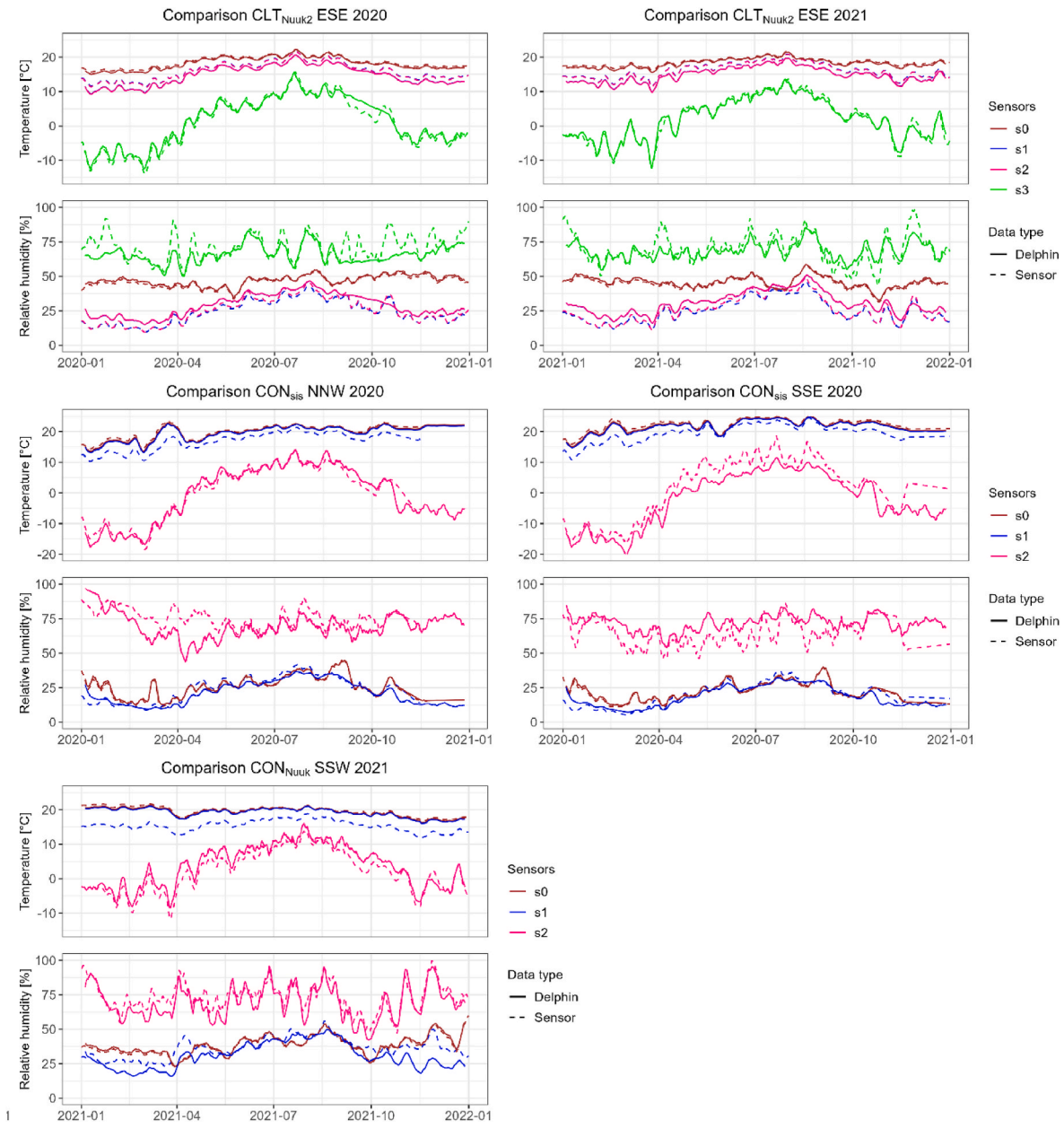

Fig. 5. (*continued*).

The conditions in HT_{Nuuk1} are very similar for both orientations, making it difficult to see the lines for NW in the graphs. The interior temperatures in HT_{Nuuk2} vary more than in the other buildings. At one point in spring 2021, the room temperature drops while the relative humidity increases to 100%.

In CLT_{Nuuk2}, the interior conditions are very different in ESE and WNW, but it does impact the conditions in the wall construction.

For the short periods in CON_{sis}, where multiple orientations are logged, the temperature and RH are similar for both orientations. The interior temperatures are, however, a bit low at the beginning and end of the measured period. In the graph for CON_{Nuuk}, the temperature difference between s0 and s1 is larger than in CON_{sis}.

Based on the graphs in Fig. 4 presenting all measured data, specific years for each house are chosen for simulations. Representative years are chosen, considering those with fewer missing data. For houses with multiple orientations, years with available data from both orientations are selected.

3.2. Comparison of measured and simulated data

3.2.1. Visual comparison

The graphs in Fig. 5 show the moving means of 7 days of the measured data compared to the simulated data produced in Delphin. The figure contains graphs for selected years and orientations, but all produced graphs can be found in the repository [49]. A general observation is that the temperature gap between s1 and s2 in constructions with vapour barriers (all five half-timber constructions) is more significant for the measured data than the simulated data. The reason for this can be traced back to the orientation of the sensing part of the sensors, which, on both sides, are installed with the backside towards the membrane, see Fig. 2. This method creates a longer distance and, thus, an increased temperature difference between the two sensors.

In $HT_{Nuuk1[NW]}$, however, the difference is more significant all year, which is also presented later by the RMSE in Table 3. All other half-timber constructions are graphically evaluated for 2021. For $HT_{sis3[NE]}$, $HT_{Nuuk1[SE]}$, and $HT_{Nuuk1[NW]}$, the tendencies are the same for 2021

Table 3
RMSE of all simulated models. Yellow cells exceed the defined success criteria. Grey cells indicate sensors, which are suspected of drifting.

	Year	RMSE of Temperature [°C]					RMSE of RH [% RH]					RMSE of RH (mm of 7 days) [% RH]					NA's	ACH [h^{-1}]
		S0	S1	S2	S3	S4	S0	S1	S2	S3	S4	S0	S1	S2	S3	S4		
Sisimiut (ERA5 weather data)																		
$HT_{sis1[W]}$	2018	0.5	4.4	5.7	8.7	8.8	1.0	8.5	10.6	5.6	9.8	0.8	5.7	9.8	5.1	8.0	7877	60
$HT_{sis1[W]}$	2021	0.5	4.7	6.2	8.2	8.5	0.9	9.7	8.9	6.5	13.3	0.5	7.5	8.1	5.7	11.9	6252	60
$HT_{sis2[NE]}$	2021	0.3	2.5	1.0	5.5	5.4	1.1	13.0	9.1	22.3	20.1	0.4	11.6	4.4	22.2	16.0	2479	90
$HT_{sis2[SE]}$	2021	0.3	3.6	2.1	3.2	3.6	1.1	11.5	9.3	8.7	13.1	0.4	9.6	2.1	6.9	6.2	2479	120
$HT_{sis2[SE]}$	2022	0.3	2.5	1.4	2.8	3.1	1.1	9.5	8.0	7.2	14.3	0.4	7.9	1.6	5.9	8.4	3	120
$HT_{sis3[NE]}$	2021	0.5	2.3	4.3	3.1	3.6	0.7	8.4	5.7	8.1	16.3	1.2	6.0	4.4	7.1	9.8	3	60
$HT_{sis3[NE]}$	2022	0.5	2.4	4.3	3.4	3.8	0.7	7.7	6.1	9.0	16.3	1.1	5.6	4.9	8.3	9.9	748	60
$CON_{sis[NNW]}$	2020	0.7	2.6	4.9	–	–	1.6	4.8	17.5	–	–	0.9	3.8	10.2	–	–	1836	60
$CON_{sis[SSE]}$	2020	0.7	2.4	7.1	–	–	1.3	4.3	19.2	–	–	0.9	3.3	10.8	–	–	2379	160
$CON_{sis[SSE]}$	2021	0.7	2.4	7.2	–	–	1.2	4.0	18.4	–	–	0.8	2.9	9.2	–	–	1732	160
$CON_{sis[SSE]}$	2022	0.7	2.9	6.2	–	–	1.3	4.5	18.4	–	–	0.8	2.8	10.8	–	–	84	160
Nuuk (DMI weather data)																		
$HT_{Nuuk1[SE]}$	2021	0.7	4.0	5.4	5.3	5.5	4.9	8.4	14.5	10.6	17.0	0.8	4.6	10.6	9.3	10.5	44	30
$HT_{Nuuk1[NW]}$	2021	1.3	5.8	7.6	3.3	3.5	4.5	7.1	15.1	7.1	14.3	0.8	3.3	13.6	5.6	9.2	286	30
$HT_{Nuuk1[SE]}$	2022	0.4	3.1	4.3	3.4	3.3	1.5	8.1	13.1	9.9	14.7	0.8	3.7	10.8	9.2	9.1	11	30
$HT_{Nuuk1[NW]}$	2022	0.5	5.1	6.9	1.4	1.4	1.6	6.9	14.3	5.9	13.1	0.7	2.1	12.5	5.1	9.4	130	30
$HT_{Nuuk2[NW]}$	2021	0.9	4.4	6.6	4.6	4.7	5.6	12.0	20.0	14.5	20.4	3.8	9.6	18.6	13.6	17.8	291	15
$CLT_{Nuuk1[NNW]}$	2022	0.4	1.0	0.9	2.0	–	1.1	2.9	2.8	9.8	–	0.9	2.6	2.2	3.6	–	3842	160
$CLT_{Nuuk1[SSE]}$	2022	0.4	1.0	1.0	2.9	–	1.1	2.6	2.8	12.0	–	0.9	2.1	2.2	6.7	–	4512	400
$CLT_{Nuuk2[ESE]}$	2020	0.4	1.0	0.9	2.0	–	1.1	2.9	2.8	9.8	–	0.9	2.6	2.2	3.6	–	12	90
$CLT_{Nuuk2[WNW]}$	2020	0.4	1.0	1.0	2.9	–	1.1	2.6	2.8	12.0	–	0.9	2.1	2.2	6.7	–	65	180
$CLT_{Nuuk2[ESE]}$	2021	0.4	1.4	1.4	3.6	–	1.9	6.3	6.1	14.4	–	1.2	5.2	4.6	8.3	–	49	90
$CLT_{Nuuk2[WNW]}$	2021	0.5	0.9	0.7	2.9	–	1.6	4.2	4.2	12.7	–	1.2	2.9	2.8	6.7	–	96	180
$CLT_{Nuuk2[ESE]}$	2022	0.4	1.3	1.3	3.1	–	1.9	6.6	6.4	12.3	–	1.1	6.0	5.3	6.4	–	24	90
$CLT_{Nuuk2[WNW]}$	2022	0.5	0.9	0.7	2.4	–	1.6	4.1	4.0	10.4	–	1.2	3.1	3.0	5.3	–	86	180
$CON_{Nuuk[SSW]}$	2020	0.5	1.1	1.1	3.0	–	1.9	5.2	5.1	–	–	1.2	4.6	3.9	–	–	18	30
$CON_{Nuuk[SSW]}$	2021	0.6	1.0	0.7	2.3	–	1.6	3.7	3.5	–	–	1.2	2.3	2.1	–	–	254	30
$CON_{Nuuk[SSW]}$	2022	0.5	4.5	5.4	5.9	–	1.9	9.3	18.2	–	–	1.0	8.5	12.3	–	–	485	30

and 2022. Delphin simulates a higher RH than measured at s3 and s4 in $HT_{sis3[NE]}$ and $HT_{Nuuk1[SE]}$. For all three facades, the measured temperatures in s1 and s2 are lower during winter than in the simulations. HT_{sis1} is not visualised due to the high number of missing data (see Fig. 4). For HT_{sis2}, the Delphin model resembles the wall facing SE more closely than NE, as the measured RH in the air cavity in the latter is much lower than the simulated values.

The graphs for CLT_{Nuuk2} are only presented for the 2020 and 2021 ESE orientation, as the tendencies are the same for WNW during all three assessed years. The graphs for 2020 are more inaccurate and have a bigger RMSE, which is presented in Table 3. The graphs for CLT_{Nuuk1} are excluded due to the well-fitted models, indicating that the wall performs as expected. The excluded graphs can be found in the repository [49].

CON_{Nuuk} is represented for the year 2021, where the humidity level in s1 is lower in the measured data than in the simulation. CON_{sis} is represented for 2020, showing that the simulation of RH is generally a bit low for NNW and a bit high for SSE, which might be a consequence of the temperature simulation being lower than the measured data in SSE. Generally, the model fits better to the measurements from CON_{sis} than from CON_{Nuuk}, despite the very similar constructions and thus similar models.

3.2.2. Root mean square errors

As explained in Section 2.2.1, RMSE is used to determine the accuracy of the simulations. Eq. (1) calculates the RMSE, and the results are presented in Table 3. The yellow cells indicate the errors, exceeding the defined success criteria of 5 °C for temperature and 10% for RH. Regardless of the weather data source and location, a general observation is that the layers close to the exterior climate perform worse than the interior layers. Additionally, the models are better fitted to temperature than to RH. This difference might partly be because the temperature development through the façade is adjusted by the thermal conductivity, λ, alone, while multiple parameters define the moisture conditions. The relative humidity also depends on the temperature, as hot air can contain more moisture than cold air. The last two columns in Table 3 describe the number of missing data (NAs) and the final air change rate (ACH) in the ventilated air cavity in the model. As the RMSE evaluation method is sensitive to outliers [33], the error for RH is also given for the 7-day moving mean to indicate how well the model follows the measured trends. The south-facing walls in Sisimiut generally have a higher ACH than the remaining orientations at this location, but there is no similar tendency for Nuuk.

The RMSEs for moving means of relative humidity are generally much lower than for the original measured and simulated data, especially in the exterior layers, close to the climate conditions, which vary more than the relatively stable interior climates.

The previous study, presented in Section 1.3 [12], found that CON_{Nuuk} did not perform acceptably, as the temperatures at s1 were very low. However, the RMSE at s1 was within the defined limitations. This discrepancy emphasises the value of including multiple indicators, e.g., statistical errors and visualisations, to identify potential issues. When comparing the error for CON_{Nuuk} at s1 with the remaining constructions, other measured data might also be critical or deviate from the simulated data. Especially the half-timber constructions including $HT_{Nuuk1[SE]}$, $HT_{Nuuk1[NW]}$, $HT_{Nuuk2[NW]}$, and $HT_{sis1[W]}$ show deviations. This observation is stressed by the graphic visualisations in Fig. 5. The RMSEs for relative humidity in $HT_{Nuuk2[NW]}$ and $HT_{sis2[NE]}$ are very high. For HT_{sis2}, the errors for the NE are larger than for the SE orientation, both regarding RMSE and visually. In $HT_{Nuuk2[NW]}$, the errors are also large for the temperatures, which might affect the relative humidity results.

3.3. Mould indexes and membranes

The mould growth indexes are calculated to identify the robustness of the constructions for the Arctic climate. Of the nine houses, HT_{sis1}, HT_{sis2}, HT_{Nuuk1}, CLT_{Nuuk1}, and HT_{sis3} are equipped with both a vapour barrier and wind barrier, while HT_{Nuuk2} and CLT_{Nuuk2} are equipped with only a wind barrier, and CON_{sis} and CON_{Nuuk} have no membranes at all.

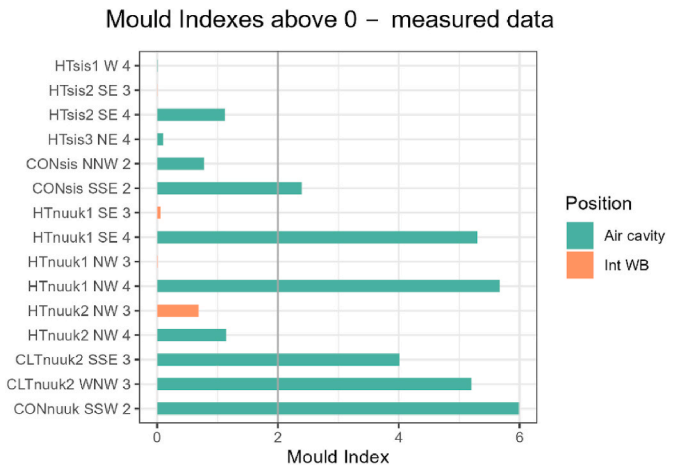

Fig. 6. Mould indexes above 0 for all measured data from the first to the last data point, with material class "very sensitive".

Despite the "very sensitive" applied sensitivity level, most mould indexes simulated with WUFI were 0, equal to no risk. Fig. 6 presents all the sensor points where the mould index was above 0. The blue vertical line indicates the threshold of 2 for an acceptable mould index. Common for all critical indexes is that the sensor point is either inside the air cavity or on the internal side of the wind barrier. According to Wang et al. [50], the risk of mould growth in a ventilated air cavity is reduced because of the constant airflow. The number of available data can impact the results, and Fig. 4 and Table 3 show the missing data for each house. One year consists of 8760 measurements, except the leap year 2020, consisting of 8784 measurements. The missing data were interpolated to create a continuous series of measurements for at least one year, which is necessary to simulate with the WUFI software.

In HT_{Nuuk1}, the mould indexes are zero at all sensor positions in the NE-facing façade, while there is a higher risk in the SE-facing façade, both in the air cavity and on the interior side of the wind barrier. None of the indexes in HT_{Nuuk1} exceeds the critical level of 2. In $CON_{Nuuk[SSW]}$, only the air cavity was at risk for mould growth; however, it was severely high.

Based on the results from Fig. 6, the number of missing data, and the interest in testing each construction type, $HT_{Nuuk1[SE]}$ (2022), $CON_{Nuuk[SSW]}$ (2021), and $CLT_{Nuuk2[ESE]}$ (2021) were chosen for the four test scenarios presented in Section 2.3. The original structure of HT_{Nuuk1}, including both membranes, is equal to Test 4, while the initial construction for CON_{Nuuk}, excluding both membranes, is equal to Test 3. The initial construction for CLT_{Nuuk2} is equal to Test 1, as it includes only the wind barrier. All initial test formats are visualised with grey cells in Table 4. For both $CON_{Nuuk[SSW]}$ and CLT_{Nuuk2}, extra membranes are implemented. New sensor names are introduced in Table 4 to keep the original connection between sensor numbers and positions. For $CON_{Nuuk[SSW]}$, "1x" describes the new sensor point on the exterior side of the implemented vapour barrier, and "2i" is the sensor point on the inner side of the implemented wind barrier. "1i" describes the interior side of the implemented vapour barrier in CLT_{Nuuk2}. The red values indicate mould indexes above 2, and the values in brackets are the indexes for the measured data. All mould indexes are calculated for a period equal to the measured period. As described in Section 2.3, the mould indexes are generally calculated for the "very sensitive" material class to identify the worst-case scenarios. For the assessments of the barriers, the indexes were also calculated for medium-resistant sensitivity in layers where the materials were fit for this definition (excluding points with no risk at higher sensitivity classes). The results for medium-resistant sensitivity are presented superscripted after an asterisk (*) in Table 4. In the air cavity of HT_{Nuuk1}, the battens keeping the cladding in place are made of raw wood. Therefore, the sensitivity is not reduced in this layer.

Table 4
Mould indexes for test scenarios in the constructions of $HT_{Nuuk1[SE]}$, $CON_{Nuuk[SSW]}$, and $CLT_{Nuuk2[ESE]}$. Brackets contain the index for measured data. Red numbers exceed the accepted index of 2. The durations vary according to the number of measured data to make the indexes comparable. Asterisks (*) followed by numbers are results for the medium-resistant sensitivity class due to the absence of wood. $HT_{Nuuk1[SE]}$ is a steel construction.

Wind barrier			+	–	–	+
Vapour barrier			–	+	–	+
	Position		Test 1	Test 2	Test 3	Test 4
$HT_{Nuuk1[SE]}$	Int VB	1	0.0	0.0	0.0	0.0 (0.0)
	Ext VB	2	–	0.0	–	0.0 (0.0)
	Int WB	3	$3.8^{*0.04}$	–	–	$3.7^{*0.04}$ (0.1)
	Air cavity	4	5.4	5.4	5.4	5.4 (5.3)
$CON_{Nuuk[SSW]}$	Int VB	1	0.0	0.05	0.0 (0.0)	0.0
	Ext VB	1x	–	0.0	–	0.0
	Int WB	2i	$0.04^{*0.0}$	–	–	$0.1^{*0.0}$
	Air cavity	2	$5.3^{*0.018}$	$5.4^{*0.021}$	5.4 (6.0) $^{*0.02}$	$5.3^{*0.018}$
	Outside	3	$6.0^{*0.026}$	$6.0^{*0.029}$	6.0 (6.0) $^{*0.029}$	$6.0^{*0.027}$
$CLT_{Nuuk2[ESE]}$	Int VB	1i	–	0.0	–	0.0
	Ext VB/ Int WB	1	0.0 (0.0)	0.0	0.0	0.0
	Ext WB	2	0.0 (0.0)	–	–	0.0
	Air cavity	3	$0.1^{*0.002}$ (4.0)	$0.1^{*0.002}$	0.0	$0.1^{*0.002}$

However, if the battens were in a more mould-robust material, leading to a medium-resistant layer, all four tests would result in a mould growth index below 0.1.

When examining the measured data for $HT_{Nuuk1[SE]}$, the risk for mould growth is only present around the wind barrier. However, according to the simulations, there is a minimal risk (less than 0.0) adjacent to the vapour barrier in the original construction (Test 4). In scenarios without a wind barrier, the mould index is zero at s1, but overall, the risk levels are similar for all membrane combinations.

With two exceptions, the indexes for the simulated constructions closely resemble those for the measured data. Firstly, s3 in the air cavity of $CLT_{Nuuk2[ESE]}$, the simulations are less exposed to risk than the measured data and secondly, s3 on the inner side of the wind barrier in $HT_{Nuuk1[SE]}$, where the situation is opposite. Implementing either a vapour membrane, a wind barrier, or both does not indicate that the mould risk could be decreased significantly.

4. Discussion

4.1. Results

The visualisations of the collected data presented in Fig. 5 and the RMSEs in Table 3 show that the models are of varying quality. Due to the similar construction types, orientations and years, the data can be used to assess the considered facades' robustness and durability. In some cases, the deviances can be justified with uncertainties. E.g., the errors for two independent façade constructions in Nuuk were generally highest in 2020, which might be caused by the reduced weather quality of the data from DMI for that specific year. In other cases, such connections are not identified, creating a foundation for discussing the façade performance. This section discusses the observations, while the uncertainties and limitations are addressed in Section 4.2.

Despite the close resemblance of the hygrothermal conditions in the two facades of HT_{Nuuk1}, slight variations were observed in the mould indexes presented in Fig. 6. In spring 2021, there was a temperature

drop in the interior climate of $HT_{nuuk2[NW]}$, affecting the entire wall construction and causing the relative humidity to reach 100% in the air cavity. Comparing the two half-timber constructions (HT_{Nuuk1} and HT_{Nuuk2}), it was found that the mould index was higher at s3 for $HT_{Nuuk2[NW]}$ than for the facades in HT_{Nuuk1}. On the other hand, HT_{Nuuk2} exhibited the least critical mould index in the air cavity (s4). This discrepancy suggests that the temperature drop in the $HT_{nuuk2[NW]}$ construction might have contributed to the increased mould index.

4.1.1. Mould indexes

Mould indexes larger than 1 were found only on the exterior side of the wind barrier, as illustrated in Fig. 6. The air cavity is comparable to an outdoor environment, and mould outdoors is usually not considered a problem [51]. Consequently, the risk of indoor climate problems due to mould in this position remains low, even when the mould index is high. Thus, a threshold value of 2 may be too strict. However, mould in the air cavity might cause deterioration and reduced durability of the adjacent materials [51].

In the context of half-timber houses, the mould indexes observed in Sisimiut were generally lower than in comparable houses in Nuuk, suggesting that the climate in Nuuk is more conducive to mould problems than in Sisimiut. This finding is supported by the test pavilion study, where similar constructions were assessed and simulated for both climates [5]. The results were reversed for concrete façades. In $CON_{Nuuk[SSW]}$, the mould index in the air cavity was 6, while in Sisimiut, it remained below 1 in $CON_{sis[NNW]}$ and 2.4 in $CON_{sis[SSE]}$. As the interior climates and the constructions are very similar for the two concrete houses, the explanation must be found in the varying climates or the labour quality in the construction phase. These results also show that the concrete façades exposed to direct sunlight are at greater risk of mould growth.

Unfortunately, there were no CLT houses in Sisimiut to compare to the CLT houses in Nuuk. The two CLT houses in Nuuk performed differently, as CLT_{Nuuk1} does not have any indexes above 0, while the air cavities in CLT_{Nuuk2} oriented to the ESE and WNW measured 4 and above 5, respectively. As the façades of CLT_{Nuuk1} were oriented towards NNW and SSE, it does not seem to relate to the orientations. A Norwegian study [51] found that the risk of mould growth in tall buildings was more related to the vertical sensor location than the orientation of the facades. In this study, however, the sensor placement was not considered.

The mould indexes in Fig. 6 and Table 4 showed that the presence of vapour and wind membranes did not significantly impact the risk of mould growth. A wind barrier can, however, increase airtightness and thus possibly reduce heat loss and increase surface temperatures. This finding is coherent with the findings in a Finnish study [7], identifying that it is safe to implement plastic vapour barriers in façades in cold climates. Unless the mould index of 2 should be a threshold value, even externally to a wind barrier, there is no indication of mould problems in any assessed construction type. Consequently, there is no ground for deeming any of the constructions unsuited for the Arctic climate; they all seem to have the needed robustness.

4.1.2. Labour quality

Despite the concluded robustness of the wall constructions, there is one more perspective to discuss: the importance of labour quality. The primary indicator of this problem is the concrete constructions, which are almost identical but relate very differently to the respective hygrothermal simulations and the risk of mould growth. They are located in different cities, and the one in Nuuk performs worse. The weather conditions in Fig. 3 show that the climate is colder in Sisimiut than in Nuuk, while the winds are often stronger in Nuuk than in Sisimiut. Thus, the issue seems to be related to the wind conditions. In the study of Vinha [6], focusing on external wind barriers, the labour quality and material choices were found essential to the airtightness of the constructions. Comparing the errors and hygrothermal conditions with the similar constructions evaluated in Ref. [5], it is clear that the constructions in this study perform worse than in a test facility meticulously constructed. This observation emphasises the essence of labour quality in the performance of the facades.

4.2. Limitations and uncertainties

In a field study of this nature, numerous factors cause uncertainties. This section aims to outline those potentially affecting the results and imposing limitations to the study.

4.2.1. Material properties

As described in Section 2.1, the sensors, which measure the fundamental data for this study, were installed after the houses were built. Even though the responsible companies have provided building project information for this study, there are many unknown details about the implemented materials, possible last-minute solutions, and project changes. Most materials were only specified generally, such as “insulation” or “OSB-board”, which leaves an extensive range of material properties to fit the description. The lack of information is a significant uncertainty to the quality of the Delphin models, despite the attempt to account for it by calibrating the material properties through iterations.

4.2.2. Model fitting and initial conditions

When fitting the models, there are endless opportunities for adjustments. It creates uncertainty that the model is based on and fitted to exact data, as these could be unexpected or faulty due to, e.g., drifting sensors or inadequate construction work. Nevertheless, in this study, the property adjustments are made within realistic limits found in literature or datasheets. Conclusively, the comparison only reveals whether the hygrothermal conditions are realistic or likely to occur for the individual construction type.

The initial conditions were set to 20 °C and 50% RH for all models. It is an uncertainty with little impact on the RMSE because of the relatively short period (approximately two weeks) until equilibrium with the dynamic boundary conditions from the interior and exterior climates. It was found sufficiently precise for this purpose, though it can be eliminated by simulating for two continuous years.

4.2.3. Sensors

As described in Section 2.1.2, the sensors are positioned to measure the hygrothermal conditions on the side opposite the membranes. It implies that they record the conditions in the air or material adjacent to the membrane instead of those directly on the membrane surface. Acknowledging this uncertainty when comparing the Delphin model results with the measurements is essential. For future field studies, it is recommended to reorient the sensors to measure as close to the membrane as possible.

Another uncertainty regarding the sensors is their tendency to drift, particularly in humidity measurements. Ideally, the sensors should be removed from the buildings after data collection for calibration and adjustments for any discrepancies in the data. However, this process presents multiple disadvantages and challenges. Firstly, it would end all measurements, though the observations from future climatic phenomena might be valuable. Secondly, it is time-consuming and expensive, requiring labour to pull out the sensors and expenses for transportation and salary.

In the results of this study, only one indication of drift was observed, specifically in $HT_{sis2[SE]}$. The suspicion is based on the temperatures being higher on the exterior side of the vapour barrier than on the inside. However, there is a possible alternative explanation. The sensor datasheet [28] describes a margin of precision, meaning that if the two temperatures were relatively close, and the internal sensor measured lower while the external sensor measured at the higher end of the margin, this could cause the observed results.

4.2.4. Evaluation method, RMSE

There are endless ways to evaluate the quality of the models. Knowing the limitations and advantages is essential, regardless of the applied evaluation method. There are two primary advantages to using RMSE. First, it is easy to interpret once the success criteria are defined, as the unit matches the investigated parameter. Second, the error does not depend on the observation value, meaning that RMSE is equally sensitive to deviances at low and high values. The primary disadvantage of this evaluation method is the sensitivity to peaks and outliers, which can lead to high errors based on a few extreme data points [32]. This issue has been dealt with using 7-day moving mean values for relative humidity.

Despite the considerations for choosing RMSE as the evaluation method to ensure equal sensitivity to errors through the constructions, the errors were generally more significant in the exterior layers than close to the indoor climate. The bigger errors near the exterior climate might be caused by the many weather parameters, affecting the measured data and challenging the accuracy when simulating the hygrothermal wall conditions.

4.2.5. Mould index and time frame

The mould indexes were calculated for periods equivalent to the measured data. As time is a significant factor in the Viitanen model [48], the mould indexes might increase if analysed for a longer time frame. However, research by Ojanen et al. [47] shows that very low indexes, in this case, many are 0, are unlikely to increase significantly over an extended time frame. The study shows that susceptible materials can attain mould index 5 in just 20 weeks when exposed to critical conditions. As all mould risk assessments in this study considered a minimum of 52 weeks for materials classified as “very sensitive”, the limited time ranges are not expected to impact the results significantly. Nonetheless, this perspective supports evaluating more sensitive materials to compensate for the limited time frames.

4.2.6. Geography and climate

This study is limited by the monitored houses being located in only two different cities, namely, Nuuk and Sisimiut. However, these locations are favourable since they represent significant proportions of the Greenlandic population, inhabiting more than 43% [24]. Still, when evaluating the suitability and robustness of the façade constructions for the overall Greenlandic climate, this restricted geographical scope must be considered a limitation.

In the previous study presenting data from the test pavilion [5], see Section 1.3, the same three construction types were analysed for five different Greenlandic climates using ERA5 weather files. Concerning mould growth risk, all constructions were concluded to be robust under varying conditions. However, the conditions in the pavilion differed from the houses because the pavilion had a controlled interior climate, and the walls were meticulously constructed under controlled conditions.

The applied climate data, especially in Sisimiut, cause uncertainties due to the production method of ERA5 weather [38]. The data from DMI has more missing data points, which also causes uncertainties. A previous study [5] found that similar Delphin simulations were insensitive to applying ERA5 weather data instead of locally measured data.

4.2.7. Relation to a previous assessment of CON_{Nuuk}

In this study, the robustness was evaluated based on the risk of mould growth. However, the façades may not perform as anticipated due to inadequate construction work. A previous study of CON_{Nuuk} [12] concluded that the temperature between the insulation and concrete was lower than expected because of airflows through the insulation, see Section 1.3. It also concluded that it might be possible to eliminate this issue by implementing a wind barrier, reducing the risk of cold wind penetrating the unevenly installed insulation layer. This conclusion is supported by Ref. [5], considering a test facility with a similar construction but implemented with high accuracy and quality control, where the measured data was in line with the expected hygrothermal conditions created by simulations. This can explain why the simulations and measurements were consistent for CON_{sis} and not CON_{Nuuk}.

4.3. Outlook

As the performance of a building is highly dependent on airtightness, the economic and environmental impact of a wind barrier might be a worthy trade-off to ensure the best quality and reduce the risk of having to redo parts of the façade. Thus, evaluating the consequences of excluding certain elements, such as the wind barrier, is recommended.

For further research, it is interesting to investigate why mould is prevalent in residential buildings despite this and other studies identifying low humidity levels and, consequently, reduced mould risks.

5. Conclusion

In this study, the hygrothermal data from 9 façade structures in Nuuk and Sisimiut were presented along with simulations representing the expected hygrothermal behaviours of the constructions. The ambition was to identify if the absence of wind barriers could cause hygrothermal issues. This study assessed two perspectives on this issue: mould and temperature. The mould indexes, presented in Fig. 6 and Table 4, showed that the risk of mould could not be eliminated by implementing a wind barrier.

Furthermore, the study intended to identify if all the represented constructions were robust to the Arctic climate. Again, this was evaluated based on the hygrothermal conditions and the risk of mould. When assessing the risk of mould growth, most of the constructions are at some risk in the outer layers, but only three half-timber constructions (HT_{sis2}, HT_{Nuuk1}, and HT_{Nuuk2}) are at risk on the inner side of the wind barrier. Furthermore, the values are so small that they will unlikely grow significantly over an extended period. Thus, the constructions can all be considered robust regarding mould. All assessed construction types have examples where the hygrothermal measurements and simulations align. However, there are also discrepant comparisons from both locations pointing toward the importance of fulfilling practical aspects.

CRediT authorship contribution statement

Naja Kastrup Friis: Writing – review & editing, Writing – original draft, Visualization, Software, Methodology, Formal analysis, Data curation. **Eva B. Møller:** Writing – review & editing, Supervision, Methodology, Conceptualization. **Tove Lading:** Project administration, Funding acquisition, Conceptualization.

Declaration of competing interest

The authors declare that they have no known competing financial interests or personal relationships that could have appeared to influence the work reported in this paper.

Data availability

Data will be made available on request.

Acknowledgements

This study was supported by DTU, DTU Byg, Grønlands Selvstyre, Kommunerqarfik Sermersooq, Greenland, Kernn-Jespersens Fond, A. P. Møllers Fond and Knud Højgaards Fond.

References

[1] J.C. Madsen, Grønlandske Boliger - Selvbyggeri Og Typehuse, Forlaget Atuagkat, 2000.
[2] E.B. Møller, T. Lading, Current building strategies in Greenland, E3S Web Conf. 172 (2020), https://doi.org/10.1051/e3sconf/202017219004.
[3] Rigsarkivet, "Nuna-Tek/GTO [Online]. Available: https://www.sa.dk/daisy/arkivskaber_detaljer?a=&b=&c=&d=&e=&f=&g=&h=&ngid=407286&ngnid=&heid=&henid=&epid=&faid=&meid=&m2rid=&side=&sort=&dir=&gsc=&int=&ep=&es=&ed=.
[4] IAPP's Committee Regarding Test Constructions, Byggeriets effektivisering, 2002.
[5] N.K. Friis, E.B. Møller, T. Lading, Hygrothermal assessment of external walls in Arctic climates: field measurements and simulations of a test facility, Build. Environ. 238 (Jun. 2023), 110347, https://doi.org/10.1016/j.buildenv.2023.110347. February.
[6] J. Vinha, Hygrothermal Performance of Timber-Framed External Walls in Finnish Climatic Conditions: A Method for Determining the Sufficient Water Vapour Resistance of the Interior Lining of a Wall Assembly, 2007.
[7] J. Langmans, Feasibility of Exterior Air Barriers in Light Weight Construction, 2013.
[8] Technical University of Denmark, Om Projektet - ABC - Arctic Building and Construction, 2022 [Online]. Available: https://abc-byg.dtu.dk/om-projektet. (Accessed 5 May 2022).
[9] E.B. Møller, T. Lading, Preliminary assessment of the building design of a new test house in Nuuk, Greenland, J. Phys. Conf. Ser. 2069 (1) (2021) 1–4, https://doi.org/10.1088/1742-6596/2069/1/012228.
[10] A. Slyngborg, Study of Energy Performance and Optimization for Buildings in Greenland A Case Study of Prøvehuset in Nuuk for Potential Purposes, 2021.
[11] U. Andersen, DTU Advarer : Ny Byggemetode Giver Kuldeproblemer I Grønland, 2020, pp. 3–5.
[12] N.K. Friis, E.B. Møller, T. Lading, Can collected hygrothermal data illustrate observed thermal problems of the façade? - a case study from Greenland, J. Phys. Conf. Ser. 2069 (2021), https://doi.org/10.1088/1742-6596/2069/1/012071.
[13] L.M. Ottosen, Lavenergihuset I Sisimiut, 2006, pp. 1–2.
[14] Direktoratet for Boliger og Infrastruktur, Bygningsreglement, 2006, p. 158, 2006.
[15] S.R. Petersen, Pivutæt Grønlandsk Lavenergihus Når Ikke Egne Energimål, 2010. Ingeniøren.
[16] C. Rode, P. Vladykova, M. Kotol, Air Tightness and Energy Performance of an Arctic Low-Energy House, October, 2010.
[17] M. Kotol, Energy Use and Indoor Environment in New and Existing Dwellings in Arctic Climates, 2014.
[18] Vejrarkiv DMI [Online]. Available: https://www.dmi.dk/vejrarkiv/, 2020. (Accessed 16 December 2020).
[19] S. Ilomets, T. Kalamees, J. Vinha, Indoor hygrothermal loads for the deterministic and stochastic design of the building envelope for dwellings in cold climates, J. Build. Phys. 41 (6) (May 2018) 547–577, https://doi.org/10.1177/1744259117718442.
[20] E.B. Møller, J. Helgason, Weather and indoor climate in Greenland, J. Phys. Conf. Ser. 8 (2021).
[21] R.J. Stanborough, A. Cattamanchi, Dry Air: How Dry Air Can Affect Your Health, Plus Prevention Tips, Healthline, 2020 [Online]. Available: https://www.healthline.com/health/dry-air. (Accessed 23 February 2023).
[22] M. Kotol, C. Rode, G. Clausen, T.R. Nielsen, Indoor environment in bedrooms in 79 Greenlandic households, Build. Environ. 81 (2014) 29–36, https://doi.org/10.1016/j.buildenv.2014.05.016.
[23] R. Krishnan, et al., An influence of dew point temperature on the occurrence of Mycobacterium tuberculosis disease in Chennai, India, Sci. Rep. 12 (1) (2022) 1–10, https://doi.org/10.1038/s41598-022-10111-4.
[24] Statistics Greenland, Greenland in Figures 19 (2022) 36, 2022.
[25] AS Boligselskabet INI, Skimmelsvamp." [Online]. Available: http://www.byginfo.gl/media/1124/ini-as-skimmelsvamp.pdf.
[26] Baumklimatik-Dresden, DELPHIN," 2022. [Online]. Available: http://bauklimatik-dresden.de/delphin/index.php. (Accessed 23 January 2021).
[27] V. Kukk, A. Bella, J. Kers, T. Kalamees, Airtightness of cross-laminated timber envelopes: influence of moisture content, indoor humidity, orientation, and assembly, J. Build. Eng. 44 (April, 2021), https://doi.org/10.1016/j.jobe.2021.102610.
[28] Innovative Sensor Technology, "HYT 221 Digital Humidity and Temperature Module." p. 3.
[29] B. Hejari, N.R.M. Sakiyama, J. Frick, H. Garrecht, Hygrothermal Simulations Comparative Study : Assessment of Different Materials Using WUFI and DELPHIN Software Bina Hejazi, 2019, pp. 4674–4681. Nayara R . M . Sakiyama , Jürgen Frick , Harald Garrecht Materials Testing Institute (MPA), University of Stuttgart , Stuttgart.
[30] M. Defo, M. Lacasse, A. Laouadi, A comparison of hygrothermal simulation results derived from four simulation tools, J. Build. Phys. 45 (4) (2022) 432–456, https://doi.org/10.1177/1744259120988760.
[31] A. Tijskens, S. Roels, H. Janssen, Neural networks to predict the hygrothermal response of building components in a probabilistic framework, in: Healthy, Intelligent and Resilient Buildings and Urban Environments, 2018, pp. 1169–1174, https://doi.org/10.14305/ibpc.2018.ms-6.04. December 2019.
[32] V. Kukk, L. Kaljula, J. Kers, T. Kalamees, Designing highly insulated cross-laminated timber external walls in terms of hygrothermal performance: field measurements and simulations, Build. Environ. 212 (November 2021), 108805, https://doi.org/10.1016/j.buildenv.2022.108805, 2022.
[33] O. May Tzuc, et al., Modeling of hygrothermal behavior for green facade's concrete wall exposed to nordic climate using artificial intelligence and global sensitivity analysis, J. Build. Eng. 33 (July 2020) 2021, https://doi.org/10.1016/j.jobe.2020.101625.
[34] S. Vogelsang, H. Fechner, A. Nicolai, Delphin 6 Material File Specification, 2013, Version 6.0.
[35] P. Mukhopadhyaya, M.K. Kumaran, J. Lackey, N. Normandin, D. van Reenen, F. Tariku, Hygrothermal properties of exterior claddings, sheathing boards, membranes, and insulation materials for building envelope design, Therm. Perform. Exter. Envel. Whole Build. 1 (2007) 1–13.
[36] Cembrit, "Cembrit Multi Force," [Online]. Available: https://www.cembrit.dk/download/SDK/montagevejledninger/montagevejledning-cembrit-multi-force, 2017. (Accessed 31 January 2023).
[37] Cembrit, "Cembrit Windstopper [Online]. Available: https://www.cembrit.com/download/CHDK/datasheets/cembrit-windstopper-basic-datasheet, 2018.
[38] European Centre for Medium-Range Weather Forecasts, ERA5 | ECMWF, https://www.ecmwf.int/en/forecasts/datasets/reanalysis-datasets/era5, 2022. (Accessed 17 January 2023) [Online]. Available:.
[39] D.G. Erbs, S.A. Klein, J.A. Duffie, Estimation of the diffuse radiation fraction for hourly, daily and monthly-average global radiation, Sol. Energy 28 (4) (1982) 293–302, https://doi.org/10.1016/0038-092X(82)90302-4.
[40] J. Langmans, S. Roels, Experimental analysis of cavity ventilation behind rainscreen cladding systems: a comparison of four measuring techniques, Build. Environ. 87 (2015) 177–192, https://doi.org/10.1016/j.buildenv.2015.01.030.
[41] J. Falk, K. Sandin, Ventilated rainscreen cladding: measurements of cavity air velocities, estimation of air change rates and evaluation of driving forces, Build. Environ. 59 (2013) 164–176, https://doi.org/10.1016/j.buildenv.2012.08.017.
[42] G.M. Girma, F. Tariku, Experimental investigation of cavity air gap depth for enhanced thermal performance of ventilated rain-screen walls, Build. Environ. 194 (2021), 107710, https://doi.org/10.1016/j.buildenv.2021.107710. October 2020.
[43] J. Brozovsky, A. Nocente, P. Rüther, Modelling and validation of hygrothermal conditions in the air gap behind wood cladding and BIPV in the building envelope, Build. Environ. 228 (November 2022) (2023), 109917, https://doi.org/10.1016/j.buildenv.2022.109917.
[44] E. Brandt, et al., SBI-Anvisning 277, Fugt I Bygninger - Teori, Beregning Og Undersøgelse, vol. 1, BUILD, 2023.
[45] A. Hukka, H.A. Viitanen, A mathematical model of mould growth on wooden material, Wood Sci. Technol. 33 (6) (Dec. 1999) 475–485, https://doi.org/10.1007/s002260050131.
[46] Fraunhofer Institute for Building Physics, WUFI® Mould Index VTT, 2022 [Online]. Available: https://wufi.de/en/2017/03/31/wufi-mould-index-vtt/. (Accessed 26 January 2023).
[47] T. Ojanen, et al., Mold growth modeling of building structures using sensitivity classes of materials, in: ASHRAE Build. XI Conf. Dec. 5-9, 2010 Cleawater Beach, 2010. Florida.
[48] H. Viitanen, T. Ojanen, R. Peuhkuri, Mould growth modelling to evaluate durability of materials, Proc. 12DBMC - Int. Conf. Durab. Build. Mater. Components (2011) 1–8.
[49] N.K. Friis, E.B. Møller, Repository for Hygrothermal Conditions in the Facades of Residential Buildings in Nuuk and Sisimiut, 2023, https://doi.org/10.11583/DTU.22212103.
[50] R. Wang, H. Ge, D. Baril, Moisture-safe attic design in extremely cold climate: hygrothermal simulations, Build. Environ. 182 (2020), 107166, https://doi.org/10.1016/j.buildenv.2020.107166. July.
[51] S.B. Ingebretsen, E. Andenæs, L. Gullbrekken, T. Kvande, Microclimate and mould growth potential of air cavities in ventilated wooden façade and roof systems—case studies from Norway, Buildings 12 (10) (Oct. 2022) 1739, https://doi.org/10.3390/buildings12101739.

V

Department of Civil and Mechanical Engineering

Section of Design and Processes, August 2023
Brovej 118
2800 Kgs. Lyngby

www.construct.dtu.dk

ISBN: 978-87-7475-755-9